Improving the urban resource nexus through urban agriculture systems with biowaste utilisation and renewable energy

Till Weidner

Exeter College



Department of Engineering Science,
University of Oxford

Thesis submitted for
Doctor of Philosophy in Engineering Science
June 4, 2021

Abstract

The food systems in developed societies face a host of challenges in the early 21st century; increasing urbanisation, supply chain shocks due to extreme climate events and pandemics, high impacts of air freight, nutrient run-off and animal farming, and tremendous amounts of wasted food and nutrients. A transformation to a more sustainable and resilient food system includes, among other pathways, increased consumption of fruits and vegetables, a localisation of food production and the recovery of nutrients in urban organic waste. Urban agriculture thus receives emerging research interest, ranging from community gardens to high-tech indoor farming. Efforts so far have focused on socio-economic aspects and life-cycle assessments of individual case studies or have described the qualitative potential of integrating urban waste streams into urban farming. Significant gaps remain in the literature about the carbon and land intensity of different growing methods when scaled-up and the quantification of productivity and nutrient recovery potentials. On the city and regional level, the design of productive food systems integrated with biowaste management and renewable energy systems has found little attention so far. These gaps are addressed in this thesis through mathematical modelling and geospatial analysis at multiple scales, including the facility, the urban area, a metropolitan area, and the regional level.

The match of supply and demand of a scaled-up urban food production system and their organic waste flow utilisation potential was assessed and compared for two urban areas, Glasgow and Lyon. Potentially convertible land and rooftop space were determined with geospatial processing, and monthly biowaste utilisation in those new farms was optimised based on nutrient requirements and CO_2 emission savings. The results showed that high self-sufficiency came with significantly increased CO_2 emissions for the productive urban food system in the colder climate due to high demand and carbon intensity of electricity for greenhouses, which also negated the benefits of utilising a large share of the biowaste.

The next project thus investigated the interplay and logistics of local composting treatment combined with low-input local farming for 76 districts in Porto from waste system perspective. Existing fields, convertible greenspaces, and compost island requirements were obtained from geospatial analysis and waste collection pilots and distance scripts informed collection and transport requirements to central facilities. The results showed that more remote districts could benefit both in cost and climate impacts from having their own decentralised biowaste systems, although mainly from collection route reduction rather than a conversion of greenspaces.

Focusing more on the contextual sustainability of high-intensive growing methods, the energy consumption of electrified greenhouses and vertical farm facilities was assessed for ten regions across the globe. A rigorous thermodynamic model for lighting and air conditioning requirements was optimised for minimum specific energy in relation to the outside climate on an hourly basis. The outcomes showed that significant energy reductions can be achieved in greenhouses with optimised climate control, while local climate conditions and design choices still have a strong impact. Vertical farms, or plant factories, had significantly higher energy consumptions, even in extreme climates.

The final project applied the learnings from the energy optimisation to a land-use based assessment of regionalised vegetable supply with renewable energy generation for nine city-regions. Potentially available land for energy generation was assessed, and the selection and sizing of solar PV and wind farms were economically optimised for the required electrical load. The results show that although greenhouse production requires oversized renewable energy systems due to higher load fluctuations, its land footprint is lower than that of open-field and vertical farming. The land use relative to existing and available land contextualised this finding, but a full regionalised vegetable supply was feasible and desirable for most of the regions.

The implications from the work are that to achieve increased food self-sufficiency and climate change mitigation, energy-efficient and low-carbon urban agriculture approaches are indispensable. Recommendations for specific urban growing systems are strongly context-dependent and many transferable aspects of relevance to decision-makers have been quantified in this work. Further, the integration of biowaste mainly provides benefits from a holistic waste management perspective and thus a multi-stakeholder approach and commitments will always be required.

Acknowledgements

Our moment in time as a collective is a critical one. But so was every moment, for somebody in some place. I feel deep gratitude to every peasant, labourer, activist and visionary that built the world as it is today but also refused to accept the status quo and fought for a more just and enlightened society. Thousands of years of common struggle gave us in Europe free secondary education, universal access to knowledge, political representation, public funding for infrastructure and amenities, the right to self-determination, independent university research agendas, and finally, scholarships for a commoner displaying some past ambition. Enjoying these fruits prior to and during my doctoral research, I can only hope that I did do some justice with my work on environmental sustainability to those before me. My thanks also go to whoever selected me for the Clarendon Scholarship and all the people behind it.

I thoroughly enjoyed learning, doing and being during the last 3.5 years. One of the main reasons that life felt smooth was my good fortune to have an incredibly devoted and kind supervisor, Aidong Yang. His guidance on my ideas, his mentorship for my ambitions, his patience with my mistakes, and his commitment to my work mean a lot and will forever be remembered. I am also thankful for having lived with some of the finest folks I have ever come across. Alex, Anis, Emma and Sage are not just bold intellectuals, generous humourists, and sweet friends but also provided comfort and calm day in and out. Living on the other side of town (an eternal ten-minute journey), my dear partner was my haven and wings. Thank you, Oxford, for bringing us together and thank you, wide cycling lanes, for bringing us closer. Franziska, your thoughts are deep, your values impeccable, your logic sharp, your heart strong, your soul kind, and your love unparalleled. My gratitude for supporting me so tenderly in this endeavour and beyond.

On my path from start to completion of this thesis, I was lucky to have received support from different people outside of Oxford. I want to thank Michael Hamm from Michigan State University for being my mentor on everything related to regional food systems and vegetable growing. João Graça was a great sparring partner for the biowaste project in Porto, and I am indebted to the whole research & development team at LIPOR. Florian Forster kindly shared his knowledge and esteemed opinions during my final project on renewable energy and land use. Despite the theoretical nature of my research, I had the opportunity to engage with practioniers and am grateful to Ketil Stoknes for hosting me in Norway and showing me his digeponic system, to Arthur Michelet for the inspiring micro-AD workshop, to Michael Martin for hosting me in Sweden and introducing me to the indoor farm companies in the

area, and to the guys at UrbanOasis that let me be part of a thriving basement vertical farm start-up for a few weeks. I am also grateful to the examiners for the helpful comments received during my Transfer and Confirmation of Status interviews.

I dedicate this thesis to every guerrilla farmer and urban gardener working hard to foster communities and reconnect people to the cycle of life.

A special place in my memory is reserved for all the amazing human beings of Extinction Rebellion Oxford. You showed me the path to fun and fierce activism. The future is on our side. I am also happy about my other extracurricular encounters at Exergy LLC and Ashoka Globalizer. In the office, many friendly and diligent individuals made for a pleasant work atmosphere – I am deeply sorry about the bouillon fumes during lunchtime.

Lastly, I would like to express my gratitude to my loving parents. You provided a gentle upbringing, acted as resourceful teachers, and honed my critical mind. Your service to humanity is deeply inspirational – may the seeds of our different work blossom one day in harmony.

List of acronyms

AD	Anaerobic digestion
ASHP	Air source heat pump
BSF	Black soldier fly
CEA	Controlled environment agriculture
CGH	Closed, non-ventilated greenhouse
CHP	Combined heat- and power units
COP	Coefficient of performance
CSA	Community supported agriculture
DLI	Daily light integral
ET	Evapotranspiration
FTE	Full-time equivalent jobs
FW	Food waste
GH	Greenhouse
GHG	Greenhouse gases
GHI	Global horizonal irradiation
GW	Green waste
HC	Home composting
HEX	Heat exchanger
HVAC	Heating, ventilation and air conditioning system
iRTG	Integrated rooftop greenhouse
LCA	Life cycle assessment
LED	Light-emitting diode
LIDAR	Light detection and ranging
OGH	Open, ventilated greenhouse
OW	Organic waste
PAR	Photosynthetically active radiation
PF	Plant factory
PFR	Plug flow reactor
PPFD	Photosynthetic photon flux density
PPM	Parts per million
PUFS	Productive urban food systems
PV	Photovoltaic
RC	Refrigeration cycle
RLC	Refraction lens cover
RTG	Rooftop greenhouse
UA	Urban Agriculture
VF	Vertical Farm
VPD	Vapour pressure deficit

Table of Contents

Chapter 1 Introduction ... 1

1.1 Background ... 1

1.2 Objectives ... 3

1.3 Thesis structure ... 4

Chapter 2 Literature Review ... 6

2.1 Introduction ... 7
2.1.1 The context of urban agriculture as part of urban food systems ... 7
2.1.2 Taxonomy of urban agriculture ... 7

2.2 Previous work on technical aspects of urban agriculture with organic waste and renewable energy integration ... 8
2.2.1 Productivity and self-sufficiency ... 8
2.2.2 Possibilities for increased resource circularity within urban agriculture ... 11
2.2.3 Distribution of urban produce and waste ... 13
2.2.4 Energy demand reduction and renewable energy integration for CEA ... 14

2.3 Previous work on environmental impacts of urban agriculture systems ... 14
2.3.1 Soil-less greenhouse growing ... 15
2.3.2 Vertical indoor farming ... 16
2.3.3 Co-location of waste conversion technologies with greenhouses ... 17
2.3.4 Carbon footprint reduction through substitution of fertiliser and growth substrate ... 17
2.3.5 Effects of distribution and changing urban logistics ... 18

2.4 Modelling techniques and optimisation of the urban resource nexus ... 18
2.4.1 Life cycle assessments and flow analysis ... 18
2.4.2 Modelling of CEA energy demand and renewable energy supply ... 19
2.4.3 Geospatial modelling for logistics and land availability assessments ... 21
2.4.4 System design: Optimisation of resource allocation ... 22

2.5 Summary of research gaps ... 23

Chapter 3 The potential of urban agriculture in combination with organic waste valorisation: Assessment of resource flows and emissions for two European cities ... 26

3.1 Introduction ... 27

3.2 Methods ... 29
3.2.1 Overview ... 29
3.2.2 Food demand and production ... 32
3.2.3 Operational requirements for growing ... 33
3.2.4 Waste generation and processing ... 34
3.2.5 Description of scenarios and operational emissions ... 35
3.2.6 Optimization of waste allocation ... 37

3.3 Results ... 38
3.3.1 Spatial analysis and climate factors ... 39
3.3.2 Influence of intensity of growing practices ... 39
3.3.3 Results for a 20% adoption level of ground-based greenhouses ... 41

3.4 Discussion ... 48
3.4.1 Implications of growth intensity ... 48
3.4.2 Remarks on resource consumption ... 49
3.4.3 Influence profile of city characteristics on outcomes ... 50
3.4.4 Assumptions, sensitivities and limitations ... 51

3.5 Key insights ... 53

Chapter 4 Comparison of local and centralised biowaste management strategies – A spatially-sensitive approach for the region of Porto ... 55

4.1 Introduction ... 57

4.2 Methods ... 59
4.2.1 Waste collection ... 61
4.2.2 Centralised waste treatment ... 61
4.2.3 Local waste treatment ... 62
4.2.4 Local sinks and land application ... 64
4.2.5 Base scenario and parametric variability ... 65

4.3 Results and discussion ... 66
4.3.1 Regional economic assessment for the base scenario ... 66

4.3.2 Regional emissions comparison for the base scenario ... 67
4.3.3 District level differences for the base scenario ... 69
4.3.4 Implications of urban farming and surplus compost ... 71
4.3.5 Analysis of alternative scenarios on the regional level ... 73
4.3.6 Nutrient recovery potential ... 75

4.4 Key messages ... 75

Chapter 5 Energy optimisation of plant factories and greenhouses for different climatic conditions 78

5.1 Introduction ... 79

5.2 Methods ... 81
5.2.1 System overview ... 81
5.2.2 Plant growth and climate settings ... 87
5.2.3 Optimisation ... 90
5.2.4 Scenario and sensitivity analysis ... 92

5.3 Results and discussion ... 92
5.3.1 Hourly optimisation and seasonal behaviour ... 93
5.3.2 Influence of physical, design and control variables ... 95
5.3.3 Location-dependent comparative performance ... 99
5.3.4 Comparison with other studies ... 101
5.3.5 Recommendations for practitioners ... 103

5.4 Conclusions ... 104

Chapter 6 Quantifying the food-energy-land nexus of low-carbon indoor farming: regional implications 106

6.1 Introduction ... 107

6.2 Methods ... 109
6.2.1 Composition and micronutrient characteristics of the vegetable basket ... 109
6.2.2 Selection and characteristics of studied regions ... 109
6.2.3 Land availability for food production ... 110
6.2.4 Land availability for energy generation ... 111
6.2.5 Productivity and land use requirement of open-field farming ... 112
6.2.6 Electricity demand for CEA facilities ... 115
6.2.7 Land use for renewable electricity supply ... 115

6.3 Results ... 116
6.3.1 Regional characteristics and land availability ... 116
6.3.2 Renewable energy systems for CEA facilities: demand and supply ... 118
6.3.3 Combined land requirements for growing and renewable energy supply ... 120
6.3.4 Regional land-use implications ... 123

6.4 Discussion and conclusion ... 125

Chapter 7 Discussion and conclusion ... 127

7.1 Summary of main work accomplished ... 127

7.2 Key learnings and outcomes ... 128

7.3 Limitations ... 129

7.4 Future work ... 131

Appendix I: Supplementary Information of Chapter 3 ... 133

Appendix II: Supplementary Information of Chapter 4 ... 142

Appendix III: Supplementary Information of Chapter 5 ... 157

Appendix IV – Supplementary information to Chapter 6 ... 192

References ... 210

Chapter 1 Introduction

1.1 Background

Our contemporary understanding of how human civilisation interacts with the planet increasingly reveals multiple crises of sustainability (Lade et al., 2020). Already today, we are consuming more resources and causing more pollution that our planet can sustainably provide and absorb. This trend is particularly troublesome for industrialised countries, where modern lifestyles are so resource-intensive that if everyone had equal standards, we would need up to five Earths to sustain us (Global Footprint Network, 2021). A major factor in this unsustainable lifestyle is the paradigm of the modern densely populated city, where valuable resources are imported from the outside and waste material is generated in vast quantities and often exported into other countries (Shinkuma & Nguyen Thi Minh Huong, 2009), large landfills or into the atmosphere (Mazzanti & Zoboli, 2011). As a subsystem of provision, the globalised food system has managed to greatly increase output over the last century through highly specialised and mechanised farms, input-intensive agriculture (e.g. pesticides and fertilisers) and conversion of forests, shrubs and moor into productive fields (Kopittke et al., 2019). However, this came at the cost of degraded soils, destroyed ecosystems and increased greenhouse gas (GHG) emissions from the use of fossil fuels in production and transportation (Springmann et al., 2018). Further, long and complex supply chains led to large amounts of food, in particular perishable items such as vegetables, going off and being wasted (Alexander et al., 2017). These linear and resource inefficient ways are a major contributor to the resource burden of cities. In addition to issues of sustainability, the current food system – with its high share of processed food and food production far removed from the consumer – has led to two intertwined issues: obesity (UNICEF, 2016) and alienation with how plants grow and farm animals live (McClintock, 2010).

Many alternatives to the current model have been proposed. The most prominent ones are changing diets from rich in processed food to rich in fresh produce, switching from animal protein to plant protein, regionalising or localising food production, repurposing agricultural residues and food waste (i.e. biowaste), and changing the way we produce, which includes more ecosystem-friendly open-field farming (e.g. agroecology) and more intensive controlled-environment agriculture (CEA) (Godfray et al., 2010). A common thread in those alternatives is an increased and more sustainable production of fruits and vegetables closer to the consumer. Another term describing these principles is peri-urban or urban agriculture (UA), provided it incorporates circular and low-carbon principles for increased sustainability. The

term UA encompasses all growing practices in or around ("peri") cities, which cater for the local demand. Although UA is only one of many puzzle pieces in the alternative food system landscape, it is a crucial one in popularising fresh and healthy produce, connecting citizens to food and soil dynamics, and enabling localised resource cycles (Bahers & Giacchè, 2019). It also promises reduced environmental impacts from the food and waste system due to shorter transport requirements, less food waste and biodiversity enhancement (Wilhelm & Smith, 2017). Despite its promises, UA is not sustainable per se, as intensive and high-input growing practices can consume substantial amounts of resources and energy (Goldstein et al., 2016), negating any benefits of reduced transport distances. This is particularly relevant for CEA practices that rely completely on artificial lighting instead of sunlight, such as indoor vertical farming (Graamans et al., 2018). Studies have shown both such detrimental and unintended impacts (Doherty, 2015) but also opportunities to increase the resource efficiency of UA practices. Many of these opportunities are related to integrating and utilising urban waste flows (Mohareb et al., 2017) and reducing the impact of energy consumption of more intensive growing practices through energy efficiency measures and renewable energy integration (Benke & Tomkins, 2017). It can be argued that a successful transformation of the food system is a delicate and context-specific matter, and that the implementation of UA needs to be done right, i.e. in a way that it delivers on the promises (Till Weidner et al., 2019). However, what is currently lacking in the literature are quantitative assessments of the benefits and implications of UA and these integration opportunities on a larger scale. Further, it is unclear how geographical, climate and urban characteristics quantitatively influence the outcomes.

This thesis is thus concerned with approaches that make UA more sustainable and resource-efficient, by considering the interplay with the urban biowaste system and the regional energy systems. The thesis is motivated by the practical relevance of this topic; providing insights and recommendations about low-carbon and circular UA can be immensely helpful to practitioners and planners, while the development of quantitative assessment methods can help researchers derive better context-specific answers. This theoretical work does not try to generate new technological innovations or advance our detailed understanding of processes but intends to synthesise previous learnings and findings from promising pilots and studies to assess system-level implications. It so differs from previous enquiries, and its novelty lies in applying geographical information systems (GIS) and process systems engineering (PSE) tools, such as mathematical modelling and optimisation, to the emerging field of urban agriculture systems embedded in the food-energy-waste-land nexus.

1.2 Objectives

In view of the challenges of a sustainable transformation of the food system with UA, the main objective is to assess the influence of context-specific conditions on the resource and GHG emissions intensity of scaled-up and integrated UA systems in industrialised countries. Necessary for this endeavour is besides developing assessment methodologies for the design of desirable and sustainable UA, biowaste and renewable energy systems. These systems interact spatially across urban and regional land, which calls for employing and developing novel spatial analysis methods. This work also aims to generate spatially differentiated insights by incorporating assessments at the urban, metropolitan and regional scale. Through applying spatial analysis, mathematical modelling and environmental impact assessments, context-specific and transferable insights shall be generated that are relevant to applied research and practitioners. The objectives are listed as follows:

1) *Assess productivity, resource flows and GHG emissions of scaled-up UA systems.* Such an assessment informs the food self-sufficiency expectations and resource implications for hypothetical fully scaled-up integrated UA systems consisting of different growing practices. The perspective is the food system, and resource flows include produce and urban biowaste and products of waste management (e.g. fertiliser, heat) that can serve as input for UA.

2) *Compare decentralised biowaste management and utilisation with current approaches.* Alternative biowaste management strategies which allow for the utilisation of waste products in UA are to be evaluated. The perspective is the waste system; collection and transport logistics, land application of waste products, and conversion of urban land to farms are to be considered.

3) *Develop methods to analyse, improve and compare the energy-efficiency of CEA systems.* Reducing the energy intensity of produce lowers the cost and environmental footprint of high-yield growing practices and is thus of paramount importance. Methods are missing which determine the ideal operating mode providing an indicative benchmark of the maximum energy efficiency that can be reached.

4) *Determine the combined land footprint or CEA systems with renewable energy.* Reducing the carbon intensity of the energy supply by generating renewable energy can be land-intensive. This indirect land use might counterbalance direct land savings achieved by employing highly productive CEA practices instead of open-field farming.

5) *Investigate the influence of local context on the resource and GHG footprint of integrated UA systems.* The different assessments not only aim to design novel systems and assess their impacts but also to understand how local factors such as climate, geography, population density and urban characteristics influence the outcomes.

6) *Provide relevant and transferable insights to practitioners and policymakers.* This work aims to generate practical insights, which can help people involved in implementing UA solutions to make better choices. This ambition is realised by generating results in a way that they can be transferred to other situations and by describing how to do so.

1.3 Thesis structure

	Study	Scale (geographical)	Details	Resolution	Assessments
Chapter 3	Urban food-energy-water-waste nexus optimisation	City (Europe)	Two cities as closed units	Patch size for available land (>3 meter) and flows and impacts on city level	• Seasonal productivity of UA • Optimized waste recovery flows • Carbon footprint comparison
Chapter 4	Design and evaluation of fully decentralised waste system	District (Metropolitan area)	Metropolitan region with surrounding land and ist 76 individual districts	Residential blocks, with flows and assessment for each district	• Economic and environmental comparison of biowaste management strategies • Logistics and sink area (including urban farms)
Chapter 5	Facility-based energy demand optimisation	Facility (Global)	Plant factories and greenhouses in 10 different locations	2000 m^2 facility	• Detail model creation space conditioning and plant interactions • Optimised specific energy use
Chapter 6	Regional food-energy-land nexus implications of different growing methods with energy optimisation and microgrids	Regional (Global)	9 regions or states, including its hinterland in a radius of up to 200 km	100 m^2 pixels within regions or states with a size < 80,000 km^2	• Load dependent renewable energy generation with grid optimisation • Land use for open-field, greenhouses and plant factories • Comparison with available land

Biowaste and energy focus Biowaste focus Energy focus

Figure 1-1: Overview of the four original work chapters, including scale and resolution

This thesis contains, besides a literature review, four chapters of original work that each present a short background to the work, gaps and research questions, methods applied and results. The objectives of this thesis are tackled in hierarchical order, with objective 5) and 6) being addressed in all four original chapters. The thesis is in the integrated form, where published or under-review papers make up the chapters (with slight adjustments in formatting). Due to the integrated form, chapters are in publication length, and further details on the methods and results are presented in the respective Appendices. Figure 1-1 provides a visual overview of the main chapters and the scale they investigate. Chapter 1 provides background, motivation, and an overview of this work, while the body of the thesis is organised as follows:

Chapter 2 evaluates the existing literature on UA itself and in combination with biowaste utilisation and renewable energy integration. The literature is reviewed critically, promising findings are reported, and research gaps are identified to develop a rationale for this work.

Chapter 3 studies the food-energy-water-waste nexus implications of scaled-up UA systems in two European cities (Lyon and Glasgow). Land availability assessments with a high resolution and mathematical modelling inform the potential self-sufficiency for fruit & vegetables relying on both CEA and open-field farming. An optimisation allocates available organic waste resources to the UA system minimising the carbon footprint of the alternative food systems.

Chapter 4 lays out the design of a decentralised waste management and utilisation system based on community composting and compares its cost and GHG emissions to three centralised waste management systems. The assessment is carried out for each of the 76 districts within the metropolitan area of Porto and the existing peri-urban farmland and potentially created urban farms act as a resource sink for waste products.

Chapter 5 optimises the energy intensity of three CEA practices in ten different geographical regions with different climate zones. To do so, it develops a detailed model of the interior climate (and its effect on hourly yield) and the air conditioning unit. It maximises the energy consumption per unit weight of produce for each hour within a year for indoor vertical farms, closed and open greenhouses. The resulting energy demand is used as a basis for the land use calculations in Chapter 6.

Chapter 6 explores the direct and indirect land-use implications of CEA practices supplied by renewable energy systems. The location-specific hourly energy demand derived from Chapter 5 is used to simulate renewable energy microgrids in nine city-regions. These microgrids are cost-optimised for the most economical balance between wind turbines and solar PV and between energy storage and overcapacity. The resulting combined land use is assessed and compared with open-field farming and with the available land for energy generation within the region.

Chapter 7 summarises the key contributions and findings of the work and their implications for practitioners. It also discusses the limitations of this theoretical work and identifies future research directions.

Chapter 2 Literature Review

Overview

This chapter explores previous work related to the topic of this thesis and identifies gaps in the literature that need to be tackled for sustainably scaling up UA systems. First, an introduction and context is given for urban agriculture. Second, technical aspects of urban agriculture systems with organic waste and renewable energy integration are discussed, and promising concepts highlighted. Third, studies are collated that report the environmental impacts of integrated urban agriculture systems and recommendations and trends are indicated. Fourth, modelling techniques employed in this area are highlighted, and some previous applications discussed. Finally, the key research gaps are listed.

Parts of this chapter have been published as: *Weidner, T., Yang, A., & Hamm, M. W. (2019). Consolidating the current knowledge on urban agriculture in productive urban food systems: Learnings, gaps and outlook. Journal of cleaner production (JCP), 209, 1637-1655.*

Among all authors who contributed to the published article, T.W. analysed and categorised the literature, conceptualised the content and story and wrote the manuscript. M.H. provided feedback on the conceptual stage and storyline and edited the manuscript. A.Y. supported the literature analysis, provided useful feedback in the conceptual stage and thoroughly revised the manuscript.

2.1 Introduction

2.1.1 The context of urban agriculture as part of urban food systems

Increasing urbanisation, population growth, deteriorating soil and extreme climate events put pressure on global food security, while a third of the global population suffers from malnutrition, through either obesity, food insufficiency, or nutrient deficiency (UNICEF, 2016; UNCCD, 2017). Additionally, the current food system contributes heavily to our global environmental challenges including biodiversity loss, climate change, fresh water pollution, deforestation, and excess nutrient accumulation (Jaramillo & Destouni, 2015; Lenka, Lenka, Sejian, & Mohanty, 2015). Innovation, dietary pattern change, and rethinking the direction of our global food system are therefore imperative in the 21st century (Tilman and Clark, 2014).

Producing food within urban boundaries has been suggested as a way to simultaneously tackle a breadth of environmental, social, and human health issues. Research has shown that in addition to achieving a certain degree of self-sufficiency (Clinton et al., 2018), potential climate change mitigation (Kulak et al., 2013) and ecosystem benefits (Wilhelm & Smith, 2017), urban agriculture (UA) has the potential to increase resource efficiency and circularity (Mohareb et al., 2017), foster social development and community cohesion (Duchemin et al., 2008), and broaden biosphere (Lin et al., 2015) and dietary diversity (Wilkins et al., 2015).

Urban agriculture (UA) as a primary production process can be viewed as a component embedded in the urban food system, which further includes processing, packaging, distribution and retail, as well as the various institutional norms, government and private sector policies, and cultural attributes in any city region. All these aspects closely interact with urban material and resource streams such as water, energy, and organic waste. In particular, urban organic waste contains valuable plant nutrients (e.g. nitrogen and phosphorus) and energy (in form of carbon compounds) but is often collected together with municipal solid waste, making nutrient and energy recovery challenging (Alvarenga et al., 2015). Nevertheless, a range of opportunities exists to (decentrally) utilise those waste streams within urban agriculture, which could significantly improve the resource circularity and reduce the overall environmental burden of such systems (Mohareb et al., 2017). The potential for waste stream utilisation has been known for many years (Smit & Nasr, 1992), but the academic discourse lacks comprehensive quantitative assessments on how those fit into and benefit urban farming.

2.1.2 Taxonomy of urban agriculture

To cope with the differing production capacity and socioecological impacts, growing practices for UA have been defined and classified depending on the paradigm of interest.

For this work, the relation between input intensity and the expected yield is of relevance. Goldstein et al. (2016b) classified practices depending on their location (ground-based or building-integrated) and the extent of controlling the climatic conditions (e.g. temperature, humidity) of their growing environment (conditioned and non-conditioned growing) and characterised the four resulting classifications by their operational characteristics, capital inputs and potential for urban symbiosis. The most common practice for conditioned environment agriculture (CEA) is hydroponics, a soil-less system in which nutrients are transported through the plant roots submerged in water. Noteworthy is also the practice of aquaponics, in which denitrifying bacteria convert the ammonium in fish faeces to readily available nitrate for plant growth in an integrated system, thus co-producing plants and different types of fish. All CEA practices achieve yields much greater than in open fields or gardens but require more infrastructure and inputs, in particular energy (Barbosa et al., 2015). First comparative studies show that this high energy requirement might be causing high environmental impacts (B. Goldstein et al., 2016; Shiina et al., 2011).

Furthermore, the term urban agriculture has been used without exact boundary definitions, e.g. a study looking at the practice in the developing world included some forms of peri-urban agriculture, meaning farms on the fringes of the city (Orsini et al., 2013). Due to the very different urban geography and food-city connections of urban agriculture in the developing world (Ellis & Sumberg, 1998), the focus of this work is mainly on activities within developed cities, for which the enquiry also benefits from better data availability.

2.2 Previous work on technical aspects of urban agriculture with organic waste and renewable energy integration

Important aspects for the quantitative assessment of the potential of combining UA with decentral organic waste valorisation are the productivity in terms of certain food items, the potential nutrient circularity pathways, novel practices that can be integrated (i.e. production of fish fed on insect larvae) and the distribution logistics for waste and produce. Aspects related to the energy intensity of high-yield practices include energy-efficient design and control as well as the integration of renewable energy generation.

2.2.1 Productivity and self-sufficiency

Productive urban food systems have the main purpose of producing food items; however, to assess and compare the potential productivity, it is crucial to look at which food crops are realistically and desirably produced within urban boundaries, which growing practices are employed and how available area is determined.

Existing studies have assumed different selections of food types, including animal products, cereals, oils and the more common fruits and vegetables. Martellozzo et al. (2014) compared an estimation for the area required to satisfy global cereal (661.6 Mha) and vegetable (47.2 Mha) demand with the global urban land area (64.3 Mha), which indicates that it is unrealistic to expect urban agriculture to provide all the calories (and protein) required for a human diet. The authors of that work furthermore shed light on the properties of micronutrient-rich foods (i.e. fruits and vegetables) as high-yield, high-value, perishable and a major indicator of dietary diversity – potentially fitting for the limited amount of land in cities and the very short supply chains. Furthermore, assessing self-sufficiency of certain food items, it is paramount to specify against which demand the supply is measured against, e.g. the actual demand or WHO recommendations for fruit and vegetables.

The choice of growing practices considered is decisive for the potential productivity as the range of employed yields for growing practices is quite large (from 1.1 kg/m^2 in non-conditioned soil-based growing (Orsini et al., 2014) to 76 kg/m^2 in conditioned hydroponics greenhouses (Benis et al., 2017b). Without high-yield CEA growing techniques such as hydroponics or high-density in-ground practices, which allow for higher plant density and/or a more controlled growing environment, it will be very challenging to contribute significantly to self-sufficiency (Richardson & Moskal, 2016). Hence previous research that has challenged that UA can contribute significantly to self-sufficiency lacked this evident consideration of high-yield practices. Another shortcoming is the lack of seasonal considerations, as the annual yield was compared to the annual demand; however, produce is likely to be harvested over the course of a few months only, requiring cold storage if the supply is equally spread over the year and consequently more space and energy requirements. Using a more nuanced approach, Colasanti & Hamm (2010) gave an indication of storage requirements and annual produce variations when different growing practices (e.g. hoop-houses) are employed to extend the growing season.

Looking at the available area, the combination of easily manipulatable geospatial data with available information on greenspace usage as well as building type, year, and function can greatly increase the accuracy of the estimation (Goldstein et al. , 2017). Ultimately, the

intended extent of a scaled-up urban agriculture system will determine which kinds of greenspace are to be included in the analysis (e.g. vacant lots only vs also including residential yards, parks and community gardens). Despite a lack of a clearly defined methodology for determining greenspace area, the technicalities of employing either geospatial data or satellite imagery to identify suitable greenspaces on the ground are very similar. When it comes to rooftops, however, different methods have led to quite different outcomes. A study using 3-dimensional satellite data by Saha & Eckelman (2017) identified

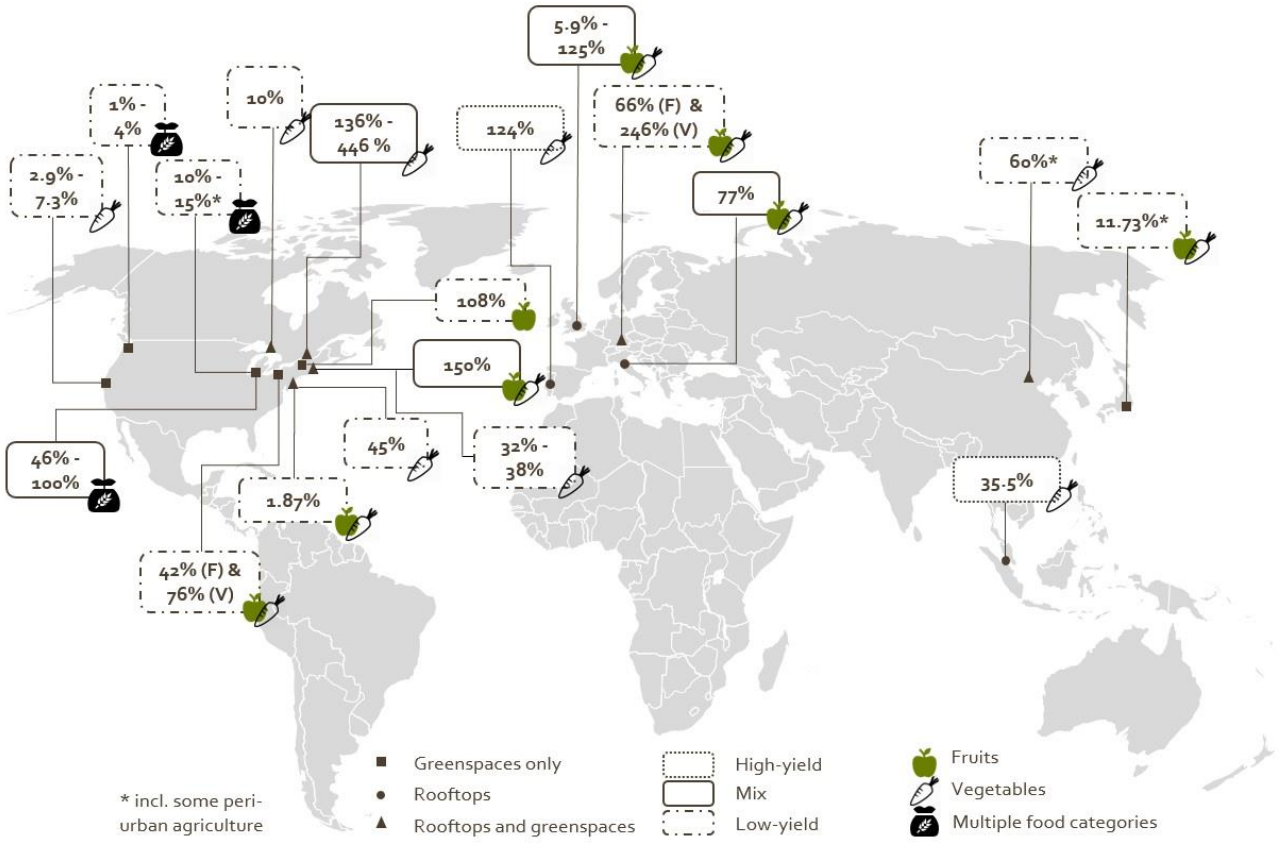


Figure 2-1: World map of self-sufficiency studies from Weidner et al. 2019

922 ha of rooftop area in Boston (equivalent to 42% of total roof area), while Goldstein et al. (2017), using tax records and geospatial data, identified for the same city 10.5 ha and 171.6 ha depending on whether the older buildings are included (equivalent to 0.46% and 7.8% of total roof area). Combining satellite data, tax records and individual building information as the most comprehensive compilation of information, Nadal et al. (2017) distilled the amount of available roof space in a Barcelona district with an economically feasible minimum size of >500 m^2 (40.4% remaining), exclusion of shaded roofs (15.2% remaining) and considering only structurally adequate roofs (2.9% remaining). Hence, previous self-sufficiency studies don't always lend themselves for direct comparison, especially if they considered only one type of potential area (e.g. greenspaces or rooftops).

Figure 2-1 gives an overview of previous self-sufficiency studies and indicates which type of available area they have used, whether high-yield or low-yield practices were employed and which food crops they considered. Some studies considered different scenarios of scaling up, hence a range of numbers is sometimes shown. The implication of those very different results is (i) that the intention of any quantitative exercise has to be aligned with the choice of growing practices (e.g. using low-yield practices for ecosystem services and disregarding productivity or high-yield for productivity) and (ii) that no definite predicament about a general potential of UA can be made. It was also found that all these studies did not consider that greenhouses and gardens have non-productive spaces (e.g. paths, tool sheds) and the shape of certain vacant lots or roofs does not allow for a full utilisation of the area for mostly rectangular greenhouses.

2.2.2 Possibilities for increased resource circularity within urban agriculture

Increasing circularity means finding new uses for waste streams or by-products instead of minimising their environmental impact by final treatment and discarding. For particular relevance within urban agriculture are organic waste streams, namely black water, green and food waste, containing plant nutrients and energy, which can be converted into soil conditioner, biogas and fertiliser (Mohareb et al., 2017).

Although some promising routes for the valorisation of waste or black water exist, nutrient extraction is currently limited and not commercially employed due to concerns about heavy metals, pathogens, and other synthetic resides (Kinney et al., 2006). Source separated food waste, on the other hand, which has not been contaminated with other types of waste (e.g. plastics) together with green waste from parks and yards, are promising candidates for nutrient and energy recovery, and collection and valorisation are already commercially applied (Mugica & Spacht, 2017). As this presents a significant untapped resource (up to 300 g/cap/day for food waste (USEPA, 2013) and 250 g/cap/day for green waste (Milbrandt, 2005)), the following paragraphs look at how source-separated and collected food, and green waste present a substantial opportunity when combined with new developments in urban agriculture practices.

Composting and decentralised anaerobic digestion

Composting, as well as vermicomposting, promises an effective and fast, one-step organic waste treatment of different types of feedstock with the potential to remediate pollutants and conserve fertilising minerals (A. Singh & Singh, 2017). Vermicompost has been used as soil

conditioner in Cuba for many years, and the humic substances generated improve plant growth performance and metabolism as well as plant defences (Hernandez et al., 2014). Compared to conventional potting soil, vermicompost as a planting base can cause an increase in yield while preventing heavy metals enrichment in plants (Grard et al., 2015). Composting, however, is only a solution for soil-based UA practices, which alone will not fulfil the productivity promises of UA as stated in the previous section.

The missing link for water-based growing practices may be small-scale AD units located close to community gardens, exhibiting similar efficiencies as large units (Walker et al., 2017). Food and garden waste is taken from the community to produce biogas (for heating) as well as digestate, which is further processed to fertiliser used in the same garden. A review of digestate use in horticulture globally found that digestate needs some form of treatment, in particular a nitrifying step, before becoming beneficial in soil-less culture (Dimambro et al., 2015). The problem may be solved in different ways. A process called multiple parallel mineralisation (Shinohara et al., 2011) employs a hydroponic system that has been inoculated with organic matter containing typical soil bacteria. When digestate is added, the ammonium and organic nitrogen is converted in vitro to mineral nitrogen available to the plants. A slightly different route was taken using a digeponic system, in which the liquid digestate is circulated through an aerated bio filter buffer tank and a vermicompost substrate with earthworms (Stoknes et al., 2016). A separated solid part of the digestate was converted via mushrooms to plant growth substrate, indicating a potential pathway to produce sustainable growing substrate locally. In their system, a bubble-insulated greenhouse is co-located with a small-scale AD unit, where the biogas is used for greenhouse heating and CO_2 supply. While both approaches seem promising, to date, no literature exists that uses their findings of such integrated systems for further quantitative assessment. Although they have achieved promising results, e.g. higher system resilience against disease as the non-organic counter-parts (Fujiwara et al. (2012), Chinta et al. (2014)) as well as higher yields than with conventional fertiliser (Shinohara et al. (2011), Stoknes et al. (2016)), more studies confirming these results are to be conducted. Compared to conventional systems that do not rely on nutrients from organic waste products, the operation and control of organic systems are less understood, with potential risks yet to be quantified. For example, one potential hazard of utilising organic waste streams in urban environments are microplastics that enter the food web, especially from commercial sources (Weithmann et al., 2018). Nevertheless, the results of the existing studies mentioned above are indicative of an opportunity to increase

yields and resilience while potentially lowering the environmental footprints of soil-less urban horticulture.

Insect rearing and aquaponics

Another completely different approach to treating organic waste, in particular poultry manure and food waste, is to feed it to insect larvae, as some species are able to thrive on this (e.g. black soldier fly), hence creating protein from waste (Xiao et al., 2018). Production can be carried out in low-tech environments and is already economically viable with post-treatment options ranging from powdering to anaerobic digestion (Joly, 2018). A critical component, negative consumer perception, might not be easily changed when it comes to direct human consumption, but when insects are fed to animals, this issue would be circumvented to some extent. The regulation landscape in the EU recently changed to allow certain types of insects to be fed to animals and be used in food products for direct humans consumption (ipiff, 2021). As certain desirable properties of animal products, such as flavour and fatty acid content, are depending on the composition, a review (van Huis, 2013) investigated studies attempting to feed organic waste to different types of insects and again feeding the insect larvae to fish. The authors found that insects purely fed on organic waste contain less omega-3 acids and constitute, therefore, at best, a small share of fish meal. Another study found that replacing 25% of fish or animal feed with insect larvae will have no negative effect (Makkar et al., 2014).

2.2.3 Distribution of urban produce and waste

Increased food production within urban boundaries also affects urban transport systems, and the distribution and retail methods can differ from conventional supply chains. In a consumer perception study, different distribution schemes were evaluated based on their sustainability, and it was found that direct on-farm sales performed the worst due to the high use of individual vehicles for small quantities of food (Schmutz et al., 2017). There is likely great potential for innovative concepts in the logistics of urban farming and organic waste. A potential solution to the problem of physically moving solid resources within the city without contributing to congestion or further GHG emission is the use of small electric vehicles. A community farm project in the United Kingdom reduced GHG emissions by transporting produce via bicycles from gardens to short-term storage and distribution centres, while small electric vans distribute the produce to the urban consumers (Kulak et al., 2013). These novel vehicle solutions could benefit from app-based technology similar to Uber, which would optimise routes and pick-up points and match supply and demand. Another aspect, especially

for household waste, is the potential of neighbourhood aggregation, e.g. in community composters, allowing collection form specific locations where residents drop off their waste (Comesaña et al., 2017). This would mitigate the potentially high environmental impacts of centralised collection of separated biowaste (Chiew et al., 2015).

2.2.4 Energy demand reduction and renewable energy integration for CEA

Greenhouse energy demand strongly depends on the greenhouse design (e.g. shape, cover material, ventilation openings), climate control capabilities and the control strategy or desired output (Bram H E Vanthoor, 2011). Determining an adequate shape may reduce energy demand by 8%, choosing a cover material according to the local climate may reduce heating energy demand up to 30%, and the possibility of ventilation can significantly reduce inside temperature (Rasheed et al., 2018). Besides design choices, using sensors and actuators to deploy advanced climate control strategies (e.g. by controlling fans, fogging sprays and ventilation openings) was found to reduce energy consumption by up to 36%, while incorporating a crop transpiration model into the controlling algorithm may provide additional savings (Zhang et al., 2020). Further methods include fluid temperature setpoints, reactive supplementary lighting and ventilation dependent CO_2 enrichment (Iddio et al., 2020). Optimising for profit instead of lowest energy consumption, it was found that a low-tech design might more profitable than mechanically conditioned greenhouses in warmer climates (such as the South of Spain) (Bram H.E. Vanthoor, Stigter, et al., 2012). The aforementioned energy efficiency measures have not yet been incorporated in any studies comparing the energy demand of greenhouses with open-field or vertical indoor farming. Possibilities exist for all CEA practices to incorporate renewable energy supply in the design (Cuce et al., 2016). For example, solar panels might be on the roof of indoor farms (Teo & Go, 2021) or as tilted panels compromising the roof of a greenhouse (Marucci & Cappuccini, 2016). In the latter case, it was found that the low conversion efficiency of panels may not compensate the reduction of solar radiation received by the plants, suggesting this application is only favourable in very sunny climates.

2.3 Previous work on environmental impacts of urban agriculture systems

Besides the technical aspect, numerous insights have been produced about the environmental performance of urban agriculture practices integrating organic waste. Of particular interest here are (climate conditioned) high-yield practices in greenhouses and vertical farms, or CEA, the effect of the co-location of growing activities and waste treatment, the replacement of synthetic inputs by organic waste products, and urban logistics.

It has to be noted that some studies comparing UA and its conventional counterpart include the structural components when they are known for both systems, while others focus on the operational footprint (e.g. inputs, climate control, distribution) only. Most of the infrastructure of the conventional or current system is already in place, hence making comparisons based on purely operational footprints avoids accounting ambiguities to some extent. A few indices or key indicator are some of the classical life-cycle assessment categories, such as weight-related water use (litre/kg produce), energy use (kWh/kg produce) and emissions (CO_2/kg produce). Others, such as the provision of ecosystem services (e.g. pollination services) or disservices (e.g. pollution, health hazards), have been subject to many studies and are excluded in this systems engineering work due to their multi-faceted and ambiguous quantification. The replacement of otherwise required external inputs is the main indices for waste utilisation, such as the replacement of fertiliser and feed as well as the benefit of energy integration through CHPs.

2.3.1 Soil-less greenhouse growing

Greenhouses can be non-conditioned, such as low-tech hoop houses, or climate-conditioned, such as metal frame glass greenhouses, with optimum day and night temperatures, moisture and CO_2 levels for maximum plant growth. When high-yielding hydroponics is employed in urban areas, the operator usually intends to maximise productivity by conditioning the environment, usually with artificial lighting as well. However, this striving for productivity comes with environmental trade-offs, and it was proven that despite the reduction in water requirements, the operational energy requirements (e.g. kWh/kg produce) are magnitudes higher (up to 82 times) than open-field production (Stanhill, (1980), Theurl et al. (2014), Barbosa et al.(2015)). Looking specifically at the influence of external climatic conditions, it was found that greenhouses in warmer climates, such as Lisbon and Singapore, have much less operational energy input than greenhouses operated in colder climates, such as Paris and New York (Benis et al., 2017a). This was mostly caused by increased heating requirements in colder climates. Compared to buildings with a sturdy and thick structure or old greenhouses with stone walls, modern greenhouses have a low heat storage capacity and hence lose heat quite quickly at night (Hall, 1989). They, therefore, benefit from an increased thermal mass when situated on building rooftops (Benis et al., 2017c) and may reduce the heating requirements for the host building due to additional insulation (Castleton et al., 2010). It seems thus sensible to locate greenhouses on rooftops, particular in colder regions. Considering another high-intensity greenhouse growing practice, aquaponics, it has been found that besides greenhouse heating, the operational input of fish feed may contribute up to

14% to the environmental carbon footprint. To date there are no studies that have investigated the potential of using feed from waste resources.

2.3.2 Vertical indoor farming

Highly conditioned indoor farming without sunlight, using optimised artificial lighting and CO_2 levels, may result in the highest obtainable yields (Touliatos et al., 2016). The industry is also booming, with multi-million-dollar investments into single projects and almost twice as much revenue per growth area as greenhouse and horizontal hydroponics operations (Agrilyst, 2017). Evaluating such promising production systems, Shiina et al. (2011) conducted a life cycle analysis to evaluate the resulting CO_2 emission from the operation of two different types of plant factories, one using only artificial light and a hybrid one with additional utilisation of sunlight. They found that the hybrid factory emitted 2.3 kg CO_2 per kg of spinach versus 6.4 kg CO_2 emitted by the total control type factory. The largest contribution in both instances was electricity used for lighting and air conditioning. To understand the effect of seasons on the associated operational emissions, conventional supply of lettuce in the UK was compared with a simulated vertical farm (Al-chalabi, 2015). Conventional produce was found to be much less energy-intensive in summer (0.33 kg CO_2/kg) than in winter (2.62 kg CO_2/kg), mainly due to the supply being satisfied from greenhouses and imports. Therefore, the associated emissions of vertical farming were only twice as high in winter (6.39 CO_2/kg) while five times as high in summer (1.78 kg CO_2/kg). Compared to greenhouses, vertical farms or plant factories were estimated to cause between 3-10 times more carbon emissions using fossil fuel-heavy electricity grids (Harbick & Albright, 2016). Another comparison considering specific electricity demand (kWh/kg) found that plant factories would require around 3.5 more energy in moderate climates but only slightly more in extreme climates (polar and arid climate zones). As artificial lighting is the main cause for the emissions, new technological developments in light emitting diode (LED) technology have been compared to conventional supplementary lighting in greenhouses, e.g. high-pressure sodium lamps (Nelson and Bugbee, 2014). While some energy savings were found, the cost per photon delivered was 2.3 times higher for LEDs, calling for the necessary development of different lighting technologies to further reduce cost and electricity consumption. Despite new advances in climate regulation, lighting technology and automation (Agrilyst, 2017), the significant gap between the current status and the desirable future means that it will probably take many years of development and need a larger share of renewable energy in the grid in order for vertical farming to become a serious contender for reducing environmental impacts of a city's food system. A first study simulating a vertical farm with rooftop photovoltaic panels and storage

achieved up to 11.6% electricity autonomy (Teo & Go, 2021), indicating that the rooftop area of such farms would not suffice to counterbalance the negative impacts.

2.3.3 Co-location of waste conversion technologies with greenhouses

Besides integrating greenhouses on rooftops with their host building, isolated greenhouses can also profit from energy integration by coupling them with certain waste conversion technologies. A commercial waste management company (SUEZ, 2017) combined a waste incineration plant with a tomato greenhouse in France, using the generated heat energy to control the growing environment, achieving operational emissions reduction of around 1 kg CO_2 per kg of tomato. Similar environmental benefits have been obtained by co-locating tomato greenhouse production with a micro-CHP gasification plant fuelled by forest residues in Norway (Nordenström et al., 2010). In their previously mentioned digeponic system, Stoknes et al. (2016) claim an operational energy demand reduction of 80% by integrating a small-scale AD and combined heat and power plant (CHP) unit with a bubble-insulated greenhouse, making use of the generated CO_2, electricity and waste heat. These studies display promising potential for integrated waste and food systems on a small scale, especially applicable in isolated, ground-based greenhouses.

2.3.4 Carbon footprint reduction through substitution of fertiliser and growth substrate

Beyond the energy-efficiency measures through either building integration or housing waste conversion technologies in or close to greenhouses, additional possibilities to further improve the environmental performance of CEA should be considered. A life cycle assessment (LCA) of an integrated rooftop greenhouse (iRTG) found that fertiliser and substrate combined made up around 40% of the emissions for summer production and around 25% of the emissions for winter production (Sanjuan-Delmás et al., 2018). This indicates that the option to recycle urban organic waste to produce fertiliser and growth substrate have the potential to bring benefits regarding the overall sustainability of urban growing practices. A theoretical assessment of waste-derived alternatives (compost and spent brewers grain) for the growing medium found GHG emission reductions of more than 60% considering all inputs except lighting (Martin et al., 2019).

Employing different types of compost instead of potting soil on rooftop growing beds in Paris and conducting an LCA, Dorr et al. (2017) found emission to be reduced by 17-47% depending on the type of crop and compost. However, a few downsides to conducting soil-based agriculture in cities exist, such as nutrient-run off. A study looking at nitrate leaching of

both intensive conventional (e.g. using mineral fertiliser) and intensive organic garden projects found that nitrogen is lost in both cases through volatilisation or leaches into the ground water (Cameira et al.,2014). Unlike high-intensity and contained systems, the aim for soil-based open-air urban agriculture should thus ideally not be to maximise productivity but to focus on providing ecosystem services and reducing negative impacts.

2.3.5 Effects of distribution and changing urban logistics

The decentral waste treatment and production of food within urban boundaries inevitably require different logistical arrangements and distribution concepts and might come with negative consequences on urban traffic and the carbon footprint of transport.

With respect to urban agriculture, it seems that some distribution models are much less efficient, up to a point where all potential environmental benefits of urban agriculture are negated. An urban farm in the United States delivers produce in small batches with a pick-up truck directly to the consumer, causing significant emissions (Goldstein et al., 2016a). Another consideration is upstream transportation requirements, e.g. for fertiliser and compost. Weber and Matthews (2008) showed that the general transport-related emissions were around 7% of the total footprint of food in the United States, which included animal feed, natural gas transport to farms and other components which might not apply to UA. At the same time, however, providing construction material or farming inputs in congested urban environments would very likely come with a greater environmental impact than on empty rural roads. Similar studies on the implications of upstream transport on the environment and traffic are yet to be carried out for UA.

2.4 Modelling techniques and optimisation of the urban resource nexus

Combining urban agriculture with organic waste valorisation and renewable energy on a large-scale requires sensible design and allocation of available space and resource to achieve the desired outcome. This could be minimum resource use and wastage, the lowest emissions possible or the highest socio-ecological benefits. To allow the weighing of options, a clear picture of resource and energy flows as well as incurred environmental impacts of any such flows is required.

2.4.1 Life cycle assessments and flow analysis

The LCA methodology provided by the ISO standards 14040,14041 and 14044 is aimed to ensure transparency and comparability between LCA studies. It consists of four steps (see Figure 2-2), starting with the definition of the goal and the scope, collecting inventory data,

applying an adequate assessment method to derive the environmental impacts relevant for the study and finally visualise and interpret the results.

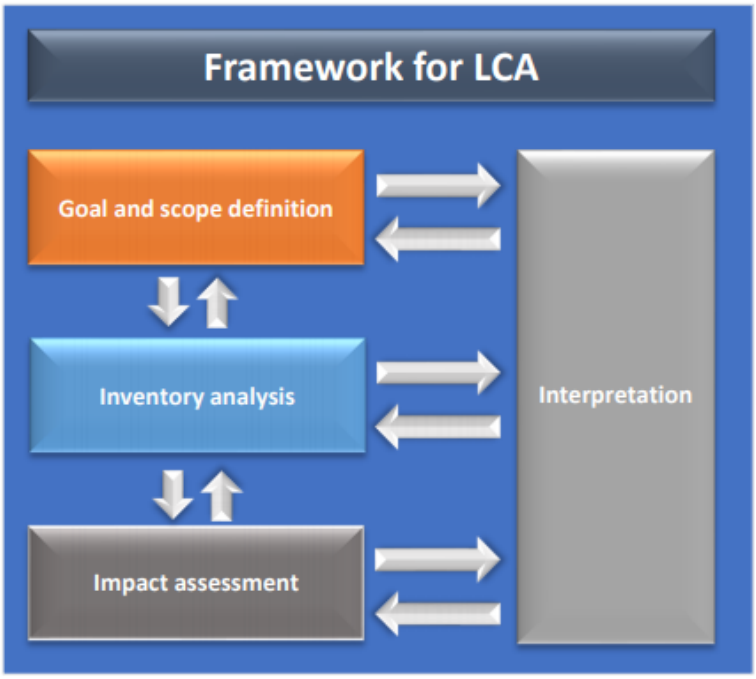


Figure 2-2: LCA Framework

However, the methodologies for urban agriculture and waste valorisation systems under inspections are not defined, and the results depend heavily on boundary conditions, assumptions and simplifications. For example, Bernstad and La Cour Jansen (2012) compared 25 LCA studies on different food waste management systems and found that results depended more strongly on the methodology rather than the chosen system. Nevertheless, the methodology can be chosen to sensibly estimate impacts for sub-parts of urban agriculture systems, such as demonstrated for insect rearing as fish fodder (Salomone et al., 2017), digestate product use and waste separation schemes (Chiew et al., 2015) as well as the studies for rooftops and hydroponic growing mentioned in previous sections. Due to limitations regarding data availability and access, meaningful results can also be obtained by focusing on one aspect of LCA, such as global warming potential (GWP) in the form of emissions (Walker et al., 2017).

Material flows are usually constructed using different sources, e.g. urban nutrient flows can be estimated via household and industry generation data (Wielemaker et al., 2018) and waste generation, composition and conversion via multi-year case studies (Hertel et al., 2015). Energy flows are either aggregated for individual projects or more locally determined for heating networks and regimes (Mago et al., 2009). No studies exist to date that combine all these components for a comprehensive assessment of the nexus between food, energy, water, land and waste.

2.4.2 Modelling of CEA energy demand and renewable energy supply

The energy consumption of CEA is one of the prime sources of environmental impacts (Benis et al., 2017b) and most of it is used for lighting and indoor climate control (Barbosa et al.,

2015; Shiina, Hosokawa, Roy, Nakamura, et al., 2011). Both these uses depend on the local climate conditions (Graamans et al., 2018) and the type of facility and level of technical sophistication (B. Goldstein, Hauschild, Fernandez, et al., 2016). Thus, context-specific and detailed studies of energy requirements have been conducted, assessing trade-offs between productivity, energy consumption and economics (Vanthoor et al., 2012) and applying different modelling techniques (Iddio et al., 2020). All methods include mass and energy balances that adhere to thermodynamic principles and consider transpiration of water vapour by the plants (evapotranspiration) (Graamans et al., 2017; Nikolaos Katsoulas & Stanghellini, 2019; F. Villarreal-Guerrero et al., 2012). The behaviour of air within the facility is modelled by simple assumptions (Shengbo Zhang & Schulman, 2017) to sophisticated dynamic models (Teitel et al., 2008), and some methods include optimisation of control parameters (Choab et al., 2019). For the greenhouse environment, studies have investigated optimal interactions between venting and heating (Van Beveren et al., 2015), fogging and ventilation (Federico Villarreal-Guerrero et al., 2012), design choices and profit (Vanthoor et al., 2012), and different temperature and lighting setpoints and their effect on yield and energy (Golzar et al., 2018). Indoor vertical farms, relying solely on artificial light, were also studied, and their energy use compared with those of greenhouses (Benis et al., 2017c; Graamans et al., 2018; L. Li et al., 2020), which revealed a possibly much greater energy requirement per kilogram of produce in less extreme climates. The studies mentioned above shine a light on many diverse aspects of CEA and already informed practitioners on how to run facilities more energy efficient. However, their shortcomings include that they do not simultaneously optimise yield and energy, have a low detail of simulation the air conditioning equipment and spatial profiles of air flows, and do not employ context-specific best-practices in comparisons between growing practices and locations.

The energy demand of CEA facilities can be supplied by renewable energy sources. From a modelling perspective, two aspects are relevant. First, how a fluctuating demand can be matched with a fluctuating supply, and second, how to best combine energy storage with sufficient generation capacity of different renewable sources. On the latter, many studies have used techno-economic analysis to determine the most economical mix of storage, oversizing and relying on dispatchable or grid energy for larger-scale systems (Deng et al., 2015; Johlas et al., 2020; Perez et al., 2019a). The studies found that energy storage is very costly and can mainly be used to account for intraday fluctuations and supply and demand mismatches. For intraseasonal fluctuations, complimentary sources of renewable electricity need to be combined, each performing best in a specific season (e.g. solar PV in summer, wind energy in

winter and hydro in spring). For smaller-scale systems, grid simulation with the HOMER software (*HOMER*, n.d.) has been applied to industrial sites (Vallati et al., 2015), autonomous irrigation systems (Ssenyimba et al., 2020), water desalination in a low-tech greenhouse (Khattab et al., 2016) and finally a vertical farm with solar PV panels (Teo & Go, 2021). The current literature lacks detailed assessments of how a load and supply mismatch for greenhouses and vertical farms influences the grid design. This necessitates location-dependent investigations of renewable energy profiles and economic trade-offs between energy storage and installed capacity.

2.4.3 Geospatial modelling for logistics and land availability assessments

Besides assessing urban land availability for assessing urban productivity within city limits as described in 2.2.1, spatial analysis and geoprocessing have also been used to assess different types of land cover and road networks to inform land availability and assessments and logistical considerations. The main application of logistics in the urban environment is for waste management, with problems surrounding location-allocation, routing and inventory-location-routing. The first includes optimum locations for centralised treatment sites (Silva et al., 2014; Sumathi et al., 2008), the placement of collection bins (Deswal & Laura, 2018), and semi-central transfer stations (Bosompem et al., 2016). Routing problems describe operational considerations, assuming the locations are fixed, and ideal transport routes have to be found (Noche et al., 2010). These types of problems can be solved mathematically, but for many years geographic information system (GIS) software has been used to tackle these tasks (Purkayastha et al., 2015). A special category is problems involving inventories as supply and demand of a good play a crucial role (Rafie-Majd et al., 2018). In relation to urban agriculture and (decentral) utilisation of biowaste, research is lacking which applies GIS methods to investigate the implications or comparative performance of switching from centralised to decentralised waste management systems and how to design those decentralised systems. Further, waste is not just treated in productive urban systems but also applied on land or used in facilities scattered around the city. No studies to data have assessed what these additional downstream (or upstream from the perspective of urban farming) logistical requirements entail and cause.

Some products from decentral treatment, such as compost or digestate, may be applied to agricultural fields (WRAP, 2016). The size and location of them can also be assessed with GIS data and software. It has, among other uses, been applied to map regional foodsheds, e.g. assessing what crops should be supplied locally to a city (Peters et al., 2012), comparing

regional self-sufficiency of city-regions (Zasada et al., 2017) and understanding the feasibility to feed the global population locally (Kinnunen et al., 2020). Besides agricultural land use and availability, GIS has also been used to assess the regional potential to deploy land-intensive renewable energy facilities, such as solar and wind farms (Wang et al., 2014; Yue & Wang, 2006). On top of the availability of a specific non-built up land-use type, the economic desirability (Koc et al., 2019) of specific locations and the interactions with the natural world have been modelled (McDonald et al., 2009). These studies lay a methodological foundation to apply GIS-based analysis to questions around the possibility and favourability of expanding CEA over other types of regional food provisioning (e.g. peri-urban open-field agriculture) through a food-energy-land nexus lens.

2.4.4 System design: Optimisation of resource allocation

Optimisation has been applied to questions pertaining to urban agriculture. For example, the choice of which vegetables are grown and how much space is used can influence the overall impact of the system. Goldstein et al. (2017) associated different global warming and land use (LU) impacts to a range of different crops, both grown on the ground and on the rooftop, and optimised the crop allocation for each block within Boston. The algorithm chosen selected for each block the appropriate crop to either reduce GWP or land use impacts. If one block could satisfy its nutritional requirements, crops were produced for other blocks, and intra-city economics were determined. Although the results show quite a different choice of crops for the two objective functions, the final choice of vegetables was strongly restricted to low-impact crops such as kale and eggplant. It is rather unrealistic and perhaps undesirable to reduce UA activity to such crops. A similar approach was taken by Ward and Symons (2017), who determined the optimum produce for different backyard garden sizes when taking into account irrigation water cost, minimum protein sufficiency and economic value. Although high-value plants like strawberries were mostly chosen by the algorithm, the diversity of crops increased for larger gardens as individuals would only require a certain amount of each crop, leading to reduced food basket savings per m^2 for larger gardens. It is likely that individuals would use cost savings as one incentive but other factors, such as experience and individual preference, are at play as well.

A more helpful approach could be considering multiple aspects and objectives and performing optimisation algorithms that satisfy a range of impacts as well as food and nutrient self-sufficiency. The inclusion of life cycle analysis and costing can help find optimum solutions that are desirable, economic and sustainable (Yue et al., 2016).

Another application of optimisation pertains to how resources such as land or money are allocated to certain technologies producing goods, energy or water satisfying a certain demand within a region. For example, a study for Qatar optimised the interplay between energy production (for fertiliser and water treatment), water extraction (for irrigation and cooling) and food production to meet 100% of the local food demand at the most favourable trade-off between cost and emissions (Namany et al., 2019). Different land allocation options have been optimised with mixed integer nonlinear programming to find the ideal mix and rotation of crops and livestock, including their waste treatment and recycling on land, which would reduce overall environmental burdens while satisfying economic and food demand constraints (Nie et al., 2018). A study by Leung Pah Hang et al., (2016) employed scenario analysis and superstructure optimisation to determine the ideal interplay between for food, energy and water provision on constrained land to supply a town with food calories, water, heat and electricity.

The process systems engineering tools of scenario analysis and optimisation have not yet been applied in the context of utilising organic waste in urban agriculture (food-energy-waste nexus) or for CEA embedded in the food-energy-land nexus through renewable energy.

2.5 Summary of research gaps

Reviewing the existing literature, it is evident that the field of urban agriculture systems which benefit from biowaste integration and renewable energy is still under-researched, particularly lacking quantitative considerations. To realise the potential and advance the field, more research is needed which addresses the following gaps.

1. The strong discrepancy between the methodologies of self-sufficiency studies calls for developing a consistent approach comparing multiple cities to derive insights. It remains unclear in this context how the selection of urban growing practices (e.g. open-field versus CEA) and the locational context (e.g. climate and space availability) influence seasonal productivity and environmental impacts of urban agriculture systems.

2. Promising findings from pilot studies integrating organic waste utilisation and food production have only been considered in isolation. Studies investing implications of scaling up such solutions are missing, including material flows at the city level, demand and supply matching and potential resource savings.

3. The environmental impacts of producing and using input for UA derived from waste, such as fish feed from insects or algae or fertiliser from digestate, have not been thoroughly studied.

4. Exploring novel technical possibilities for co-locating waste treatment with food production, such as distributing heat locally or storing it seasonally, as well as economic and environmental considerations of the materials and infrastructure requirements of such integrated systems on smaller scales.

5. Environmental implications of local supply chains for urban agriculture products (downstream), including novel forms of urban transport (e.g. cargo e-bikes), circular packaging and reduced storage and food loss, made possible through the producer-consumer proximity of urban farms.

6. Environmental implications of local supply chains for inputs to urban agriculture (upstream), e.g. transporting compost and fertiliser from treatment sites to farms.

7. How to design decentralised waste management systems for households so that they are practical, economical and desirable is yet unclear. This includes what level of neighbourhood or community waste aggregation is required and what intermediate logistics points might be necessary.

8. Assessing the comparative performance (e.g. life cycle costs and environmental impacts) of decentralised organic waste treatment systems versus conventional centralised systems, including aspects of collection, transportation, treatment and land application. Of specific interest here are how factors such as urban layout and population density influence the performance.

9. The application of mathematical optimisation to CEA growing systems for increased energy efficiency, with detailed considerations of the exterior climate, the interior space and climate control facilities.

10. It remains unclear how best-practice greenhouses and vertical farms compare against each other from an energy-intensity perspective and what influence the local climate, design choices and operational strategies have.

11. The potential of greenhouses with tilted solar panels from an economic and environmental perspective under different climatic influences.

12. Simulations of renewable energy grids using solar PV, wind and energy storage for CEA systems have not yet been carried out. Insights are needed on how supply and demand mismatches can best be met economically by employing energy storage, dispatchable energy and oversizing the renewable energy supply.

13. Assessments of the land use of CEA systems when considering the indirect land use of renewable energy generation.

14. Comparisons of different urban agriculture systems with renewable energy (including open-field and CEA) to supply local food to larger cities and their rural hinterland, including the trade-offs within the food-energy-land nexus.

The gaps, particularly points 1 to 3 (Chapter 3), 6 to 8 (Chapter 4), 9 and 10 (Chapter 5) and 12 to 14 (Chapter 6), have motivated this DPhil project which aims to address them by answering the research questions presented in Chapter 1.

Chapter 3 The potential of urban agriculture in combination with organic waste valorisation: Assessment of resource flows and emissions for two European cities

Overview

This chapter presents the following published article: *Weidner, T., & Yang, A. (2020). The potential of urban agriculture in combination with organic waste valorisation: Assessment of resource flows and emissions for two European cities. JCP, 244, 118490.*

Among all authors who contributed to the published article, T.W. conceptualised the study, performed the modelling and wrote the manuscript. A.Y. supported the conceptualisation and the modelling steps and revised the manuscript.

This first original work has been carried out to lay a foundation for understanding different crucial aspects of scaled-up UA systems. Among those aspects are the ones related to urban agriculture itself as such, including the maximum but realistic (local) self-sufficiency that can be achieved, the carbon footprint of employing different growing practices, and a comparison with the current food supply system. Further, a design of an urban resource nexus is proposed, incorporating organic waste treatment technologies and rerouting a share of the generated waste (household biowaste and green waste) to UA. This work's novelty, among others, is thus the quantification of urban organic waste utilisation within such scaled-up UA systems. Optimisation was carried out to determine alternative resource flow arrangements that provide the highest GHG emissions reductions. Two European cities were chosen to investigate the influence of climate and city characteristics on all the mentioned aspects.

The results from this study show that a substantial amount of energy is needed for supplying fresh produce in winter through greenhouses, and that this energy demand can have an unsustainable carbon footprint if electricity is not supplied from low-carbon sources. It also shows that utilising organic waste reduces the carbon footprint of such systems but assimilation potential when considering only urban agriculture is limited. The energy aspect was most decisive, leading to further inquiry of energy intensity (Chapter 5) and regional energy supply (Chapter 6). The waste integration was done considering the city as one unit, excluding logistical and spatially sensitive aspects. These additional considerations are addressed in Chapter 4, which approaches biowaste utilisation in UA systems from the perspective of the waste management system.

3.1 Introduction

Pressures on the current food supply chain in connection with climate change, increasing population and socio-environmental concerns call for alternative modes of food production and consumption. As a potential solution with multiple socio-economic implications, food production within urban environments has attracted considerable interests (Koegler et al., 2017). The productivity of large-scale urban agriculture (UA) for a city is determined by its potentially available area, which in recent years has been studied via geographic information systems (GIS) in 2D and 3D for a range of cities in the global North (Haberman et al., 2014; Saha & Eckelman, 2017; Sioen et al., 2018). Additionally, the yield per unit area is a decisive factor and differs depending on the growing practices, which range from open-air community gardening over soil-based rooftop gardens to high-tech hydroponic and aquaponic greenhouses (Goldstein et al., 2016; Love et al., 2015). The environmental sustainability of these practices differs (Goldstein et al., 2016) and geographical location and the associated climatic factors play a decisive role (Benis et al., 2017). Building integration (Sanjuan-Delmás et al., 2018) and new distribution models (Kulak et al., 2013) provide a first step towards increased sustainability, but there is a strong need to further lower the footprint of this alternative food supply.

The main inputs for urban agriculture are plant nutrients (fertiliser), water and energy in the form of heating and electricity, allowing for year-round production. It has been suggested that some urban waste streams can be synergistically used within UA (Mohareb et al., 2017) and urban nutrient flows currently considered as waste could satisfy fertilising needs of urban farming endeavours (Wielemaker et al., 2018). Thus, to preserve resources and improve nutrient circularity, urban agriculture can be combined with bespoke organic waste management, making use of source separation and conversion technologies. Novel urban food and waste systems could be created that exchange nutrients, energy and other resources, while making use of a decentralised structure.

The urban utilisation of products derived from organic waste is promising, such as nutrient-rich digestate in organic hydroponics (Shinohara et al. 2011, Kawamura-Aoyama et al. 2014, Rayns 2015), compost and digestate fibre in soil-based growing (Baltzell 2011, Grard et al. 2015, López-Mosquera et al. 2011) and insect protein production from organic wastes (Joly 2018, Salomone et al. 2017). The technologies for organic waste conversion, such as anaerobic digestion (AD), are well understood in isolation (Banks et al. 2011, Chiew et al. 2015) and are more recently integrated within a productive greenhouse (Zhang et al., 2013,

Walker et al. 2017, Stoknes et al. 2016), allowing local heat utilisation and production of fertiliser.

Despite the promising findings, there is currently a lack of detailed studies assessing the potential material and energy flows and associated environmental impacts at the city level of such novel urban food systems, which combine different growing practices with waste conversion, nutrient cycling and energy integration (e.g. provision of heat and upgrading of biogas). It also remains unclear how the choice between low-intensity gardening and high-intensity greenhouse growing affects the environmental performance of such systems (Weidner et al., 2019). Urban planning, investment decisions and resource allocation by decision-makers and stakeholders could be enhanced by an understanding of what a city can expect if such systems are scaled up.

This work takes a quantitative modelling approach, synthesising isolated literature information to investigate theoretical resource flows of a novel type of integrated UA & decentralised waste management system. To assess how decentralised waste valorisation can be symbiotically designed to cover resource needs of UA, this work undertakes the necessary step of determining the monthly production of food and by-products and the resulting resource requirements. Refined seasonal and crop granularity is employed to provide a more realistic description of the system. As the productivity depends strongly on the intensity of the growing practices, a variable ratio of growing intensities is investigated. Using the cities of Lyon, France, and Glasgow, UK, as case studies, the purpose of this work therefore is:

- To compare the influence of space and population characteristics of typical European cities and the intensity of the growing practices on the potential monthly self-sufficiency obtained for a selection of typical UA crops and fish;
- To assess the water, nutrient, electricity and heating requirements for the UA activities and how they are influenced by a different climate;
- To understand how the organic waste flows can best be utilised to support the UA activities from a nutrient and energy perspective; and
- To compare the operational greenhouse gas (GHG) emissions of the current food system with the proposed integrated UA and waste management system on a monthly basis.

3.2 Methods

3.2.1 Overview

This study evaluates the productivity (i.e. self-sufficiency), resource requirements and carbon footprint of an integrated UA & decentralised waste management system via mathematical modelling and optimisation of monthly material and energy balances. The overall methodology is illustrated in Figure 3-1. For the benefit of comparing different urban space and population characteristics, the dense urban City of Lyon (i.e. the 9 arrondissements) and the more spread out Glasgow City Council area were chosen (climate and population characteristics are listed in Table 3-2 in the result section). Glasgow has ongoing urban

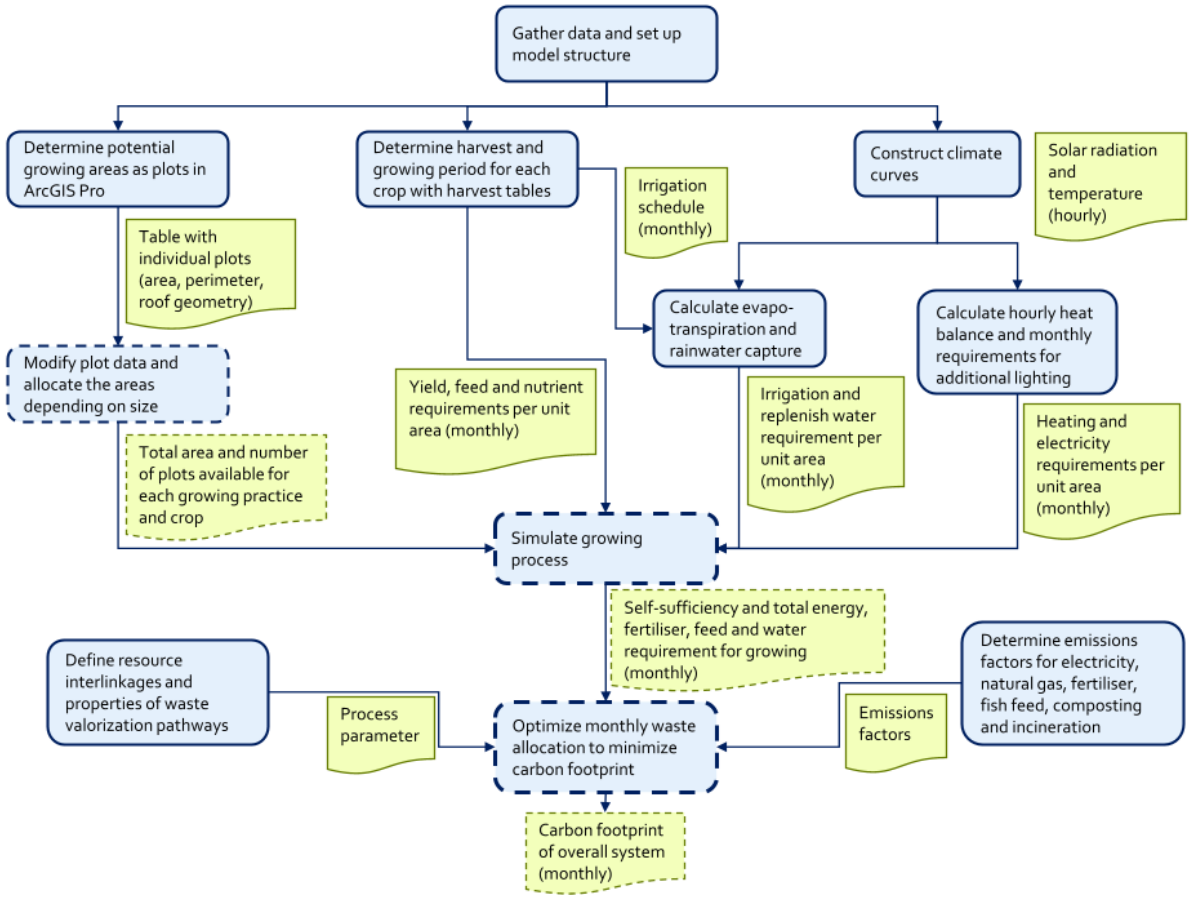


Figure 3-1: Overall methodology, the steps in dotted lines were repeated for different levels of growing intensity

agriculture projects (White & Bunn, 2017) and Lyon is a pilot city for novel decentralised organic waste valorisation in UA (www.decisive2020.eu/lyon). To allow for a reliable assessment of the potentials of waste integration, a robust approach on the productivity and resource requirements of UA was followed. Two main tasks were therefore performed, the simulation of the growing process and its related resource requirements, and the optimization of the waste management aimed at minimizing the carbon footprint. The first task includes

determining the available area (described in Appendix I, 1.1), assessing season-dependent food production and fertigation needs, and climate-dependent energy and water requirements. Of those, the determination of available growing area includes the allocation of areas to specific growing practices with differing resource intensities (illustrated in Figure 2). This allocation was represented by ratios between the practices (see Table 3-1). The second task includes defining the possible waste management pathways (referred to as the resource nexus), quantifying the carbon footprint of all inputs and operations within the system considered and optimizing the allocation of waste streams between possible destinations.

Table 3-1: Area use and ratios applied in spatial analysis

Growing practice	**Maximum area use or ratio**	**Details**
Public greenspaces	50%	Maximum realistic or desired amount of conversion
Private yard spaces	25%	Maximum realistic or desired amount of conversion
Flat rooftops	20%	Adjusted considering structural integrity and access with minimal retrofit (Nadal et al., 2017)
Open-air vs hoop-houses	50/50	Equal share, hoop-houses extend growing season but open-air gardens could offer more urban ecosystem services
Professional vs community gardens	50/50	Equal share, focus either on productivity (higher yield, automated drip irrigation) or social benefits
Greenhouses versus gardens, on large ground plots (>750m^2)	Variable, detailed study on 20/80	Affected by preferred level of resource intensity (with greenhouses being more intensive), and public acceptance (e.g. aesthetic reasons)
Aquaponic vs digeponic greenhouses, on ground	50/50	Both equally desired (Alshrouf, 2017; Bowman, 2017; Pantanella et al., 2012)

Gardens vs greenhouses, on large rooftops	25/75	Assumption that on 25% of applicable flat roofs greenhouses are not allowed (e.g. fire safety) or desired, else greenhouses are preferred on rooftops
Aquaponic vs hydroponic greenhouses, on rooftops	25/75	Assumption that only 25% of applicable flat roofs have required structural integrity

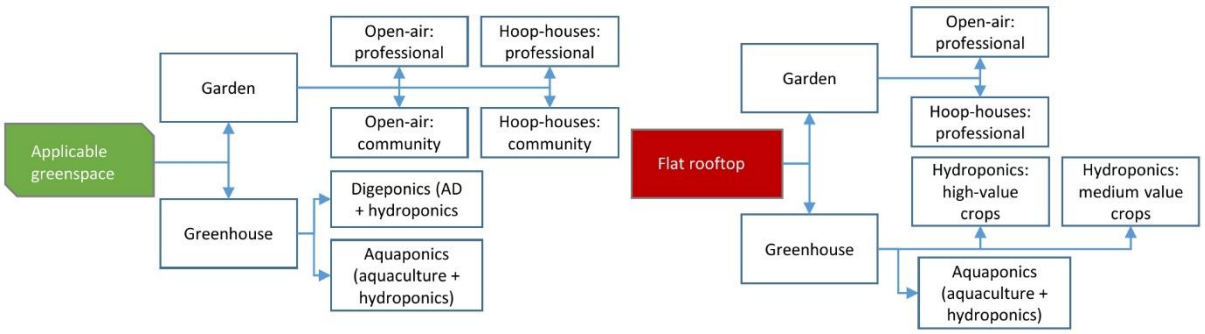


Figure 3-2: Different growing practices employed on greenspaces and rooftops

The resource nexus that encompasses the considered material and energy connections between waste processing, resources extraction and growing is shown in Figure 3-3. The organic waste (brown) generated from different sources (dark grey) is converted via the

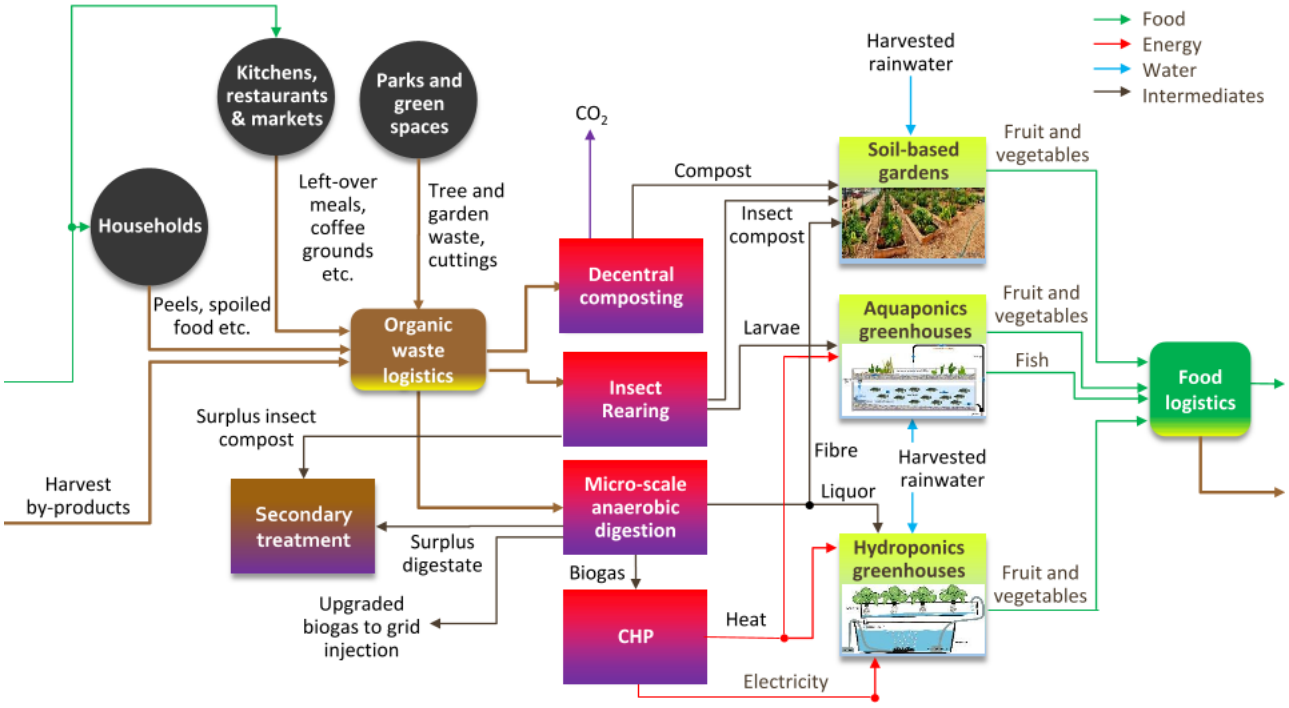


Figure 3-3: Resource nexus of integrated UA and waste management system

decentralised treatment pathways (red) to inputs for the UA practices (light green), which in turn produce food (dark green). Surplus products from waste treatment have to undergo secondary treatment (brown-lilac) before final disposal. The term digeponic is used to describe hydroponics fertililsed by digestate by-products (Stoknes et al., 2016), but in this study, the term hydroponics will be used irrespective of the origin of fertiliser. Details on waste generation and processing are given in section 3.2.4. Details on system boundaries, i.e. which flows were considered to calculate resource requirements and carbon footprints, are described in sections 3.2.3 to 3.2.5 and visualised in AppxI-Figure 5.

3.2.2 Food demand and production

The assessment of resource flows and emissions intended by this study needed to build on the selection of appropriate crops for UA, their demand profile and yield figures, the growing and harvest periods, as well as fertilization requirements. Crops were selected based on their applicability for UA in the Northern hemisphere as discussed in other studies (Clinton et al., 2018; Colasanti & Hamm, 2010), including specifically six fruits and 14 vegetables, which constitute a significant share by weight of the fruit and vegetables consumed in the EU. To allow a comparison of self-sufficiency between the two cities, the recommended amount of 500 g/day/person of fruit and vegetable (Haberman et al., 2014) was split by 1:2 between fruit and vegetable (Health Canada, n.d.) and excluded exotic fruits (e.g. banana and pineapple, considered to be 50% of fruit demand), resulting in 433 g/day/person. This amount was then distributed over the 20 crops according to actual consumption patterns in the EU. Yield figures for soil-based growing were determined by adjusting FAOSTAT yield data from 2016 (www.fao.org/faostat) by a factor of 0.75 for community gardens and of 1.25 for professional gardening, which served as a feasible average of other studies with similar classification (Grewal & Grewal, 2012; Haberman et al., 2014; Sioen, et al., 2017), and 5% loss through refuse was assumed (which is referred to as “plant biomass” in this study). Hydro- and aquaponic yields for eight applicable crops were employed from case studies mentioned in Haberman et al. (2014).

As one of the aims of this work is to quantify the potential monthly productivity of UAs, the annual yields for open-air gardens and hoop-houses were split up on a monthly basis according to a harvest table, which included potential growing season extension in hoop-houses for 9 crops and potential storage of 5 crops (Colasanti & Hamm, 2010). Together with crop growing cycles (KZNDARD, n.d.; Orsini et al., 2014), the harvest tables were used to determine the additional productivity of crops that benefit from increased yield through

season extension in hoop-houses. It was assumed that the nine crops which benefited from the growing season extension would be grown in equal ratios in hoop-houses while the remaining 11 crops would be grown in equal ratios in open-air gardens. The allocation of crops within year-round high-tech greenhouse growing was determined such that the increase in self-sufficiency due to greenhouse growing is equal between different crops. Further information on demand profiles, yield values, food imports, spatial and crop distribution for growing practices and harvest tables can be found in the SI of Weidner & Yang (2020).

Aquaponic greenhouses produced not only the eight hydroponic crops but also fish, including carp, catfish and tilapia. The available area was divided by the ratio in consumption of those fish (Fisch-Informationszentrum, 2016).

3.2.3 Operational requirements for growing

Energy was used by the system primarily as electricity (for artificial lighting, irrigation pumps and other equipment) and as heat for greenhouse climate control, insect rearing and AD operations (see section 3.2.4). Assessing the monthly heating and additional lighting requirements of greenhouses required solar radiation and ambient temperature profiles, which were created from 30-year average data. Solar noon, average daily solar radiation, sunrise and sunset information, as well as minimum and maximum daily temperature values were used to construct the curves. It was assumed that solar radiation follows a positive sin curve profile and temperature was assumed to increase linearly from its minimum at sunrise with its maximum sometime after solar noon. The electricity requirements for artificial lighting were then calculated according to the difference between plant-specific photosynthetically active radiation (PAR) needs as daily light integral (DLI) (Shao etl al., 2016) and the naturally provided PAR, incorporating molar efficacy of the lighting system and shading and transmittance factors (see AppxI 1.2). Heating requirements in greenhouses were calculated on an hourly basis employing the constructed climate curves, fixed day- and night-minimum temperatures and relations for five predominant fluxes while omitting any thermal inertia from the structure. Furthermore, reduced heating requirements for the host buildings in the case of rooftop greenhouses were considered similar to Goldstein et al. (2017), hence the typical user heating requirements for France and the UK were assumed to be reduced by 3%. Parameters related to the heating and lighting demand are shown in AppxI-Figure 2.

Irrigation and replenishment water requirements were calculated for both, open-air (Lupia et al. (2017)), hydroponic (Nadal et al. (2017b)) and aquaponic growing (Forchino et al., 2017).

Rainwater harvested in the integrated scenario on hoop-houses and greenhouses, used for irrigation and to supply AD feed water, was investigated considering three different scenarios:

a) No rainwater storage

b) Short-term local storage, i.e. use within a month in the same facility only

c) Shared reservoir, i.e. distribution network with intra-monthly storage capacities

To assess nutrient supply, nitrogen, phosphorus and potassium (NPK) were considered individually as essential plant nutrients. It was assumed that aquaponics farms can satisfy their nutrient needs internally while hydroponically grown plants rely on added nutrients recirculating in solutions, determined by their nutrient uptake of the (edible) crops (Fink et al., 1999; Health Canada, 2005) and the nutrient uptake of non-edible plant material (considered to be 25% of the crop weight, e.g. leaves and stems), also accounting for some recovery loss (Bugbee, 2004). The fertigation of soil-based growing was according to FAOSTAT fertiliser rates for France and the United Kingdom.

3.2.4 Waste generation and processing

It was assumed that both households and commercial sources generate 0.2 kg/day/capita of source-separated food waste each (Mugica & Spacht, 2017; Wielemaker et al., 2018) while yard waste generation depended on the season (David, 2013) and non-built up area (1 kg/m^2/year) (Adwiraah et al., 2012). It is important to note that the generated food waste stems from the supply and consumption of all food products, not just UA produce. Relevant composition parameters, including NPK content, were employed for food waste (Banks et al., 2011), green waste (Hertel et al., 2015) and insect compost (Salomone et al., 2017). It was assumed that refuse generated as a harvest by-product has the same composition as yard waste and they together constitute the generated green waste (GW).

As the most traditional conversion technology, aerobic decomposition via small decentralised composting units (www.ridan.co.uk) was considered in this study to convert organic waste into soil conditioner that provides nutrient for open-air growing. Co-located near greenhouses, insect rearing of black soldier fly (BSF) fed on food wastes was employed to supply protein for the fish raised in aquaponic greenhouses. It was assumed that the dry mass of live BSF larvae can replace 25% of conventional fish meal without fish growth reduction (Salomone et al. 2017). Mesophilic wet anaerobic digestion via small- and micro-scale digesters co-located with greenhouses was employed to convert various organic wastes into digestate and biogas (Banks et al., 2011; Møller et al., 2009), which is either upgraded and fed to the grid or

burned in a combined heat and power Stirling unit (CHP) if there is sufficient heat demand in greenhouses. The digestate was locally separated into liquid (liquor) and solid (fibre) using a small-scale centrifuge and the liquor made available as fertiliser for hydroponic growing, also called digeponic (Stoknes et al., 2016), and the fibre as fertiliser for soil-based growing. Any surplus digestate products had to be treated semi-centrally for final disposal and the final concentrate was sent to incineration together with surplus insect compost. For all three main conversion technologies, a processing time of 1 month was assumed, hence changes in feed composition and quantity had an effect on the products only in the following month. Further, it was assumed that waste products are converted in close proximity to UA operations and thus, transport impact was omitted. All process parameters are listed in AppxI-Figure 3.

3.2.5 Description of scenarios and operational emissions

To compare the benefit of integrating decentralised waste valorisation, three different scenarios were carried out:

- The integrated scenario (referred to as “integrated”), in which scaled-up urban growing operations may be supplied by feed and fertiliser from converted waste products and benefit from co-locating CHPs for heat integration and electricity generation. The material and energy flows were determined via optimization as described in Section 3.2.6.
- A scaled-up UA scenario but without integration or decentralised waste valorisation (referred to as “UA+Ext”). All inputs to UA were externally supplied (fish feed, chemical fertiliser, natural gas, grid electricity) and all waste streams externally (i.e. outside the city boundaries and the UA system) treated (incineration with energy recovery and windrow composting)
- The current system (referred to as “current”), in which food is supplied from outside of city boundaries (as described below) and waste treated externally as in the “UA+Ext” scenario

Emissions and resource use were compared on an operations-only basis (compared to the full life-cycle), hence they do not include impacts from facility construction and other equipment and materials required for setting up and running the system (for implications see Section 3.4.4). Even though this study is guided by the LCA ISO standard 14040 (e.g. defined scope and system boundary, inventory data collection), it was not fully adhered to. The varying adoption of greenhouses changes a) total food production and the ratio between fruits,

vegetable and fish, and b) the amount of organic waste assimilated and thus considered; hence the carbon footprint of the whole system is the basis for the assessment, rather than a functional unit, e.g. a kg of crop. To assess the carbon footprint benefits of the "integrated" UA scenario versus the operations of the "current" scenario, it was assumed that the produce would replace either imported or nationally produced food. The share of supply that was considered imported was determined using production, export and import data from FAOSTAT and then distributed over 12 months in the year according to the harvest table and other considerations (e.g. year-round greenhouse production of tomatoes and cucumber in the UK, required lighting for reported yields for the crops (Shao et al., 2016)). The carbon footprint of national and imported food supply for the UK was based on Audsley et al. (2009), which estimated the associated emissions per crop for production and transport until the regional distribution centres. The carbon footprint of national and imported food supply for Lyon was extracted from the Agribalyse and Agri Footprint databases (farm-gate) and adjusted for transport emissions similar to the UK values (Watkiss, 2009; Webb et al., 2013). The carbon footprint of externally supplied food thus comprises all the emissions during the entire process of food production and supply, including those linked to energy and water use at various stages. The GHG emissions for fish production were taken from Robb et al. (2017) and from Ziegler et al. (2003) for transport. The carbon footprint of the produce distribution within the city was then assumed to be the same for the "integrated", "UA+Ext" and "current" scenarios and thus excluded in the assessment. Fish type specific production and distribution emissions were used for the "current" scenario. Insect meal would replace the share of equivalent soy meal (Salomone et al., 2017) as part of the overall accounted feed in the "integrated" scenario. The associated emissions for the production (for both soil-based and hydroponic growing) and application of externally supplied chemical fertiliser (for soil-based growing only) were taken from EU guidelines. The carbon footprint of grid electricity was accounted with 0.06 and 0.41 kg CO_2e/kWh for France and UK, respectively, natural gas heating with 0.27 and 0.20 kg CO_2e/kWh for France and UK respectively and water with 0.15 kg CO_2e/m^3. The low carbon footprint of electricity in France is due to nuclear energy provision and can be viewed as a representative of a low carbon electricity grid, such as one with a high-level penetration of renewables. Relevant carbon footprints and emissions factors are listed in AppxI-Figure 4.

In the "current" scenario, it was assumed that food waste is not source-separated and is thus incinerated together with municipal solid waste (waste-to-energy) while green waste is composted in windrows, both outside of the city boundaries (20 km distance, diesel truck).

This work does not consider the final treatment of incineration ash but takes into account the energy recovery in incineration facilities (Astrup et al., 2009). The end use of compost from windrows was not considered as (i) the majority was considered not to be used in commercial food production and (ii) the benefits as fertiliser replacement were found to be negligible compared to the process emissions. The emissions during incineration were dependent on the (biogenic) carbon content and the total mass of the processed material. Gaseous losses during the composting process constituted the emissions for both decentralised and windrow composting. For the "integrated" scenario, any concentrate of surplus waste products processed semi-decentrally were also treated outside the city (co-incineration). The emissions arising from treating the fraction of the primary waste (i.e. food and green waste) that was not used in the "integrated" scenario was not included in the calculation for any of the three scenarios, because this part of the emissions would be identical for all the scenarios and therefore not necessary to include for comparison. The applied (insect) compost and digestate fibre in the "integrated" scenario released 0.5% and 0.75% of available N as N_2O, respectively, and accounted for as well were the emissions from biogas burning, energy requirements for secondary treatment of surplus waste products, and the credits of biomethane (grid injection) for the replacement of natural gas (production only, excl. combustion).

3.2.6 Optimization of waste allocation

The sensible allocation of primary waste (i.e. food waste and green waste) to valorisation technologies and how waste products are allocated to either urban agriculture or secondary treatment would be a primary concern for future integrated productive urban food systems. Among the options of reducing external material input (e.g. fertiliser and feed), overall energy requirements and the carbon footprint, the last one was taken as the overall sustainability indicator. Non-linear optimization was conducted to minimise the total GHG emission from all months as shown in the objective function (Eq. (3-1)). Monthly GHG emissions from external heating (Q^{Ext}), electricity (P^{Ext}), NPK fertiliser ($Fert^{Ext}$) and fish feed ($Feed^{Ext}$) requirements are multiplied with the respective GHG footprints, (i.e. the GWP terms) and added to the GHG emissions (i.e. the GHG terms) resulting of biogas combustion (GHG^{Biogas}), fertiliser application (GHG^{Fert}), waste incineration ($GHG^{Incineration}$) and composting ($GHG^{Composting}$).

$$\text{Min} \quad GHG^{Total} = \sum_{m \in M} \begin{bmatrix} Q_m^{Ext} * GWP^{Gas} + P_m^{Ext} * GWP^{Power} + Fert_m^{Ext} \\ * GWP^{Fert} + Feed_m^{Ext} * GWP^{Feed} + GHG_m^{Biogas} \\ + GHG_m^{Fert} + GHG_m^{Incineration} + GHG_m^{Composting} \end{bmatrix} \qquad \text{Eq. 3-1}$$

The decision variables were the amount of food and green waste sent to each valorisation pathway and the amount of waste products assimilated by the UA operations. The constraints included:

- Over-fertilization was not allowed, meaning that when one of the plant growth nutrients was saturated through waste products while the other nutrients were still insufficient, the shortage would be met by corresponding externally supplied fertilisers;
- Composting to be an option only for existing demand in the following month;
- The feed into AD to consist of at least 50% food waste;
- The feed into composting to consist of at least 25% food waste;
- Insect rearing was chosen only up to the point where larvae constitute up to 25% of fish feed; and
- The CHP units to be running when and only when the heating requirements of the co-located ground-based greenhouses was no less than the potentially available heat extracted from CHP, in order to avoid undesirable loss or unrealistic derivation of surplus heat
- No secondary treatment of digestate liquor, i.e. all digestate liquor that is produced had to be used for hydroponic growing (but without overfertilization)

The introduction of the last constraint was due to the following considerations: From an initial assessment of the material flows, it was found that the optimization - without restricting the secondary treatment of streams arising from waste processing units - led to all waste being treated within city boundaries via either AD, composting and insects while generating a large surplus of digestate products. This extensive generation and decentralised treatment of surplus waste product is most likely not practical nor desired in urban areas, hence the additional constraint of no decentralised treatment of digestate liquor was introduced (more liquor than fibre was used in the system, surplus fibre was still allowed and underwent secondary treatment).

The detailed mathematical model, including the list of constraints, variables and parameters is described in Appendix I section 1.5. Excel in combination with What'sBest!® was used for modelling and optimization.

3.3 Results

3.3.1 Spatial analysis and climate factors

Table 3-2 lists the main differences between the two case study locations with respect to urban layout, climate and the resulting energy demand by greenhouses. The urban layout influences the potential productivity and the possible split between year-round greenhouse growing and seasonal harvests in gardens. Population-wise, the city of Lyon is almost twice as dense as Glasgow (6819 vs 3560 people/km2), consequently the share of greenspaces and other non-built up area (e.g. waterways, trees) is smaller while buildings constitute a larger share. The relative share of flat roofs is much higher in Lyon (21.5% vs 7.3%), while the relative share of applicable greenspaces is higher in Glasgow (20.3% vs 12.4%).

Table 3-2: Relevant spatial and climatic factors for Glasgow and Lyon

Aspect	Sub-aspect	Glasgow	Lyon
Spatial factors	Total area (km^2)	186.86	47.09
	Population density (people/km^2)	3560	6819
	Share of flat rooftops of total rooftop area (%)	7.3	21.5
	Share of applicable rooftop area of total urban area (%)	0.8	4.7
	Share of applicable greenspace area of total urban area (%)	8.1	3.1
Climate factors	Average temperature (°C)	8.73 °C	11.59 °C
	Annual rainfall (mm)	1200	844
	Average daily light integral (mol PAR / m^2)	13.8	18.8
Greenhouse energy demand	Heating intensity (kWh/m^2/year)	353	237
	Lighting intensity (kWh/m^2/year)	252	143

3.3.2 Influence of intensity of growing practices

The resource intensity of soil-based gardening and high-intensity greenhouse growing – with heating and artificial lighting – is quite different. Thus, the extent to which the latter is used on larger ground-based plots is a key variable in the assessment of the carbon footprint.

Figure 3-4 shows the carbon footprint of the optimised system for a varying ratio of greenhouses versus gardens on large ground plots (0%-100%), normalised for the "current" scenario. Also shown are the self-sufficiency achieved and waste assimilation (in relation to total waste and food waste only) for the varying ratio of greenhouses versus gardens. The

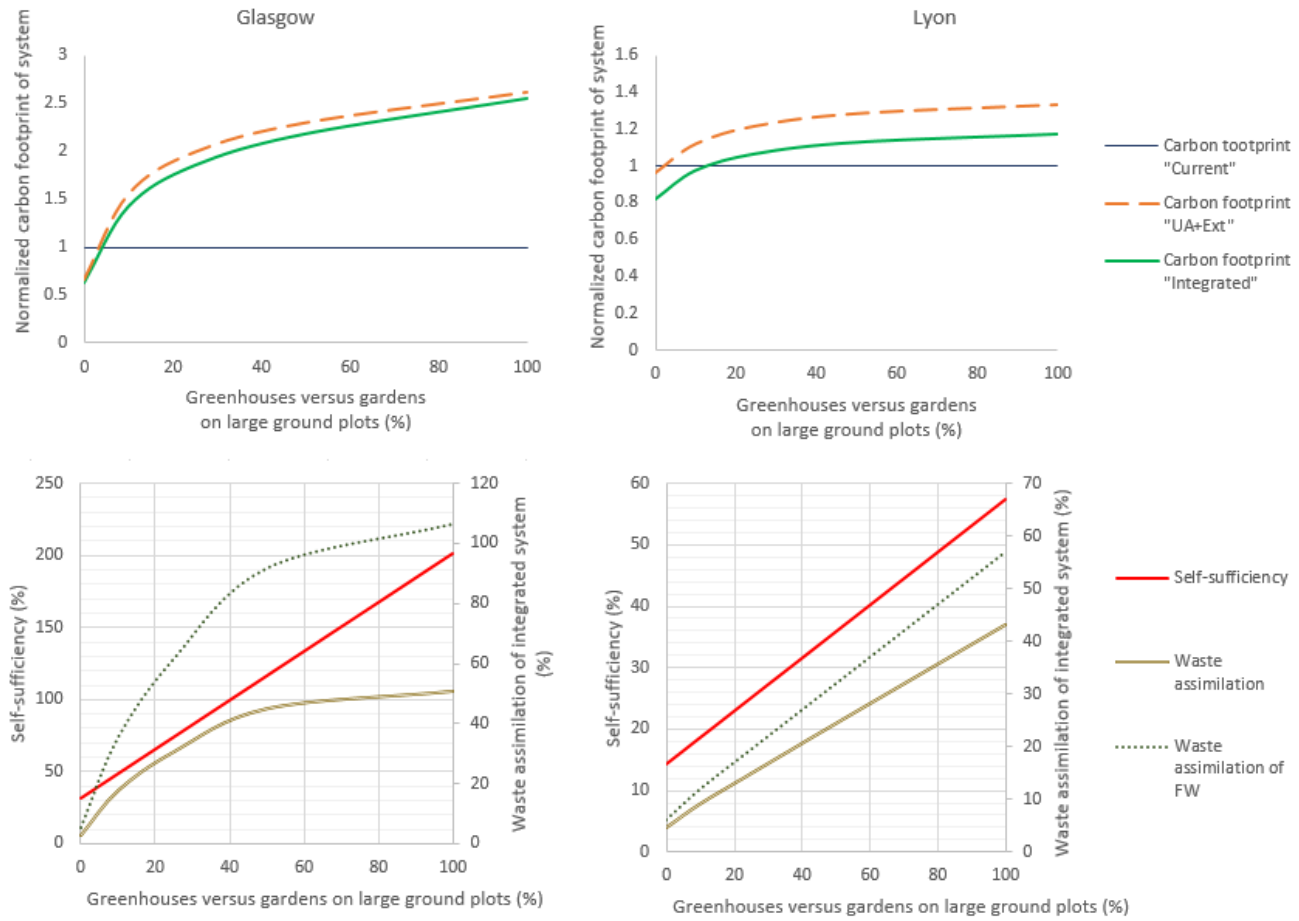


Figure 3-4: Impact of greenhouse to garden ratio.

waste assimilation is calculated on a mass basis and includes waste products used as fertiliser, fish feed or as biogas in CHPs but excludes biogas injected into the grid. It has to be noted that in the case of 100% ground-based greenhouses, soil-based garden growing will still be practiced on smaller plots and in the case of 0% ground-based greenhouses, there will still be production in rooftop greenhouses. Furthermore, with an increasing share of high-intensity greenhouse growing, the productivity of the system rises, and the carbon footprint of the hypothetic operation of not only the "integrated" and "UA+Ext" but also in the "current" scenarios becomes greater as the consequence of producing the same elevated levels of output.

For both cities, supplying higher levels of self-sufficiency via greenhouses results in a higher carbon footprint than the current system. In both cities, equal carbon footprints between the

"integrated" and "current" scenario are only reached at lower percentages of greenhouse growing, i.e. 4.1% for Glasgow and 13.3% for Lyon. The assimilation of waste at high ratios of greenhouse growing approaches 50% in Glasgow due to the limitation on green waste as feed for AD.

Subsequent assessments and visualizations in this work that compare material and energy flows, monthly carbon footprints and integration benefits rely on a fixed ratio of greenhouses versus gardens for larger ground plots. As this work aims to also evaluate the influence of urban geography and climate, it is desirable to choose the same ratio (i.e. adoption level of greenhouse growing) for both cities, hence a few considerations have to be made. First, although a higher adoption level of greenhouses leads to higher self-sufficiency and waste assimilation in both cities, it also leads to a much higher carbon footprint than the "current" scenarios. Second, it is unrealistic to picture a scenario in which all applicable large urban greenspaces are converted to greenhouses, which are likely less (socially) inclusive and aesthetic than gardens. Third, for a resilient urban food system, it is likely advisable to supply a good proportion of, but not all, fruits and vegetables from within urban boundaries, even during winter months. Thus, a compromise is assumed at 20% greenhouses and 80% gardens on large plots, resulting in a similar carbon footprint for at least one of the cities, Lyon, between the "integrated" and the "current" scenario while still providing a considerable level of winter crop production and assimilation of organic waste in both cities.

3.3.3 Results for a 20% adoption level of ground-based greenhouses

Self-sufficiency

Figure 3-5 shows how the harvest and fish production each month satisfies the demand in each city. As expected, the seasonally limited production in open-air and hoop-house growing leads in both cities to a drop in production during the winter months. The self-sufficiency in winter can be seen as "baseline" supply from all-year operating greenhouses, indicating the maximum realistically achievable fresh food supply during those months. Combining fruit and vegetables, UA in Glasgow achieves on average 65.4% self-sufficiency and 22.9% in Lyon.

Resource intensity

Table 3-3 shows the resource use and other metrics for both cities. The water use is split by the three rainwater harvesting scenarios for both soil-based and soil-less growing and only meets the irrigation and replenishing water requirements of the urban produce. The negative

values for hydroponics in the shared reservoir scenario occur because more rainwater is harvested throughout the year than the annual requirements for hydroponic greenhouses. For

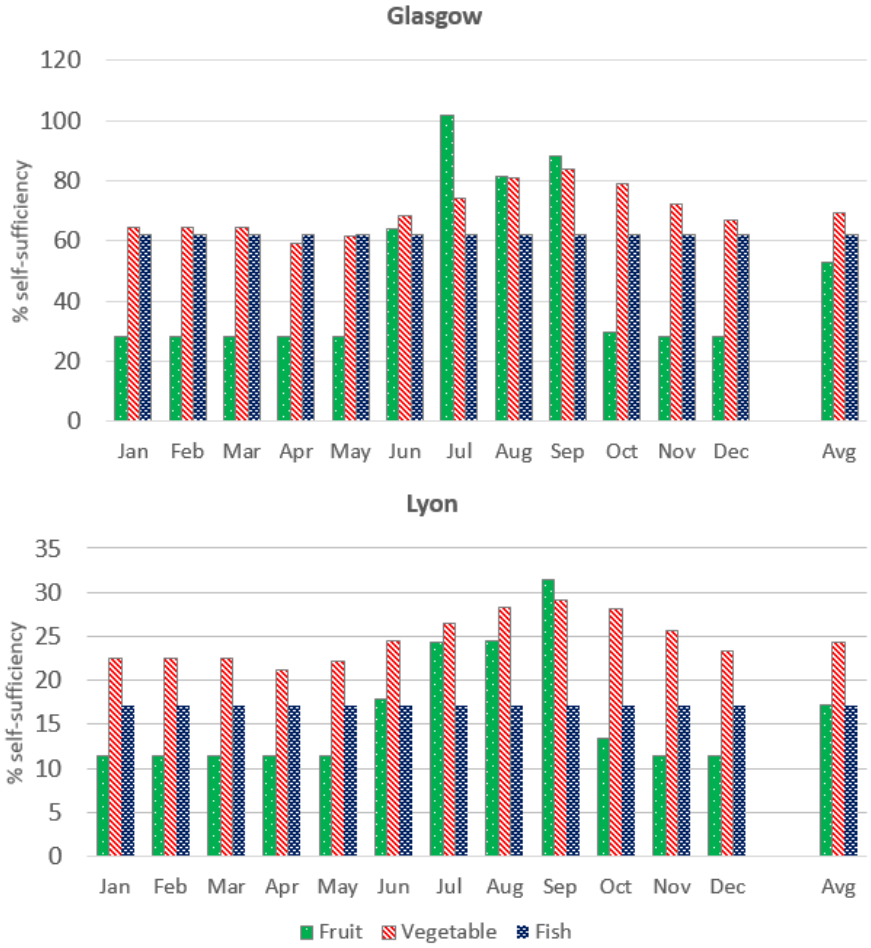


Figure 3-5: Annual self-sufficiency profiles for Glasgow and Lyon

Glasgow, the shared reservoir scenario covers all remaining water requirements within the whole system boundary (incl. water for AD and insect rearing operations). The use of external fertiliser is higher overall in Glasgow due to a higher crop production, while in both cities the "integrated" scenario still requires some external fertiliser due to the mismatch between the nutrient demand and the nutrient profile of the waste products, in particular for hydroponics.

The carbon intensity of growing tomatoes in greenhouses may serve as a comparison between the cities and with other studies, which are discussed later in the paper. It considers all electricity and heating requirements for the "UA-Ext" scenario and in addition the effect of the local heat utilization from the CHP and that of the use of digestate liquor fertiliser for the "integrated" scenario but excludes credits from biogas injection. Reductions are with 1.13% for Glasgow and 1.99% for Lyon rather small.

The waste integration parameters describe the (nutrient) circularity factors of the "integrated" scenario. In both cities, the assimilation of the primary waste, in the form of products derived from waste processing that are consumed within the system (i.e. excluding streams undergoing secondary treatment and the biomethane for grid injection), is far from complete, meaning that only a small share of the generated organic waste may be utilised by a considerably scaled-up UA system. Considering food waste only, the potential assimilation would increase and in the city of Glasgow reach around 50%. The CHP utilization, i.e. the percentage of time the CHPs are operated within the year, is constrained by heating requirement rather than biogas quantity. The large share of non-assimilated waste correlates with the low recovery of phosphorus as shown in table 3.

Table 3-3: Resource metrics for Glasgow and Lyon

Aspect	Sub-aspect	Feature		
Water use (l/kg)	Soil-based gardening	No harvesting	Glasgow	191.4
			Lyon	224.1
"Integrated" scenario		Short-term storage	Glasgow	108.9
			Lyon	144.7
		Shared reservoir	Glasgow	18.8
			Lyon	69.6
	Hydroponics greenhouses	No harvesting	Glasgow	23.3
			Lyon	28.3
		Short-term storage	Glasgow	1.1
			Lyon	5.3
		Shared reservoir	Glasgow	19.3
			Lyon	0.3
Fertilizer use (tonne/y)	Gardening and hydroponics	"UA+Ext" scenario	Glasgow	1774
			Lyon	322
		"Integrated" scenario	Glasgow	519
			Lyon	60
Carbon intensity (kg CO2e/kg)	Tomatoes from greenhouses	"UA+Ext" scenario	Glasgow	3.88
			Lyon	1.97
		"Integrated" scenario	Glasgow	3.83
			Lyon	1.93
Waste integration (%)	Assimilation within UA-System	Total decentral utilisation	Glasgow	25.8
			Lyon	13.0
"Integrated" scenario		Considering food waste only	Glasgow	51.7
			Lyon	16.9
	CHP operation	CHP-utilisation	Glasgow	68.7
			Lyon	53.5
	Resource recovery	P-recovery	Glasgow	13.5
			Lyon	5.5

Concerning the feasibility of allocating urban space for waste conversion, the total area required for insect growing in Glasgow and Lyon was 177,813 m^2 and 24,416 m^2, respectively (0.095% and 0.050% of total city area), and the total digester volume required to convert the waste in Glasgow and Lyon was 4951.1 m^3 and 1315.4 m^3, respectively.

Waste allocation

For both cities, material flow diagrams are presented, which show the waste valorisation pathways and the annual mass flow in kilo tonnes between them, determined by solving the optimization problem (Figure 3-6). In those diagrams, each pair of text (e.g. “Food waste”) and number (e.g. “93.086”) relates to the bar to its left for the first two stages and to the bar to its right for the last two stages. The products of incineration and windrow composting have no

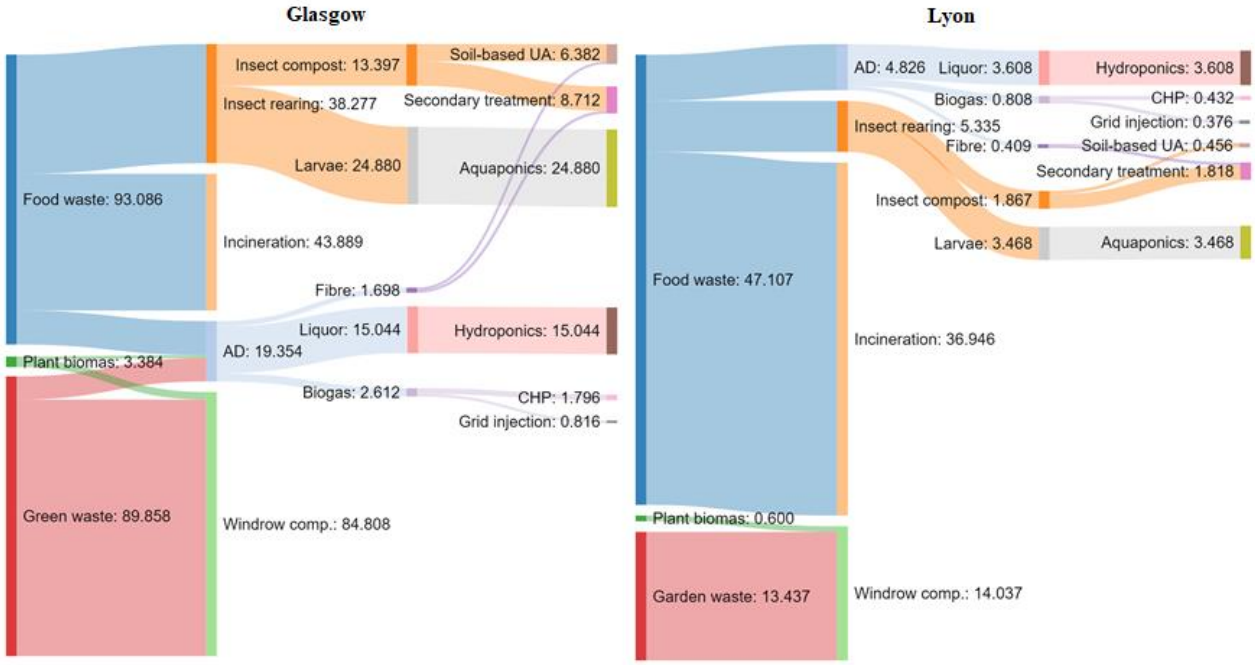


Figure 3-6: Sankey diagram for waste flows in Glasgow and Lyon (kt/year)

final use in the UA system and are thus not continuously displayed beyond the first panel. For Glasgow, the AD takes in the maximum permissible amount of green waste, despite the resulting lower biogas yield. This is because for Glasgow, the emissions from windrow composting of green waste (0.443 kg CO_2e/kg green waste, same as Lyon) is higher than those from the incineration of food waste (0.414 kg CO_2e/kg green waste, slightly lower than that for Lyon). In both cities, the primary waste that is assimilated goes to AD and insect rearing and none to decentralised composting as chosen by the optimization based on the lowest emissions. Hence, insect compost and digestate fibre are chosen for the fertigation of soil-based UA. Due to the different nutrient profiles, combining the two sources allowed maximization of the total amount of organic fertiliser applied and hence minimization of the secondary treatment emissions. On the other hand, production of digestate fibre and insect compost in both cities is about twice as high as the use potential, making half of it an unwanted by-product to be treated. The prevention of overfertilization with a single nutrient

was in both cities the limiting factor for further utilization of organic fertiliser; in soil-based growing N had to be externally supplied and in hydroponics P and K.

Carbon footprint comparison

Figure 3-7 displays the monthly emissions for the "integrated" and "current" scenarios for both cities, split by heating, electricity (excl. secondary waste treatment), other inputs (fish feed, external fertiliser and water), and all emissions related to waste management (incl. production of organic fertiliser and secondary waste treatment). The total carbon footprint is strongly influenced by the carbon intensity of the electricity grid, which is much higher in Glasgow. The figures show significantly increased emissions for the "integrated" scenario in the winter months, mostly driven by artificial lighting needs and heating requirements. For

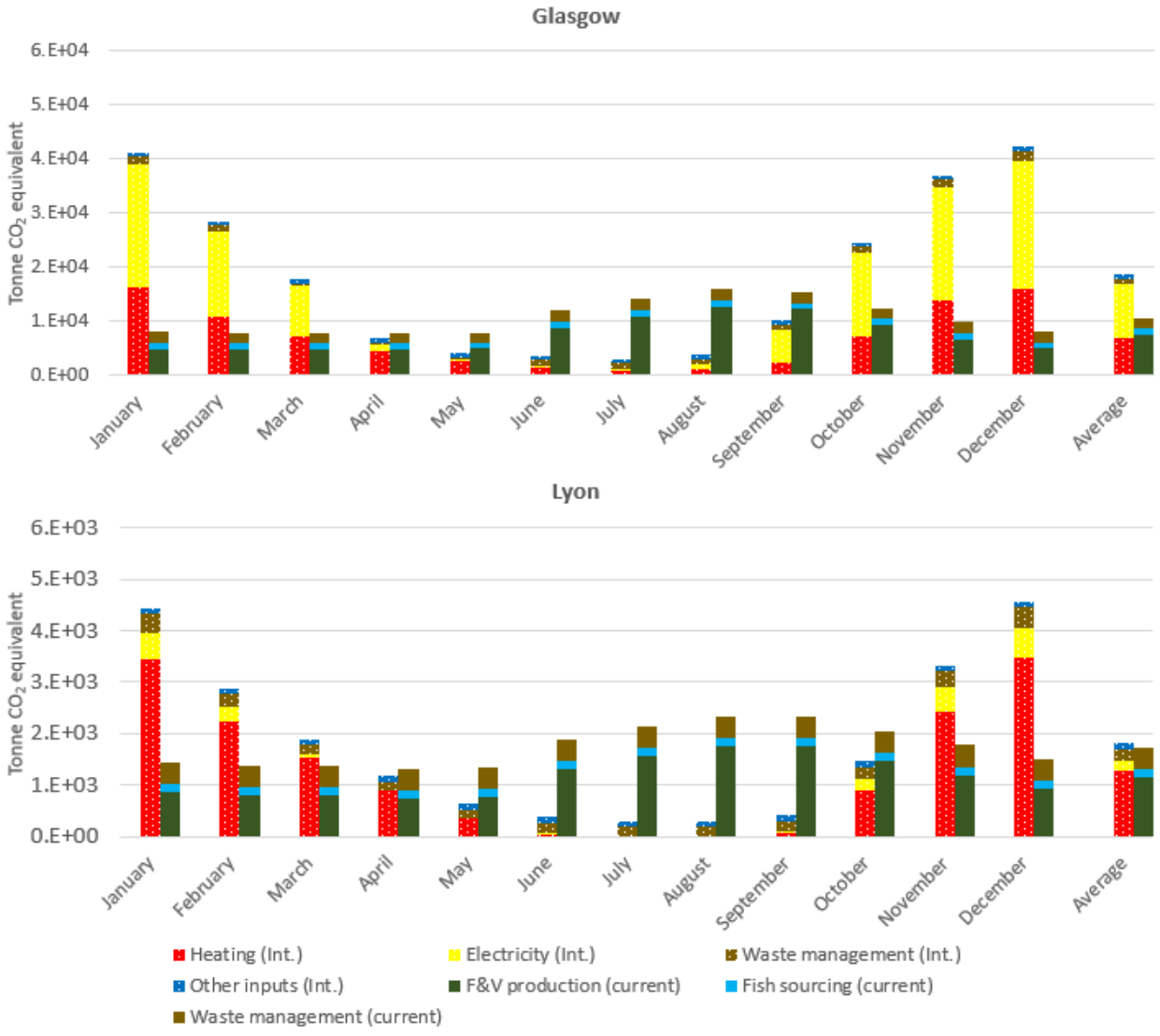


Figure 3-7: Annual emission profile of the "integrated" and "current" scenarios for Glasgow and Lyon

both cities, the "current" scenario has a significantly greater footprint in summer. This is partly because the F&V production accounted for within the "current" scenario was assumed to match the higher productivity of the UA system in summer. It has to be noted that the share of imported food with a larger carbon footprint is higher in Glasgow than in Lyon, resulting in greater average emissions (1.39 and 1.23 kg CO_2eq/kg produce for Glasgow and Lyon, respectively). Comparing the average carbon footprints, the "integrated" scenario emits significantly more CO_2e than the "current" scenario in Glasgow (by 75.1%) and slightly more than the "current" scenario in Lyon (by 4.3%).

Benefit of integrating UA with waste management

Figure 3-8 shows the difference in annual emissions between the "UA+Ext" scenario without integrated waste valorisation and the scenario of UA combined with decentralised organic waste valorisation for both cities. To compare the two cities despite their different production levels, the emissions are displayed per kg of produce (derived from the total annual production of fruits and vegetables in each city).

Due to the higher productivity relative to the waste assimilation (which is the waste accounted for in the "UA+Ext" scenario) and the lower associated emissions for incineration in Glasgow, the per-kg-produce emissions for waste are lower than in Lyon.

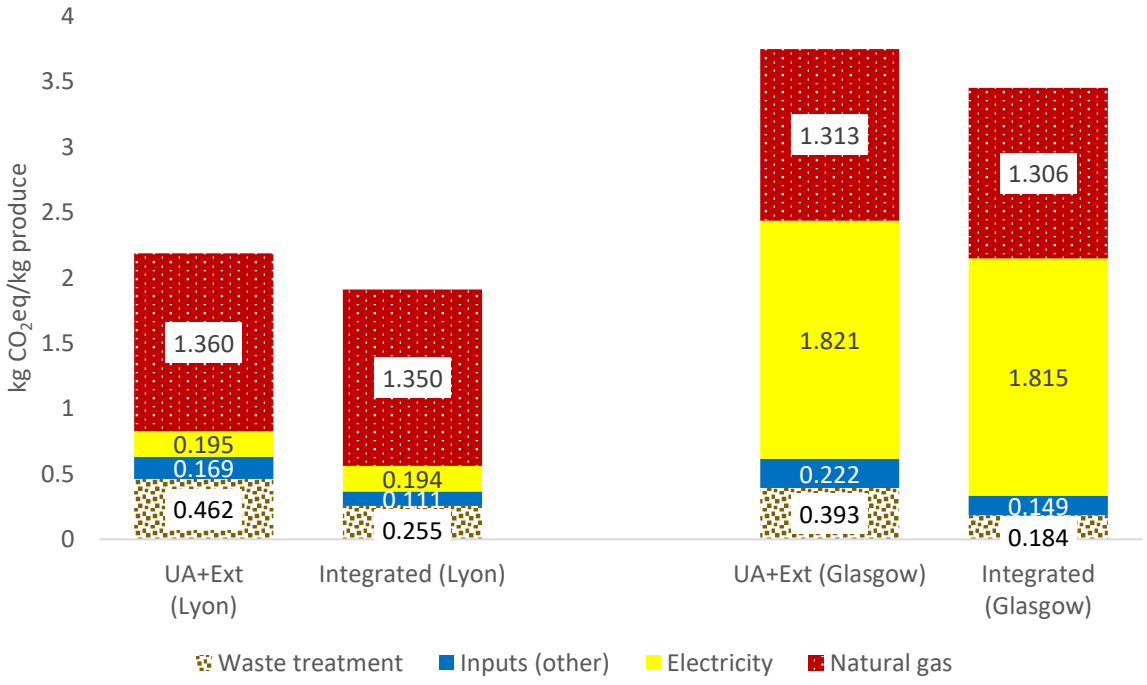


Figure 3-8: Emission intensity of the "UA+Ext" and "integrated" system for Glasgow and Lyon

Despite the production of electricity and heat by converting biogas in a CHP, the "integrated" scenario has a rather insignificant reduction in emissions from grid electricity and gas use compared to the "UA+Ext" scenario with external waste treatment. This is mainly due to (i) the parasitic electricity requirements for the operation of the AD and the centrifugal solid/liquid separation and (ii) the high heating requirements in relation to the heat produced.

In both cities, the emissions associated with waste treatment receive significant reductions in the "integrated" scenario. Further, compared with the lowering of the carbon footprint of energy inputs enabled by the integration between UA and waste management, the replacement of chemical fertiliser with waste products and especially of fish feed with insect larvae had a considerably larger effect (included in the "Inputs (other)"). In total, the reduction of emissions (per kg of produce) due to the integration between UA and waste management was 7.9% for Glasgow and 12.6% for Lyon.

So far, the carbon footprint has been assessed from a UA perspective, where emissions are determined by the resource demands of urban food production and how these demands are met; the latter is particularly affected by the partial supply of inputs derived from organic waste products (electricity, heat, fertiliser, feed). This assessment has shown an apparent mismatch between (1) the high amount of digestate provided relative to the fertiliser requirements of UA and (2) the low amount of energy provided by AD relative to the energy requirements of UA. This mismatch leads to a low level of waste assimilation at the city level and reliance on further external energy inputs. From a waste management perspective, the potential benefits of waste valorisation within a UA system (which may have been established for a much broader range of benefits) can be examined by assuming full assimilation of all waste products. Table 3-4 lists a few carbon footprint metrics for the treatment of 1 kg of food waste. The carbon balance compares these replacement benefits with the emissions for process inputs (e.g. natural gas, electricity) and biogas combustion; a negative sign means the replacement benefits are higher than the process emissions. The carbon balance for the integrated system is influenced by the ratio of primary waste sent to the more favourable insect rearing route (insect rearing benefits: -0.136 and -0.140 kg CO_2e/kg FW for Glasgow and Lyon, respectively, versus AD with 0.154 kg and 0.168 kg CO_2e/kg food waste for Glasgow and Lyon, respectively). In both cities, using the products from insect rearing and AD locally in urban agriculture provides significant benefit versus incineration with energy recovery. Theoretically, the benefits for AD could also hold true for centralised organic waste

recovery and on-field application, although it can become difficult to utilise CHP waste heat and to keep transport requirements low.

Table 3-4: Carbon footprint metrics related to the treatment of 1 kg of food waste in the different scenarios

City	AD to insects ratio for primary waste	Carbon balance of "integrated" waste management	Carbon balance of incineration	Benefit of "integrated" waste management versus incineration
Glasgow	0.64	- 0.0225 kg CO_2e/kg FW	0.4141 kg CO_2e/kg FW	- 0.4366 kg CO_2e/kg FW
Lyon	0.90	0.0063 kg CO_2e/kg FW	0.4904 kg CO_2e/kg FW	- 0.4841 kg CO_2e/kg FW

3.4 Discussion

Implications of the results are discussed and a guide to transpose results to other cities, i.e. how spatial, population and climate factors influence the outcome, is provided. Relevant assumptions, sensitivities and limitations of this study are discussed and key learnings are then summarised. Comparisons with the results from other studies for some specific findings are discussed in Appendix I, 2.1 and 2.2. It is important to note that the learnings from this study relate only to resource consumption and carbon footprints of urban farming. Other equally crucial considerations (e.g. economic opportunity, food and nutrition equity, higher affinity for plant-based diets, ecosystem services and disservices) of such systems have not been considered.

3.4.1 Implications of growth intensity

The variation of the ratio between greenhouse growing and urban gardening shows an inverse proportional relationship between self-sufficiency and system emissions with a clear trade-off. Further, the monthly self-sufficiency profile for both extremes lends insight into how a UA system may be shaped depending on how its socio-ecological benefits are weighed against the perspective of productivity and food security. Giving more emphasis to the former,

options such as urban gardens would be preferred, leading to more inclusive development but also likely the need for storage and processing facilities. In contrast, if stabilised year-round production is more emphasised, the system would favour options such as high-intensity greenhouses, which come with a potentially much higher carbon footprint but a steady supply and thus simpler logistics. Another consideration is public perception, as more exclusive and less aesthetic greenhouses are likely undesired in many urban settings. Besides, the choice between these two types of options may be affected by the local circumstances. In general, a comprehensive assessment of the advantages and disadvantages of the various growing options would help decision-makers to assess the necessary trade-off in the scale-up of urban agriculture.

3.4.2 Remarks on resource consumption

In the water use scenarios analysed in this work, rainwater harvesting brings significant benefits up to the point of reducing the water input to zero when shared distribution and storage is assumed in a location with extensive rainfall. The difference in water demand between the cities is primarily caused by the difference in annual rainfall. Making use of low-tech hoop-houses with rainwater harvesting equipment can reduce water requirements for gardens by half, and can further minimise the external water requirements with some decentralised storage capacity. It could be claimed that if urban agriculture is to be scaled up, new infrastructure should incorporate rainwater harvesting facilities, although the possibility of sharing reservoirs and installing inter-monthly storage of rainwater would be somewhat limited. Technical aspects such as disinfection after longer storage or distribution losses are yet to be considered in future work.

Fertiliser use was greatly reduced through utilisation of waste products. The use of chemical nitrogen fertiliser in soil-based growing in the “integrated” scenario occurred mainly due to the differences in plant availability assumed for the nutrients in compost and digestate fibre: The nitrogen had a very low plant availability, thus P and K became the constraining factors for further waste nutrient addition. In reality, different countries use varying fertilization rates of nitrogen for soil-based growing, and growers obtain similar crop yields whether grown with chemical fertiliser or with compost only (Cleveland, 1997), hence it may be projected that the waste products from decentralised waste conversion could make chemical fertiliser obsolete for soil-based growing. Hydroponic growing solutions, on the other hand, require exact dosing and fertiliser levels for maximum productivity. Hence it is likely that growth is adversely affected by nutrient deficiency (e.g. reduced yields or change

in taste). Therefore, considering more advanced nutrient recovery technologies capable of concentrated extraction of a single plant nutrient would allow to better tailor the nutrient supply to the plant needs in hydroponics.

This study likely overestimated the energy inputs and thus emissions for the yield figures employed: (i) a modelling study by Benis et al. (2017b) for Paris used higher daily light integral values (20 vs 13.5 mol/m^2 in this work) and thus higher yields (75 versus 42.9 kg/m^2 in this work) while only requiring 93 kWh/m^2 of lighting (versus 143 kWh/m^2 in this work), (ii) a study for a vertical farm in Lyon only had a life cycle impact of 0.39 kg CO_2e/kg lettuce (Romeo et al., 2018) and (iii) an empirical study by Theurl et al. (2014) operated a greenhouse in Austria without artificial lighting while achieving similar yields to this work. The latter study also found that heating-related annual carbon footprint could be almost halved by not running the greenhouse for 1-2 months in winter (Theurl et al., 2014).

The more food is produced in urban environments, the higher the potential waste assimilation. Considering food waste alone, a large-scale UA system in a less dense city such as Glasgow could assimilate half the generated amount, which would equal either the share of household or commercial food waste, thus allowing for tailored collection strategies. In terms of closing the nutrient loop, it seems that a great amount of phosphorus would still be lost, calling for holistic solutions for recovery in a range of waste streams.

3.4.3 Influence profile of city characteristics on outcomes

The differences between the two cities (see Table 3-2) have influenced the results significantly. Figure 3-9 shows how specific characteristics have influenced a certain outcome and enables transposing the results to other cities.

The integration benefit (percentage improvement, not shown) concerning heat and electricity consumption depends mainly on the ratio between absolute heating requirements (determined by the self-sufficiency and a high share of greenhouses) and the potential amount of heat generated. If the ratio of digeponic to aquaponics increases, higher demand for digestate leads to a higher AD throughput, resulting in more biogas and thus energy generated but a lower larvae demand and thus reduced input replacement benefits. For the integration benefit associated with waste treatment, a lower ratio of greenhouses versus soil-based growing reduces secondary treatment requirements of the surplus digestate fibre.

	Spatial			Climate			Other			
Outcome	Population density	green-space as % of urban area	Flat roof-space as % of urban area	Temperature	Solar radiation	Rainfall	CF of electricity grid[1]	Productivity level[2]	Ratio Digeponics / Aquaponics[3]	Ratio greenhouse / soil-based growing[4]
Heating intensity				- -	-					
Lighting intensity					↓					
Differences in seasonal production				(-)	(-)					++
Self-sufficiency F&V at 20% GH	↓	++	+							++
Self-sufficiency fish at 20% GH	↓	++							- -	++
Water use efficiency (SB, no harvesting)				-		++				
Fertilizer use reduction										+
Carbon intensity of system ("UA+Ext" and "integrated")				-	-		++			↑
Waste assimilation								↑	-	++
CHP-utilisation				-						+
P-recovery								↑		+
CF benefit assuming full waste product assimilation							-		-	

1 0.41 kg CO_2 eq/kWh for Glasgow and 0.06 kg CO_2 eq/kWh for Lyon

2 "Productivity level" is the chosen degree of self-sufficiency, hence every factor that influences self-sufficiency outcomes also affects the other outcomes marked in the table as being affected by "productivity level"

3 1.136 for Glasgow and 1.917 for Lyon

4 Ratio by weight for annual produce, 1.832 for Glasgow and 2.605 for Lyon

Figure 3-9: Influence matrix, meaning of symbols: ↑↓(approximately) proportional or inversely proportional, ++ -- strong influence (increasing or decreasing), +- weak influence (increasing or decreasing), () Expected, not calculated in this study

3.4.4 Assumptions, sensitivities and limitations

This modelling exercise of relevant material and energy flows relied naturally on a range of assumptions and simplifications to allow for a quantitative assessment of the feasibility, desirability and sustainability of such integrated systems. For example, the compositions of food and garden waste (assumed to be constant) have a direct effect on the monthly nutrient balance and biogas yield and likely fluctuate throughout the year. It was also assumed that the carbon footprint of the logistics network for both, the distribution of food and management of waste, is the same in all scenarios and therefore not included in the assessment. While some argue that switching to source-separation of food waste increases emissions overall (Chiew et al., 2015), alternative logistic arrangements are available, such as aggregation at neighbourhood collection points for semi-decentralised conversion facilities (Guo et al., 2018) or cargo-bike schemes for the collection of wastes (Walker et al., 2017), both with

considerably lower footprint than household pick-up with large diesel trucks. A more direct delivery of urban produce, e.g. through bike couriers (Wrighton & Reiter, 2016), electric vans (Kulak et al., 2013), mobile markets (Widener et al., 2012) and local pick-up points (Opitz et al., 2017) could also reduce refrigeration and storage emissions. Another influential assumption was the limits set to the maximum scale-up, i.e. area use. Naturally, if all applicable areas were used in this study, the self-sufficiency would be proportionally higher. It could be claimed that the limits used in this work are already too high and unrealistic; they nevertheless serve as an indication and benchmark to allow comparison and facilitate discussions about the potential. The yield values also have an effect on the expected productivity (and the energy intensity of soil-less production), however, the chosen range of crops and thus diversified yield figures likely capture reality better than estimates focusing only on one specific crop. On the energy balances, a strong effect on the results comes from the K-value (2.27 $W/m^2/K$) for heat lost to the surroundings in greenhouses, with almost full proportionality for the resulting heating requirements. Other studies have used higher figures around 5-6 $W/m^2/K$ (Nadal et al., 2017) while novel types of greenhouses, e.g. with bubble-insulation, promise K-values as low as 0.9 $W/m^2/K$ (Stoknes et al. 2016). The demand profile for fruit and vegetable and the distribution of crops between growing practices were assumed the same for both cities to offer a simple basis for the comparison, but the actual demand profiles for both countries differ quite substantially. In reality, the crop choice of the growers is most likely also influenced by economics and consumers' preference rather than assuring proportional demand satisfaction. Further assumptions or simplifications have been applied to allow the modelling of this work, such as using general fertilization rates and excluding among others the shading effects of buildings, the influence of the urban heat island effect, CO_2 enrichment, humidification, micronutrient availability, labour requirements, nutrient and waste run-off, and the germination and nursing processes.

Lastly, this work only considers the operational footprint, similar to many other studies (Barbosa et al., 2015; Benis et al., 2017a; Sanyé-Mengual et al., 2018; Shiina, Hosokawa, Roy, Nakamura, et al., 2011). Clearly, structural components for greenhouses, building retrofits, waste conversion facilities and local gardens will have an environmental footprint. At the same time, the infrastructure for the existing global supply system is already in place and constantly refurbished, making the inclusion a complex exercise. In a study by Boulard et al. (2011), emissions from the raw materials and construction of a greenhouse for a 20-year project duration were included and found that they only contributed a small amount (0.14 kg CO_2e/kg product, or 6.8% of the total footprint) in comparison to the operational

inputs such as heat and fertiliser. The validity of the outcomes of this work is therefore unlikely to be significantly affected by only considering the operational footprint. Overall, the learning from this study can be seen as indicative and providing first ballpark figures rather than aspiring to obtain fully conclusive results.

3.5 Key insights

The primary purpose of simulating and optimizing the organic waste valorisation pathways for use in urban agriculture was to understand the associated material flows in relation to urban space and population characteristics and to find out which pathways are the most promising for reducing emissions. A few insights can be gathered from the outcomes:

1. The carbon footprints of the two UA scenarios are highly influenced by the adoption level of energy-intensive greenhouses growing in winter months which may result in a significant increase in emissions. At the same time, less intense lighting and heating schedules could reduce the operational footprint of greenhouses substantially. Further, fully renewable – and thus low-carbon – electricity grids in the future favour the UA scenarios in terms of GHG emissions. The advantages of a warmer and wetter climate with more sunshine can be seen in the resource intensity of high-intensity greenhouse production and make integrated UA and decentralised waste management systems more attractive in such climate conditions.

2. Even a fully-scaled up productive urban food system is unlikely to assimilate all the food and green waste generated in a city, as a large share of digestate products would not find an urban sink, even in less dense cities such as Glasgow. External or central treatment of organic waste is therefore always required, and matching the throughput of small-scale neighbourhood AD facilities with local fertiliser requirements or the sizes of other local sinks could be the most sensible approach.

3. Insect rearing on food waste for fish feed was the most preferred pathway in the optimization. This renders a promising combination of technologies for increased protein self-sufficiency and reduced waste burden while likely adding economic opportunities. The direct feeding of larvae to fish, rather than the energy-intensive drying and processing to powder (Salomone et al., 2017), makes live BSF larvae a low-footprint feed, while the local production and fresh consumption of fish could reduce emissions during transport and storage (Ziegler et al., 2003). The required

urban area is also minimal since the operations can be carried out in multi-story buildings.

4. Co-located small- and micro-scale anaerobic digestion is a strong contender for the decentralised treatment of food wastes if local sink capacity is available, as the produced biogas and biofertiliser has major environmental advantages over waste-to-energy schemes and composting. The localized utilization of heat during biogas combustion complemented by the injection of biomethane into a low-pressure urban grid or fuel stations represents a major advantage of decentralised or co-located AD against centralised AD. Pick-up schemes and collaborations with businesses as currently investigated by an EU-funded project with pilot cases in Lyon could facilitate the waste logistics and create a stable AD feed supply (http://www.decisive2020.eu/). Given the space constraints in urban environments and community gardens, total digester volume would have to be distributed to a number of smaller units (e.g. 2-50 m^3) co-located with greenhouses, calling for more scattered locations of smaller AD facilities. Besides in greenhouses, AD facilities could also be co-located in gardens with adjacent heat sinks (e.g. bakeries, community cafés) to ensure the benefits of CHP heat use (see Walker et al. (2017)).

5. The nutrient, feed and water requirements for urban growing operations can be met by a significant degree via integration with waste management and incorporating rainwater harvesting. If mainly open-air gardens, low-tech hoop-houses and a few greenhouses with less-intensive growing schedules (e.g. reducing supplemental lighting) are employed, well-designed urban agriculture and waste management systems mean no additional burden to the resource use and the carbon footprint profile of a city while contributing to a more resilient urban food system.

Chapter 4 Comparison of local and centralised biowaste management strategies – A spatially-sensitive approach for the region of Porto

Overview

This chapter presents the following published article: *Weidner, T., Graça, J., Machado, T., Yang, A., 2020. Comparison of local and centralised biowaste management strategies – A spatially-sensitive approach for the region of Porto. Waste Manag. 118, 552–562.*

Among all authors who contributed to the published article, T.W. conceptualised the study, performed the modelling and wrote the manuscript, J.G. helped with data provision, aided to conceptualise the study, reviewed the model and edited the manuscript, T.M. provided insights on community composting, reviewed the methods and edited the manuscript. A.Y. supported the conceptualisation and the modelling steps and revised the manuscript.

This second original work was inspired by the potential to reduce a city's carbon footprint by utilising organic waste within a city. A second inspiration was the desire to collaborate with practitioners to provide insights related to the new requirement to source-separate and treat or collect biowaste locally within the EU from 2024 on. The previous chapter did not give any indication of how a local or decentralised treatment and utilisation would affect the collection and transportation of biowaste and how the utilisation (or land application in this case) would depend on land availability and transport distances of biowaste products. It also showed that biowaste assimilation is limited when only considering UA within the city boundaries. This chapter addresses these concerns by designing an alternative biowaste management system that consists of community and home composting, district-level aggregation of compost and subsequent land application in urban and peri-urban agriculture. The original hypothesis of this work was that converting urban land to productive farms, which allows for increased local use of compost, would significantly reduce logistical requirements and thus costs and carbon footprints of the decentralised system. Although this hypothesis was eventually disproven, new learning was generated of the alternative decentralised system, with and without additional urban farms, through comparison with centralised treatment systems relying on biowaste collection. One of the latter was anaerobic digestion, which was already identified by the previous chapter as promising. The assessment was carried out for 76 districts within a metropolitan area to obtain insights into how the rural-urban characteristics

influence comparative costs and carbon footprints and provides context-specific and transferable recommendations for biowaste management systems after 2024.

4.1 Introduction

In many countries, expanding urban areas face great challenges in biowaste management and resource recovery. From 2024, all household biowaste in the EU must be treated at source or collected separately (*Proposal for a Directive of the European Parliament and of the Council Amending Directive 2008/98/EC on Waste*, 2018). In preparation for this, many municipalities are currently facing the task of restructuring their waste management systems. While this fundamental change presents opportunities, it also raises questions as to which treatment systems best address climate change mitigation and circular resource flows for different types of municipalities, among other desirable outcomes.

Many studies have compared different centralised food waste treatment systems, reaching mainly similar but sometimes contrary conclusions due to different system boundaries for substituted products and different weighting of environmental factors (Vieira & Matheus, 2019). For example, while most studies rated separate collection with anaerobic digestion (AD) as having the lowest impacts, in-vessel composting performed either worse (Kibler et al., 2018; Lundie & Peters, 2005; Slorach et al., 2020) or better (Edwards et al., 2018; Parry, 2016; Righi et al., 2013) than landfill or incineration of mixed waste. A potential trade-off between nutrient recovery and GHG emissions is noted in all studies, and some studies point out the strong dependency of the results on transport distance (Mayer et al., 2020), bin size (Purkayastha et al., 2015), collection frequency (Jaunich et al., 2016) and efficiency (Teixeira et al., 2014) of separate biowaste collection. However, these studies do not consider in detail the local sink capacity for waste products and how the impact of inner-city logistics for collection and compost distribution changes for different urban layouts. Moreover, some of these studies omit the potentially significant emissions from land application of the biowaste treatment products (Boldrin et al., 2009). Besides the relatively high cost of biowaste collection and centralised treatment (Forkes, 2007), centralised facilities are often located outside city boundaries, making it difficult to engage communities in the circular economy and utilise resource flows locally. Decentralised or local biowaste treatment with utilization in peri-urban or urban farming is an alternative that has the potential to close these resource loops and deliver a host of positive social outcomes, such as community cohesion and more varied and healthy diets (Aubry et al., 2017). This practice can also be seen as increasing resource sovereignty, effectively empowering citizens to be less dependent on global supply chains, promoting environmental stewardship and creating employment opportunities (Dehaene et al., 2014).

Several challenges of community or decentralised composting and their potential solutions have been studied. For example, paid and locally engaged technical personnel are recommended to overcome issues of low participation (Comesaña et al., 2017; Pai et al., 2019), odour and public acceptance (Keng et al., 2020; Parry, 2016; Purkayastha et al., 2015), correct segregation and poor process performance (Comesaña et al., 2017). Furthermore, implementing compost islands in the neighbourhood close to residents (as opposed to e.g. only in public parks) could overcome limited processing capacity (Pai et al., 2019), unfavourable drop-off distances and low acceptance of decentralised solutions (Deswal & Laura, 2018; Lunag et al., 2020), increase quantities of bulking material for home composters (Keng et al., 2020) and ensure high quality of compost and low maintenance cost (Bruni et al., 2020). The need for personnel and thus limited revenue and financial self-sufficiency can be addressed through active management by local authorities (Bruni et al., 2020; Comesaña et al., 2017; González-Sierra et al., 2019). Investment costs for auxiliary equipment, such as wood chippers and scales, can also be reduced by semi-central processing stations sharing such equipment (Keng et al., 2020). The limitations of local composting studies include missing system-level considerations, such as the potential of local compost application (Vázquez & Soto, 2017) and the difference in GHG emissions between large- and small-scale composting (Parry, 2016; Vázquez & Soto, 2017).

On local nutrient recovery, first assessments have been carried out to understand the impact of composting with urban farming, which is shown to perform better than landfill systems (Trlica, 2016). It was found that a significant share of farmers on the fringe of the city would accept compost from urban waste as soil amendments (Nigussie et al., 2015). However, a city-wide assessment has identified that local sink capacity may be limited when decentralised schemes are scaled up (Till Weidner & Yang, 2019), thus being a potential barrier for implementation which would not be encountered by isolated community composting projects. Excessive land application of nutrients in urban environments (beyond their assimilation capacity) may cause pollution of groundwater (Hart et al., 2004) while collecting compost locally for long-distance transport outside city boundaries could potentially incur considerable costs and GHG emissions. We posit that increasing local sink capacity through the conversion of urban land to organic community farms may mitigate these impacts while ensuring that nutrients are recovered locally.

In this work, we present the design of a realistic system for full decentralization of biowaste management, i.e. treatment at source via home and community composting with local land

application of compost. This design is compared with conventional practices for centralised biowaste treatment in terms of costs and environmental implications. Addressing local biowaste utilization, the assessment has also included the effects of creating additional urban farms on compost assimilation, cost, and emissions of the decentralised system. Furthermore, this assessment aims to offer a reliable comparison between local and centralised treatment systems for different urban typologies (represented by districts), which requires the incorporation of spatial details such as population density and distance between waste sources, treatment facilities and application areas. To the authors' knowledge, this work is the first study that compares cost and climate impact metrics of centralised and decentralised treatment strategies considering both (1) the spatially sensitive sink potential for biowaste treatment products and (2) the required logistics for a specific district type (e.g. for bulking material and surplus compost).

4.2 Methods

The metropolitan region of Porto, Portugal, has been chosen as a case study. The diverse typology of the municipalities of this region provides an interesting range of settings in terms of availability of peri-urban land, population density and distance to central treatment facilities. Furthermore, the public waste management company for the region, LIPOR, operates an incineration plant for mixed waste, a tunnel composting plant for biowaste (mainly commercial food waste and green waste), and has established local composting and organic urban farming programs (LIPOR, n.d.).

This work focuses on household biowaste and excludes biowaste from commercial sources. Five different systems for biowaste management are compared through a life cycle assessment (LCA) and annualised cost approach, including three centralised (with household collection and remote treatment) and two local (with treatment at source and local land application) approaches (see Table 4-1). The assessment considers annualised cost, rather than net present value as the cost per tonne is the most common indicator relevant for waste management organisation. The area assessed in this study consists of seven of the eight municipalities covered by LIPOR (1 municipality was not included as no suitable geographical information data was available). These seven municipalities comprise 76 districts. The spatially sensitive data source used, at the level of residential blocks, assumed a total population of 834,853 people. The models included in this study consider the locations of LIPOR's existing incineration and composting plants (the latter being also considered as the potential site for the AD plant).

The LCA was carried out employing both EASETECH software (v.3.17, http://www.easetech.dk/) and Excel using the parameters described below and in Appendix II section 3. The ISO 14040 standard for LCAs served as a guideline. The goal, step 1, was described in the introduction and the functional unit for each district was a tonne of biowaste generated. The system boundaries of the five systems are visualised in AppxII-Figure 1. The life cycle inventory, step 2 in an LCA, was composed of calculated and fixed parameters from EASETECH and literature as described in section 4.2 and listed in AppxII Figures 3,4,6,8 and 9. The impact assessment method (step 3 according to the standard) was ILCD 2011 Prosuit Global NR w/o LT. Biogenic CO_2 emissions were excluded. The project duration was considered to be 25 years. The substitution method was applied where biowaste products or electricity was generated and the use of equivalent products was considered to be avoided. The comparison between different systems was based on the midpoint indicator global warming impact (GWP100), which is a pressing concern globally and the case study locale.; further assumptions used in this study are provided in Appendix II, 11. Information about the modelling in EASETECH in Appendix II, 4., and the studied scenarios are described in Section 4.2.5. The interpretation of the results (step 4) can be found in sub-section 4.3.

Table 4-2: Details of the five biowaste management systems investigated

SYSTEM	CENTRAL INCINERATION (CENT.-INCINERATION)	CENTRAL ANAEROBIC DIGESTION (CENT. AD)	CENTRAL COMPOSTING (CENT. COMPOSTING)	LOCAL COMPOSTING (LC)	LOCAL COMPOSTING + URBAN FARMING (LC+UA)
TREATMENT	Energy recovery	Biogas production and upgrading, digestate separation	Tunnel composting	Composting islands and home composting	Same as LC
FACILITIES	1 per region	1 per region	1 per region	Multiple within residential areas and 1 semi-central per municipality	Same as LC
HOUSEHOLD COLLECTION	3 x week, mixed	3x week biowaste only, 1x week mixed waste	3x week biowaste only, 1x week mixed waste	1x week mixed waste	Same as LC
OTHER LOGISTICS				Surplus compost and bulking material	Same as LC
LOCAL LAND APPLICATION		Considered in surplus land application	Considered in surplus land application	Peri-urban farmland (except in “no peri-urban farming” scenario)	Same as LC and on urban farms
SURPLUS LAND APPLICATION	Bottom ash landfill	Composted digestate: 50% for farming outside region, 120 km average transport distance. (100% in “external land application” scenario) Liquid digestate: 100% in”external land application” scenario	50% for farming in- and outside of region,120 km average transport distance (100% in “external land application” scenario)	Only non-farming, 120 km average distance (100% for farming in “external land application” scenario)	Same as LC

STORAGE (SEASONAL)		Liquid digestate (in "external land application" scenario)	Short-term (semi-) central	Same as LC

4.2.1 Waste collection

To ensure consistency between the scenarios, the same amount of household biowaste was considered for treatment for each system, which included food and garden waste, their sortation rate and degradable fractions. Also, for each separate biowaste treatment system, a similar waste collection process was assumed for all the municipalities. For the incineration system, mixed waste is collected three times a week to prevent excessive biowaste degradation. For all the other systems, the biowaste is either collected separately or treated at source, thus allowing the mixed waste to be collected only once a week. Since the analysis focuses on the organic part, the collection cost and environmental impact attributable to the organic portion of the mixed waste in the current collection scheme was quantified by the difference between (i) the actual cost and global warming impacts of the current mixed waste collection and (ii) those of a mixed waste collection where only non-bio waste is collected at a reduced frequency of once a week (further details in Appendix II, 2.1).

For centrally collected waste, it was assumed that every municipality carries out the collection for their districts and delivers the waste (without backhauling) to the central treatment facility. The methodology used was inspired by Boskovic et al. (2016) and the calculations accounted for collection parameters (i.e. the collection frequency, pick-up rate [tonne/hr] adjusted for population density, the non-collection driving time, driving distance and fuel use, and unloading and preparation time) and cost information (i.e. working hours and shift length, required amount of trucks and personnel per municipality, kitchen and collection bins required, annualised capital and maintenance cost of trucks). The driving distance to transport waste from each district to central facilities was assessed using Google Distance API Script. The less frequent mixed waste collection benefited from an increased pick-up rate as described in Appendix II 2.2. Since the collection routes are intra-municipal, the total municipal cost and emissions were attributed to each district according to its required collection time and fuel (calculations in Appendix II, 6.). The calculated average cost per collection shift was in the range of the real costs reported by LIPOR (+/-5%).

4.2.2 Centralised waste treatment

The district-specific amount of household biowaste was used to calculate treatment costs and emissions. Capital costs were included in the total annualised cost, together with the annual maintenance and operational costs. An LCA was conducted by modelling the systems in

EASETECH by selecting appropriate modules and end-uses. The GHG emissions from capital goods were excluded from the LCA, mainly due to the lack of data for the decentralised systems and because the contribution of capital goods in waste management systems is usually negligible (Brogaard & Christensen, 2016). The contributions of electricity to GHG emissions were assessed separately and as a function of different carbon intensity scenarios of the grid. For energy recovery in the incineration system, the electricity generation was adapted to the lower heating value of biowaste compared with the values from mixed waste. In the anaerobic digestion system, the digestate was assumed to be subjected to phase separation with the solid part composted and the liquid part undergoing nitrogen removal to allow sewage discharge. One scenario ('External land application') considered the liquid fraction to be stored on-site for an average of 2 months in appropriate vessels with subsequent transport and land application. Biogas was assumed to be upgraded via membrane separation and compressed for grid injection. All relevant parameters for centralised waste treatment are described in Appendix II, 3., including a mass balance for anaerobic digestion (Appendix II, 3.2) and further details on tunnel composting (Appendix II, 3.3).

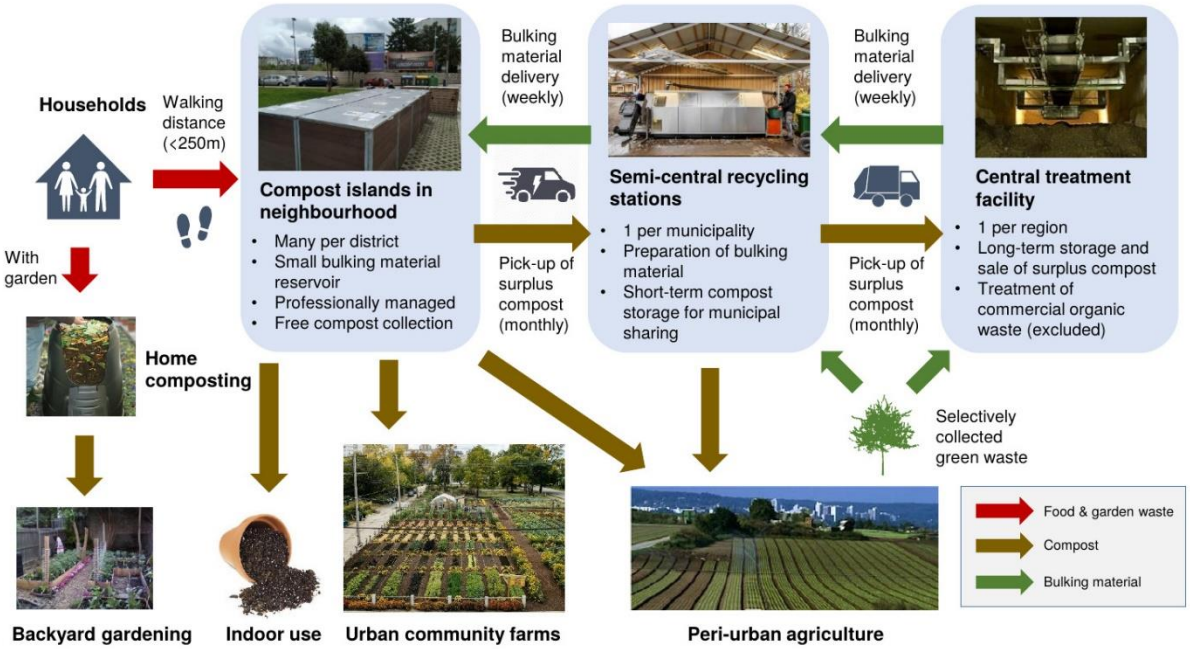


Figure 4-1: Design of local compost system and resource flows with (peri-)urban sinks

4.2.3 Local waste treatment

The model developed for the present study includes operational learnings and considerations from the community composting systems implemented in Pontevedra and Itsasondo in Spain

(González-Sierra et al., 2019). Figure 4-1 provides an overview of the design with the following considerations:

Compost islands: Professional and active monitoring and use of sufficient bulking material are crucial for providing pest- and odour-free urban operations, ensuring optimum aerobic conditions, and creating public awareness. Every compost island consists of 3-12 composting cubes, each with 1000 litre capacity. Each composting cube should cover a maximum of 60 residents to ensure adequate maturation. One technician was assumed to be responsible for churning and monitoring 30 cubes. The numbers of islands and cubes per district were determined via a location-allocation algorithm in ArcGIS Pro, ensuring a maximum walking distance of 250m (further described in Appendix II, 5.).

Home composting: Home composting was considered for residential blocks classified as semi-rural and semi-urban according to their built-up and population density (further described in Appendix II, 5.). Households involved in home composting were considered to apply the compost in their garden and were not associated with compost islands.

Bulking material and compost: The existing municipal recycling centres (*Ecocentros*) were considered to be semi-central locations for intermediate storage of surplus compost and for preparation (shredding) and delivery of bulking material. The transport of bulking material to each composting island was carried out with small electric vehicles. A deficit in bulking material was compensated for and collected from the central composting facility.

Compost usage: It was considered that the technicians would inform farmers and citizens when the compost in a cube is matured and ready for collection (for free). Surplus compost not utilised locally (see below for local sinks) was considered to be picked up by small electric vehicles for monthly storage at the respective recycling centre, which could send the compost either to other districts within the municipality, if there is local demand, or to the central treatment facility.

The assessment for bulking material and surplus compost was carried out for each season, as the volume of green waste and the potential for land application differs throughout the year. Similar to the waste collection, the capital investment (cubes, shredder, bins, trucks), labour, fuel costs, distances and driving times were considered in the total annualised cost. Further information related to the local waste treatment can be found in the SI in Appendix II: modelling in EASETECH (4.) relevant parameters and information on emissions (AppxII-

Figure 9), adjustment for the different composing processes (AppxII-Figure 7), and calculations (6.).

4.2.4 Local sinks and land application

The local application of compost from compost islands on peri-urban fields and organic urban farms (i.e. local sinks) was assessed via spatial analysis in ArcGIS Pro, the impacts were assessed in EASETECH. To evaluate the effect on cost and GHG emissions of increased local sink area, one of the local systems considered assumed that vacant land and greenspaces would have been partially converted to urban organic farms. The term "productive" application in this work means compost is used where it substitutes synthetic fertiliser, e.g. for growing food or public gardens.

The following assessments were carried out for the two systems with local waste treatment for each district: (1) existing area of peri-urban farmland, employing different data sources (2) existing urban farms and their size; (3) area convertible to urban farms (green spaces and vacant land); (4) seasonal productive compost application on peri-urban fields and urban farms, depending on the seasonal share of the annual application rate; (5) seasonal productive compost application in household gardens, depending on garden size (determined via linear interpolation as a function of population density); (6) productive compost uses indoor, e.g. for potting (with replacement of peat); (7) surplus compost from districts was considered to be distributed via recycling centres if productive land was still available in other districts from the same municipality; (8) surplus compost not used up within a municipality would be delivered to the central treatment facility once a month and applied to land without productive use (e.g. not replacing fertiliser); (9) the economic potential of the applied compost product (the compost generates no direct revenue as it is provided for free to the citizens); (10) emissions related to productive and non-productive land application. Transport emissions were neglected for the local sinks because: a) collection by citizens would be non-motorised, b) farmers would normally drive to collect their synthetic fertiliser and soil conditioner anyway and c) a rough assessment resulted in negligible GHG emissions.

GHG emissions of productive land application were assessed according to EASETECH, which included plant nutrient uptake and run-off, fertiliser substitution rates, tractor fuel (fields only), gaseous emissions, soil carbon storage (100-year horizon) and other soil benefits (i.e. effects of increased water retention and reduced soil erosion). The impacts of land application (e.g. fertiliser substitution) of compost generated in a different district in the same municipality were accounted for in the district where the compost was applied. Although this

work focuses on compost application for food production, any public use could also be represented in the greenspace conversion in the LC+UA system.

For the centralised treatment system (tunnel composting and anaerobic digestion with composting of the solid fraction), it was assumed that a share of compost product is distributed in the wider region (120 km return) and sold as a soil amendment for crop production. For the municipal surplus compost in the local system, non-productive land application was considered (accounting only for soil carbon storage, with no other positive effects of compost application). This reveals any differences in cost and GHG emissions (i) between the districts (in LC and LC+UA) and (ii) incurred by increased urban farming (by comparing LC and LC+UA). To allow a fair comparison with the centralised systems, one scenario (for scenario analysis, described below) considers 100% productive use of the surplus compost produced in the local system, equal to the centralised systems in that scenario. Details of all related calculations can be found in Appendix II, 6.

4.2.5 Base scenario and parametric variability

The parametric sensitivity was evaluated for several key parameters and assumptions that can have a strong and non-linear impact on the results of the assessment, especially concerning GHG emissions. The outcome of the LCA can also be affected by the adopted underlying data (e.g. diesel emission intensity). In this work, however, the focus has been given to the significant settings that can effectively lead to different scenarios of the future operation of the waste management system.

The assumptions for the base scenario were selected to represent a plausible implementation towards the middle of the project duration: (1) the electricity grid features 80% of total power consumption from low-carbon sources such as solar, as pledged by the Portuguese government in their Carbon Neutrality Roadmap (https://descarbonizar2050.pt) for 2030 (roughly the middle of the project duration); (2) 0%/50%/50% productive application of compost outside the region for the local composting systems, centralised composting and composted digestate solids, respectively; liquid digestate is treated for sewage disposal; (3) peri-urban farmers with 75% compost adoption rate for commercial food growing; (4) 50% of vacant land and 25% of urban green spaces converted to urban farms; (5) 25% of the population was assumed to maintain their compost well, modelled as compost islands in EASETECH, the rest was modelled as non-turned tumble composters.

Further scenarios deviating from the base scenario were evaluated to assess the sensitivities: (1) no changes to the grid: the carbon intensity of electricity reflects the power consumption pattern in 2018; (2) external land application: 100% productive application of all biowaste products (surplus outside of region, 120 km), including liquid digestate; (3) no peri-urban farming: commercial peri-urban farmers would not adopt compost application (adoption rate 0%) and compost would be applied non-productively; (4) maximum urban farming: 75% of vacant land and 50% of urban green spaces converted to urban farms; (5) optimised home composting: 100% of the population was assumed to maintain their compost well, leading to reduced CH_4 and N_2O emissions (emissions, mass balance and application impacts chosen from compost island process).

4.3 Results and discussion

4.3.1 Regional economic assessment for the base scenario

The result of the economic assessment of the five waste treatment systems (base scenario) for the Porto metropolitan area are shown in Figure 4-2. This assessment considers the annualised

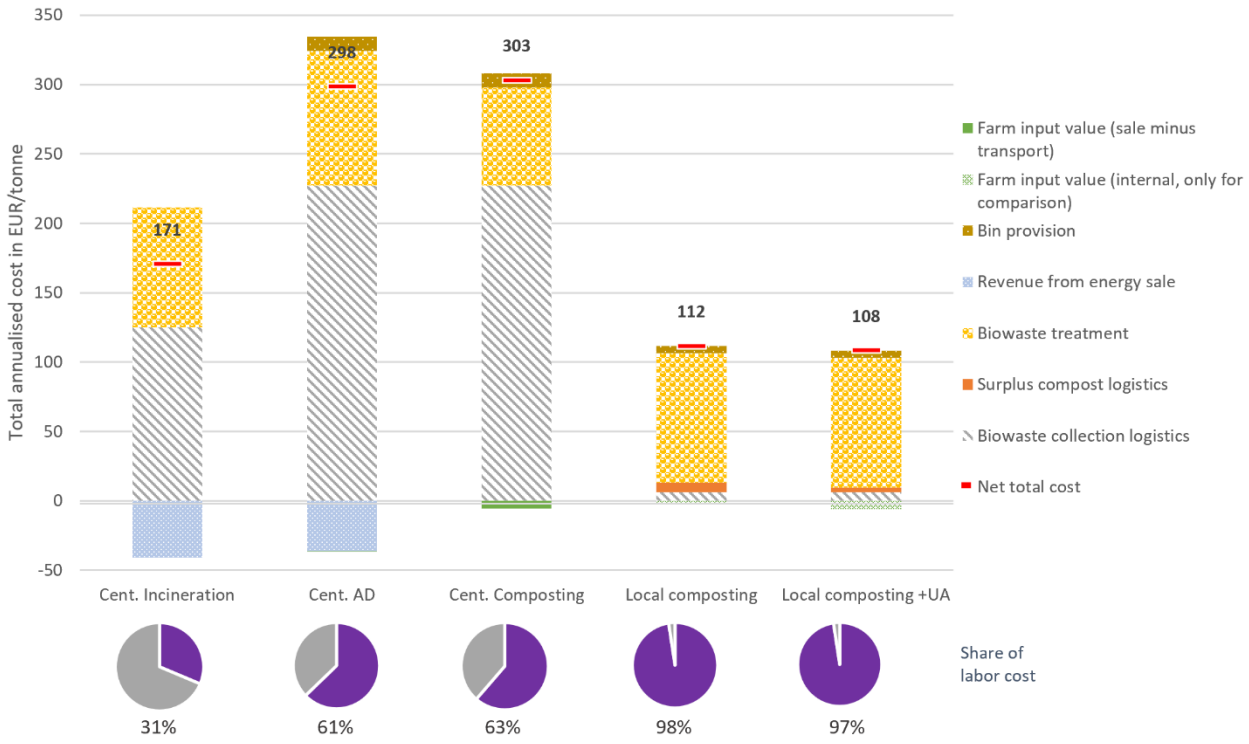


Figure 4-2: The economic balance (in EUR per tonne of treated waste) and share of labour cost for the five systems. Biowaste collection logistics, surplus compost logistics and biowaste treatment costs include labor and non-labor (infrastructure, material and fuel) components, all other costs compromise only non-labor components. The farm input value from fertiliser in the local composting systems is not included in the net total cost.

cost per tonne of waste treated (69,241 tonnes in total), including capital and operational cost and the revenues from the sale of electricity, biomethane, and compost. The cost of waste treatment was significantly different between the five systems assessed.

Local composting systems encompass the lowest total cost of all systems. The surplus compost logistics cost is significantly lower than the labour costs for the technicians looking after the compost islands. They therefore constitute only a small portion of the total costs and increasing the local sink capacity through urban farming only reduces these costs marginally.

For centralised biowaste treatment, collection logistics represent the fraction with the highest share of costs, from 64% to 86% of the total costs for the municipalities, depending on the system and urban setting. Waste collection costs were more affected by the population density (which impacts the pick-up rates) than by the distance to treatment facilities. Centralised composting and AD have the highest logistics cost because these systems require separate collection of biowaste. Nevertheless, collection costs are also significant for the incineration system as the collection frequency of mixed waste is higher and the pick-up rate lower when no separate collection or local treatment option is implemented. It must be noted that the waste collection frequency in Porto is quite high compared with other municipalities in Europe, partly due to safety and odour concerns in warmer environments; collection costs might thus be substantially lower in regions with less frequent collection (Bianchi-Aguiar et al., 2011).

The share of labour in total costs varies significantly in the different systems. For local composting, labour represents most of the annualised costs (98%, equivalent to 433 full-time equivalent jobs or FTE). For centralised composting and AD, labour also represents the largest share of the total costs (61-62%, equivalent to 758 and 760 FTE) since the separate collection scheme involves high labour costs. Incineration involves a significantly lower share of labour in total costs (31% or 387 FTE). The higher share of labour costs in the local systems means that those become comparatively less favourable in regions and cases where labour costs are higher and more favourable where labour costs are lower.

4.3.2 Regional emissions comparison for the base scenario

The contribution to global warming of the different waste treatment systems, estimated by LCA on the base scenario, is displayed in Figure 4-3. AD showed the best performance regarding GHG emissions (-21.9 kg CO_2e/tonne) with biomethane, the product of AD, replacing natural gas from fossil sources. The high share of low-carbon electricity assumed in

the base scenario results in modest credits for avoided electricity production from energy recovery in incineration. Despite this, incineration exhibits lower emissions (27.4 kg CO_2e/tonne) than centralised composting (89.3 kg CO_2e/tonne) and the local composting systems with and without urban farms (53.0 and 63.9 kg CO_2e/tonne, respectively).

Collection logistics is the main source of GHG emissions in centralised systems, especially for separate biowaste collection in the centralised AD and composting systems. Population density and distance to central treatment facilities were found to influence the environmental



Figure 4-3: Annual GHG emissions for the base case per tonne of household biowaste processed for the five systems, excluding the impact of capital goods. Biowaste treatment includes inputs (e.g. electricity) and gaseous emissions. Land application, use and logistics includes gaseous emissions after application, carbon storage, mechanized compost application and 120 km transport. Avoided emissions include fertiliser replacement, soil erosion, and water retention benefits.

impact of collection, with closer and denser districts performing better. This reflects the importance of efficient route planning and multi-household collection strategies with their respective trade-offs (Gallardo et al., 2010). The outcome, however, could be altered if future waste collection trucks are powered by renewable electricity, which has the potential to reduce transport-related emissions by up to 93% (see Appendix II, 8.). Collection emissions stem from diesel combustion only, hence the indicated values would proportionally change when employing deviating emission intensity values (3.83 kg CO_2/l chosen in this study).

Despite having no collection associated emissions, local composting systems entailed high GHG emissions from treatment and use of compost, which could not be compensated for by the avoided emissions through productive land application of compost. The reason for this is that CH_4 and N_2O are emitted in the composting process and after land application, especially when it is not well managed, as it is frequently the case in home composting. The environmental performance of home composting schemes could be improved if composting technicians are actively involved in educating, monitoring and providing feedback and if suitable bulking material can be sourced, particularly in winter (González-Sierra et al., 2019). Moreover, the benefits of compost on GHG emissions considered in this study may be underestimated as some of its long-term effects are less well studied. Further limitations of the study are described in Appendix II, 11.

Regarding the potential of UA, creating additional urban farms provided a moderate reduction in emissions, mainly due to reduced surplus compost logistics and increased avoided emissions from land application. The transferability of the insights by district typology to other cases is described in Appendix II, 10.

4.3.3 District level differences for the base scenario

The regional results shown above were obtained by aggregating the economic and environmental impacts of individual districts. The results at the district level (base scenario) are shown in Figure 4-4. The districts of the Porto metropolitan area exhibit considerable differences in population density (Figure 4-4-A), distance to the central treatment facilities (indicated in Figure 4-4-A), and amount of peri-urban farmland (Figure 4-4-C), all with a strong influence on the outcomes. Population density directly affects the potential for home composting implementation (Figure 4-4-B).

The main factor influencing the cost of waste management in the different districts for the local composting system (Figure 4-4-D) was the potential for home composting (applicable for 29.4% of all citizens). Home composters require less infrastructure, maintenance, and monitoring than composting islands, and therefore encompass lower costs to operate. A study of different biowaste management options in Canada reported similar cost differences between home composting ($42/tonne) and community composting ($118/tonne)(Adhikari et al., 2010). The highest cost of treatment per capita was observed in districts with a low population density and low potential for home composting. These areas are mostly constituted by distant semi-urban houses without gardens and therefore, its composting islands are used by a lower number of citizens than the islands in urban areas (AppxII-Figure 12). These

results suggest that the design of a new biowaste management system should consider such local peculiarities. The cost per capita in this system in general was not significantly

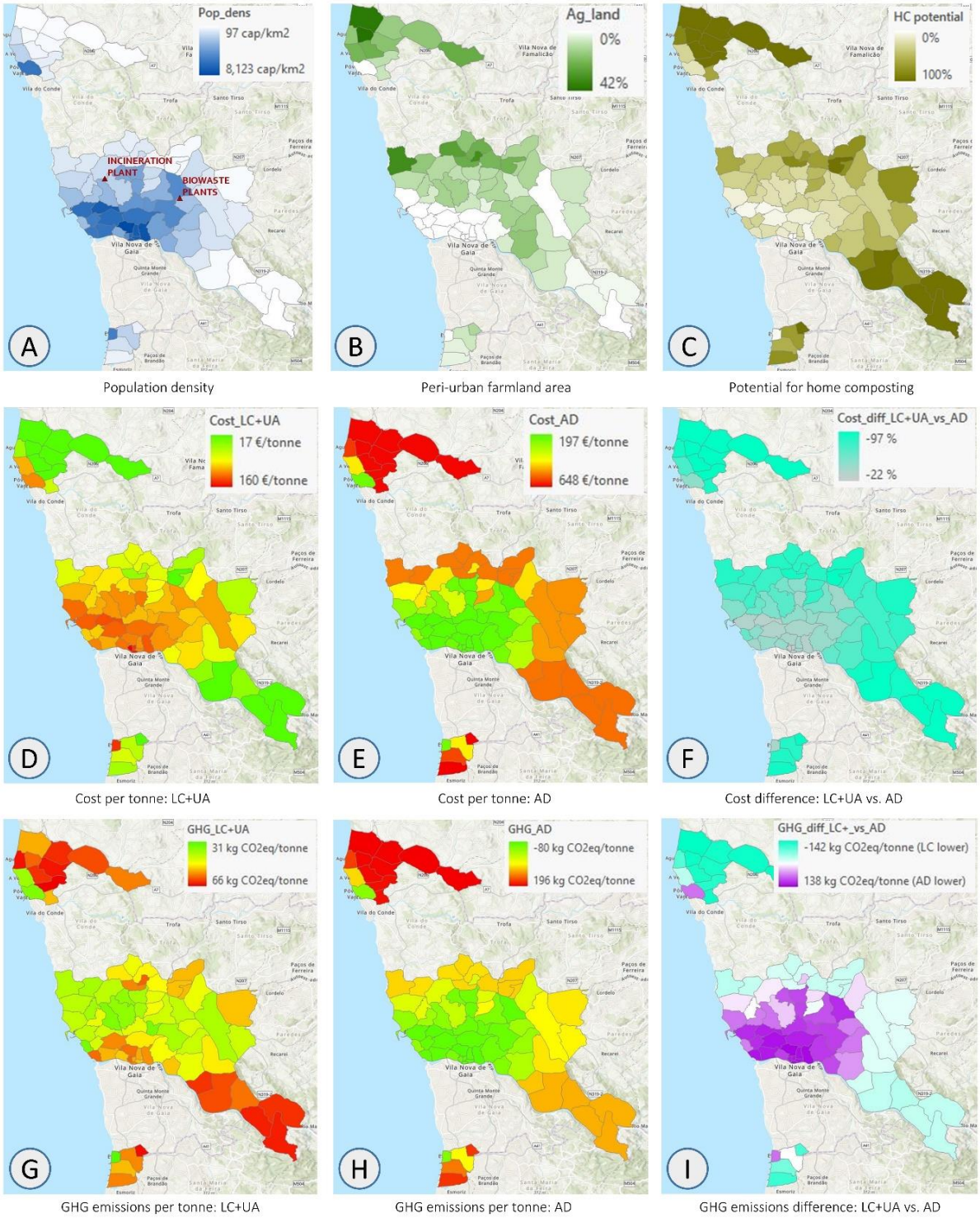


Figure 4-4: Particularities of the districts (4-A and 4-B), potential for home composting implementation (4-C) and district-level outcomes for annualized cost (4-D to 4-F) and GHG emissions per tonne (4-G to 4-I) for the local composting + urban agriculture, the centralised AD system and comparisons between the two systems. The indicator for the biowaste plants (4-A) describes the location for the industrial composting and the anaerobic digestion plant.

A district comparison of the waste management cost of local composting and Cent. AD is shown in Figure 4-4-F. Local composting allows savings between 17% in urban areas closer to the central treatment plants to 97% in more rural areas further from the central treatment plants.

District comparisons of the annual GHG emissions per capita are displayed for the LC+UA system (Figure 4-4-G) and the Cent. AD system (Figure 4-4-H). The main factor influencing GHG emissions in the local composting system was the home composting potential. Home composting would produce more emissions than composting islands since it would not be continuously monitored by a technician. Another key factor influencing GHG emissions in this system per capita was the sink area available to mitigate the negative emissions through productive land application.

The main factors influencing GHG emissions in the different districts for the Cent. AD system were population density and distance to the treatment facilities. The GHG emissions were highest (195.52 kg CO_2e/tonne) in the more remote districts with a low population density. The main reason for this is the increased emissions from collection and transport.

A district comparison of GHG emissions between the local composting system and the centralised AD system is shown in Figure 4-4-I. AD has a better environmental performance than local composting in districts with a higher population density and closer to the treatment units (shown in purple). Conversely, local composting has a better environmental performance than AD in districts with lower population densities and more distant to treatment facilities (shown in cyan). Similar findings were observed for the district comparison of local composting with centralised composting and incineration (data not shown).

A district-level comparison was also carried out to estimate the effect of increasing the sink potential in waste treatment costs and GHG emissions of the local composting systems (LC vs LC+UA). The effect of increasing the sink potential on cost savings was small, only up to 6.3% in denser urban areas with a high potential for urban land conversion. Conversely, the effect of increasing the sink potential on GHG emissions was more pronounced, with emissions savings of up to 60% in dense urban areas with a high potential for urban farms.

4.3.4 Implications of urban farming and surplus compost

Although the compost produced in the local composting systems is primarily destined for the citizens using the composting islands and for the local farmers, surplus compost, which has to

be transported out of the region, might be generated. The concept of increased urban sink area with productive use (e.g. through increased urban agriculture) allows more compost to be used locally, especially when it can easily be shared between districts through short-term storage at recycling centres.

The implications of the available local sink area on annualised cost and GHG emissions for the different municipalities were assessed for two different scenarios (Figure 4-5). Municipalities differed in the amount of existing peri-urban farmland (excluding any private garden land), land potentially convertible to urban agriculture and the potential for home composting implementation (reducing the amount of compost generated in compost islands).

In the base scenario, the main sink for compost was the peri-urban farmland and sufficient productive sink area is available in most municipalities to assimilate the compost produced by the local composting systems. In both scenarios, creating additional urban farms would only

	Aspect	Farmland per person (excl. HC)	Land to UA conversion possible	Potential for home composting	Compost surplus (LC)	Compost surplus (LC+UA)	Difference LC+UA vs LC	Difference LC+UA vs LC
	Municipalities	*m2/cap*	*%*	*%*	*%*	*%*	*Cost*	*Emissions*
Base scenario	Espinho	32.0	2.7%	48.2%	29.4%	0.0%	-2.4%	-19.0%
	Gondomar	47.5	0.4%	41.4%	18.7%	3.6%	-0.9%	-12.7%
	Maia	78.8	0.5%	38.3%	0.0%	0.0%	-0.5%	0.1%
	Matosinhos	26.7	0.6%	19.0%	34.9%	26.3%	-1.1%	-21.8%
	Porto	0.1	1.5%	13.9%	93.1%	64.2%	-2.5%	-39.9%
	Povoa de Varzim	267.2	0.4%	48.9%	0.0%	0.0%	-1.1%	-0.1%
	Valongo	33.1	0.4%	36.6%	28.0%	12.9%	-1.1%	-17.5%
Scenario 'no peri-urban farming'	Espinho	Same as above			91.3%	0.0%	-5.5%	-42.1%
	Gondomar				92.4%	39.2%	-3.0%	-34.8%
	Maia				91.2%	37.1%	-3.2%	-37.5%
	Matosinhos				94.2%	65.6%	-2.3%	-38.1%
	Porto				93.9%	65.0%	-2.5%	-40.0%
	Povoa de Varzim				90.7%	20.1%	-5.4%	-37.8%
	Valongo				93.5%	43.2%	-2.9%	-38.1%

Figure 4-5: The influence of increased urban agriculture in the local composting systems on surplus compost, annualized cost, and GHG emissions. The alternative scenario considers that compost from compost islands is not used for food production on existing peri-urban fields. Any surplus compost is considered to be applied to land non-productively

marginally reduce costs since surplus compost logistics (transporting compost from islands to semi-central short-term storage and central long-term storage) have little weight on the annualised cost.

For GHG emissions, converting land for urban agriculture would be more beneficial, especially in the denser municipalities of Matosinhos and Porto. Nevertheless, more urban

farms would not be able to assimilate all compost generated in such areas. In the scenario where none of the compost is applied on peri-urban farms, there is a higher impact of creating additional urban farms in the reduction of emissions (37.5-42.1%). The outcome of this analysis suggests that city planners would need to consider whether the benefits of local composting and urban farms justify the land footprint they require, particularly in denser neighbourhoods. Nevertheless, the positive experiences from urban farming and community composting trials with face-to-face interactions across Spain (Comesaña et al., 2017) and the Horta à Porta urban farm program in Porto have shown that the engagement of citizens in waste and farming practices could bring a range of other benefits, including facilitated education and awareness about food waste reduction, resource circularity, and changes in diet (Benis & Ferrão, 2017; Slater & Aiken, 2015).

4.3.5 Analysis of alternative scenarios on the regional level

The base scenario, described in the methods section, is based on the most likely development for key assumptions such as renewable content of the electric grid, productive application of compost, adoption of compost in peri-urban farms, amount of land convertible to farms, and performance of the composting process. A scenario analysis was conducted to assess variations of these parameters and assumptions.

The outcome of the scenario analysis had a generally low impact on waste management costs. The biggest impact on costs is the scenario “external land application”, in which the possibility of spreading liquid digestate on land would decrease the cost of the Cent. AD system by 4.3%. Conversely, in the scenario ‘no peri-urban farming’, the cost of local composting would increase by 2.6% and 1.1% in the systems without and with urban farming, respectively.

The outcome of the scenario analysis was more significant for GHG emissions (Figure 4-6). The scenario ‘no changes to the grid’, which considers the carbon intensity of the electricity grid existing in 2018, results in higher carbon benefits for the electricity generated by the incineration plant and more process emissions for centralised AD and composting. According to this scenario incineration would have a better impact than AD on GHG emissions; similar results have been reported by previous studies (Chiew et al., 2015; Salemdeeb et al., 2018). Further comparison with literature can be found in Appendix II, 9.

If regulations for liquid digestate application favour land use (see scenario ‘external land application’), the AD system would become even more attractive in this study, while the three

composting systems were also shown to reduce their GHG emissions slightly. To realize the benefits, farmers would have to reduce their synthetic fertiliser application to prevent overfertilization. A mixed solution, featuring local composting and a more central AD plant, would provide farmers with a variable choice of organic fertiliser and soil amendments.

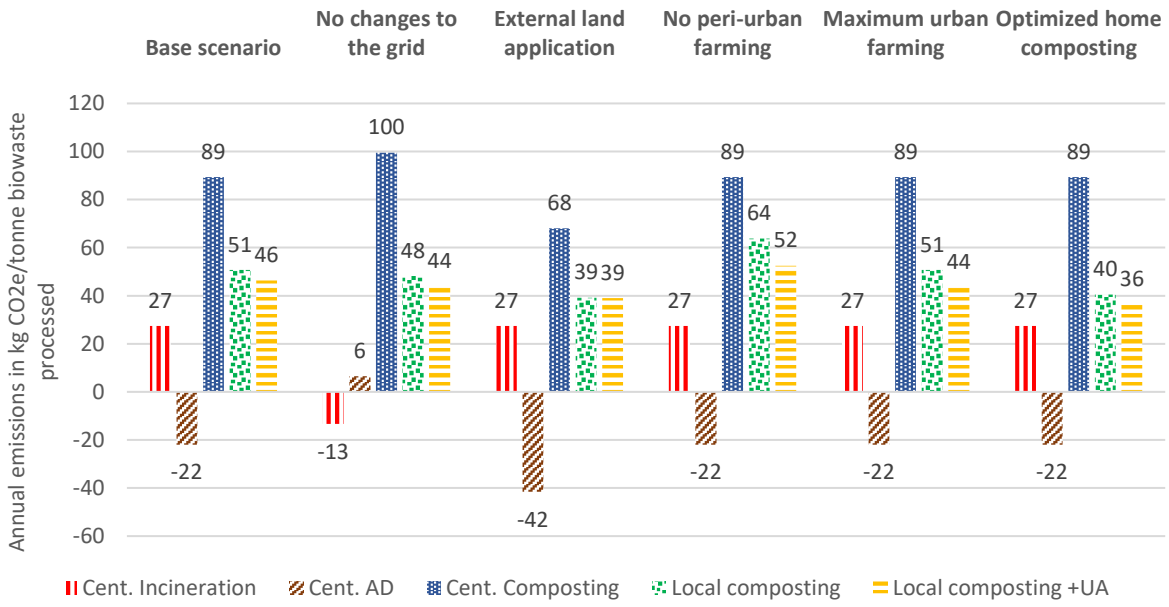


Figure 4-6: The influence of the different scenarios and their parameters on annual GHG emissions for the five biowaste management systems.

In the scenario 'no peri-urban farming', where farmers do not use the locally produced compost, emissions would increase for the local composting systems, in particular without additional urban agriculture.

In the scenario 'maximum urban farming', by increasing green and vacant land conversion to urban farms, emissions could be reduced slightly for the LC+UA system. This was mainly due to the reduction in emissions attributed to productive land application. The results indicate that the GHG emission benefits of productive land application of compost (e.g. including fertiliser replacement and reduced top-soil run-off) are significantly higher than the emissions related to transport of compost outside of the municipality. This means that prioritising productive over non-productive applications of compost is more critical than choosing the location of compost application; a strong argument for the creation of additional urban farms is their role in ensuring a (local) productive application of compost.

Lastly, in the scenario 'optimised home composting', better performance of the home composting would lead to a decrease in process emissions. This could be achieved by

educating and enabling households to monitor and churn their compost to prevent anaerobic decomposition.

4.3.6 Nutrient recovery potential

In addition to GHG emissions, a key factor of biowaste management is the circularity of nutrients, in particular critical raw materials such as phosphorus (P). The annual potential of the products of the different waste management systems to replace mineral P was estimated (based on the recovery rates indicated in the SI 3.3, 3.5 and 6). The estimated replacement rate was 72.2 tonnes for centralised composting, 55.3 tonnes for AD, and 63.4 tonnes for the local composting systems (considering surplus compost is used productively). This would respectively cover 47%, 36% and 32% of the regional needs for P use, when assuming an application rate of 30.1 kg P/ha farmland (FAOSTAT). The differences observed in P content in the products of the different management systems are due to processing losses (e.g. AD pre-treatment), and non-productive applications (for home composting). The difference between the two composting systems sheds light on the importance of the final (productive) use of compost.

4.4 Key messages

This study investigated the waste management costs and environmental impacts of three centralised and two local biowaste management systems, taking into account different scenarios. The novelty of the study lies in the application of spatially sensitive modelling to (1) evaluate the influences of local details such as population density and productive sink area available, and (2) design and assess a scaled-up local composting system with urban farms. An overview of benefits is given in table 2. The main learnings derived were:

1. Local composting has lower costs than centralised models.

Considering the region-wide outcome, local systems had significantly lower costs than centralised models, with labour representing 97-98% of the operational costs. This makes biowaste management through local composting an attractive choice for municipalities.

2. The creation of urban farms has a small impact on the reduction of treatment costs and emissions associated with local composting.

The conversion of urban areas to farms can provide a local destination for the surplus compost produced in local composting systems but the cost reduction associated with the creation of

urban farms is not significant. A small positive impact on global warming can be achieved when additional urban farms ensure that compost is applied productively (i.e. cycling nutrients by replacing synthetic fertiliser) or in urban municipalities with no or little peri-urban farming.

3. The generation of GHG emissions associated with the different biowaste treatment methods is dependent on the local context. Expected changes to electricity grids and trends in compost and digestate application favour anaerobic digestion.

The renewable content of the electricity grid and the possibilities for the productive utilization of compost and digestate are key factors for influencing the GHG emissions associated with the different treatment methods; increasing the share of low-carbon sources in electricity generation reduces the benefits of producing electricity from the incineration waste.

4. Local composting can benefit from improved home composting practices.

Home composting with poor monitoring and non-productive land application make composting less favourable. Better education and capacity building could improve this.

5. Regionally integrated biowaste management plans combining different systems are the best option to achieve cost-effectiveness and emissions reduction.

Municipalities should adopt waste management solutions tailored to their different needs. For instance, separate collection of biowaste and treatment in a centralised AD plant can be implemented in denser and central neighbourhoods, and local composting can be implemented in more remote and less dense neighbourhoods of the same municipality.

Table 4-3: Summary of expected economic and environmental impacts of the biowaste management systems. Benefits are displayed as + and ++ according to the relative performance compared with the other systems.

Aspect	Cent. Incineration	Cent. AD	Cent. composting	Local composting	Local composting + urban agriculture
Cost	+			++	++
GHG emissions	+	++		+	+

Nutrient circularity	+	++	+	+
Soil benefits	+	++	++	++
Job creation	++	++	+	+

Chapter 5 Energy optimisation of plant factories and greenhouses for different climatic conditions

Overview

This chapter presents the following accepted article currently in production: *Weidner, T., Yang, A., Hamm, M., 2021. Energy optimisation of plant factories and greenhouses for different climatic conditions. Energy Conservation and Management (accepted 24th May 2021).*

Among all authors who contributed to the accepted article, T.W. conceptualised the study, performed the modelling and wrote the manuscript, A.Y. supported with the conceptualisation, provided feedback on the modelling and revised the manuscript, M.H. proposed the concept, reviewed the results and revised the manuscript.

This third piece of original work picks up on the insights generated in Chapter 3, which show that the carbon footprint of UA systems employing greenhouse production is very sensitive to energy demand. This chapter also addresses the upcoming trend of vertical farming identified in Chapter 2, which was so far excluded from assessments in previous chapters due to its negligible direct land implications. This study was inspired by the need to operate CEA facilities (including greenhouses and vertical farms) as energy-efficient as possible and the lack of up-to-date comparative modelling studies that assume best practice cases and assess a broad range of climate zones and design and operational choices. The hourly energy demand was simulated by incorporating the external and internal climate conditions into a detailed model of the air conditioning system. The hourly yield was modelled dependent on the interior climate, and the climate control strategy was optimised to minimise the specific energy demand, i.e. the kWh per kg produce. This optimisation was carried out for 19 parameters in one location for two months and in multiple locations with a best-practice design for the entire year. The key finding was that ventilated greenhouses can have substantially lower energy intensities than vertical farms in milder climates, also compared with previous studies. The simultaneous optimisation of yield and energy brought improvements over an energy or yield-only optimisation approach. Additionally, crucial design and operating parameters were identified. The energy intensity of CEA facilities in different locations, obtained in this chapter, forms the input to an assessment of the indirect land use of renewable energy systems supplying CEA facilities, which is the subject of Chapter 6.

5.1 Introduction

The consumption of both a good quantity and variety of fruits and vegetables is paramount for a healthy diet (Willett et al., 2019) and their steady supply is thus of critical importance to regional food systems. Increasing stress on supply chains from crises such as extreme weather events, geopolitical uncertainties and epidemics (Harris et al., 2020) leads to calls for more resilient food systems (Béné, 2020). One way of achieving this is to focus on more regionalised food systems that simultaneously help achieve the UN Sustainable Development Goals (Hamm et al., 2018). This includes the scaling up of localised high-yield controlled-environment agriculture (CEA) systems, such as greenhouses (GH) and indoor vertical farms or plant factories (PF) (O'Sullivan et al., 2019). Although these enable vegetable production in any climate or location, the space conditioning and additional lighting require high energy inputs (Barbosa et al., 2015). The demand for energy, and in particular electricity, is projected to grow and it is often still sourced from fossil fuel due to the slow transition to renewable sources (IEA, 2019). Therefore, a high carbon footprint penalty might be incurred for any potential gain in resilience (Shiina, Hosokawa, Roy, Orikasa, et al., 2011) or self-sufficiency (Till Weidner & Yang, 2019). It is thus recommended to operate as energy-efficiently as possible (Iddio et al., 2020), consider electrification opportunities (Ahemd et al., 2016) such as heat pumps (Y. Tong et al., 2012), use renewable energy (L. Li et al., 2020) and choose the CEA system that is more favourable in the local climate (Graamans et al., 2018). The favourability of specific CEA systems over others rests on multiple trade-offs, such as a closed CO_2-enriched environment versus an open ventilated system or the use of natural sunlight versus a more opaque structure with reduced heating and cooling needs, which is especially relevant in very hot or cold climates (Benis et al., 2017a). These complex trade-offs all affect the comparative energy intensity or specific energy use (i.e. kWh per kg produce), and policymakers and practitioners can benefit from knowing the expected energy use depending on local climate conditions and how it can be reduced through facility design and climate control.

A range of studies have been performed to address this complex challenge for the GH environment(Choab et al., 2019). Most relevant for this work, Van Beveren et al. [17] created a dynamic model which optimises ventilation and heating control based on adjustable setpoints to achieve substantial energy savings of up to 75% during colder days. Cooling via fogging and ventilation was assessed by Villarreal-Guerrero et al. [19], deriving combinational strategies to reduce energy consumption. Vanthoor et al. [18] developed an

economic model incorporating yield and energy use for operational and GH design heuristics, revealing that adapting to local climate conditions through seasonal whitewash, appropriate cover materials, thermal screens and variable cooling systems can reduce energy intensity. A comprehensive model including interactions between yield and energy demand was developed by Golzar et al. [20] and applied to different temperature, light and CO_2 setpoint scenarios, reporting specific energy benefits from optimised lighting and deviations from typical temperature setpoints in climate control. They also applied their model for different locations and found that heating and cooling requirements and thus CO_2 emissions varied greatly.

A simulation-based tool by Benis et al. [21], including vertical indoor farming revealed considerable climate-dependency of the CEA systems for tomato production; substantially lower energy consumption for the GH compared with vertical indoor farming in Lisbon but similar operational energy consumption in Paris, where it is colder (Benis et al., 2017a). A comprehensive comparison of CEA practices for lettuce in three different locations was carried out by Graamans et al. [14], based on PF specific models for evapotranspiration (Graamans et al., 2017). They confirmed the climate-dependency and revealed the potential benefits of PFs over GHs in cold (Sweden) and hot (United Arab Emirates, UAE) climates from an energy perspective. However, for GHs, they did not consider the impact of providing the same light and temperature conditions assumed for PFs throughout the year. A slightly different approach, by Li et al. [13], compared the resource intensity and profitability of open-field farming with CEA practices for several crops. They optimised the net present value based on operating parameters, including their effect on crop yield, and found that PFs with solar PV might be favourable for climate conditions in Singapore.

Previous efforts have highlighted certain aspects of comparing and improving CEA systems. However, it remains unclear how best-practice CEA systems would perform against each other in a given region. Simple heating and cooling needs derived from energy balances are usually considered, rather than the actual performance of electrified heating and dehumidification systems. Further, in the comparative studies, more rigid climate setpoints instead of optimisation are employed (Benis et al., 2017c; Golzar et al., 2018; Graamans et al., 2018; Harbick & Albright, 2016), potentially favouring one system over the other. Thus, a comprehensive assessment is still missing, which a) considers daily and annual fluctuations of outside climate conditions, b) incorporates energy-efficiency heuristics in facility design, c) models the air conditioning system and the spatial climate profile within a facility, d)

optimises climate control and parameters affecting the yield of staple vegetables, while e) applying the same methodology for greenhouses and plant factories.

Addressing the above limitations of existing work, this study develops a new functional model which can optimise hourly space conditioning and specific energy consumption based on outside climate conditions for three types of CEA systems, namely plant factories and closed (non-ventilated) and open (ventilated) greenhouses. With the aid of the use of a reference vegetable basket, this has for the first time allowed these CEA systems to be compared, in their optimised performance, for a common set of diverse regions. The impact of the most relevant parameters and operational strategies has also been assessed to reveal how these factors may affect the comparative performance of these systems.

5.2 Methods

This work focuses on electricity consumption for lighting and climate control as they make up most of the energy consumed (Barbosa et al., 2015; Benis et al., 2017a). The specific energy consumption (i.e. energy consumption per unit output of produce), was optimised for three CEA systems, taking into account outside climate conditions at different locations. The energy consumption is equivalent to electricity consumption in this work. The optimisation models consist of mass and energy balances within the growing facilities and the air conditioning system and consider crop responses to internal climate conditions.

5.2.1 System overview

This sub-section explains the characteristics of the three systems, the mass and energy balances to simulate the interior conditions, technical aspects of the air conditioning system and the choice of crops.

Controlled-environment agriculture system design

The design of the CEA systems was derived from reported energy-efficiency measures with the aim of enabling a fair comparison between the systems based on the best technology available. Table 5-1 shows the main differences between the systems. The PF is an opaque, well-insulated and sealed structure. GHs are transparent structures that experience more pronounced heat exchange with the environment as well as some air infiltration and air exchange through ventilation (only for open ventilated greenhouses, OGH). Thus, GHs lose some of the irrigation and fogging water to the environment, while PFs were considered to have a closed water circuit with continuous dehumidification. The PF benefits from multiple growing layers, increasing the ratio of growing to floor area (T. Kozai et al., 2019). The

volume was chosen to be equal between the CAE systems to enable a fair comparison of space conditioning requirements. As the current best practice to increase the productivity in GHs, sunlight is considered in this work to be supplemented with artificial light from light-emitting diodes (LEDs) (Hemming et al., 2019), to match the target daily light integral (DLI) of the plant. The standard efficacy of the LEDs was assumed to be 2.7 µmol/J (equivalent to an efficiency of 59%). LEDs were the only source of light in PFs, and, contrary to the GHs, the photoperiod was at night. A detailed description of the lighting calculations can be found in section 1 of Appendix III, further details on the systems can be found in section 1 in the Supplementary Information of Weidner et al. (2021).

Table 5-1: The most relevant design parameters for the three CEA systems.

Category	**Aspect**	**Plant factory (PF)**	**Closed greenhouse (CGH)**	**Open ventilated greenhouse (OGH)**
Dimensions	Floor area (m^2)	1,250	2,500	2,500
	Productive space	60%	82%	82%
	Growing layers	4	1	1
	Growing area (m^2)	3,000	2,050	2,050
	Height (m)	8	4	4
	Volume	10,000	10,000	10,000
Exterior	Walls	Opaque structure	North-facing[1] wall solid, other walls and roof translucent	North-facing[1] wall solid, other walls and roof translucent
	Cover type	Insulated concrete	Ethylene tetrafluoroethylene (ETFE) or Polycarbonate (PC)	ETFE or (PC)
	Thermal transmittance or U-Value ($W/(m^2*°C)$)	0.3	2 (ETFE), 2.27 (PC) or 0.5 (Reflective lens cover, RLC)	2 (ETFE), 2.27 (PC) or 0.5 (RLC)

	Solar transmissivity	0	83% (ETFE), 70% (PC) or 28% (RLC)	83% (ETFE), 70% (PC) or 28% (RLC)
	Infiltration rate (vol/h)	0	0.25	0.25
Space conditioning	Radiation at canopy vs at light source	89% (reflective surfaces)	79%	79%
	LED cooling ratio	85% of waste heat	Flexible, up to 85% of waste heat	Flexible, up to 85% of waste heat
	CO_2 level (ppm)	1600 ppm	1600 ppm	Variable supply (see SI 2.3)
	Water loss	None, fully recirculating	Loss only through infiltration	Loss through infiltration and venting
	Heating, ventilation and air conditioning (HVAC) system	Always dehumidification	Dehumidification or cooling only	Dehumidification or cooling only or none
	Other cooling options	-	Fogging	Venting and fogging
	Lighting	LED at night	Sunshine & LED during the day	Sunshine & LED during the day

[1] For locations in the Southern hemisphere, this would be South facing.

Mass and energy balances

Simulating the interior of a CEA facility can be done in multiple ways, e.g. by using simplified assumptions such as considering the space as well-mixed (Stacey & Hildebrandt, 2018; Shengbo Zhang & Schulman, 2017), or by a more complex calculation of the spatial profile using computational fluid dynamics (Kittas et al., 1997; López et al., 2012; Teitel et al., 2008), which, however, makes optimisation very challenging. For this work, it is crucial to capture the interactions in the facility between the plants, the exterior climate and space conditioning efforts, which requires modeling some degree of spatial heterogeneity (Arbel et al., 1999; Ghoulem et al., 2019). Thus, a pragmatic approach was developed which

differentiates three zones; inlet, centre, and outlet. The space was more well-mixed at lower venting (F_{vent}) and HVAC flowrates (F_{hvac}) and with a directional temperature and humidity gradient for higher venting and HVAC flowrates. The HVAC outlets were considered to be more distributed than venting inlets, hence venting elicited a more pronounced gradient than space conditioning through an HVAC. The main mass and energy flows used in the three systems are visualised in Figure 5-1 and described in detail in AppxIII 2.1. Heat exchange occurred between the outside and inside ($Q_{structure}, Q_{solar}, Q_{infliltration}$) of the facility and between the inside air and LEDs ($Q_{LED,PAR}$ and $Q_{LED,heat}$ influenced by $f_{LED,cooling}$,), plants (Q_{SH}), cooling through fogging (Q_{fog}) and fans ($Q_{fans,hvac}$). Water was introduced into the air through infiltration ($m_{w,infiltration}$), plant evaporation ($m_{w,evap}$), fogging ($m_{w,fog}$) and ventilation (due to the difference in water vapour content), and was extracted as condensate ($m_{w,out}$). The air in the three different zones inside the facility and the HVAC inlet and outlet was described through the main properties including temperature (T_{suffix}), water vapour content (ω_{suffix}), relative humidity (RH_{suffix}) and enthalpy (h_{suffix}) where "suffix" refers to the specific locations in the system.

The HVAC operated either in dehumidification mode (including a reheating step), in cooling-only mode or in heating-only mode (only applicable to GHs). The conditions at the inlet and outlet of the HVAC were used to determine the air conditioning requirements. The centre conditions of the CEA facility were used to determine evapotranspiration and the effect of infiltration. Lower and upper climate parameter bounds were applicable at all three locations. In the OGH, the flow into the GH was made up of outside and conditioned air. The total electricity consumption (Equation 5-1) was determined by adding the electricity consumption of the air-to-air cooling, ($E_{fans,a2a}$), refrigeration cycle (E_{RC}), the air-source heat pump (E_{ASHP}), the LED ($Power_{LED}$)and the LED cooling ($E_{cool,LED}$), the fans inside the growing facility ($E_{fans,hvac}$), the fogging system (E_{fog}, GH only), and the ventilation fans ($E_{fans,vent}$, OGH). The loss of water and CO_2 due to infiltration and venting was also considered (see AppxIII 2.1).

$$E_{total} = E_{RC} + E_{fans,a2a} + E_{ASHP} + Power_{LED} + E_{cool,LED} + E_{fans,hvac} + \left[E_{fog} + E_{fans,vent}\right] \quad \text{Eq. 5-1}$$

More detail on the employed calculations can be found in AppxIII: the primary mass and energy balances in 2.1, exchanges with the environment in 2.2, CO_2 level in the OGH in 2.3, thermodynamic relations in 2.4 and physical relations in 2.5.

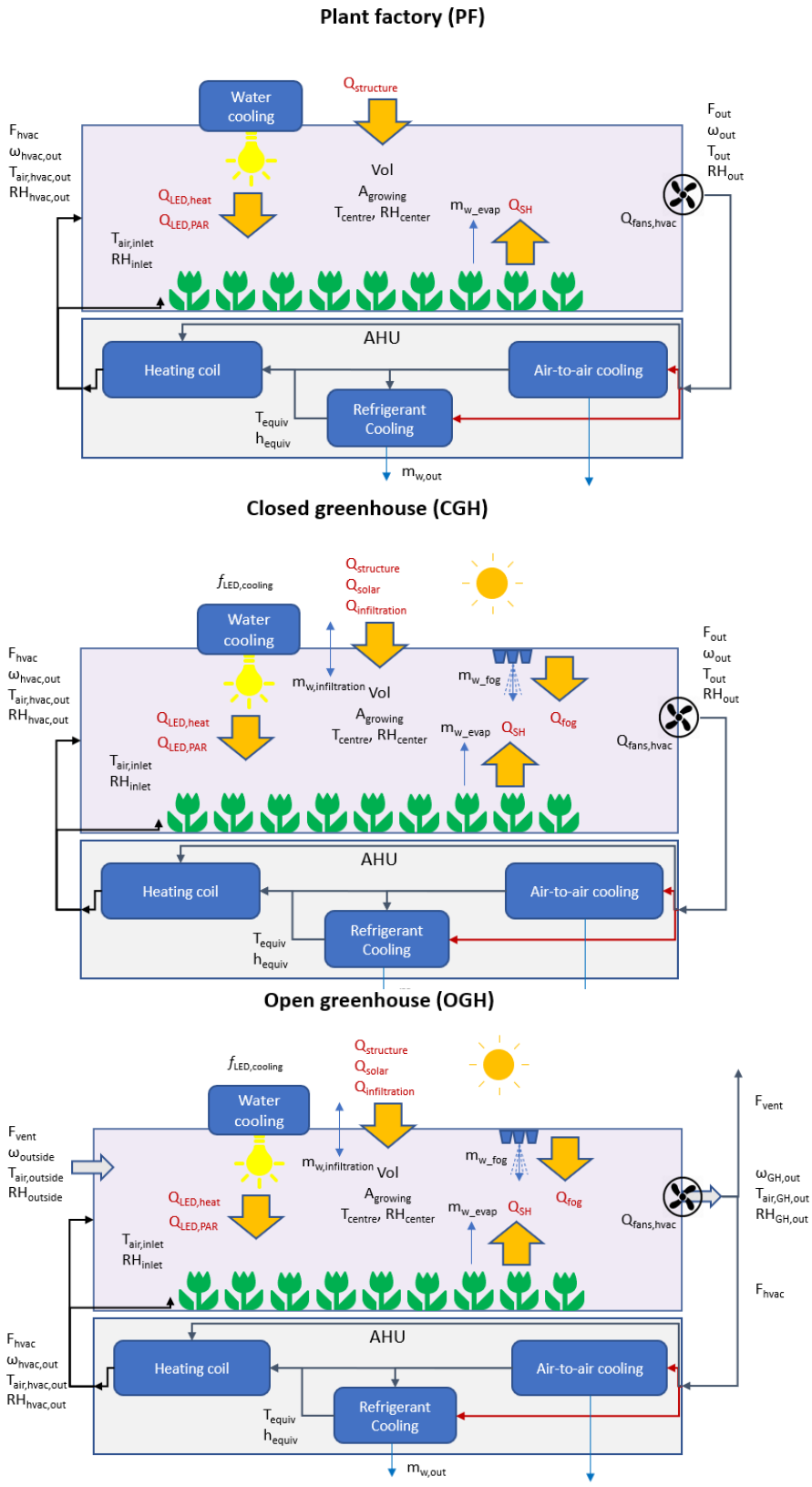


Figure 5-2: Schematic of the mass and energy balances of the three CEA systems. The large arrows depict energy fluxes and the small arrows material flows.

Air conditioning system

Besides heating and cooling requirements, indoor growing facilities need to remove moisture generated by the plants. To adequately assess and optimise the energy use of CEA facilities, the behaviour of the HVAC system has to be explicitly modelled (Graamans et al., 2020), and this work does so by incorporating variable interior and exterior climate conditions. Although currently most GHs are heated with fossil fuels (Russo et al., 2014), this work considers air-source heat pumps (ASHP) for the heating requirements. First, significant carbon abatement potential exists by electrifying the equipment (Bakos et al., 1999; Russo et al., 2014; Y. Tong et al., 2012), in particular with electricity from renewable sources. ASHPs were chosen over slightly more efficient ground-source heat pumps due to significantly lower upfront costs and lower dependency on shallow aquifers (Nemś et al., 2018). A schematic of the HVAC is shown in Figure 5-2, which together with the ducts and fans makes up the HVAC system.

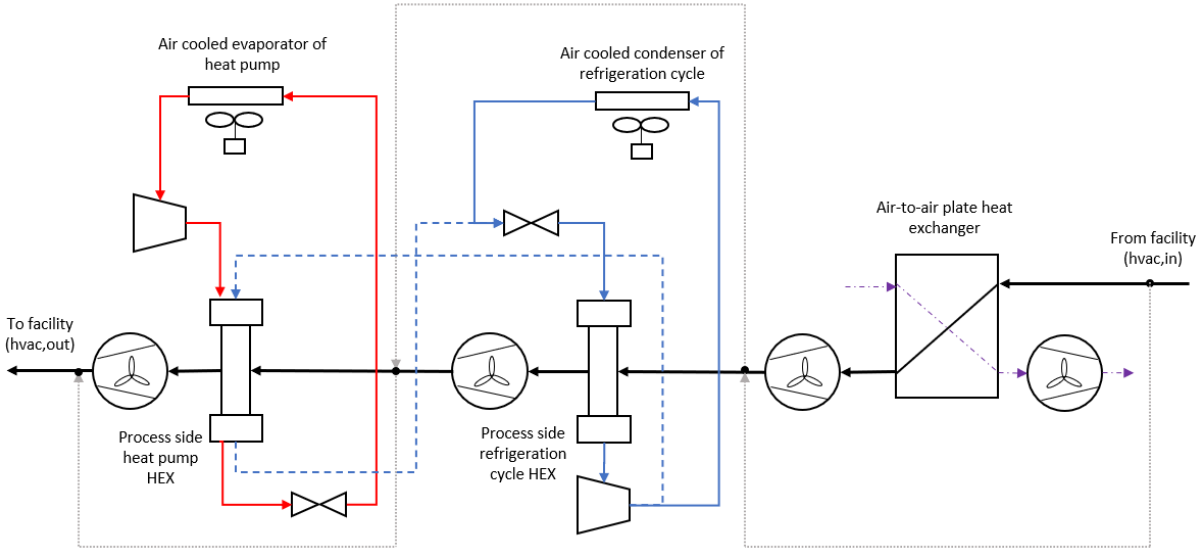


Figure 5-3: Schematic of the HVAC unit, including a counter-flow plate air-to-air heat exchanger, a refrigeration cycle with a cross-flow finned tube heat exchanger for cooling and dehumidification and an air-source heat pump with a cross-flow finned tube heat exchanger for heating. After condensation, the process side heat exchanger of the heat pump can also operate as the condenser of the refrigeration cycle.

The HVAC features a typical refrigeration cycle (RC) in which the heat gained by the refrigerant in the cooling process may either be rejected back to the stream (for reheating after dehumidification) or, for cooling-only processes, to an air-cooled condenser. The concept of the (upstream) air-to-air heat exchanger was inspired by Graamans et al. [33] and expanded

with the option for partial bypassing to reduce the use of this heat exchanger (HEX) at warmer ambient conditions (where this HEX would become inefficient due to a lower heat exchange temperature difference). This was mathematically realised by combining the NTU method (Incropera et al., 2006) and a cooling ratio term to iteratively calculate the heat exchange area used for cooling-only and the cooling plus condensation section of the HEX. The relevant state variables of the RC were related to operating conditions via polynomials to allow for a flexible optimisation of these conditions, including particularly a detailed calculation of the coefficient of performance (COP), which also depends on the outside climate. The COP of the LED water cooling was approximated using the same concept. Considered for the electricity consumption were the two compressors, the outside and inside air fans of the RC and ASHP and the two fans of the air-to-air HEX (inside and outside air flows). Further details about the concepts, functionality and dimensions can be found in AppxIII 3.

Vegetable selection

Crops differ in their characteristics; hence optimum settings of the climate system are crop dependent. Since this study intends to assess the production of staple vegetables in GHs and PFs, a vegetable basket, i.e. a proxy, has been defined reflecting the properties of the six most consumed vegetables (www.fao.org/faostat/en/) that can be produced in soilless growing systems (tomato, bell pepper, lettuce, broccoli, spinach, summer squash). A vegetable basket proxy ensures that a global comparison of electricity use is not favouring a particular cultivar (e.g. high yield vs low yield (T. Kozai et al., 2019)) or climate (e.g. hardy vs tender vegetables) while also approximating the actual demand that would need to be satisfied. The vegetable basket is composed of lettuce, broccoli, bell pepper, spinach, zucchini (12.5% each) and tomato (40%). The vegetable basket requires a DLI of 13.7 mol/day with a photoperiod of 14 hours (in the PF), resulting in a reference yield of 38 kg/m2/year. The properties of the crops making up the basket are detailed in AppxIII 4.4.

5.2.2 Plant growth and climate settings

This sub-section explains how evapotranspiration, productivity, the interior climate boundaries and exterior climate conditions were determined.

Evapotranspiration

To calculate the amount of water transpired by the plants (i.e. evapotranspiration), this work uses the method employed by Graamans et al. [22], which balances the latent and sensible

heat with the radiation received by the plant. Equation 5-2 [22] computes the latent heat (LH) equation, depending on the vapour concentration difference (VCD), the leaf area index (LAI), the heat of vaporization at the leaf surface (λ_{leaf}), and the aerodynamic (r_a) and canopy resistance (r_c).

$$LH = LAI * \lambda_{leaf} * \frac{VCD}{r_c + r_a} \qquad \text{Eq. 5-2}$$

The canopy resistance is derived from the stomatal resistance and is calculated differently to Graamans et al. [22] as it includes a radiation term, a vapour pressure deficit (VPD) term and a CO_2 term (Nikolaos Katsoulas & Stanghellini, 2019; Stanghellini, 1987; F. Villarreal-Guerrero et al., 2012). A detailed explanation and rationale for the method and values chosen, including the equations employed, is described in AppxIII 4.1, and a description of all terms is provided in the nomenclature in AppxIII.

Yield and specific energy consumption

The optimisation aims to determine the minimum energy requirements per kg crops produced. This specific energy as electricity (kWh/kg crop) requires an approximation of the daily or hourly crop growth, influenced by temperature, PAR received, and CO_2 levels of the inside air. Crop or yield modelling has been carried out by many studies (Kuijpers et al., 2019; Manikandan & Vethamoni, 2017) and applied explicitly to indoor farms in similar assessments combining energy consumption and crop yield (Golzar et al., 2018; L. Li et al., 2020). In general, the yield models differ in their estimated yield and accuracy due to a limited understanding of the physical and biological processes for each crop (Manikandan & Vethamoni, 2017). Adapted models were therefore selected for this work that were both (1) straightforward to apply and (2) featured parametric sensitivities that reflect results from experimental studies and reports from growers. Although structural (e.g. cells) plant growth also occurs at night, the main driver for it is the existence of photosynthesis products generated during the photoperiod (Van Henten, 1994). In this work, it is thus assumed that reference yields in kg m^{-2} $year^{-1}$ for year-round production ($Y_{ref,annual}$) with artificial light supplementation can be converted to daily growth values which are distributed over the photoperiod (t_{photo}, see AppxIII 4.3) as shown in Equation 5-3 to obtain hourly growth or yield (Y_{hourly}). Deviations from the reference conditions are reflected in a change of the yield factor (YF_{total}) which is determined for each of the spatial zones within a CAE by relations between yield and PAR, yield and temperature, and yield CO_2 levels (see SI 4.2). The specific

hourly energy (SE_{hourly}, Equation 5-4) to be optimised for the photo or day period was then assessed by using this hourly yield (AppxIII 4.2), the growing area ($A_{growing}$) and the total electricity consumption (from Equation 5-1). Finally, the average specific energy for the given day ($SE_{product}$, Equation 5-5) was assessed by aggregating the hourly yield during the photoperiod (from t1 to t2) and dividing it by the total energy use during the day.

$$Y_{hourly}(t) = \frac{Y_{ref,annual}}{365\frac{days}{year} * t_{photo}} * YF_{total}(t) \quad \text{Eq. 5-3}$$

$$SE_{hourly}(t) = \frac{E_{total}(t)}{Y_{hourly}(t) * A_{growing}} \quad \text{Eq. 5-4}$$

$$SE_{product} = \frac{\sum_1^{24} E_{total}(t)}{\sum_{t1}^{t2} Y_{hourly}(t)} \quad \text{Eq. 5-5}$$

Interior climate

For the day or the photoperiod, the minimum and maximum permissible temperatures at the inlet and the outlet of a GH or PF were such that the hourly yield is at least 85% of its optimum value. This was done to ensure that the specific energy consumption is not maximised by sacrificing yield through shutting off the climate system since this would be contradictory to the business model of high-tech farming operations. For the night or dark period, the permissible temperature range, which was assumed to not negatively affect the yield, was obtained by reducing the optimum day temperature by 8 °C (Benis et al., 2017c) and allowing a temperature of +/- 4 °C around the optimum night temperature (Rijsdijk & Vogelezang, 2000). To capture the different preferred temperature ranges of certain cultivars and crops in the vegetable basket, the sensitivity to the temperature ranges (shown in Table 5-2) has been assessed in the scenario analysis.

Table 5-2: Permissible day- and night-time temperature ranges and optimum temperature used in the optimisation model for three different crop climate preferences.

Preferred climate	**T_{opt} (C)**	**T_{min}, T_{max} (photo, °C)**	**T_{min}, T_{max} (night, °C)**
Mild (basket)	22.1	15.6, 28.0	10.1, 18.1
Warm	27	20.6, 32.5	15, 23

Cold	16	10.5, 21.2	4, 12

Evapotranspiration is directly dependent on the VPD rather than through the water pressure or the relative humidity. It is thus a more relevant factor for determining a range of climate conditions conducive to optimum plant growth (Shamshiri, Kalantari, et al., 2018). Several studies have reported different VPD ranges that have not negatively affected crop growth in their experiments, sometimes with an optimum range and an acceptable range (Shamshiri, Jones, et al., 2018; Yoder et al., 2005). For this work, a permissible range of 4 hPa to 12 hPa was chosen to constrain VPD inside the CEA facility for all locations.

Exterior climate

Hourly optimisation of the climate control system requires knowledge about outside temperature, vapour pressure and incoming solar radiation (global horizontal irradiation, GHI) for every hour of the day. Since the optimisation was carried out for each hour within a typical day for a given month, available data on the average minimum and maximum daily temperatures within a particular month were used to construct temperature curves while average daily solar radiation and sun-hours were used to construct the solar radiation profile. For the sun-hours, second-order polynomials were developed, which relate the latitude to the average daily hours of sunshine set according to the 15th day of the respective month (see SI 5.1). The GHI values used (daily average) already accounted for the effect of cloud cover. The vapour pressure was assumed to be constant throughout the respective day but never exceeding the saturation level. The data was obtained from https://www.worldclim.org/ and is described in Fick and Hijmans (Fick & Hijmans, 2017); the methodology to construct temperature and solar radiation curves is described in Weidner and Yang (Till Weidner & Yang, 2019) the solar noon was set to 12:30 PM. Eighteen metropolitan regions were selected for this analysis, covering most of the habitable climate zones on Earth (see AppxIII-Table3). They were chosen to ensure a sufficiently different combination of latitude (seasonality), temperature, humidity and solar radiation. Further information on the derivation of sun-hours and the geoprocessing steps can be found in AppxIII 5.1 and 5.2, respectively.

5.2.3 Optimisation

The optimisation of the specific energy was carried out for each CEA system on an hourly basis in order to obtain sufficiently accurate prediction (Van Beveren et al., 2015). This results in a 24-hour operational profile that describes the performance of the CEA system for the given location on a typical day within the given month. This calculation was then repeated

for every month in multiple locations to obtain the average annual specific energy consumption. The inside air flowrate through the HVAC (F_{hvac}) and the share of it sent through the air-to-air HEX ($f_{a2a,share}$), together with the temperature ($T_{hvac,out}$) and relative humidity $\left(RH_{hvac,out}\right)$ of the HVAC outlets and the external airspeed through the air-to-air HEX ($u_{air,a2a,ext}$) were adjusted by the optimisation to achieve minimum specific energy consumption. Further variable elements of control were the fogging flowrate ($m_{w,fog}$) in both GHs and the venting flow rate (F_{vent}) in the OGH. The system was constrained by a minimum air exchange rate (AER_{min}), a suitable VPD and temperature range at the inlet (VPD_{in}, T_{in}) and outlet (VPD_{out}, T_{out}) zones, a minimum temperature (T_{equiv}) after the condensation step to prevent ice formation in the HVAC system, and by ensuring conservation of energy around the crop ($I_{net} - LH - SH \ = 0$). Further, a maximum fogging flow ($\dot{m}_{w,fog,max}$) and LED waste heat absorption by the water cooling $\left(f_{LED\ cooling}\right)$ should not be exceeded. At the night or dark period, the total (as opposed to specific) energy consumption was minimised (with different temperature setpoints) as the high sensitivity of yield to lighting and temperature was assumed only for the photoperiod. Mathematically the optimisation can be expressed as:

Minimise $\begin{matrix} E_{total} & if\ I_{net} = 0 \\ SE_{hourly} & if\ I_{net} > 0 \end{matrix}$

By setting hourly values for

$F_{hvac}, T_{hvac,out}, RH_{hvac,out}, f_{a2a,share}, u_{air,a2a,ext}$ for PF

$F_{hvac}, T_{hvac,out}, RH_{hvac,out}, F_{air,a2a,ext}, u_{air,a2a,ext}, m_{w,fog}$ for CGH

$F_{hvac}, T_{hvac,out}, RH_{hvac,out}, F_{air,a2a,ext}, u_{air,a2a,ext}, m_{w,fog}, F_{vent}$ for OGH

Subject to

$AER_{vent} + AER_{hvac} > AER_{min}$

$VPD_{min} < \ VPD_{in}, VPD_{out} \ < VPD_{max}$

$T_{min} < T_{in}, T_{out} < T_{max}$

$m_{w,fog} < \dot{m}_{w,fog,max} * A_{growing}$ for GHs

$0 < f_{LED\ cooling} < 0.85$

$$I_{net} - LH - SH = 0$$

$$T_{equiv} > 3$$

A description of the terms can be found in the nomenclature of AppxIII, and details of how the optimisation was carried in a computational algorithm can be found in AppxIII 6.

5.2.4 Scenario and sensitivity analysis

There is a host of parameters that will influence the outcome of the optimisation. Some of these are assumptions related to physical behaviour, which may vary within a certain range, and others can be directly influenced by the grower, either through facility design or the level of climate control automation. For practical relevance, a comprehensive range of scenarios or settings of these parameters is assessed for a winter month (short daytime) and a summer month (long daytime) in Stockholm, further described in AppxIII 7. and shown in Figure 5 and 6 in the results section. The standard settings are as described in the previous sections and as listed in the parameter table (Table 5-1); the assessed crop is the vegetable basket proxy. Further assumptions adopted in this work, as well as some limitations, are explained in section 8 in the Supplementary Information of Weidner et al. (2021) .

5.3 Results and discussion

First, the functionality of the model and the climate control operations in the three CEA systems are visualised on an hourly basis. Figure 5-3 shows the optimised hourly climate profiles and the specific energy consumption, while Figure 5-4 shows the water and CO_2 loss of the three systems for a winter month and a summer month, respectively, in Stockholm. The location and the months have been chosen to demonstrate how the climate control regulates the conditions in the OGH differently.

Second, the results of the scenario analysis are presented to assess the parametric sensitivity of the model by way of the difference to the base case for space conditioning energy (i.e. climate control) and specific energy consumption. Figure 5-5 shows the results for winter and Figure 5-6 for summer conditions. The difference in resource consumption (water and CO_2) for each scenario is shown in AppxIII 8. for winter (AppxIII-Figure 3) and summer (AppxIII-Figure 4).

Third, the optimisation results for the different locations are shown, broken down into the contributions by equipment to the specific energy consumption (Figure 5-7) and the water and CO_2 loss (AppxIII-Figure5).

5.3.1 Hourly optimisation and seasonal behaviour

Figure 5-3 reveals how the climate control affects inside climate conditions and Figure 5-4 how it affects energy and resource consumption. For GHs in winter, night-time heating is alternated with low space conditioning requirements during the day, while ventilation was not chosen by the optimisation in the OGH to achieve high CO_2 levels and reduce heating requirements. The higher CO_2 levels from the start in the CGH result in a slightly higher yield and more favourable specific energy consumption but also higher CO_2 loss from infiltration (green dotted line). The PF, in turn, benefits from colder outside temperature during the night-time photoperiod, resulting in increased air-to-air cooling and refrigeration cycle efficiency. This benefit is lost in July as temperatures are higher than in winter. However, the year-round electricity consumption of LEDs was in great excess compared to the low energy consumption for air conditioning. The warmer summer puts the OGH at a considerable advantage over the CGH, in which ventilation, paired with fogging at the highest daytime temperatures, was chosen by the optimisation to regulate the climate. However, this comes at the cost of considerable water loss. In summer, the yield in the CGH is higher than in the PF due to the slightly higher radiation despite light seasonal whitewash, which was chosen by the optimisation to reduce cooling requirements. Despite the slightly lower yield in the OGH due to near-ambient CO_2 levels, specific energy consumption is lower compared with the CGH, which only relies on mechanical dehumidification and cooling. It is worth noting that in the modelling for regions with hot summers in which the outside temperature is higher than the permissible maximum temperature, venting was not an option, and the OGH behaved like the CGH, with dehumidification and fogging used to control the climate.

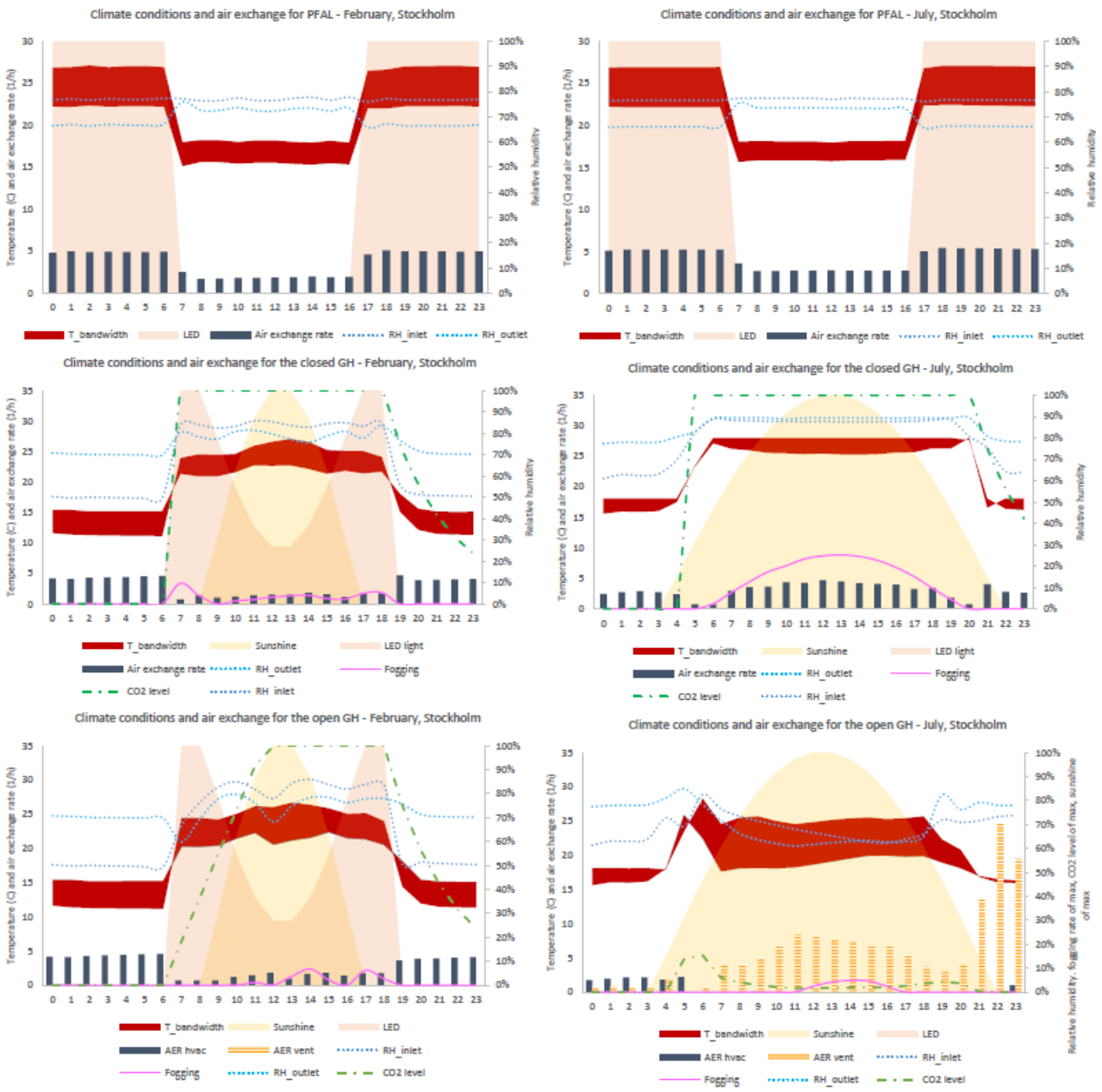


Figure 5-3: Optimised hourly climate control profile of the three CEA systems for a typical day in February (winter, left) and July (summer, right). The temperature is shown as a bandwidth between inlet and outlet zone, the air exchange rate displayed as a bar is in volumes/h (first y-axis), the solar radiation, LED intensity, relative humidity (inlet and outlet zone), CO2 level and fogging are displayed as percentage of their maximum (second y-axis).

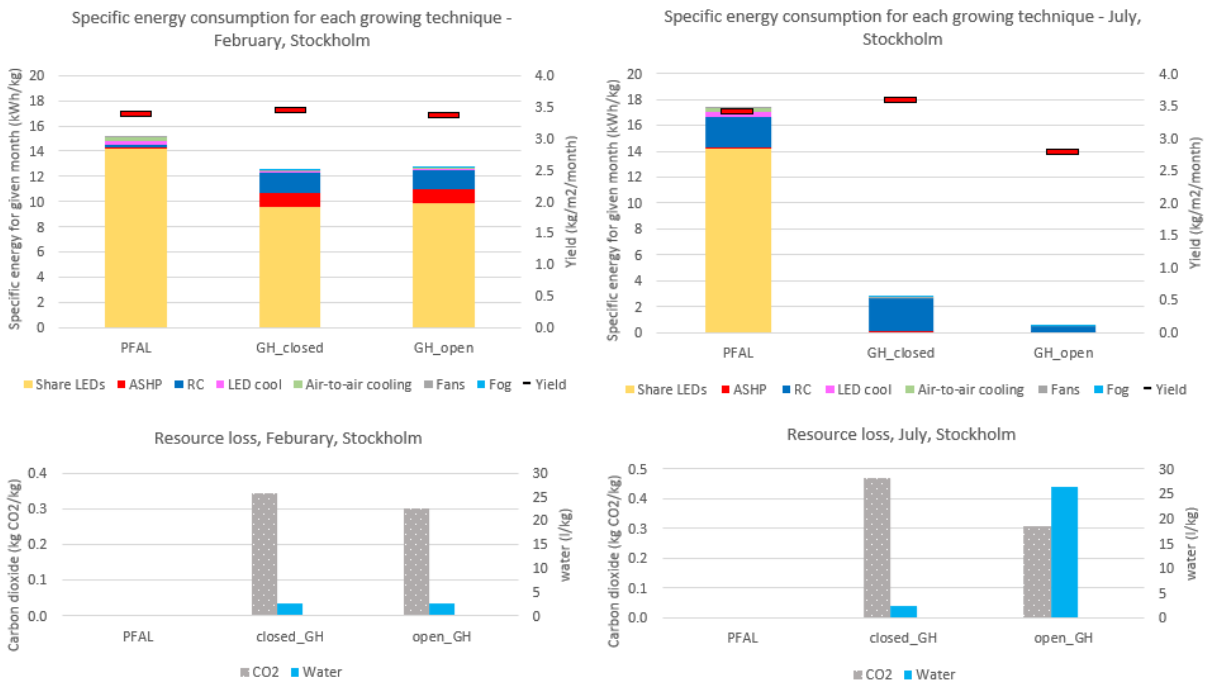


Figure 5-4: Specific energy consumption and resource intensity of the three CEA systems for a typical day in February (winter, left) and July (summer, right). All values are given per kg of edible produce and the obtained yield for the respective month is indicated in the second y-axis. Fan electricity consumption is displayed for HVAC duct and venting fans (Fans) and the process and air side fans of the (re)heating system (ASHP) and cooling cycle (RC). Plant uptake of water and CO_2 was equal and comparatively small and is thus excluded in this comparison.

5.3.2 Influence of physical, design and control variables

The variables describing the physical behaviour of plants and equipment show some sensitivity affecting the comparative results between the CEA system (Figures 5-5 & 5-6):

- The sensitivity of specific energy consumption to stomatal resistance (scenario 1) is generally very little and was highest when it would affect the venting performance in the OGH.
- A narrower VPD range (scenario 2), which some crops and growers might prefer, would greatly reduce the benefit of open venting compared to closed GHs.
- Increased LED efficiency (scenario 3) is more beneficial to plant factories than to open or closed GHs.
- A higher U-value (scenario 4, e.g. from cheaper cover material), significantly increases climate control energy consumption for GHs but slightly reduces it for PFs

(similar to Graamans et al. [33]). Due to increased heat loss, cool morning air in the Scandinavian summer could not be used for ventilation in the OGHs anymore without violating the permissible minimum temperature (thus reducing the ventilation benefits in OGHs). The lower U-value helps with daytime cooling in the CGH.

- All systems benefited slightly from a lower (heat exchange) temperature difference in the condenser and evaporator of the refrigeration cycle (scenario 5); however, this would require more heat exchange area than specified in the assumed design, when operating at the highest loads.

Scenarios 6 to 14 describe facility design and operation choices that the grower can influence:

- If the growing space is smaller (while keeping the dimensions of the HVAC system unchanged, scenario 6), the cooling efficiency becomes higher in summer for CGH and PF and also in winter for PF.
- Incorporating a square geometry (scenario 7) reduces the temperature and humidity gradient slightly and thus favours summer venting in the OGH.
- Halving the size of the heat exchangers (scenario 8) increases velocity and pressure drop at the same duty, hence leads to reduced air conditioning efficiencies, especially for cooling as the air-to-air cooling duty is reduced as well. The appropriate sizing of the HVAC units is thus of paramount importance.
- Aiming to boost production by doubling the DLI received by the plants (scenario 9) increases the specific energy consumption in the CGH and PF as the yield increase is less than the increases in the electricity consumption for LEDs and their cooling. In some cases, this might still lead to higher profits; hence this trade-off needs to be carefully considered. The OGH differs as the increased cooling load in summer can be realised through ventilation.
- The OGH also benefits in summer from an unconstrained CO_2 supply (scenario 10) but this comes at high resource costs (increase from 0.3 to 10.1 kg CO_2/kg crop, see SI S11). The influence on specific energy consumption of the preferred temperature of grown crops (scenarios 12 and 13) is significant and the results are somewhat counterintuitive. A colder climate preference leads in all cases to greatly increased cooling and dehumidification requirements, in particular in the OGH when venting alone was no longer sufficient, suggesting that some cold temperature crops might best

be grown outside in some locations. It needs to be noted, however, that the specific energy consumption of the OGH is ~7 times less than that of the CGH in the base scenario to which those percentage values refer. Studies comparing GHs and PFs could unintentionally favour one system over the other by using disadvantageous colder climate setpoints in GHs (e.g. Graamans et al. [14]). If plants prefer warmer temperatures, electricity consumption goes up in winter for all three systems but the response differs in summer; the CGH benefits from reduced daily average cooling requirements while the OGH needed to resort to mechanical dehumidification in the early evening (contrary to the purely positive response to higher temperatures from Golzar et al. [49]). This means that despite achieving artificial climate conditions in GHs, the choice of crop should still be tailored to the local climate for maximum resource efficiency (L. Li et al., 2020). Switching to mild temperature cultivars or climate setpoints in PFs in winter could reduce electricity consumption for the HVAC by over 50%. The lettuce crop (scenario 11) is closest to the cold climate preference but has a significantly higher yield than the vegetable basket proxy. Small increases in air conditioning requirements were counterbalanced by higher yields in winter, while this yield increase was not sufficient in GHs in summer to balance the much higher air conditioning requirements.



Figure 5-5: Percentage change of climate control and specific energy consumption for the three CEA system and 19 scenarios compared with the base scenario for February (winter) in Stockholm

The remaining scenarios considered cases with less sophisticated climate control capacities:

- Opting to not have water-cooled LEDs (scenario 14) had significant negative consequences in the PF, while, for GHs the cost of such systems needs to be weighed against modest improvements in specific energy consumption.
- Scenario 15 investigated the effect of employing fixed-intensity LEDs. In the PF, this led to longer but less intense photoperiods (18 instead of 15 hours), which showed to be beneficial for climate control. However, some plants might require longer dark periods for healthy growth. Contrary to initial expectations, the constant supply of light and heat in GHs in winter had only a small effect on specific energy consumption. Growers need to evaluate the trade-off between higher control complexity and small total energy savings.
- If a control system aims to merely consider minimised energy consumption (scenario 16), the specific energy consumption would increase due to lower yields. Although this effect was relatively small, higher productivity has the most impact on profit which would justify a combined yield-energy approach.
- Scenario 17 describes facilities that do not employ air-to-air cooling. In winter, this led to a considerable increase in energy consumption, in particular for the PF, which benefits from colder night-time temperatures during the photoperiod. The effect in summer was negligible. The other cooling device, the fogging system, was of paramount importance. Cooling through “ventilation and mechanical cooling only” lead to dramatic increases in specific energy (data not shown) for March in Singapore (+279% and +158%% for the CGH and OGH, respectively) and considerable increases for July in Stockholm (49% and 0.4% for the CGH and OGH, respectively).
- LED cooling might be detrimental for GHs if it is always on and takes away otherwise useful heat, as shown by scenario 18 (the base scenario considers flexible cooling).
- Optimising solely for hourly yield resulted in very high energy consumption for climate control in all cases. The increase in specific energy was particularly significant for greenhouses in summer (6.6 and 18.2 times as much for the CGH and OGH), when intensive mechanical cooling was used to closely control the climate, rather than venting. The increase in yield, however, was comparably insignificant in PFs (2-2.4%)

and small for GHs in summer (10.8% for the CGH and 38.9% for the OGH), not enough to justify controlling the facility in this way.

The sensitivity of the scenarios on water and CO_2 loss through venting and infiltration is small (AppxIII-Figure 3 and 4); the biggest effect on water loss is observed for increasing the DLI and for lettuce (scenario 9 and 11, specific consumption drops as yield increases), for warm climate preferences (scenario 13, increased loss due to higher water vapour storage capacity of air), in the OGH due to increased venting for no air-to-air cooling during winter (scenario 17), in summer for cold climates (scenario 12) and in summer when maximising the yield (scenario 19). The response to the parameters can be divided into positive or negative proportional (scenarios 3,5,6,8,10,12,14,16,18) and non-proportional or non-linear (scenarios 1,2,4,7,9,11,13,15,17,19), with the latter responses fully depending on the CEA system and the outside climate. This means that results obtained in the study may be proportionally adjusted to other cases only for the proportional parameters.

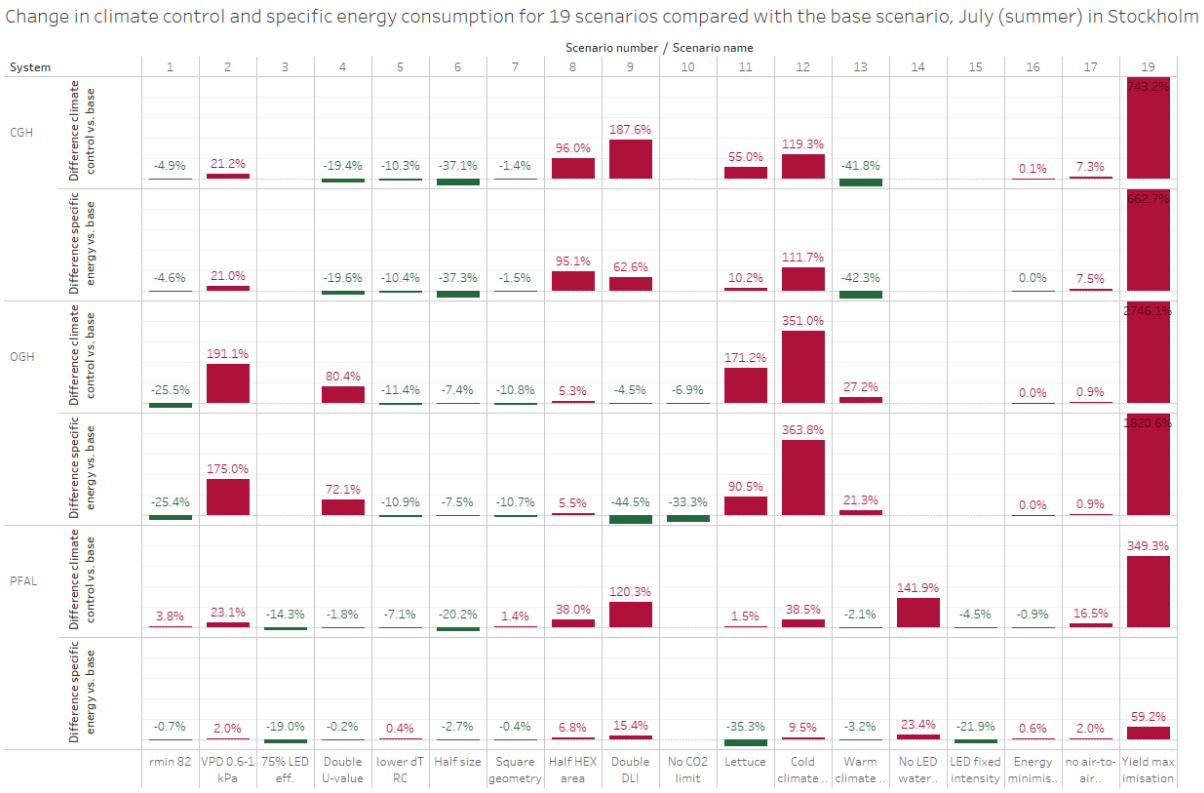


Figure 5-6: Percentage change of climate control and specific energy consumption for the three CEA system and 19 scenarios compared with the base scenario for July (summer) in Stockholm

5.3.3 Location-dependent comparative performance

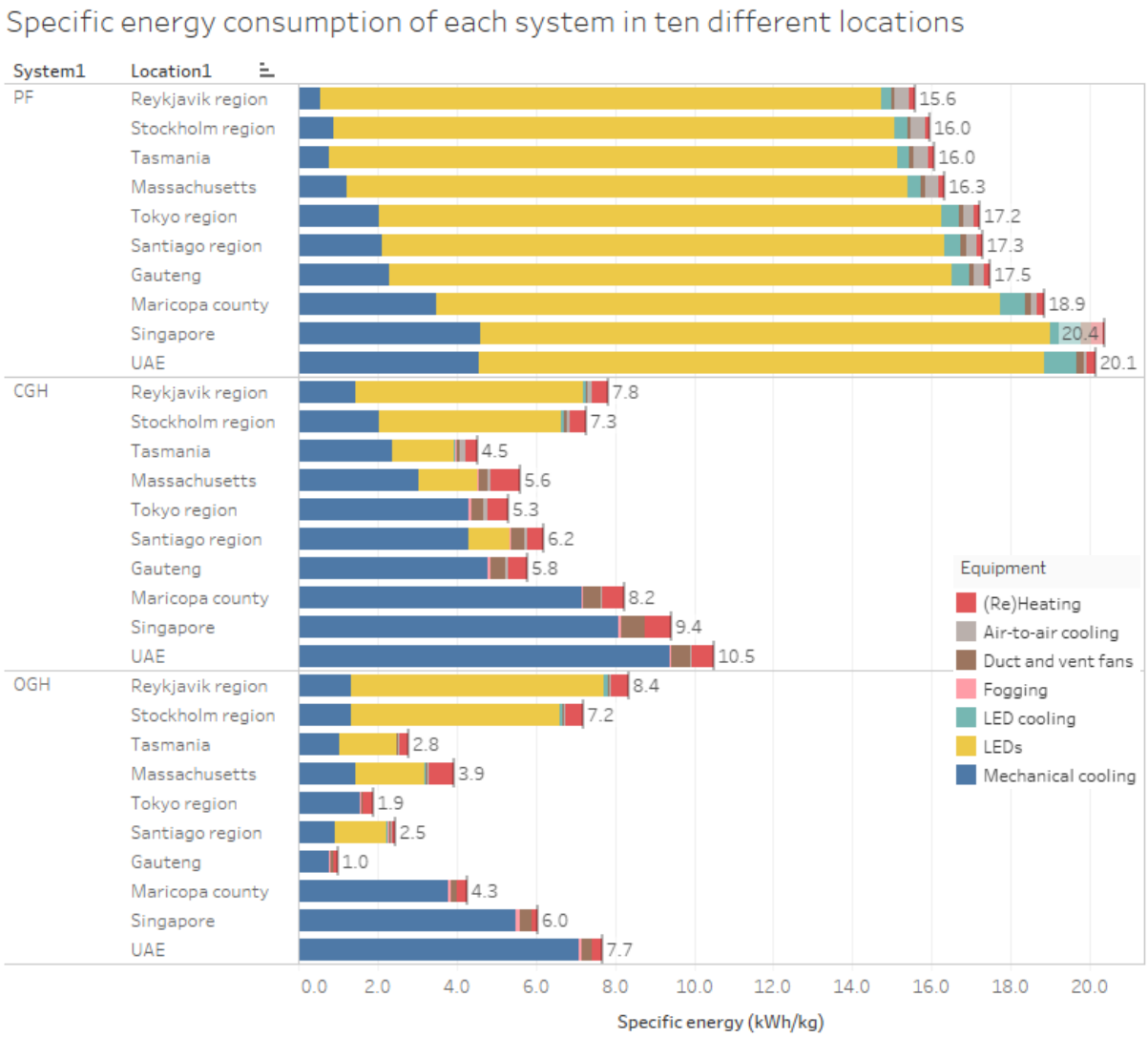


Figure 5-7: Average annual specific energy consumption of the three systems (PF, CGH, OGH) at different locations. The locations are sorted by their average annual temperature in ascending order. Process side fan electricity consumption was allocated to (re)heating and mechanical cooling.

Figure 5-7 shows great differences between the three systems and between the locations, in particular for the OGH. The PF has increased specific energy consumption in hot regions where mechanical cooling is more challenging and higher specific energy requirements in all locations. Interestingly, despite a higher average temperature in UAE compared with Singapore, a lower night-time temperature during peak cooling demand led to lower specific energy consumption in PFs in UAE. The effect of seasonal temperature extremes becomes apparent in the GHs; while Tokyo's average annual solar radiation is lower than in Tasmania or Santiago (listed from lowest to highest solar radiation in Figure 5-7), it does not require additional lighting. On the other hand, constantly high temperatures are detrimental for Singapore and Maricopa in a GH without venting but with the option to vent, the specific

energy can be lower than in the colder regions of Stockholm and Reykjavik. In UAE, temperatures are too high for venting most of the time, leading to only a slight reduction in specific energy consumption for the OGH. In very cold regions such as around Reykjavik, ventilation was not chosen by the optimisation as it would significantly increase heating requirements, which means OGH and CGH have similar results. The reason for the higher specific energy in OGHs in Reykjavik is due to a restriction of hourly CO_2 supply in OGHs imposed in the model to avoid unacceptable CO_2 loss in ventilation, which lead to lower yields in the morning hours (see green dashed line Figure 3). In general, the reduction of specific energy in OGHs compared with CGHs is highest when ventilation could be used as a major contributor to climate control. AppxIII-Figure 5 shows the water and CO_2 loss incurred from the exchange with the environment in GHs for all locations. The CO_2 loss per kg crops is relatively constant, with ~0.35 kg for the CGH and ~0.31 kg for the OGH. Venting in the OGH significantly increases water loss and represents thus a trade-off with energy consumption in water-scarce regions.

None of the locations had sufficient solar radiation to justify installing a refraction lens cover as described by Pakari and Ghani (Pakari & Ghani, 2019). This was due to a lower target DLI considered optimum for plant growth in their work (8.1 mol/m^2/day compared with 13.7 mol/m^2/day in the current study). A calculation of the effect of the cover for the hottest months in UAE by adjusting the yield akin to scenario 9 resulted in a reduction of both cooling requirement and specific energy consumption of around 40% for both GHs. If the solar transmission of the lenses can be increased (e.g. by reducing the spacing between them), it constitutes an attractive option for energy-efficient high-yield GH production in the desert.

5.3.4 Comparison with other studies

Comparison of the results from this work and those from previous studies is far from straightforward due to differences in both the adopted problem settings (e.g. temperature preference, DLI requirements and growing intensities of individual crops) and the slightly different choice of locations. Nevertheless, an attempt has been made to make the results of several relevant studies as comparable as possible. Here, key contrasts to the specific energy consumption of GHs and PFs are presented in Figure 5-8 – which needs to be interpreted with caution due to the aforementioned discrepancies between different studies. Those differences that can be sensibly linked to the variation in the modelling approaches are discussed below. Further comparison with other studies related to operational aspects are described in AppxIII 9.

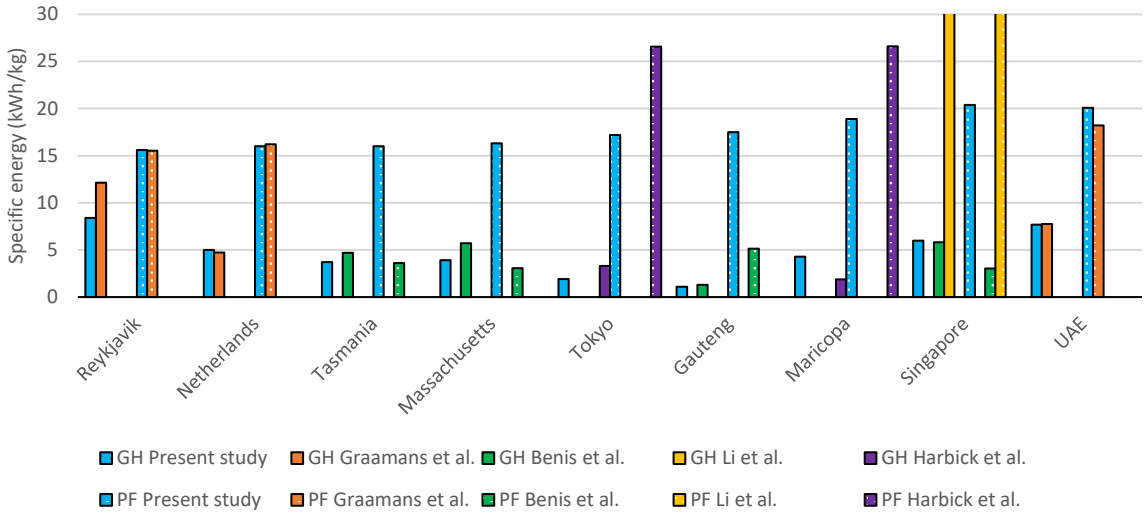


Figure 5-8: Specific energy comparison of this work with previous studies, adjusted for yield according to light levels (see SI 10). The adjusted specific energy for Li et al. is 113.9 kWh/kg for GHs and 59.1 kWh/kg for PFs.

Comparing the results from this study with those from Li et al. [13], who conducted an optimisation for glass-covered (similar to OGH) and opaque (similar to PF) shipping containers for Singapore, it was found that cooling electricity requirements were significantly different. Cooling was a magnitude more energy-intensive in GHs (explained by their equal electricity consumption and cooling needs in kW terms implying a COP of 1, compared with an average COP of around 6.5 for Singapore in this work) and multiple times more for PFs in their work (due to a higher U-value of the walls).

Benis et al. (Benis et al., 2017a) reported a similar water consumption per kg produce and a slightly higher specific energy consumption for the OGH. The difference can partly be explained by the optimised interplay of mechanical cooling, fogging and ventilation in the present study. The opaque shipping containers had a similar share between the energy consumption for cooling and lighting. However, their specific energy consumption was significantly lower compared with the present study. This can be explained by the reported ~3.2 kWh lighting per kg crops (or 47 W/m^2 for 13 hours), which is significantly below what the current study considers necessary to achieve the reported yield with current LED technology.

An indicative comparison with Graamans et al. [14] showed similar energy intensities except in a few cases. In the cold climate, the lower specific energy consumption is due to the modelling of consistent production using supplemental lighting during winter months in this

work, making them more favourable in such climates. In UAE, this work had a higher specific energy consumption, mainly due to higher energy use for climate control, which likely stems from the fixed COP assumed in their study compared with a detailed variable model for the COP in this work. Their work did not report data for locations that particularly benefitted from a more sophisticated GH climate control, where it would be possible to greatly reduce energy demand for OGHs.

The difference for the PF in Harbick and Albright (Harbick & Albright, 2016) is primarily due to their high heating requirements from a poorly insulated building, with lower light efficacy playing a minor role. The lower specific energy consumption in Phoenix for the GH in their work is due to their model relying on evaporative cooling, which would have caused excessive moisture levels in this work. The higher specific energy consumption in the milder location is likely due to sub-optimal climate control.

5.3.5 Recommendations for practitioners

From the parametric sensitivity and scenario analysis reported in section 5.3.2, recommendations can be derived to reduce the energy required for growing. CEA systems benefit from tailoring crops and cultivars to the ideal climate conditions (e.g. tolerating higher temperatures) and adequate sizing of the HVAC system. GHs benefit from covers with low U-values and advanced control systems which can regulate ventilation, fogging and mechanical cooling according to outside conditions. In water-stressed regions, the degree of ventilation can be assessed on a temporal basis (e.g. the extent of seasonal rainfall). Fully closed GHs make sense only if the pest risk is constantly high and significant productivity increases can be realised through high CO_2 levels. There is less justification from an energy perspective for greenhouse operators to invest in LED water cooling (unless symbiotic effects with a host building can be realised), air-to-air cooling in combination with electricity-driven heating and cooling (as process side heat recovery is preferred) and complicated LED dimming schedules. However, those technologies, together with efficient LEDs, are highly recommended for PFs. Indoor growers need to be aware that maximising yield may come at higher specific energy requirements and thus environmental footprints.

The choice of CEA system and design in a given location depends on many factors. The source of electricity (i.e. fossil vs renewable) combined with the specific energy consumption will dramatically influence the carbon footprint of the produce. Although the specific energy consumption is a prime aspect for the sustainability of controlled-environment vegetable production, other factors, such as profitability or land availability, might be more important

for growers. Thus, if land is scarce and expensive, PFs might still be favourable as growing layers and rooms can be stacked as desired. Additionally, existing (urban) space such as empty parking lots and abandoned buildings reduce the upfront cost and environmental impact from the structure. Nevertheless, rooftop and peri-urban GHs, compared to other CEA options, present the most favourable alternative to open-field farming in most cases.

5.4 Conclusions

This work investigates and compares the best-practice energy intensity of CEA systems (plant factories and open and closed greenhouses) for several climate zones. A novel optimisation approach was developed that combines detailed modelling of electrified climate control systems in relation to the outside climate conditions (temperature, humidity, solar radiation) with spatially and temporally varying vegetable yields dependent on the interior climate conditions realised in these systems. It provides a consistent and improved basis for comparison between not just the three CEA systems but also different climate conditions and technical or operational choices and their effect on specific energy and resource consumption.

The approach has been used for hourly optimisation of CEA systems for a whole year in ten different human habitat locations representing a diverse range of climatic conditions. The results indicate that plant factories (i.e. vertical indoor farming systems) are more energy-intensive than greenhouses in all climates. The specific energy consumption of ventilated OGHs is significantly lower than the other two systems, even in more extreme climates, although at a higher level of water consumption. While the lower energy intensity of OGHs is not always contrary to previous studies, the extent of the difference between OGHs and other options identified in this work is stronger than generally reported. This increased favourability of GHs, and especially OGHs, in this work is mainly due to the possibility of optimising greenhouse control.

In addition to the assessment of different locations using the representative parameter settings, the optimisation approach has also been applied to one location for a comprehensive range of parametric sensitivities to understand the impact of assumptions and technical and operational variations. These changes do not significantly change the overall favourability of OGHs but do offer some recommendations for practitioners. The most relevant ones for energy-efficiency are harmonising crop choice (and their preferred temperature range) with local climate conditions in GHs, considering operating at modest DLI levels and installing LED water cooling in PFs.

A range of open research questions for energy-efficient CEA remains. From a plant science perspective, the breeding of high-yield cultivars thriving in controlled environments is yet in its infancy, and an open-access compendium relating yield values of multiple crops and cultivars to light intensity (and respective climate conditions during experiments) would bring substantial benefits to the CEA community. From an energy perspective, the quantitative benefits of geothermal and waste heat for GHs (for direct heating but also enabling vapour absorption refrigeration), the influence of seasonal and daily solar heat storage and transparent PV panels in GHs, and industrial and building symbiosis for GHs and PFs require further assessment. From a life-cycle assessment perspective, the trade-off between building PFs in existing structures close to the consumer and GHs with higher transport (crop and workers) requirements need to be assessed, in particular in locations where the difference in specific energy consumption was less pronounced. Future studies should consider the influence of climate setpoints and crop selections when comparing PF and GH in different locations and consider choosing different crops for different seasons in modelling studies.

Finally, it is important to note that obtaining the performance indicated in this study requires advanced climate control devices, which might not always be available to growers. The modelling methodology employed in this study may be used to determine the optimum (hourly) setpoints for energy-efficient operations, while the actual sensing and actuator control needs to be programmed via control loop mechanisms (not addressed in this work). Results derived in this work for the vegetable basket can be adapted to specific crops by figuring out the respective yield at light levels of 13.5 mol/m^2/day and adjusting the specific energy consumption proportionally. The influence of different climate setpoints is akin to the changes described in section 5.3.2.

Chapter 6 Quantifying the food-energy-land nexus of low-carbon indoor farming: regional implications

Overview

This chapter was submitted to the journal Nature Sustainability and was still under review at the time of submission of this thesis. The title of the publication is "Quantifying the food-energy-land nexus of low-carbon indoor farming: regional implications" and the study was carried out under the supervision of Aidong Yang and in collaboration with Michael Hamm (Michigan State University) and Florian Forster (Boston Consulting Group), who provided some guidance with the conceptualisation of the study and the manuscript.

This last piece of original work continues the enquiry of the previous chapter into the energy aspect of CEA. It describes a novel approach to assessing environmental and resource sustainability as it considers land as one of the central scarce resources in a low-carbon future where renewable energy (typically of a low area density) has a high electricity grid penetration. To provide nutritious produce to city dwellers year-round, the combined total and relative land use of two CEA practices (greenhouse growing and indoor vertical farming) were compared with open-field vegetable farming (with preservation for off-season months). The indirect land use from renewable energy systems, namely solar PV and wind turbines, was simulated, and multiple aspects related to grid design economically optimised. The scale of the investigation is the city-region, which includes the metropolitan area and the rural hinterland. Nine such city-regions were chosen globally for investigation. The spatial extent of the land considered for open-field farming and energy generation (to operate CEA) is more extensive than that of the land use in traditionally defined (peri-)urban agriculture. However, this was necessary when considering a fully regionalised supply of produce as the urban space alone could not provide sufficient quantities of produce through open-field farming (a learning derived from Chapter 3) or generate sufficient renewable energy for CEA. The results from this enquiry show once more that the outcome is very context-dependent and provides recommendations for the considered regions. It thus helps planners and policy-makers to assess which UA approach they should promote within their region for a resilient and sustainable fresh food supply in the future. Providing insights into UA integrated with renewable energy systems completes the enquiries of this thesis.

6.1 Introduction

Food security in highly globalised supply chains was under pressure in the recent pandemic (Béné, 2020), and further shocks due to extreme climate events are expected in the future (FAO, n.d.; Vogel et al., 2019). Calls for increased supply chain resilience (Davis et al., 2021) and higher demand for regional and fresh produce (Shoup, n.d.) lead to a trend of increasing the regionalisation of food production (Richards & Rickard, 2020; Zasada et al., 2017). The fastest growing sector in industrialised countries addressing this development is controlled-environment agriculture (CEA), in particular greenhouses with supplemental lighting and vertical indoor farming (VF) for vegetable production (Agritecture, 2020; S2G Ventures, 2020). Such high-tech growing methods promise improvements on a host of sustainability metrics (Benke & Tomkins, 2017) but perform poorly on energy intensity (Avgoustaki & Xydis, 2020; Barbosa et al., 2015; Graamans et al., 2018). The prospect is that renewable energy will mitigate potentially high carbon emissions associated with energy supply (Avgoustaki & Xydis, 2020; Benke & Tomkins, 2017; Teo & Go, 2021). However, this potentially contradicts claims by the sector related to land savings (Herrero et al., 2020; S2G Ventures, 2020) since most new renewable energy projects are based on solar photovoltaic (PV) or onshore wind energy (IEA, 2020), both of which require large amounts of land (Saunders, 2020). A limiting factor in a low-carbon economy will be land (Gao & Bryan, 2017), with competing uses between biodiversity/conservation (Xie et al., 2020), carbon sequestration (Foley et al., 2005), biofuels (Calvert & Mabee, 2015; Graham-Rowe, 2011), food (Nie et al., 2018) and energy (Leung Pah Hang et al., 2017; Namany et al., 2019). These trade-offs will have to be evaluated on a sub-national level to distribute benefits and impacts (Sasse & Trutnevyte, n.d.) and reduce import dependencies of food and energy (Poggi et al., 2018; Sliz-Szkliniarz, 2013). Thus, the direct and indirect land use implications of food production will be of major importance. Currently, there is a lack of rigorous quantification of these implications, which hampers our understanding of the potential of regional up-scaling of CEA.

For the regionalisation of food production, localising the supply of fresh produce seems to be more desirable (Mead et al., 2021; Ruiter et al., 2016) and feasible (Kinnunen et al., 2020) compared with non-perishable staples or animal products (Peters et al., 2012), with recommendations to convert agricultural land to fruit and vegetable production (Peters et al., 2012; Ruiter et al., 2016) from its current use. CEA facilities often grow fresh produce for local demand (Agritecture, 2020), while advances in electrified transport create opportunities for low-carbon peri-urban field production (Martins-Turner et al., 2020). This work investigates the food-energy-land implications of localised vegetable supply in nine city-regions, selected for their existing interest in VF and their differing climatic and geographical conditions. The satisfaction of daily nutrient requirements via a selection of typically

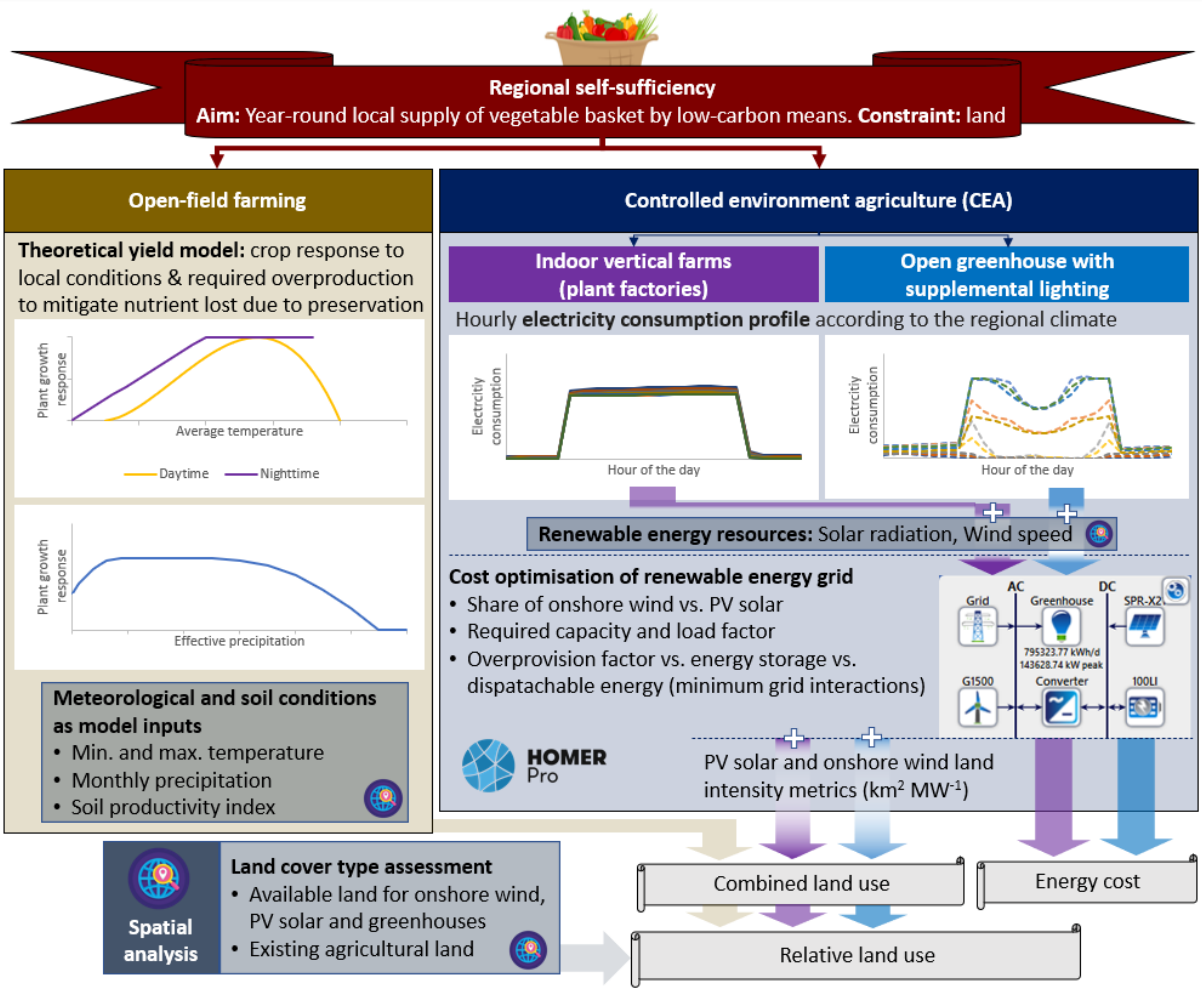


Figure 6-1: Overview of the land-use comparison approach for open-field farming and two CEA farming practices.

consumed vegetables is chosen for comparison of different options for production. The best practices of three growing strategies are compared (see Figure 6-1): plant factories (PF) and ventilated greenhouses (GH) with supplemental lighting and advanced climate control

(Agritecture, 2020) optimised for the lowest specific energy consumption (kWh/kg)(Hemming et al., 2019), and low-input open-field production constrained only by the local climate and soil conditions (but not by poor practice). The open-field option has considered the requirement for food preservation (and the associated losses of micronutrients (Drew & Rhee, 1980; M. Li et al., 2019)), due to the fact that in most latitudes it is unable to produce vegetables year-round. We optimised the climate control systems of the two CEA systems to determine energy consumption patterns and then modelled renewable energy supply systems to cover this need. Each system has a minimum interaction with the larger grid (Laugs et al., 2020; Teo & Go, 2021) and minimises its cost by the best combination of wind and solar PV (Kazem et al., 2017; Khattab et al., 2016) and the balance between overcapacity and energy storage (Johlas et al., 2020; Perez et al., 2019a) to tackle intermittency (Dujardin et al., 2017; Johlas et al., 2020).

The aim of this work is to assess a) the regional characteristics of the renewable energy system required for CEA facilities, b) the combined land use of growing and energy provision, and c) the relative land use against the regional land availability for agriculture and renewable energy generation (see Figure 6-1).

6.2 Methods

6.2.1 Composition and micronutrient characteristics of the vegetable basket

The six vegetables in the basket were chosen based on their relevance in global consumption patterns (FAO, 2021), the feasibility of growing them indoors (usually hydroponically) and micronutrient composition of fresh and processed forms. Tomato is by far the most produced crop and considering a significant share of production for processed use (EU fruit and vegetables market observatory, 2020), it received a share of 25% in the basket, the other five crops received an equal share of 15%. The satisfaction of 50% of the daily recommended nutrient intake (RNI) was used as a basis and resulted for the basket in around 318 grams of fresh vegetables per person per day (see AppxIV-Table S1). This number is consistent with recommendations for a healthy and sustainable diet (Willett et al., 2019). Nine relevant micronutrients for human consumption were considered for this work (Ca, Fe, Zn, ascorbic acid, thiamine, riboflavin, niacin, vitamin B-6, folate and vitamin A), and their content in fresh and preserved (frozen or canned) vegetables was obtained from nutrient tables (Sokolow et al., 2019).

6.2.2 Selection and characteristics of studied regions

Since this study examines how different geographical, climatic, and societal conditions influence growing practice's favourability over another, a selection of regions was chosen. These are in different continents and climate zones but also a) have an existing or upcoming vertical farming industry, b) have a capital city or otherwise prominent city in their centre, and c) country-level data is available on the FAOSTAT portal (FAO, 2021). The regional selection was also in line with our previous work, to enable the use of electricity load profiles of CEA farming facilities. The following heuristics determined the extent of a region considered for this analysis. If the prominent city or region of interest was in a sufficiently small country, the whole country was chosen (Singapore, UAE). If the city or region had an established boundary definition for research, business or statistical purposes that included the whole extent of the urban conglomeration (incl. satellite towns) and sufficient rural hinterland, the established boundary was chosen (Greater Tokyo Area (Wikipedia, n.d.-a), Combined Statistical Area of Boston(Wikipedia, n.d.-c), Stockholm-Mälaren region (Wikipedia, n.d.-b)). If there was no established boundary that would satisfy the conditions, all lowest-level administrative areas (*GADM*, n.d.) (usually municipalities) with their centre within 125 km of the centre of the central city were selected using ArcGIS Pro (Reykjavik, Phoenix, Santiago, Johannesburg). The following steps were carried out in ArcGIS Pro for such cases. The regional population (CIESIN, 2018) was determined through Zonal Statistics. The total regional area was obtained by calculating the geometry attributes. Monthly precipitation, average minimum, and average maximum temperature were obtained from WorldClim (Fick & Hijmans, 2017) and extracted for the regions through Feature To Point and Extract Multivalues to Point. The data set for the land cover types was primarily the Copernicus Global Land Cover (Buchhorn et al., 2020) (100m resolution), with more detailed information on agricultural land from the Corine Land Cover dataset (EEA, n.d.) for Europe and from the USGS (USGS, 2016) for the United States.

6.2.3 Land availability for food production

The existing agricultural land was used as a basis for the land-sparing potential of switching from open-field farming to CEA farming practices. Although only a fraction of agricultural land is typically used for vegetable production (Ruiter et al., 2016), this study conceptualises regional self-sufficiency with a dietary preference for vegetables. Thus, all land currently used for agricultural purposes is considered in this work; code 40 in the Copernicus dataset, code 555-557 in the USGS dataset and code 211-224 in the Corine dataset. The geoprocessing sequence in ArcGIS Pro was Extract by Mask, Reclassify and Zonal statistics (sum). Due to differences between planar and geodesic measurements, each region's total number of raster

pixels was extracted for each land cover type raster. The number of pixels obtained by assessing the respective land cover type was then divided by the total number of pixels and multiplied by the region's geodesic area, allowing accurate determination of the available area for agricultural and renewable energy generation purposes. To determine the regional annual yield per unit area as described in a subsequent paragraph, the average regional values for Soil Productivity Index (UNEP, n.d.) (reclassified to exclude water areas), Moisture Index (Willmott & Feddema, 1992) and Growing Degree Days (derived from WorldClim (Fick & Hijmans, 2017) monthly data according to Ramankutty et al. (2002) raster were obtained by multiplying their source raster with the reclassified agricultural land raster (indicating the location of farmland) and using Zonal statistics (mean). This way, only the on-the-ground conditions at the farmland locations determined those regional values. The direct land use of greenhouses was allocated to the agricultural land and subtracted from the open-field farming land sparing potential. Although greenhouses can also be built on bare land and flat rooftops (Nadal et al., 2017), it was assumed here that primarily it is the experienced farmers who would build them and they would do so on their land. The direct land use of plant factories was not considered as it is often negligible particularly with an increased number of stacked growing beds, and they can be operated underground.

6.2.4 Land availability for energy generation

The brief discussion about the selection of land cover types and their availability is described in AppxIV 1.2. This work's philosophy is to be more on the technically feasible side; we treated land in this way to avoid political differences in land use regulations across regions and time. Straightforward land availability values were chosen for the main scenario reported in the figures, with land cover types shrubland, herbaceous vegetation and sparse vegetation allowing 50% of the land area for onshore wind and solar PV. Also, 5% of the urban land area was considered available for solar PV and 50% of the open forest area (with tree cover between 15-70%). The latter reflects the emerging practice to place newer wind turbines in or close to open forests with minimal destruction, since the actual footprint of turbines and access roads is only between 3-6% (Fthenakis & Kim, 2009; McDonald et al., 2009; McGowan & Connors, 2000) of the considered land and the increased hub height has low detrimental effects on the ecosystem (*Wind Farms Adapt to Forest Conditions - Renewable Energy World*, n.d.). Land cover types completely excluded were closed forests, wetlands, snow and ice, cultivated land, and water. The existing agricultural land was also excluded in this work. Although it is likely desirable to develop renewable energy alongside agriculture (Cho et al., 2020; Miskin et al., 2019), it is currently not common practice and might interfere

with mechanised field operations such as ploughing or harvesting. Additionally, any energy generated on open-field farms could either be used for transporting, processing and storing the open-field produce (Zappa & van den Broek, 2018); excluding the potential use of agricultural land for energy generation thus prevents any double-counting.
Additional constraints for installing solar PV were a maximum slope of 5 degrees (assuming a 2.5 per cent slope (C. D. Yue & Wang, 2006) for all directions and a third of slopes facing SW, S or SE with up to 20 per cent (Deng et al., 2015; Dhunny et al., 2019)) and for wind a maximum slope of 15 degrees (26.8%) (Deng et al., 2015; Hoefnagels et al., 2011). Both were constrained by a relative altitude of 1000 m above the city level (C. D. Yue & Wang, 2006) (due to considerations of difficulties in access and maintenance). Finally, the following were used as constraints for wind turbine siting: 500 m buffer zones around urban areas; land cover by water, snow, and ice (Q. Wang et al., 2014); and insufficient wind speeds for a wind turbine's economic operation (Dhunny et al., 2019) (wind speeds at 50 meters below 5 m s^{-1}). The described heuristics result in some land being potentially available for both technologies. In this case, it was assumed that co-located hybrid plants would be possible and economically preferred (Dhunny et al., 2019; Koc et al., 2019; Sliz-Szkliniarz, 2013) since they save land and the effects due to shade and access restrictions are limited and less than the benefits derived from co-location (Yin et al., 2020). For those locations, a conservative turbine footprint of 5% (in which no solar PV panels can be placed) was used to describe the dual-use of land (Saunders, 2020). An alternative scenario assumed 100% availability of the non-forest land cover types mentioned for solar PV and wind, 10% for solar PV in urban areas and 100% of the open forest areas. These percentage figures mean that the region-specific results reported in this work can be linearly and proportionally adapted to differing land availability assumptions.

6.2.5 Productivity and land use requirement of open-field farming

Reported yield figures by the FAO (FAO, 2021) were insufficient for this work as they are influenced by high-yield greenhouse-based production and are only available at the country (as opposed to regional/local) level. Another issue is the varying level of current agricultural development and intensity between countries; this work intends to compare best practices based on geophysical constraints, rather than social, economic, or political constraints. A hypothetical yield model was thus established to estimate the impact of monthly deviation from the optimum conditions leading to maximum vegetable yields. Three local peculiarities were used in this hypothetical yield model: monthly temperature, monthly precipitation and soil characteristics. A discussion about the influence of temperature and precipitation can be

found in AppxIV 1.3. For daytime temperature, the PGDD (photo growing degree days) method described by Aslam et al. (2017) was used as a basis, incorporating a modest influence from the length of the photoperiod and a minimum (5 °C), optimum (27.7°C) and maximum (40 °C) growing temperature for the vegetable basket (S. Singh, 2018). The yield response to temperature for a given month was then the curve's daytime temperature deviation from the optimum in per cent. The region's photoperiod was correlated to its latitude via polynomials, as described in Appendix III of Chapter 5. The night-time temperature is a linear curve (Parthasarathi et al., 2013) with optimum growth above 19.7 °C and halting of growth at 0° C. Daytime and night-time correlations are shown in AppxIV-Figure 1. The effect of solar radiation on plant growth (relating daily global horizontal irradiation values to photosynthesis) was excluded; we found that adding its effects to that of the temperature-yield response led to a minimum difference and was thus considered negligible.

Besides temperature, the amount of seasonal precipitation affects yields (Huang et al., 2015; Sabiiti et al., 2018), but irrigation and drainage reduce negative influences of low or excessive precipitation (van der Velde et al., 2012) and stretches optimality conditions. A fair comparison with high-tech indoor growing techniques assumes such practices. This work combines the principles discussed in AppxIV 1.3 to a yield response curve relating potentially sub-optimal monthly precipitation conditions to their yield impact (AppxIV-Figure 2). A sensitivity analysis for the precipitation response was carried out, and results are shown in AppxIV-Figure 3.

The last influential variable was the soil characteristics; previous studies considered soil carbon density and soil pH (Ramankutty et al., 2002) or soil depth and nitrogen content (Archontoulis et al., 2020). A fair comparison with indoor farming assumes optimum plant care to supply nutrients (fertilisation) and compost application for soil depth. The productivity of the soil (describing carbon content and pH) was accounted for with a soil productivity index (UNEP, n.d.) (SPI). It can take seven different values (0-6), ranging from prime to bare land (Calvert & Mabee, 2015) and is linearly correlated to yield (Seifert & Moss, 2020) according to Equation 6-1 with a minimum value of 0.5.

$$Yield\ soil\ factor = \begin{cases} \frac{SPI - 1}{10} + 0.5 & if\ SPI > 1 \\ 0.5 & if\ SPI \leq 1 \end{cases} \quad \text{Eq. 6-1}$$

The monthly temperature and precipitation response factors were multiplied (Eq. 6-2) and finally correlated to the maximum achievable yield to determine the local yield (in kg/m^2/year) as shown in Equation 6-3 and 6-4.

$$Monthly\ yield\ response = yield\ response\ to\ temperature * yield\ response\ to\ precipitation \quad \text{Eq. 6-2}$$

$$Local\ annual\ yield\ factor = \frac{\sum_1^{12} Monthly\ yield\ response}{12} * yield\ soil\ factor \quad \text{Eq. 6-3}$$

$$Local\ annual\ yield = \frac{Local\ annual\ yield\ factor}{SF} * maximum\ reported\ yield \quad \text{Eq. 6-4}$$

The maximum yield was determined using the highest reported figures (FAO, 2021; USDA, 2020) (discounting for high-yield greenhouse production) listed in Table S1; its average for the basket is 8.3 kg/m^2/year. A scaling factor (SF) was introduced to account for the fact that year-round perfect conditions do not exist, even for the locations which reported the highest yields for a specific vegetable. Its value (0.74) was the maximum local annual yield factor determined for 25 locations in different climate zones and continents. The results of the hypothetical yield model are compared in AppxIV-Figure 4 with a) the reported yield values from the FAO (FAO, 2021) for the selected vegetables, and b) with conventional GDD and moisture index as used by Ramankutty et al. (2002) with the values of curve parameters determined by linear regression using the FAO yield data for the 16 smaller countries mentioned above. The effects of extreme anomalies (with yield losses of up to 20% (Powell & Reinhard, 2015)) and the potential change to growing conditions due to climate change were out of the scope of this study. Nevertheless, a yearly average of 5% yield loss due to extreme anomalies was accounted for and is also AppxIV-Figure 4.

Since this study takes the satisfaction of daily nutrient requirements as a basis, the reduced nutrient content of preserved food needs to be accounted for by producing more fresh crops during the growing season. Besides the initial nutrient loss from preservation (e.g. blanching or shock freezing, around 24% as an average for the vegetable basket), the subsequent storage loss in freezers or cans was determined as 0.1% per day as an average of reported figures from Drew and Khee (1980) and Rickmann et al.(2007). The total nutrient storage loss, and thus the need to overproduce, was dependent on the length of the growing period (LGP). The LGP (days per year) was determined in monthly intervals; the average minimum temperature had to be above 0 C° and the average maximum temperature below 40 °C (S. Singh, 2018). The months in between were assumed to be productive with a harvestable fraction of the vegetable basket (due to different harvesting periods for the chosen crops), except the first

month. An overproduction factor (OP) was defined for these considerations and is further described in AppxIV 1.4.

Besides yield and overproduction, the land use is affected by an additional footprint of paths and other infrastructure, resulting in a land coverage of growing beds of 82%, equal to greenhouses (Federico Villarreal-Guerrero et al., 2012). This was combined with the yield, the overproduction factor and the daily requirements described earlier to obtain the open-field farming land use per person (in m^2 $person^{-1}$), as shown below.

$$Land\ use\ per\ person = \frac{1}{local\ annual\ yield\ * \frac{1}{OP} * 82\%} * 0.318 \frac{kg}{day} * 365\ days \qquad \text{Eq. 6-5}$$

6.2.6 Electricity demand for CEA facilities

The hourly electricity demands (i.e. load) to produce vegetables in the CEA facilities are needed to reliably estimate the extent and cost of the renewable energy infrastructure required. This demand was modelled by combining established principles and sub-models employed in the literature of plant factory and greenhouse modelling, while incorporating several novel methods for climate regulation and yield-energy optimisation (detailed methodology in Chapter 5). The optimisation determined the minimum electricity input per kilogram of produce for plant factories and open (ventilated) greenhouses with electrified humidity and temperature regulation. The calculated hourly loads were calculated for a typical facility size. To estimate the regional energy requirements, those values were extrapolated based on the annual facility yields, the number of inhabitants of each region, and the required vegetable production to satisfy 50% of daily RNI.

6.2.7 Land use for renewable electricity supply

The land required for renewable energy facilities depends on the required installed capacity of solar PV and onshore wind and their respective land-use efficiencies (i.e. square metres per Watt capacity). The required capacity depends, apart from the load profile, on the amount of energy storage available (in equivalent storage days) and the interactions with the existing electricity grid. A brief discussion about the assumptions and trade-offs is provided in AppxIV 1.6.

The CEA facilities act as quasi-independent prosumers. Therefore, the maximum interactions with the regional grid are set to 10% of the annual load (assuming access to dispatchable low-carbon energy), while the economic trade-off between storage and overcapacity is evaluated with the Homer Pro (*HOMER*, n.d.) software, using near-term projected equipment costs.

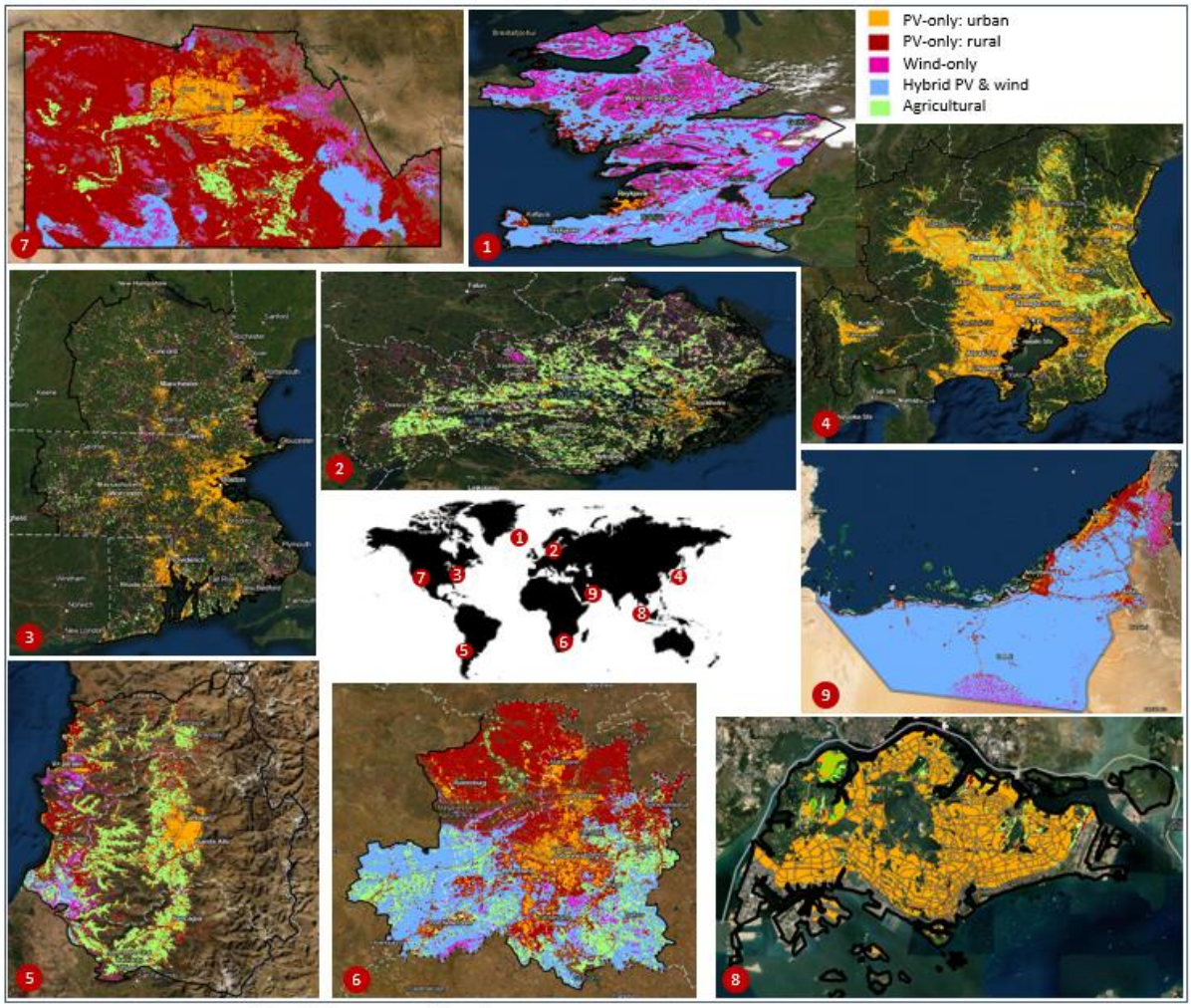
Homer Pro is a grid simulation software for renewable energy applications initially developed by the National Renewable Energy Laboratory in the US and is used to evaluate the set-up and cost of microgrids (Kazem et al., 2017; Khattab et al., 2016; Vallati et al., 2015). Considering plant factories, the annual dispatchable energy restriction resulted in storage days and overcapacity similar to the results from the studies mentioned in AppxIV 1.6. The standard grid purchase price is set at 0.10 USD/kWh, inflation and discount rate are set at 2% and 6%, respectively, and sell-back to the grid was not permitted to avoid sizing a facility more towards a renewable energy investment project instead of one for powering CAE. The potential revenue from grid sales as an alternative scenario was calculated for visualisation. The wind speed values were scaled according to the regional average for suitable locations described in the land availability section. If an initial analysis of combined land use resulted in exceeding land available for wind while occupying only a small share of the land available for solar PV, another optimisation was carried out in which a maximum wind capacity was set (Boston and Tokyo). Wind energy was fully disregarded in the optimisation if there was no suitable land for wind turbines (Singapore). Other project settings and equipment efficiencies are described in AppxIV 1.7. A scenario analysis encompassing alternative grid interactions, zero-cost storage, night-time operations, and a single energy source (offshore wind and solar PV) was also carried out to assess their impact on the required power generation capacity.

The second factor determining the required land is the ratio of capacity to land (or land-use efficiency). A brief discussion is provided in the SI 1.6; this study assumes 6 MW/km^2 for onshore wind energy and 76.6 MW/km^2 for solar PV. As described above for co-located plants, 5% is added on top of the solar PV land use to account for wind turbine footprint and other interactions. The corresponding equations for the per person and relative land use are further detailed in AppxIV 1.8.

6.3 Results

6.3.1 Regional characteristics and land availability

The investigated regions are either state or national capitals with their rural hinterland and, in some cases, a region constitutes an entire (small) country. Figure 6-2 shows the current agricultural land and the potential land area available for renewable energy generation. Our



	Population density (people km-2)	Windspeed at 50 meter (m s-1)	Solar radiation (kWh m-2 day-1)	Share of land currently allocated to agriculture	Available area for renewable energy
1 Reykjvaik, Iceland	23	8.0	2.1	2.7%	41.7%
2 Stockholm, Sweden	93	5.3	2.8	12.7%	3.5%
3 Boston, US	315	5.0	3.7	5.6%	2.8%
4 Tokyo, Japan	1,210	4.8	3.8	8.6%	1.7%
5 Santiago, Chile	265	4.9	5.5	16.9%	32.4%
6 Johannesburg, South Africa	300	4.9	5.6	15.6%	34.1%
7 Phoenix, US	142	4.6	5.4	6.0%	37.7%
8 Singapore	8,423	0.0	4.6	0.4%	2.5%
9 UAE	131	5.3	5.9	0.7%	46.7%

Figure 6-2: Top: Location of agricultural land (green) and land suitable for renewable energy generation via PV solar (yellow and orange), onshore wind (pink) and co-located wind and solar (blue) within the 9 regions, on top of a satellite image. Bottom: Characteristics of the studied regions. The windspeed at 50 m is the average of all locations considered suitable for onshore wind energy generation. The order of countries is according to their average annual temperature (ascending).

methodology constrained the latter with conservation uses such as forests or due to built-up areas (shown in orange, which have a small potential for solar PV). Four of the regions (Stockholm, Boston, Tokyo, Singapore) thus feature a rather limited land availability for renewable energy generation. Some regions had very few (Tokyo) or no (Singapore) suitable locations with sufficient wind speeds for economic wind turbine operations. Of interest in this work was the technical feasibility to deploy renewable energy facilities, irrespective of political constraints. Besides the land cover, regions differed greatly in climate characteristics and population density (Singapore being one of the most densely populated regions globally), leading to vastly different scales of produce production required. The population density did not correlate with the current agricultural land in a region as regions such as those chosen in this study import most food today (Kummu et al., 2020). The soil productivity average was best in temperate climates. Precipitation is low in Phoenix and the United Arab Emirates (UAE).

6.3.2 Renewable energy systems for CEA facilities: demand and supply

The climate influenced the energy intensity of CEA (Figure 6-3a). GHs would require more energy in very cold (with less sunshine and more light supplementation) and very hot months (increased cooling), and annual energy intensity was particularly low for regions with comparatively sunny winters and cloudy or not too hot summers, such as Tokyo and Johannesburg. PFs tend to have a steadier load profile with some outliers when very hot weather makes air-to-air cooling not possible (AppxIV-Figure 5). Further investigation of climate control and specific energy aspects is the subject of another work by the authors.

A fully CEA-based regional vegetable supply was hypothesised in Figure 6-3b to compare it with the current regional electricity consumption. A high percentage indicates that a complete conversion to CEA is either infeasible (due to the hard constraints of generation potential) or requires the electricity sector to drastically adapt. A lower percentage means it is more feasible with the current system. Reykjavik is noteworthy: its already high per capita electricity consumption and favourable wind profiles mean that upscaling indoor production in PFs has little effect on the existing generation capacity. Contrastingly, Johannesburg and Santiago have a low per capita electricity consumption and thus fully scaled-up CEA would need almost half as much electricity as is consumed today. Regional self-sufficiency in renewable electricity generation for CEA facilities meant minimal interactions with the national grid and thus a need for energy storage. Increasing the installed capacity and thus factoring in curtailment of overgeneration reduces energy storage needs (at the cost of

increased land use). Thus, an economic optimum was found for the ratio between wind and

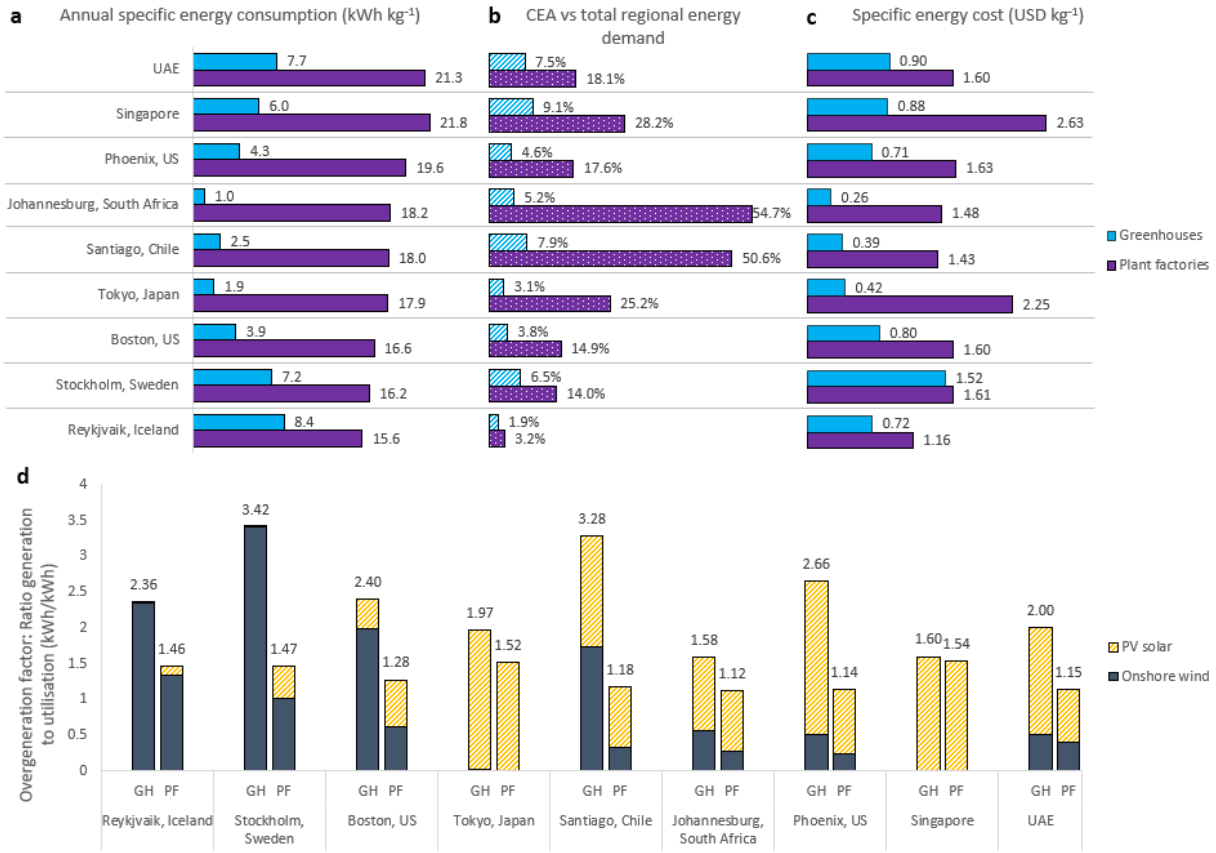


Figure 6-3: Top left (a): Annual specific energy consumption, describing the annual electricity consumption for either type of a growing facility divided by the annual production of produce. Top middle (b): The hypothetical electric demand (i.e. load) of scaled-up CEA farming compared with the current regional demand for either of the two CEA systems, derived from national figures and population adjusted. A higher share of CEA-farming makes it more challenging to utilise the overgeneration indicated in the bottom graph. Top right (c): The specific energy cost per unit mass of produced vegetable. It is the product of the specific energy consumption (A) and the levelised cost of energy (Figures S11 and S12), not considering grid sell-back. Bottom (d): The ratio of generated electricity to electricity utilised in the respective CEA types. This ratio describes how much overgeneration is required to cover the annual electricity requirements under the project constraints (grid supply limited to 10% of the annual demand, economic trade-off between overgeneration and storage). It is influenced by local solar and wind energy generation potential and the mismatch with the utilisation profile. Singapore had no and Tokyo limited land availability for wind, thus the share of solar PV is higher in those cases. Depending on the local context, this overgeneration could be used for other industrial and residential purposes, improving the values indicated in this figure.

solar PV capacity and for the balance between energy storage and overgeneration, the latter differing between the regions and the CEA systems (Figure 6-3d). The steadier load of PFs, contrasting with the seasonally and hourly fluctuating loads of GHs, necessitated less overgeneration. Some regional peculiarities were observed for GHs: (1) sub-optimal wind conditions and strongly varying seasonal demand led to the highest overgeneration ratio in Stockholm; (2) in Santiago, supplemental lighting in the morning and evening hours of winter (AppxIV-Figure 5) and the otherwise very low energy demand led to the 2nd highest ratio; (3) hot summers led to high cooling requirements in Phoenix; and (4) the more seasonally uniform temperature profiles (and hence uniform cooling needs) of Singapore and UAE led to lower overgeneration factors. For PFs, a higher share of solar PV in the energy mix reduced the required overgeneration due to the temporal match with daytime indoor lighting. However, locations heavily relying on solar PV (Singapore and Tokyo) needed increased overgeneration due to the lack of the use of wind turbines to mitigate the seasonal nature of solar PV.

Potentially, the excess electricity can be used for other applications within the region if it matches temporal demand, thus reducing the levelised cost of energy (LCOE) through sell-back (AppxIV-Figure 6 and 7) and the land theoretically allocated to energy generation for CEA production. The LCOE, together with the regional energy intensity (Figure 6-3a) determines the specific cost of energy for produce (Figure 6-3c). The latter cost was consistently lower for GHs with the lowest cost in less extreme climates. CEA production in PFs is more costly, particularly when only (Singapore) or predominantly (Tokyo) one form of renewable energy is used. A discussion of findings regarding the LCOE and storage needs and the sensitivity of results to the discount rate and grid interaction can be found in AppxIV 2.2.

6.3.3 Combined land requirements for growing and renewable energy supply

For open-field farming, only direct land requirements for growing were considered. The annual area-based productivity, i.e. yield, of open field farming was simulated on a regional basis. Combined with preservation requirements due to seasonal production, the yield determines the land requirements to supply year-round vegetables to the local population. Excessive rainfall (Singapore) and low rainfall in summer (Santiago, Phoenix, UAE), potentially prohibitive for growing (AppxIV-Figure 3), was assumed to be mitigated by good practice (e.g. drainage, drip irrigation), which allowed this analysis to assume feasible open-field production in those otherwise challenging climates. By our calculation, yields in those arid regions were still lower than in wetter regions with similar temperatures, leading to

slightly lower yields than those reported by the FAO (AppxIV-Figure 4). The discrepancy likely stems from the inclusion of polytunnel and greenhouse production in the FAO-reported values, which may also explain a lower simulated yield for colder regions, such as Reykjavik and Stockholm. A steady harvest quantity throughout the growing season was assumed due to different seasonal preferences of selected crops and incorporation of growing practices such as plastic soil cover colour to help regulate fruiting. The growing season was influenced by temperatures below freezing and above 40°C; Reykjavik, Stockholm and Boston had the shortest season (6 months), followed by UAE (7 months), Phoenix (9 months) and Tokyo (11

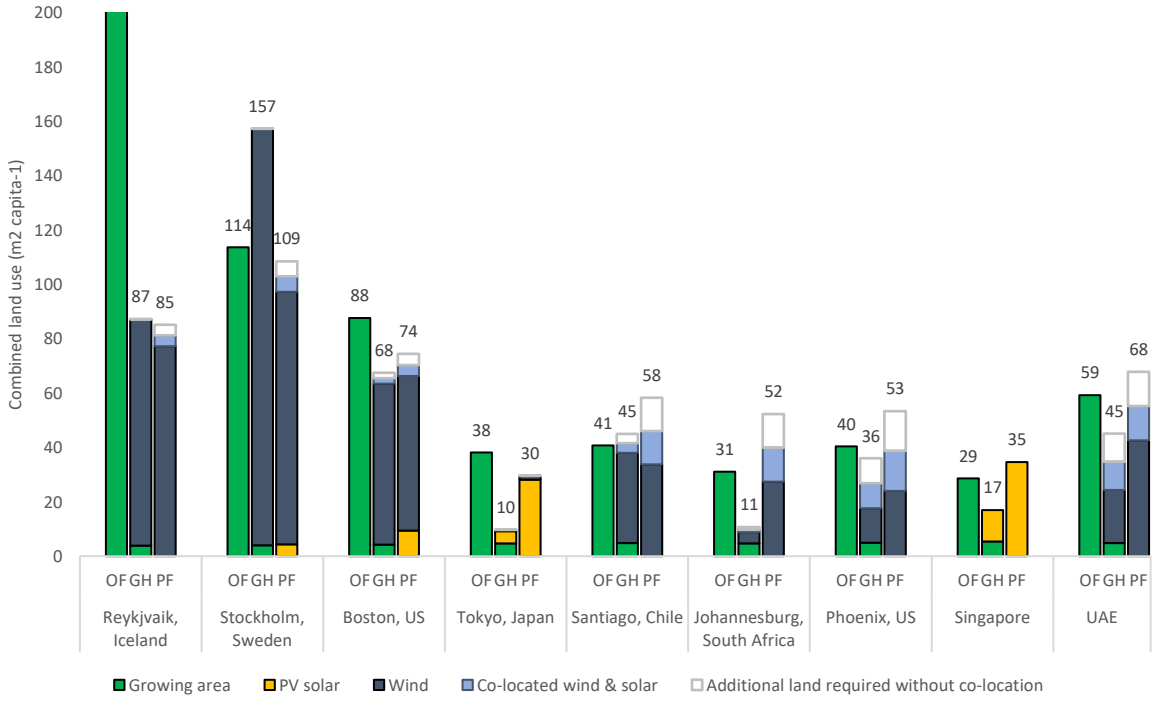


Figure 4: Combined land use requirements of the three growing techniques accounting for the land required to generate the required electricity. Co-location is included and preferred, if feasible. The savings due to co-location are shown in the translucent bar and the value indicates the land use without the savings. If the land available for co-location was restricted, PV solar and wind were allocated to land exclusively available for it. Singapore had no and Tokyo limited land availability for wind, thus solar PV is predominantly used in those cases. This figure only considers the direct and indirect land required to satisfy nutrient requirements for one person, without accounting for limitations due to regional land availability. The value for open field farming in Iceland is 305.1 m^2/capita.

months), with Santiago, Johannesburg and Singapore having year-round open-field

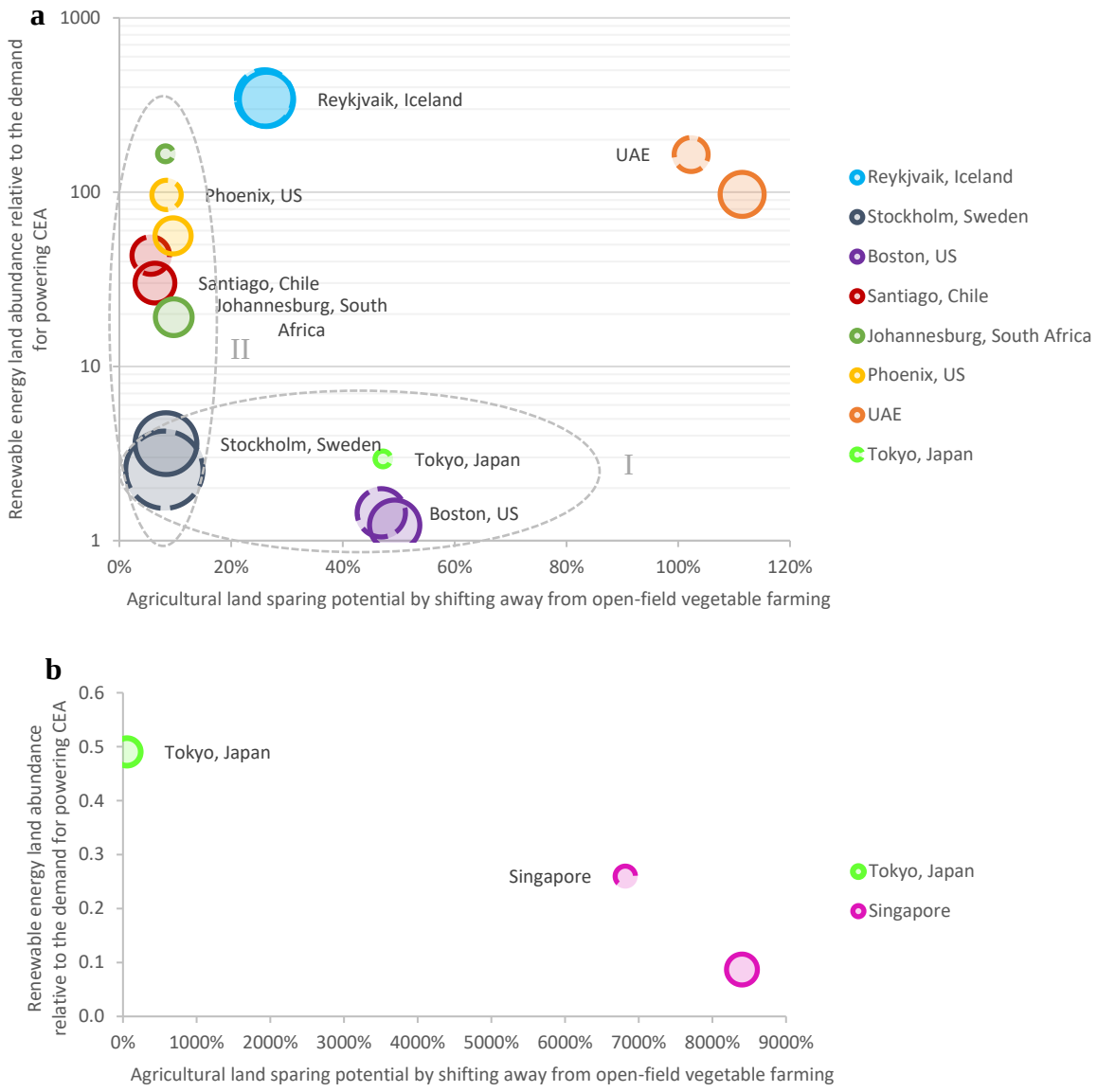


Figure 6-5: Regional land use requirements of CEA practices; measured by the sparing potential of agricultural land by avoiding open-field vegetable farming compared with the total agricultural land available (x-axis, a higher value is better), and the ratio of total land available for renewable generation versus that which would need to be used to supply the CEA farming technique (y-axis, logarithmic in 6-5a, a higher value is better). The bubble size depicts the net land use per person subtracted with savings of co-locating solar PV and wind. The dashed-line circle is for greenhouses and the solid-line circle is for plant factories. The characteristics of the regions in cluster I and II are described in the text. 6-5a only shows regions and CEA practices for which sufficient land would be available to generate the energy required for fully scaled-up CEA. 6-5b shows the cases in which insufficient land is available to upscale CEA.

production. Preservation of nutrient losses required overproduction (up to 49% for the coldest

regions) to continuously satisfy daily nutrient needs. Low yields and oversupply requirements in Reykjavik meant a high per capita land use for open-field farming (Figure 6-4). Warm and wet climates had the lowest land requirements, with more than a magnitude difference between the Reykjavik region and Singapore. The indirect land requirement per person for CEA production is the land required to generate renewable electricity, which depends on the required capacity of wind turbines and solar PV panels and their land-use efficiency. Direct land use by growing was only considered for GHs, not for PFs. Figure 6-4 visualises land requirements for a land-use efficiency of 76.6 W/m for solar PV and 6 MW/km for wind turbines. GH production tends to have significantly lower energy intensity than PF and thus requires less land for energy production, despite higher overgeneration requirements. The combined land use of GHs is higher than that of PFs only in Reykjavik and Stockholm, since in these locations the difference between the two growing systems in the specific energy (Figure 6-3a) is less than that in overgeneration required (Figure 6-3d). Regions where wind energy is more economical than solar PV, such as Reykjavik and Stockholm, also have a higher combined land use than those where solar PV is more economical. Johannesburg, Santiago, Phoenix and UAE have significant land savings due to a high co-location potential of solar PV and wind farms. The co-location savings are generally higher for PFs since the higher share of more land-efficient solar PV is not a limiting factor. Figure 4 implies that GH production is the most land efficient in most cases, although PFs may perform better in very cold climates. Santiago is the only region where open-field farming requires a similar land area to GH production with renewable energy provision (not considering co-location savings). This is mainly due to very favourable (open-field) growing conditions and seasonally and hourly fluctuating GH loads which necessitate overgeneration. In Singapore and Tokyo, the combined land use of PFs is relatively low (in comparison with other locations) due to the high land-use efficiency of solar PV. Land used for wind only (not co-located facilities) might also be available for other uses. The factors influencing the differing combined land uses for PFs is highlighted in AppxIV 2.3 and AppxIV-Figure 9. Sensitivities for the combined land use, i.e. no constraints on land availability (AppxIV-Figure 8), yield increase (AppxIV-Figure 10), regional use of excess energy (AppxIV-Figure 11) and solar land use efficiency (AppxIV-Figure 12) are discussed in SI 2.3.

6.3.4 Regional land-use implications

The combined land requirements need to be put in context with the locally existing land for agriculture and potential energy generation. The land considered for energy generation was separate from agricultural land, resulting in two land occupation metrics. Figure 6-5 visualises

these metrics and puts the combined land use in a regional context for fully scaled-up CEA. The land-sparing potential describes the amount of existing agricultural land freed up assuming local vegetable production is replaced by CEA. In regions with abundant land for renewable energy generation, the required solar and wind farms for CEA would leave sufficient land for other uses (Reykjavik, UAE, Phoenix, Santiago, Johannesburg). The regions in cluster I (Figure 6-5a) had rather limited land available for renewable energy generation, and shifting to CEA would require dedicating a substantial share of the available land to this end-use of energy. Insufficient land for energy generation was available to entirely switch to CEA in Singapore and for PFs in Tokyo (Figure 6-5b). The land sparing potential is high in regions with little existing farmland compared to the population, such as UAE, Boston, and Tokyo. Contrastingly, not much agricultural land is spared in the regions in cluster II (Figure 6-5a). Since the land-sparing potential also infers how much of the existing agricultural land would be required to fully localise vegetable production (which is likely not to be the case), regionalised vegetable supply would only use up around 10% of the farmland in the regions in cluster.

The relative importance of farmland sparing to the occupation of land suitable for energy generation is a political choice the regions must make; the more to the right and top a region sits in Figure 6-5, the more favourable CEA is, irrespective of the absolute combined land use (bubble size) of any of the three growing techniques. This differing implication between combined and relative land use was particularly striking for Stockholm, where the combined land use would indicate the favourability of CEA; however, a large amount of existing farmland compared with the small amount of land available for energy generation relativises these results. A significant difference between the two CEA practices was observed for Johannesburg as GHs can be run with moderate energy input there. For Singapore, its high population density means that regionalisation of food production is infeasible from the land use perspective (Figure 6-5b), both for open-field farming, as it would require more than 90 times as much land as currently dedicated to agriculture, and for CEA, as it would require between 4 (GH) and 10 (PF) times more land than what is available to produce the electricity required. On the other hand, the ratio between agricultural land sparing potential (indicated by the x coordinates in Figure 6-5b) and relative land requirements for energy generation (indicated by the inverse of the y coordinates) for PFs is close to 10 (GHs around 20), primarily due to significant potential for rooftop solar PV. This implies that about 10% or 20% agricultural land savings could be achieved by every per cent of the land for energy generation allocated to PFs or GHs; therefore, localising some food production through CEA

in Singapore could be sensible despite the infeasibility of full upscaling. In Tokyo, this ratio is less than 1 for PFs (Figure 6-5b) as sparing 50% of agricultural land would necessitate the occupation of twice the available land required for energy generation in the whole region. Contrastingly, the ratio is higher than 1 for GHs (Figure 6-5a) since a similar level (~50%) of agricultural-land sparing can be achieved with only 34% of the available land for energy production. The above results have considered the aggregated land use by solar PV and wind energy; their separate contributions to land use (AppxIV-Figure 13 and 14) show that the economic optimum of combined wind-solar generation, as adopted in this work, has led to a higher usage of the land available for wind turbines than that for solar panels, except where feasibility constraints on wind exist (Singapore, Tokyo).

An alternative scenario could be when agricultural land is also used for energy production via solar PV panels installed above crops with a low filling ratio (limiting shade throw) and wind turbines placed along the field lines. This practice would allow Tokyo to fully scale up CEA within the land constraints and significantly reduce land requirements for energy production in Boston and Stockholm (AppxIV-Figure 15), where the ratio of available agricultural land to available land for energy generation is high. In hot and sunny regions, placing solar PV panels above crops might reduce irrigation requirements and stabilise yields (Miskin et al., 2019).

6.4 Discussion and conclusion

Plant factories have been touted by many as the future of agriculture. Current private sector developments in this area typically frame their value around low water and land use as well as market proximity and freshness. Energy is typically underappreciated in these discussions – yet it is clear that their energy use is extensive. For the first time, this work investigates total land use of vegetable production and the required energy production through comparing several systems. We showed that the favourability of a specific production strategy (GH, PF, and open field) differs across regions. No single global recommendation can be given across these systems. Nevertheless, an observed tendency is that GH production with electrified and advanced climate control (as modelled in this work) requires the least amount of land and has lower energy expenses than PF production. We showed that the fluctuating nature of the energy load in GHs requires oversized renewable energy systems, which could benefit from local demand for the excess energy. More generally, CEA seems particularly recommendable for extreme climates with abundant wind or solar energy resources (e.g. Reykjavik, UAE), and to some extent, for highly urbanised regions with little farmland compared to land for

energy generation (e.g. Singapore). Besides, some countries already produce a major share of their electricity from other low-carbon sources (e.g. hydro and nuclear in Sweden, geothermal in Iceland, nuclear in Japan). Thus, they are potentially able to cover the additional load requirements for their main city-regions without significant additional land occupation for energy generation.

Notwithstanding the recognition of other advantages of indoor growing by PFs, such as pesticide-free production, micronutrient content adaptation and freshness (S2G Ventures, 2020), we challenged generalised claims about land savings of PFs. We also demonstrate that land for renewable energy production is limited in most regions studied in this work, which – given the host of other potentially more pressing end uses – could strongly limit the scale-up potential of PFs in a low-carbon world, particularly within the setting of regional food and energy independence. Furthermore, given the high resource footprint (Bloomberg, 2019) and ecosystem fragmentation impact (Kim et al., 2021; Saunders, 2020) of solar panels and wind turbines, CEA might be less favourable when open-field farming has a similar total land footprint (e.g. Santiago), even more so when open-field production is done in an ecosystem-friendly way. More broadly, additional considerations related to customer preferences, local customs or political possibilities need to be considered when opting for policy to support any of the growing methods.

The insights from this work apply to other regions with similar characteristics. Nevertheless, a few limitations present opportunities for further comparisons between CEA practices and open-field vegetable farming. The embedded resources and energy in infrastructure and the criticality of scarce raw materials might be prohibitive for the vast renewable energy systems required for CEA. Operational aspects such as labour intensity, labour availability, and automation potentials likely differ between practices and approaches and could be an important factor in regional decision making. The cost of land was excluded in this assessment and is likely relevant when it is scarce or expensive. For the respective growing practices, some adaptations deserve further assessment: the feasibility and viability of adjusting LED timings in PFs to intermittent renewable energy resources, utilising waste or geothermal heat in GHs, and employing hoop-houses to save water, extend seasons and increase the yield of open-field vegetable farming. The interactions with and proximity to the consumer might have downstream effects on sustainability (Mead et al., 2021), which vary between urban and rural hinterland production. Finally, cultural and socio-economic aspects also play a role in regionalising agriculture, on top of the food-energy-land nexus.

Chapter 7 Discussion and conclusion

7.1 Summary of main work accomplished

The work accomplished in this thesis is a comprehensive review of the literature (Chapter 2) and four pieces of original theoretical modelling work (Chapter 3-6) about urban and peri-urban agriculture integrated with organic waste utilisation and renewable energy provision. It starts with a novel design of an urban resource nexus, combining a productive urban food system with organic waste treatment (Chapter 3). A detailed assessment of monthly self-sufficiency for fruits and vegetables realised through different UA practices was carried out, based on a granular adjusted spatial analysis method applied to two European cities. The resource requirements to accomplish this productivity, including water, fertiliser, fish feed, electricity and heating, were determined. Then, employing mathematical optimisation, the monthly flow regimes within the resource nexus were obtained to minimise GHG emissions. This system was subsequently compared with the current food system, and an investigation into the effects of different spatial and population characteristics was performed. Next, the focus was put on the biowaste management system and how UA could potentially affect decentralised schemes (Chapter 4). Such a decentralised scheme was developed for the metropolitan area of Porto through a realistic and desirable design of community and home composting systems with local land application of recovered products. The subsequent assessment employed spatial analysis to solve a location-allocation problem (compost bin locations), determine transport requirements (waste collection, bulk material delivery and compost surplus logistics) and land availability. It also employed life cycle analysis using bespoke software to model five different biowaste treatment routes and their life cycle impacts. Lastly, mathematical modelling determined the overall costs and carbon footprint of these five different systems for 76 districts within a municipality.

In Chapter 5 and 6, the focus was put on the energy demand of controlled-environment agriculture practices and the implication on cost and land use when considering renewable energy provision. An energy intensity model was set up that incorporates influences from outside climate conditions, detailed modelling of air conditioning equipment, the impact of the interior climate on hourly productivity, the spatial profile within the facility and a range of variable design and operational parameters (Chapter 5). This model was built for greenhouses, with and without ventilation, and indoor vertical farms, i.e. plant factories. The energy intensity, or specific energy, was then optimised on an hourly basis for the whole year in ten different geographical locations by adjusting lighting and climate control variables. Further,

the influence of the design and operational parameters on the energy intensity was investigated in one location. These hourly energy demand values of greenhouses and plant factories were used in the final piece of work to simulate renewable energy systems in nine of the previously chosen locations. The renewable energy systems were economically optimised using a grid simulation software, balancing overcapacity with energy storage requirements. Additionally, a theoretical yield model was developed that estimates the annual yield for vegetables based on the local climate and soil conditions. Finally, the indirect and direct land use of greenhouses, plant factories and open-field farming was assessed and related to locally available land.

7.2 Key learnings and outcomes

A few overarching learnings can be derived from this work. First, scaled-up regionalised food production for local demand can substantially contribute to the food securities of cities but requires some form of CEA in densely populated cities. This local supply can be sustainable from a carbon footprint and land use perspective but the ideal choice of growing practices depends on the local context. Provided the energy comes from renewable sources and energy-efficiency measures are implemented, most countries or states would benefit from an upscaled greenhouse vegetable production. Places with extreme climate conditions may also advance indoor vertical farming. The integration of biowaste reduces emissions but the assimilation potential of organic waste within the city boundary could be rather limited, and the effect of this integration on the cost and carbon footprint of the waste system is small. Hence, such integrated solutions are recommendable where the local biowaste generation matches the local application potential, which mainly occurs at lower population densities (semi-rural areas), where decentralised biowaste management solutions could be most favourable.

More specifically, the learnings from combining urban agriculture with organic waste utilisation are as follows (Chapter 3 and 4): The amount of organic waste generated in cities is too large to be absorbed by urban or peri-urban agriculture alone. Other sinks are required for complete assimilation, such as gasification or pelletisation of dried compost and digestate for export. The feeding of insect larvae is a promising route to the valorisation of biowaste but was not modelled in great detail as more experimental studies are required. The nutrient, fish feed, and water requirements of massively scaled-up systems could be fully met through organic waste products. Further, the integration of biowaste reduces the carbon footprint of urban agriculture somewhat but the source of energy and the energy efficiency are more decisive aspects than the biowaste integration. It was found that a potentially fully

decentralised biowaste management system would be preferable for less densely populated districts but the creation of additional urban farms did not significantly affect cost and carbon footprint. This was due to neighbourhood aggregation, which already massively reduces logistical requirements. Crucial in decentralised systems is that good practice for home compost need to be ensured to prevent excessive gaseous emissions. Renewable electricity grids make incineration less favourable and biowaste utilisation more favourable in the future.

Regarding the energy aspects, it was found that the adjustment of climate control to minimise specific energy instead of just yield or energy can significantly reduce greenhouse energy intensity (compared with previously reported studies and the results of less optimal operational settings in this work) and bring it close to zero in some temperate climates (Chapter 5). Indoor vertical farms always have a higher energy requirement than greenhouses, even in more extreme climates. The crop choice (and its temperature preference) has a major effect on energy intensity, followed by using water-cooled LEDs in plant factories and growing with only moderate daily light integral levels. To meet the energy demand of CEA, considerable amounts of land resources are required, significantly exceeding the direct growing area (Chapter 6). Greenhouses have the lowest combined land use, even compared with open-field farming, in most climates. Exceptions to this were extreme climates with abundant renewable energy resources (where PFs were more favourable) or very temperate climates with long growing seasons (where open-field farming was more favourable). The fluctuating energy demand of greenhouses combined with the intermittent renewable resources means a high degree of overcapacity is necessary in the renewable energy facility, calling for local demand balancing or having to waste excess electricity. Although some land area can be saved with CEA, it is unclear if resource and infrastructure footprint makes it worthwhile. Fully localising vegetable supply through CEA requires a major share of the available land for energy, which needs to be justified, particularly when more pressing purposes are present in the future.

7.3 Limitations

The accuracy of the results derived from the modelling in this work depended greatly on the validity of the input parameters. This was particularly relevant for reported yield figures, emissions data from life cycle inventories, and land use efficiencies of renewable energy. Although scenario and sensitivity analysis were employed for many parameters, their varying nature introduces some degree of uncertainty. This was mitigated, besides through scenario analysis, by taking the average of multiple values found in the literature. In theory, a

probability distribution approach could have been employed but this was not feasible given the modelling techniques and calculation software package used in this work (mainly spreadsheet modelling with Excel with inputs from ArcGIS Pro and EASETECH). Another major limitation was the lack of model validation through experiments. This was mitigated as much as possible by employing a range of experimentally validated equations and principles from literature.

Limitations in the assessments of integrated waste and UA system in Chapter 3 include the simplification of not considering inner city logistics for UA and waste products (partly addressed in Chapter 4) and the less detailed cooling energy simulation due to the exclusion of moisture considerations (addressed in Chapter 5). Another limitation was the focus on only the carbon footprint among all the LCA categories in Chapter 3 and 4. Some LCA impact categories might get worse through decentralised treatment and utilisation but were not considered. This exclusion was necessary to allow for optimisation and scenario analysis without diluting the main message. Further, only the operational footprint was investigated, not considering the entire life cycle impacts of infrastructure and decommissioning (which are typically small for systems with a long life span). In Chapter 4, the study relied on patchy monitoring data from collection pilots and controversial literature on the long term global warming effects of compost and digestate application. In addition, the location-allocation problem did not incorporate whether compost bins could actually be placed at the identified locations.

In the energy intensity modelling, variable yield equations (depending on temperature, light and CO_2) were mainly indicative and only based on one study. The advanced climate control modelled in this study has not yet been realised in practice and thus validated. The three spatial zones considered in Chapter 5 were a simplification and not fully reflecting best practice; in reality, ventilation and air conditioning inlets could be distributed across the space and flow regimes improved, thus further reducing energy demand. Hourly temperature and solar radiation curves were constructed from monthly climate data and are thus simplified without fluctuations. Such fluctuations can reduce energy efficiency (e.g. a cloudy sky means more supplemental light is required, while a cloud-free sky for multiple days increases heat gain and cooling needs). The land use assessment employed only the two most relevant renewable energy sources for the energy transition. Other, more local renewable energy sources, such as hydro and geothermal were not considered due to the desired universal applicability of the method. Naturally, their inclusion would drastically alter (reduce) land

use. The land cost was also excluded due to its substantial variation between the regions and within the regions, including it could change the design of the optimal grid. The remaining limitations are that low-tech greenhouse growing could not be considered due to insufficient empirical data, and the land between wind turbines (not the hybrid locations with solar PV) was considered occupied, even though it could be used for other purposes.

7.4 Future work

The enquiries have revealed some promising opportunities which call, together with the limitations of this work, call for further research. It was found that aquaponic production, where fish are fed partly by (live) insects, comes with a particularly low carbon footprint compared with conventional fish and vegetable production. Of interest here is a holistic LCA including different other sustainable feed options and their complementarity. As indicated in Chapter 2, more facility-based studies could be conducted where anaerobic digestion is paired with greenhouse production. The relevant aspects here are how the waste products can fully replace all inputs and how large the waste collection area should be for a given size of greenhouse to absorb the biowaste fully. Similar, small-scall decentralised AD in neighbourhoods (akin to the community composting scheme in Chapter 4) require further research into realistic and feasible operating modes (e.g. who runs them, how to mitigate harm and risk, how to transport digestate, or if biogas is better used as a transport fuel or for electricity production). For such units, the potentially unfavourable economies of scale need to be compared with the savings from waste collection. Other biowaste conversion technologies where local use for products might exist, e.g. gasification or pyrolysis, should be assessed from a biowaste system perspective.

On CEA, practitioners and academics would benefit from detailed studies assessing daily or weekly yields or plant growth at different combinations of temperature and DLI levels. The exploration of geothermal and waste heat for direct heating in greenhouses or vapour absorption refrigeration in all CEA practices could be promising. The breeding of cultivars adapted to perfectly harmonised indoor conditions could provide a substantial increase in yields (sacrificing not required resilience for growth). In general, this work did not consider infrastructure capital in the LCAs, which could be considered for material-intensive CEA and renewable energy systems. An investigation of differences between labour requirements and automation potential between open-field vegetable farming, greenhouse production and vertical farming would also be warranted. Finally, the use of intermittent lighting in plant

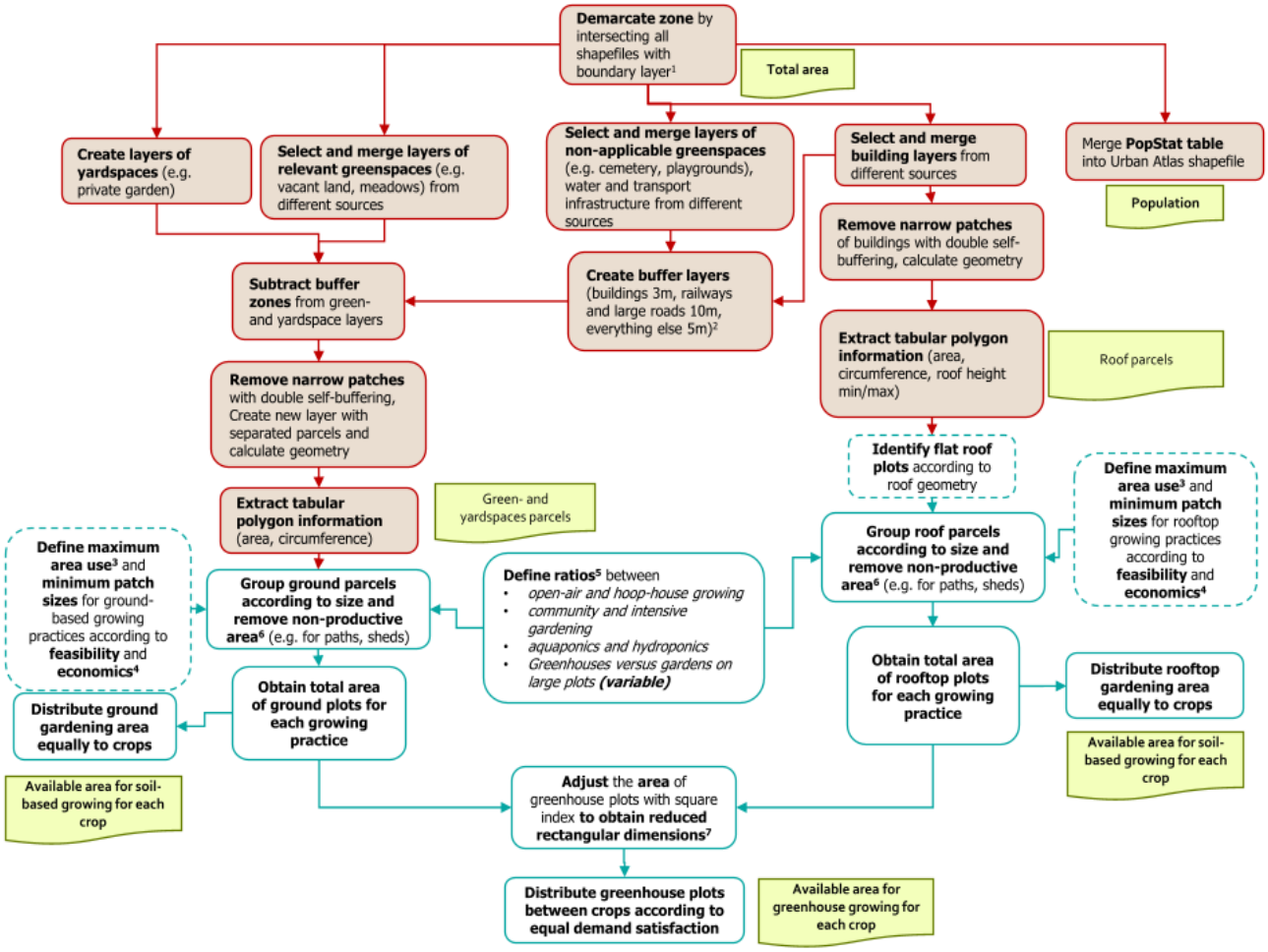
factories and the effect on crop growth would harmonise such growing practices with renewable energy sources.

Appendix I: Supplementary Information of Chapter 3

1. Further methodological details

1.1 Spatial analysis and area assessment

To assess available area, ArcGIS Pro 2.1 (https://pro.arcgis.com) was used for spatial analysis, for which information was extracted for further processing. This flow diagram shows the steps undertaken in ArcGIS Pro 2.1 (red boxed) and in Excel (white boxes). The green flags show the resulting output used in the calculation.



AppxI–Figure 1: Methodology to assesses available growing area

A range of data sources was used for land use information as no single source alone was able to reflect reality appropriately. Building on previous studies and introducing several novel treatments, spatial data was stepwise refined:

- Each target city was zoned to obtain the correct population and appropriate area within the data layers (Goldstein, et al. 2017)

- Non-applicable areas (e.g. playgrounds, roads, cemeteries) including a buffer zone were deducted from selected greenspaces (e.g. parks, allotments, grass and vacant land)(Saha & Eckelman, 2017)
- Narrow stretches were removed in each plot (double buffering)
- Flat rooftops were identified by extracting geometric data, which were provided by the utilised building footprint layers (e.g. minimum and maximum roof height)
- To account for structural integrity and access logistics, the maximum available flat rooftop area was constrained (see table 1 and Nadal et al., (2017))
- To account for desirability and realistic expectations, the maximum area use of applicable ground-based greenspaces was defined (see Table 1 in Chapter 3)
- The resulting parcels were distributed between different growing practices (see figure 2 in main text). This was done by economic and practical considerations for minimum patch sizes and sensible ratios between them (see table 1 in Chapter 3)
- The total area of greenhouse plots and rooftops was further reduced by adjusting the shape to account for non-rectangular geometry
- Non-productive growing area was subtracted based on assumptions (e.g. for sheds, paths)
- For determining the final areas when varying ‘greenhouses versus gardens on large ground plots’, all steps in the white boxes with a continuous outline were repeated.

1.2 Calculation of heating and lighting demand

The lighting requirements were calculated according to Shen et al. (2018), heating requirements were calculated according to Bakos, Fidanidis et al. (1999) and the USDA Virtual Grower software (https://www.ars.usda.gov/midwest-area/wooster-oh/application-technology-research/docs/virtual-grower/). Losses through the cover were considered through walls and roof, solar influx only through the roof, and exchanges with soil and roof (constant temperature assumed) only through the floor. Only the productive area within a greenhouse was considered for the evaporative losses. The space heating was distributed according to Vallati et al. (2015).

Parameter	Value	Source
K-value for polycarbonate greenhouse walls (K_{cover})	2.27 W / m² / K	Proksch 2016
Solar transmittance of cover (τ_{cover})	0.835	(Nadal et al., 2017)
Shading effect (shading)	0.9	(Shen et al., 2018)
Air replacements per hour (n_{air_change})	0.5	(Harbick & Albright, 2016)
Temperature set in greenhouse	24 °C (7 AM – 7 PM) and 16 °C (7 PM – 7 AM)	(Nadal et al., 2017)
Greenhouse height	3 m	Assumption
Coefficient radiation	1.2	Kirtsitis 1982
Specific heat capacity of air (C_{air})	0.837 kJ/m³/K	(Bakos et al., 1999)
K-value soil (K_{floor})	0.34 W/m²/K	(Papadakis & Kyritsis, 1989)
K-value roof (K_{floor})	0.525 W/m²/K	(Castleton et al., 2010)
Temperature roof of host building	20 °C	Assumption, to calculate heat flow to and from host building
Enthalpy water (ΔH_{water})	2450 kJ/kg	N/A
Density water (ρ_{water})	1000 kg/m³	N/A
Typical space heating France	134 kWh/m²/annum	https://www.ovoenergy.com/guides/energy-guides/how-much-heating-energy-do-you-use.html
Typical space heating UK	133 kWh/m²/annum	https://www.ovoenergy.com/guides/energy-guides/how-much-heating-energy-do-you-use.html
PAR transmittance of cover	0.7	(Proksch, 2016)
LED molar efficacy	8.33 mol/kWh	(Philips, 2018)
Rainwater harvesting efficiency	0.7 (hoop-houses), 0.9 (high-tech greenhouses)	(Angrill et al., 2012)
Application efficiency of irrigation	0.45 (surface, community), 0.9 (drip, intensive)	(Lupia et al.,2017)

AppxI–Figure 2: Parameters used to calculate heating and lighting demand

1.3 Overview of process parameters and emission intensities

Aspect	Parameter	Value	Source
Anaerobic digestion	Additional feed water	0.3786 l /kg feed	(Banks et al., 2011)
	AD – biogas potential	156 Nm3/tonne food waste & 78 Nm3/tonne green waste	(Banks et al., 2011; Hertel et al., 2015)
	AD – biogas composition	62.7% CH4, 34.8% CO2, 2.5% H2O	(Banks et al., 2011)
	Total solids – digestate	5%	Assumption based on (Dimambro, 2015)
	Total solids - fiber	32.62%	Based on mass balance and TS split according to (Eriksson & Runevad, 2016)
	Total solids - liquor	2.27%	Based on mass balance and TS split according to (Eriksson & Runevad, 2016)
	Volumetric yield	1.59 Nm3 biogas/m3/day	(Banks et al., 2011)
	Parasitic electricity requirements	59.112 kWh/tonne waste	(Banks et al., 2011)
	Parasitic heating requirements	0.11 kWh / kg feed	(Banks et al., 2011)
	CHP heat generation	12.12 kWh / Nm3 biogas	50% thermal efficiency (Walker et al., 2017)
	CHP electricity generation	1.68 kWh/Nm3 biogas	(Walker et al., 2017)
	CHP parasitary electricity	0.042 kWh/kWh produced	(Banks et al., 2011)
	Lower calorific value of biogas and natural gas	23 and 37 MJ/Nm3 biogas	(Møller etl al., 2009) (Walker et al., 2017)
	AD – biogas upgrading efficiency	95.2%	(Nock et al., 2014)
	Nutrient availability – fiber	50% N, 100% P, 100% K	(Chiew et al., 2015)
	Electricity consumption decanter centrifuge	4 kWh/m3 digestate	(Drosg et al., 2015), density was assumed to be 1000 kg/m3 due to the high water content
	Liquor content as share of original content in digestate	Mass: 91%, TS: 42%, TC: 35%, TN: 76%, TP: 38%, K: 91%	TS is total solids, TC is total carbon, TN is total nitrogen, TP is total phosphorus, K is Potassium (Eriksson & Runevad, 2016)(Drosg et al., 2015), fibre content according to mass balance (e.g. for total solids, 58%)
Secondary treatment	TS in concentrate (Ultrafiltration and reverse osmosis for liquor)	25%	(Rehl & Müller, 2011)
	TS in concentrate (Belt press for fiber)	90%	(NNFCC, 2016)
	Electricity consumption belt press	635 kWh/m3 feed	(NNFCC, 2016)
	Electricity consumption liquor membrane filtration	20.5 kWh/m3 feed	(WRAP, 2012)
	Density liquor	1000 kg/m3	Assumed same as water
	Density fiber	620 kg/m3	(WRAP, 2012)
Insect rearing	Insect bioconversion	17.5% (mass conversion from feed to larvae; the latter contains a moisture content of 62.4)	http://enterrafeed.com, (Salomone et al., 2017)
	Insect compost production	35% of feed	(Joly, 2018)
	Water use	61.1 l / tonne waste	(Salomone et al., 2017)
	Area use	45 m2 / tonne waste	(Joly, 2018)
	Natural gas use	20 l / tonne waste	(Joly, 2018)
	Electricity use	12.9 kWh/ tonne waste	(Salomone et al., 2017)
Composting	Compaction	63% mass loss	(Andersen et al., 2011)
	Composting - gaseous losses	55% of N, 69% of C	(Andersen et al., 2011; Eklind & Kirchmann, 2000)
	N2 loss as N	97.615%	(Cobo et al., 2018)
	N2O loss as N	1.400%	(Cobo et al., 2018)
	NH3 loss as N	0.985%	(Cobo et al., 2018)
	CO2 loss as C	95.0%	(Andersen et al., 2011)
	CH4 loss as C	3.9%	(Andersen et al., 2011)
	CO loss as C	0.08%	(Andersen et al., 2011)
	Processing capacity	14.25 kg/m³/day	www.ridan.co.uk
	Nutrient availability – compost	17.5% N, 50% P, 100% K	(Chiew et al., 2015; Wielemaker, Weijma, & Zeeman, 2018)
	Density finished compost	650 kg/m3	Assumption

Aquaponics	Water use	20 l/kg fish	(Forchino et al., 2017)
	Tank density	30 kg/m^3	(Forchino et al., 2017)
	Growth period - carp	10 months	(FAO, 2014)
	Growth period – Catfish	9.5 months	(FAO, 2014)
	Growth period – Tilapia	7 months	(FAO, 2014)
	Feed ratio	50 kg/month/m^2	(FAO, 2014)
	Feed conversion ratio - Carp	1.6	(Fry et al., 2016)
	Feed conversion ratio - Catfish	1.3	(Fry et al., 2016)
	Feed conversion ratio - Tilapia	1.6	(Fry et al., 2016)
	Electricity use	10.1 kWh/m3/year	(Forchino et al., 2017)
Equipment (other)	Electricity use irrigation pumps – intensive farming	0.2432 kWh/m3	(Smajstrla et al., 2002)
	Hydroponics control and conveyance	0.1778 kWh/kg/year	(Barbosa et al., 2015)

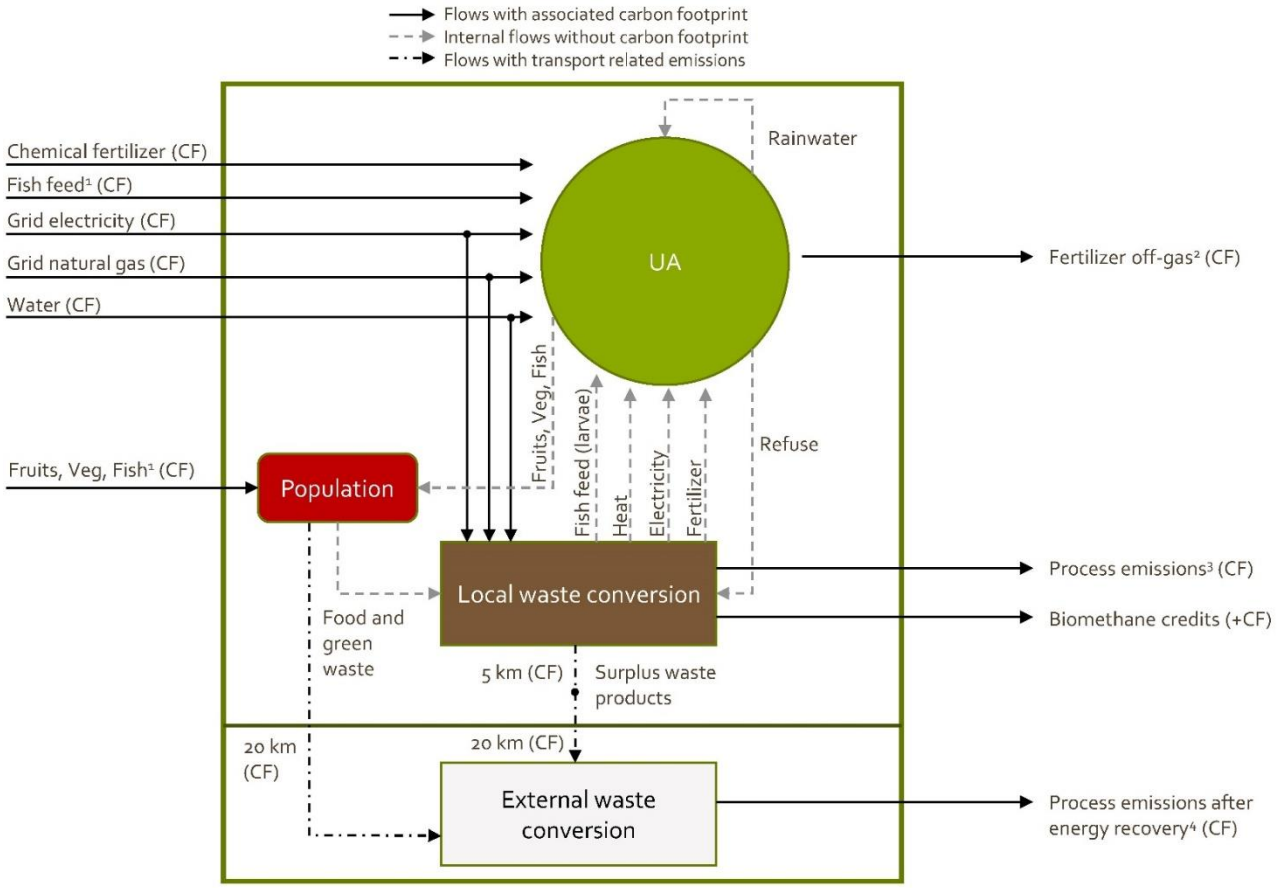
AppxI–Figure 3: Parameters for waste conversion technologies

Type	Parameter	Emission value	Sources
Fertilizer	Production N (hydroponics use)	0.680 kg CO_2-eq / kg N	Calcium Nitrate (Fertilizers Europe, 2014)
	Production P (hydroponics use)	0.542 kg CO_2-eq / kg P	(Møller et al. 2009)
	Production K (hydroponics use)	0.417 kg CO_2-eq / kg K	(Møller et al. 2009)
	Production and application N	8.9 kg CO_2-eq / kg N	(Møller et al. 2009)
	Production and application P	1.8 kg CO_2-eq / kg P	(Møller et al. 2009)
	Production and application K	0.96 kg CO_2-eq / kg K	(Møller et al. 2009)
Emissions factors	Natural gas grid – France	0.27 kg CO_2 / kWh	(Møller et al. 2009)
	Natural gas grid – UK	0.204 kg CO_2 / kWh	(DECC, 2011)
	Electricity grid – France	0.0604 kg CO_2 / kWh	http://www.compareyourcountry.org/climate-policies?cr=oecd&lg=en&page=2
	Electricity grid – UK	0.410 kg CO_2 / kWh	(DECC, 2011)
	Diesel emissions	3.15 kg CO2 / l diesel	(Møller et al. 2009)
	Diesel use	0.03 l / tonne / km	(Møller et al. 2009)
	Water provision	0.15 kg CO_2 / m^3	(Møller et al. 2009)
	Biogas combustion	1.816842627 kg CO2/kg biogas	Based on mass balance
	Replacement natural gas (production)	0.052 kg CO_2/kWh	(Exergia, 2015)
Greenhouse gas equivalents	CH_4	25 kg CO2/kg	https://www.epa.gov/energy/greenhouse-gas-equivalencies-calculator
	N_2O	298 kg CO2/kg	https://www.epa.gov/energy/greenhouse-gas-equivalencies-calculator
	NH_3	2.11 kg CO2/kg	https://www.epa.gov/energy/greenhouse-gas-equivalencies-calculator
	CO	1.57 kg CO2/kg	https://www.epa.gov/energy/greenhouse-gas-equivalencies-calculator

AppxI–Figure 4: Emission intensity values used to estimate the global warming potential (part of the life cycle inventory)

1.4 System boundary overview for carbon footprint accounting

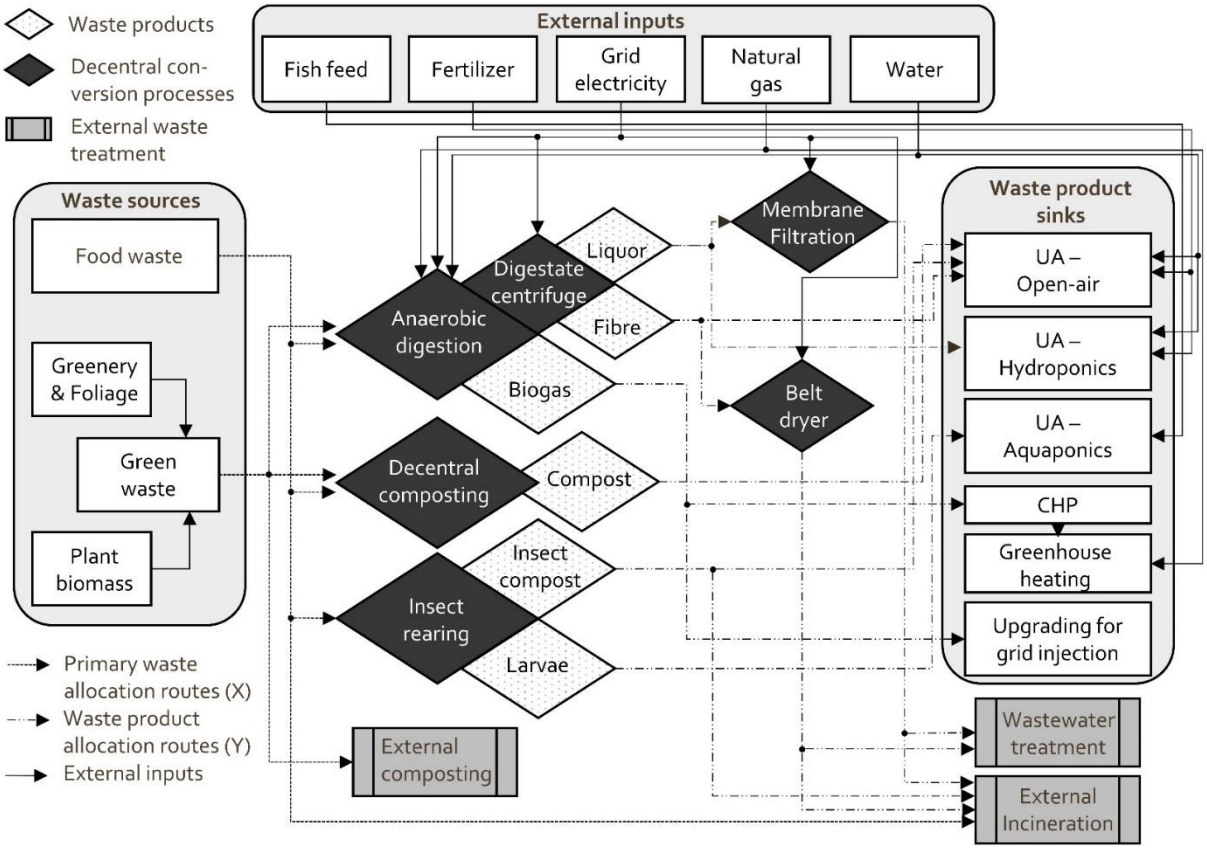
AppxI-Figure 5 visualises the flows considered, which either were accounted via their associated carbon footprint (CF) (incoming and outgoing flows, transport emissions) or were internal flows that had no incurred emissions but which affected the flows across the boundary by substitution (e.g. local production of fertiliser reduces the need for externally supplied fertiliser). Biomethane credits across the boundary are marked with a + symbol as these had a beneficial carbon impact.



AppxI–Figure 5: System boundaries for the life cycle assessment

1.5 Optimisation

The optimization routine used the resource nexus as superstructure, illustrated in the following schematic. The external or secondary treatment of surplus waste products through either membrane filtration of a belt dryer leads to two waste streams, waste water (which goes into the sewage and waste water treatment) and dried concentrate (which is incinerated).



Appx I – Figure 6: Superstructure for the optimisation

Mathematical formulation

The decision variables were the allocation of food and green waste to the different waste conversion technologies (all X's) and the allocation of waste product to UA (the Y's).

$X_m^{i,j} \in [0,1]$

$Y_m^k \in [0,1]$

$i \in \{Food_waste, Green_waste\}$

$j \in \{AD, In\,sec\,t_rearing, dec_composting, external_composting, external_incineration\}$

$k \in \{In\,sec\,t_compost, Fibre, Liquor\}$

Besides the constraints described in the main paper, all waste had to be allocated, and the waste products were either allocated to UA practices or had to be centrally treated.

$$X_m^{FW,AD} + X_m^{FW,Ins} + X_m^{FW,C} + X_m^{FW,CI} = 1$$
$$X_m^{GW,AD} + X_m^{GW,C} + X_m^{GW,CC} = 1$$

The following equations ensured that all nutrient requirements were met and no overfertilization occurs, and no more insect larvae is produced than required as feed for aquaponics production:

$$Fert_{n,m}^{Ext,soil} = Fert_{n,m}^{Re\,qSoil} - Y_m^{Fibre} * Fibre_{n,m} * A_n^{Fibre} - (Y_m^{insC} * C_{n,m}^{Ins} + C_{n,m}^{Compost}) * A_n^{compost}$$

$$Fert_{n,m}^{Ext,HP} = Fert_{n,m}^{Re\,q.HP} - Y_m^{Liquor} * Liquor_{n,m} * A_n^{Recovery}$$

$$Feed_m^{Ext} + Feed_m^{Larvae} = Feed_m^{Re\,q}$$

The hourly heat balance and monthly electricity balance determined the additional input required from the grid.

$$Q_{t,m}^{Ext} + I_{t,m}^{CHP} * Q_{t,m}^{Bio} + (1 - I_{t,m}^{CHP}) * Q_{t,m}^{Bio} * Z_{t,m}^{Injection} = Q_{t,m}^{GBG} + Q_{t,m}^{RTG} + Q_{t,m}^{AD}$$

$$P_m^{Ext} + \sum_{t \in T}^{t} I_{t,m}^{CHP} * 30.5 * Z^{CHP} = (1 - Y_m^{Fibre}) * Fibre_m^{Mass} * Z^{Dryer}$$
$$+(1 - Y_m^{Liquor}) * Liquor_m^{Mass} * Z^{Filtration} + (X_m^{FW,AD} * W_m^{FW} + X_m^{GW,AD} * W_m^{GW}) * Z^{AD}$$
$$+X_m^{FW,Insc} * W_m^{FW} * Z^{Ins} + P_m^{Irr} + P_m^{GH-Light} + P_m^{GH-Ops}$$

$$t \in T, T = \{1,2,\ldots 24\}, m \in M, M = \{Jan, Feb, \ldots, Dec\}, n = \{N, P, K, Ca\}$$

Appx I – Table 1: Nomenclature of optimisation

Symbol	Variations	Meaning
X^{FW}	AD,Ins,C,CI	Share of food waste going into either of the conversion pathways
X^{GW}	AD,C,CC	Share of green waste going into either of the conversion pathways
Y	InsC,Fibre,Liquor	Share of waste product used in urban agriculture
Q	Ext, Bio, GBG ,RTG, AD	Heat flows (external, from biogas, ground-based greenhouses, rooftop greenhouses, anaerobic digestion)
I	CHP	Integer for CHP operation (0,1)
P	Ext, Irr, GH-Light, GH-ops	Electricity user or supply (grid, irrigation equipment, greenhouses)
Z	CHP, Dryer, Filtration, AD, Ins, Injection	Mass or throughput dependent electricity use factor for different conversion technologies
W	FW, GW	Amount of waste
Fert	Ext, Req / soil,HP	Amount of fertiliser
A	Fibre, compost, recovery	Plant availability or recovery loss factor
C	Ins, Compost	Amount of compost
Feed	Ext, Larvae, Req	Amount of fish feed
GWP	Gas, Power, Fert, Feed	Global warming potential factors

CO2	Other	gaseous emissions composting, incineration, digestate application, biogas burning

2. Discussion of results

2.1 Comparison with other studies – Spatial analysis

The obtained share of applicable greenspace (3.1%) and flat rooftop area (4.7%) for Lyon is lower than in other studies looking at dense urban centres, e.g. for a district in Munich, 23.6% of the total area was identified as applicable growing spaces and 9.8% of total area as flat roofs while the share of total roof area was similar (Gondhalekar & Ramsauer, 2017). For the less built-up city of Glasgow, a comparable study was done for Boston, in which of the total urban area a share of 10% as greenspaces and 7.4% as flat rooftop area was considered applicable (versus 8.1% and 0.8% in Glasgow) (Saha & Eckelman, 2017). The difference can partly be explained by different architecture styles and urban layouts but also by more restrictions considered by the methodology in this work, e.g. taking into account the shape of the area, an assumption for a realistic maximal scale-up and subtraction of non-productive spaces within a garden. Both of the previous studies therefore predicted higher levels of self-sufficiency than the two urban areas in this work. From this first study that simulates the production of a range of crops with multiple growing practices on a monthly basis, the results show nevertheless a still remarkable level of self-sufficiency, in particular for Glasgow. Many previous studies do not necessarily arrive at this outcome, which is sometimes due to consideration of only soil-based growing or the omission of rooftops spaces (Weidner et al., 2019). It should be noted that, within certain crop categories, it might not be desired to become fully dependent on urban produce, as extreme climate events or earthquakes would constitute severe supply risks.

2.2 Comparison with other studies – Resource requirements

Benis et al. (2017b) have simulated tomato production in a rooftop greenhouse in Paris with a similar climate to Lyon and obtained a heating intensity of 233 kWh/m2 and a lighting intensity of 93 kWh/m2 (versus 252 kWh/m2 and 143 kWh/m2 in this study). The heating intensity is comparable (Paris is slightly warmer). Another study has obtained a similar intensity for the south of France (240 kWh/m2)(Boulard et al., 2011). However, the lighting intensity for tomato production differs significantly, especially when considering that this work used DLI values for tomatoes of 13.5 mol/m2 PAR while Benis et al. (2017b) used 20

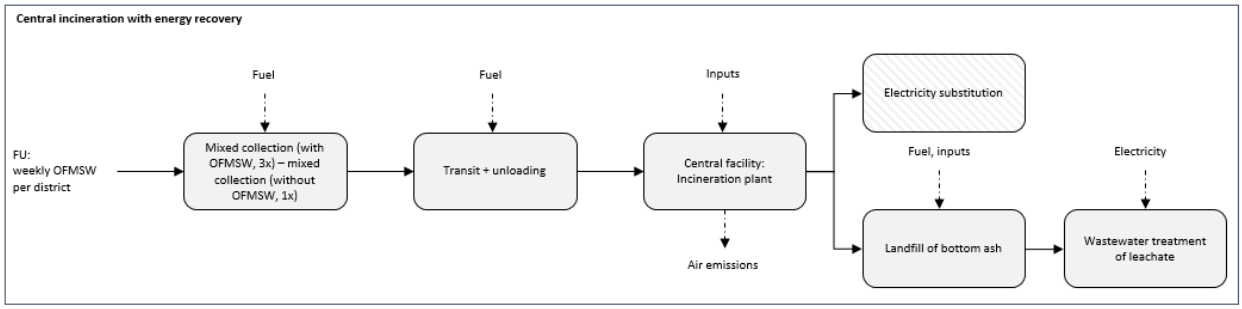
mol/m2 PAR, achieving roughly proportionally increased yields (42.9 versus up to 75 kg/m2) but also necessitating more supplemental lighting. The assumed shading and transmissivity losses in this work might contribute to, but does not fully explain this large difference.

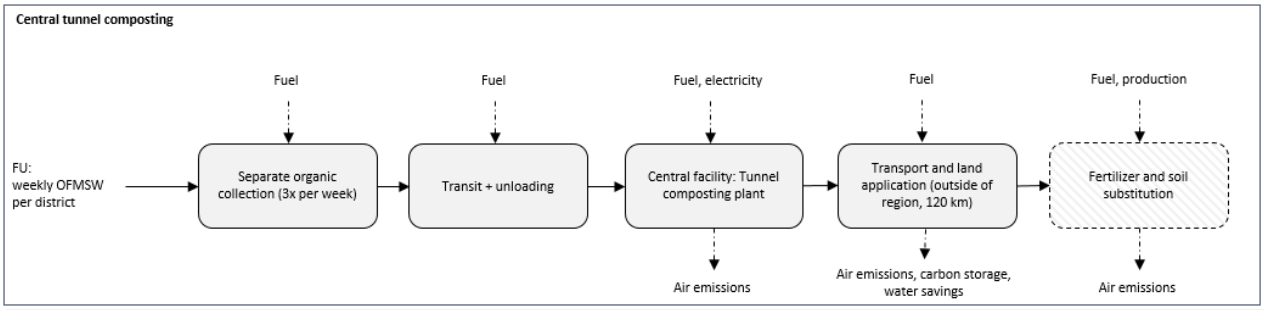
The net water use for hydroponic growing calculated in this work is slightly lower than in the comparable Paris study (28.3 l/kg versus 36 l/kg). Comparing the contributions to the carbon intensity of production, emissions calculated in this work are in a similar range as in other studies. Boulard et al. (2011) conducted an LCA analysis on heated greenhouses in the south of France and found the contribution of heating to CO2e emissions to be around 1.6 kg CO2e/kg tomato (versus 1.57 CO2e/kg in this work).

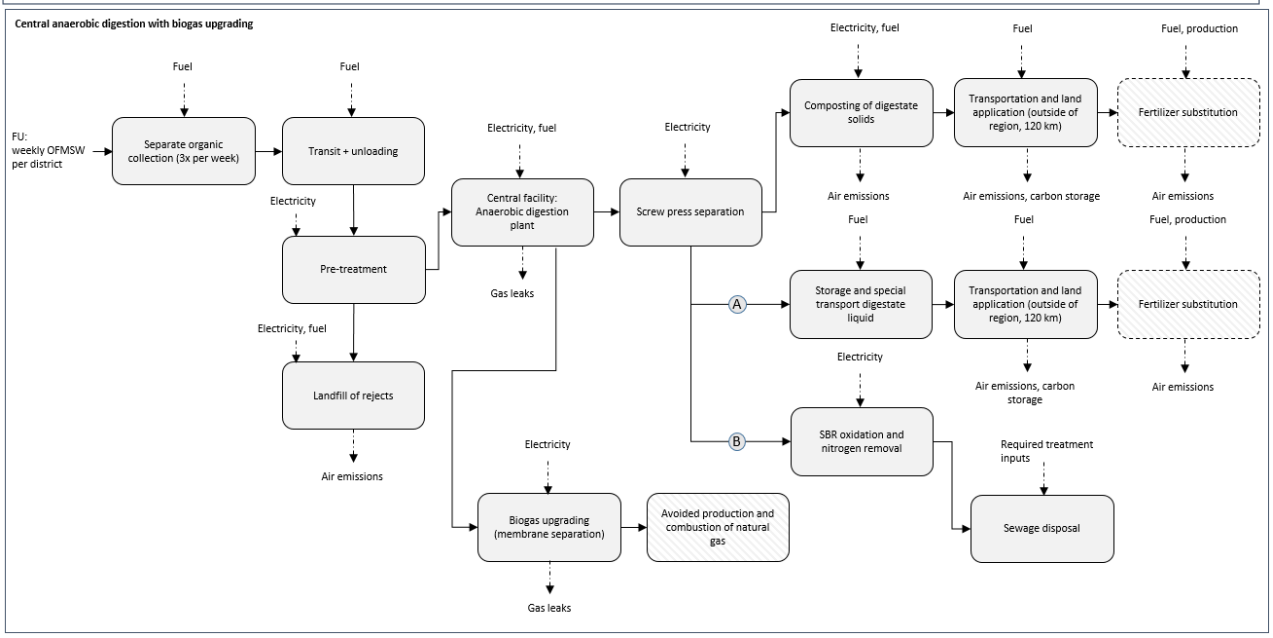
Goldstein et al. (2017) have assessed the amount of organic waste avoided if food waste compost is used in urban agriculture and the per-capita greenhouse gases for fruits, vegetables and nuts in both the current system and a soil-based UA system. The first metric relates to the waste assimilation investigated in this study. They found that for a population of 617,000 people, 9% of municipal organic solid waste (12,000 ton/a) could be assimilated when using 28.8% of Boston's urban space (125.4 km^2) as greenspaces and 1.3% as rooftops in the subtractive scenario. In their "Nutrition (-)" scenario, this leads to a self-sufficiency of 100% for vegetables. This may be compared to the 0% GH scenario in Glasgow, where 2.6% of organic waste is assimilated and 31.4% self-sufficiency is reached. Hence, for a self-sufficiency of 100%, around 8.3% organic waste would be assimilated, which is not too different in this work. The second metric, which is given in kg CO_2eq/capita/annum, relates to the produce emissions for the "UA+Ext" scenario at 0% GH. In their work, the baseline footprint for the category "fruits, veg, nuts" is around 200 kg, while this work arrives at around 125 kg CO2 eq./capita/annum. This may be explained by the fact that exotic fruits and nuts are included in their study. It is not possible to compare the carbon footprints of urban produce accurately as they have done a full LCA study on their crops while in this study, only emissions from irrigation and fertigation have been accounted for urban open-air produce. Further, from the data provided in their SI, the footprint varies widely between crops and farms. For example, the average carbon footprint for tomato in this work is 0.091 kg CO_2eq/kg produce while in their work it ranges from 0.104 to 0.134 kg CO_2eq/kg produce for open plot farming and 0.625 kg CO_2eq/kg produce for open rooftop farming.

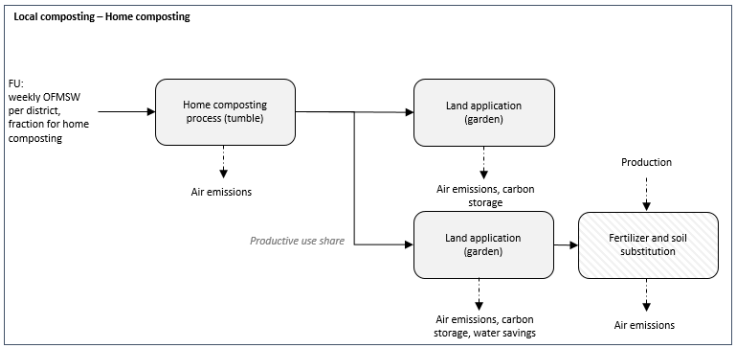
Appendix II: Supplementary Information of Chapter 4

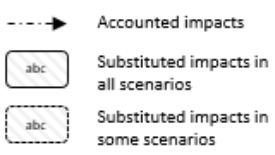
1. System boundaries and assumptions for the life cycle assessment

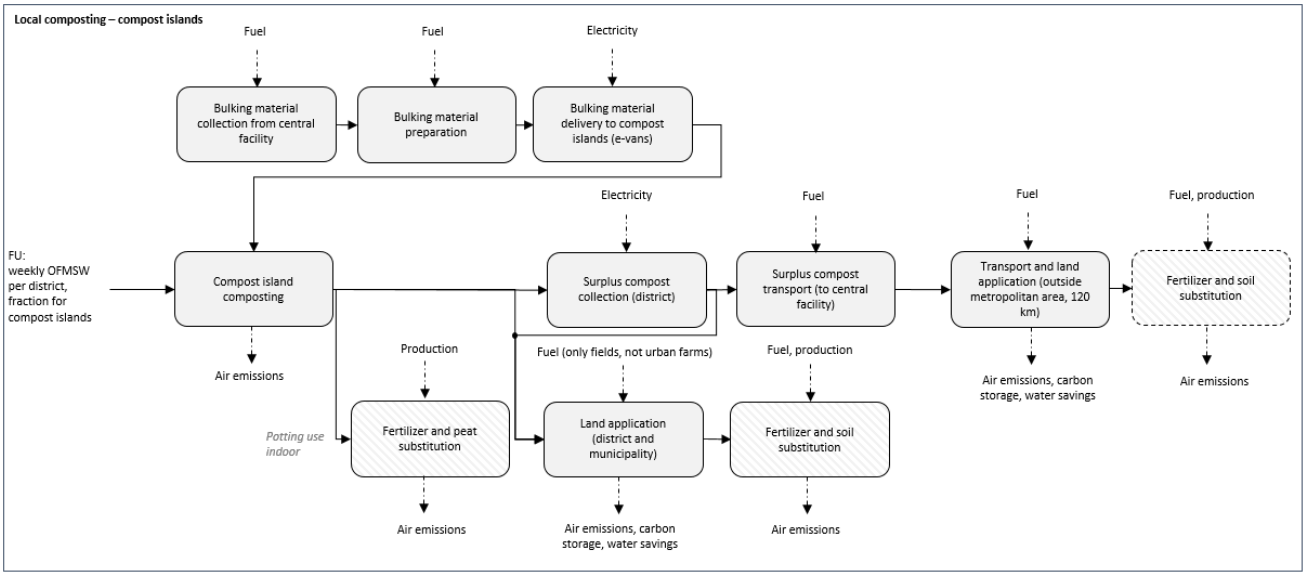








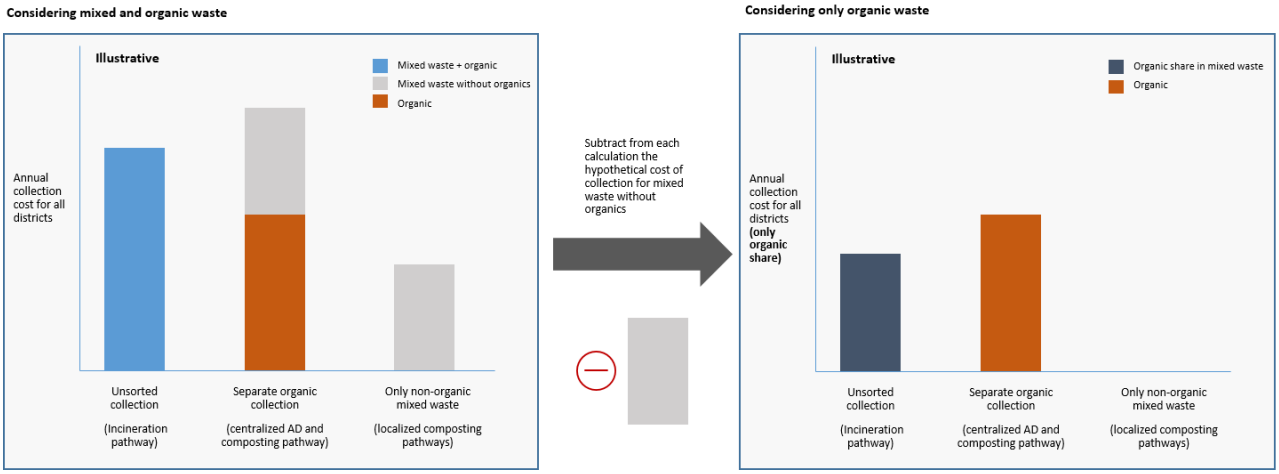




AppxII-Figure 1: System boundaries of the different systems for the life cycle assessment of the global warming impact

2. Calculations for centralised biowaste treatment and collection

2.1 Attribution of the biowaste fraction to mixed collection



AppxII-Figure 2: Illustrative overview of collection cost calculation. The biowaste fraction in the mixed waste was attributed to the unsorted collection according to the difference in cost between a more (3x per week) and less frequent (1x per week) collection.

2.2 Determination of collection pick-up rates and driving speeds

Truck monitoring information from the door-to-door collection pilots carried out in the associate municipalities of LIPOR was used to provide indicative figures for these parameters. The monitoring information for mixed waste collection (incl. biowaste) three times a week exhibited pick-up rates between 812 and 2016 kg/hour, with the former being a peri-urban district and the latter an urban area with larger residential buildings. A visual inspection of the

districts in ArcGIS allowed for an approximation to equate those rates with population densities of 1000 and 4000 people/km2, respectively. These constitute the lower and upper bounds, and in between a linear relation was used to determine the pick-up rate (as shown in 3 ff.). Monitoring information for separate biowaste collection exhibited pick-up rates between 147 and 491 kg/hour and the same methodology was applied. For the mixed waste collection excluding biowaste, and comprising a reduced frequency of collection (once per week), it was assumed that the household and curbside bins would have a higher fill level, thus increasing the pick-up rate. The proportionality factor applied (46%, with 100% being fully proportional) was determined by two circuits that followed the same route with different quantities of waste per collection point. The driving speed during collection was also recorded, and was depending on the time of day (influence neglected), the sprawl of the collection points (a higher population density resulting in lower driving speeds) and the type of truck (the smaller biowaste collection truck being faster). Similar to the pick-up rates, the population density was used as the x value in a linear relationship (m*x +b) with the mixed waste collection averaging 5.3 in urban and 6.7 km/h in peri-urban areas (8.4 and 13.6 km/h for biowaste collection). A subsequent analysis of the results from the heuristics showed that driven distances obtained through the driving speed equation were roughly in line with the actual length of the collection routes.

3 Parameters

3.1 General and incineration specific parameters

Category	Parameter	Value	Unit	Source
Biowaste	Food waste generation	0.276	Kg/person/day	Waste composition analysis (LIPOR) – 24% of food waste in mixed waste
	Mixed waste generation	1.15	Kg/person/day	Waste production data (LIPOR)
	Degradable share of food waste	90	%	Waste composition analysis (LIPOR)
	Food waste sortation rate	60	%	Assumption based on different collection schemes
	Green waste sortation rate	80	%	Assumption based on different collection schemes
	Density biowaste	600	kg/m3	Waste composition analysis (LIPOR)
Food waste composition	Dry matter	25	%	Chemical analysis (LIPOR)
	Organic matter	88.7	% of DM	Chemical analysis (LIPOR)
	Total organic carbon	12.3	%	Chemical analysis (LIPOR)
	Total K	0.9	% of DM	Chemical analysis (LIPOR)
	Total P	0.4	% of DM	Chemical analysis (LIPOR)
	Total N	0.9	%	Chemical analysis (LIPOR)
Location metrics	Average household size	2.3	People/hh	CENSOS https://censos.ine.pt
	Pop. Density defined as "urban"	4000	People/km2	Assumption based on Histogram of Urban Atlas data for Porto
	Pop. Density defined as "peri-urban"	1000	People/km2	Assumption based on Histogram of Urban Atlas data for Porto
	Carbon intensity of electricity grid (2018)	0.307	Kg CO2/kWh	https://www.aib-net.org/facts/european-residual-mix
	Carbon intensity of electricity grid (2030)	0.07	Kg CO2/kWh	Value from FRANCE, assumed to be equivalent to high renewables penetration https://www.electricitymap.org/
	Carbon intensity of natural gas grid	0.27	Kg CO2/kWh	(Møller et al., 2009)
Economic data	Cost of electricity	0.1	€/kWh	Operational data (LIPOR)
	Cost of diesel fuel	1.35	€/l	https://www.globalpetrolprices.com/ Portugal/diesel_prices/
	Hourly salary	10.5	€/hour	Operational data (LIPOR)
	Project duration	25	years	Assumption
Collection	Shifts per day	1.5	1/day	Operational data (LIPOR) - average shifts throughout the week
	Shift duration	7	Hours	Operational data (LIPOR)
	Non-collection shift time (preparations)	2	Hours/day	Operational data (LIPOR) - twice 1 hour, including driving time to start route
	Duration at waste facility	10	min	Operational data (LIPOR) – includes queuing and procedures prior to weighing
	Fuel use during collection	0.367	l/km	Factor 1.3, see (WRAP, 2010)
	Fuel use travelling	0.254	l/km	Factor 0.9, see (WRAP, 2010)
	Emissions from diesel fuel	3.83	Kg CO2/l	(Ng et al., 2019)
	Personnel per truck	3	people	Operational data (LIPOR)
	Driving speed – collection, urban	5.3 / 8.42	Km/h	Operational data (LIPOR) - for mixed waste / biowaste (smaller truck with higher speed)
	Driving speed – collection, semi-urban	6.7 / 13.6	Km/h	Operational data (LIPOR)- for mixed waste / biowaste (smaller truck with higher speed)
	Driving speed – travelling	37.7 / 42.5	Km/h	Operational data (LIPOR)- for mixed waste / biowaste (smaller truck with higher speed)

AppxII–Figure 3: Parameters used in all systems

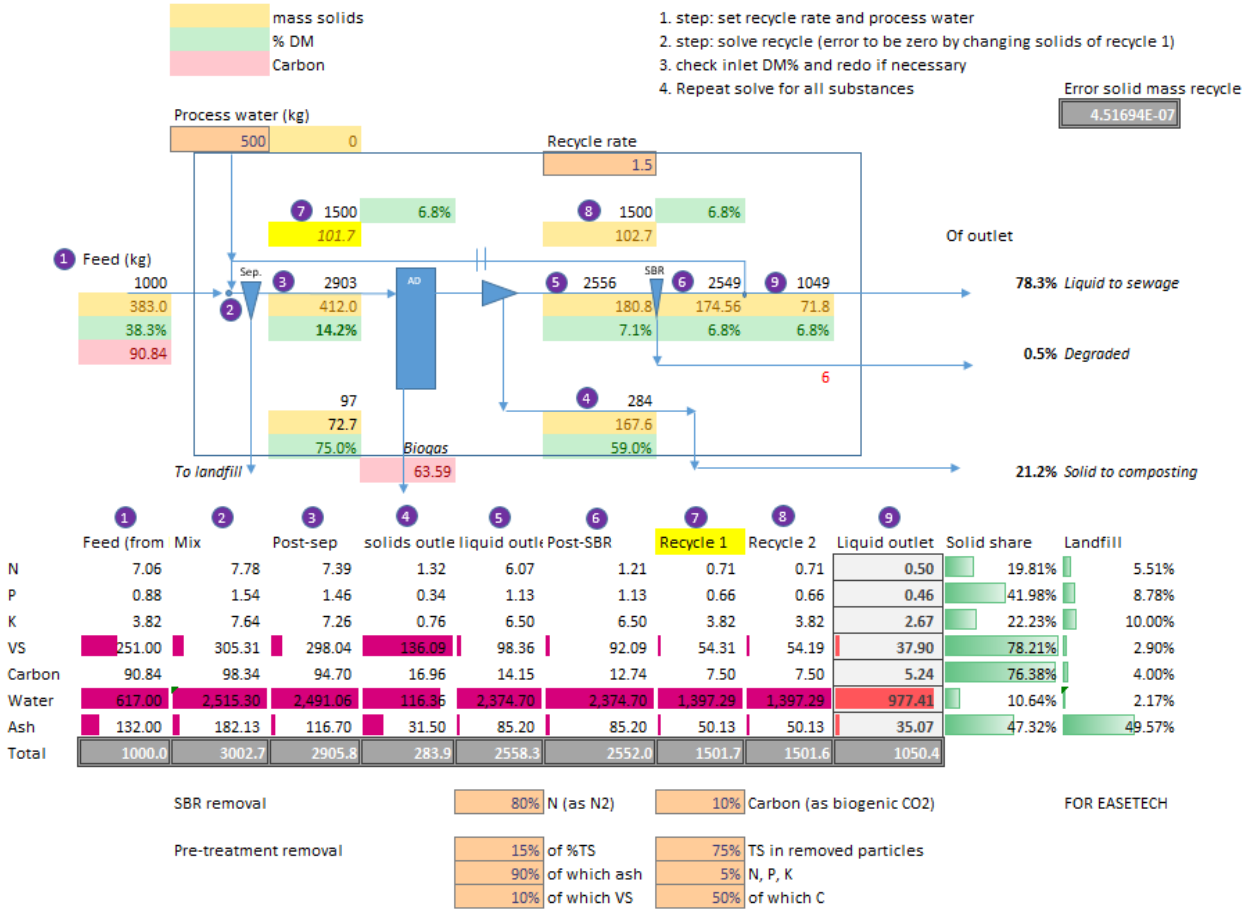
Category	Parameter	Value	Unit	Source
Collection	Pick-up efficiency mixed - urban	2016	Kg/h	Operational data (LIPOR) - extrapolated from dataset obtained from monitoring of waste truck fleet
	Pick-up efficiency mixed – semi-urban	812	Kg/h	Operational data (LIPOR)- extrapolated from dataset obtained from monitoring of waste truck fleet
	Proportionality of pick-up rate to waste generation	46	%	Based on LIPOR collection monitoring data, for the same route with different bin fill rates, means that if bins are twice as full, the pick-up efficiency increases by 46%
	Maximum truck capacity	22,000	kg	Operational data (LIPOR)
	Collection frequency – mixed waste	3	1/week	Assumption based on the door-to-door collection models (LIPOR)
	Collection frequency – mixed waste without biowaste	1	1/week	Assumption based on the door-to-door collection models (LIPOR)
	Investment cost collection truck (22t)	130,000	€	Market data (LIPOR), own analysis
	Lifetime collection truck	10	years	Operational data (LIPOR)
	Annual maintenance expenses	13,000	€/year	Assumption of 10% of investment costs
Treatment	Operational cost incineration plant	54.7	€/tonne	Operational data (LIPOR)
	Investment cost incineration plant	800	€/tonne	Inflation adjusted investment cost for the incineration plant of LIPOR - 170 m EUR
	Lifetime incineration plant	25	years	Assumption of project duration
	Share of labor cost incineration plant	10	%	(Calixto, 2017)
	Calorific value biowaste	3.6	MJ/kg	Operational data (LIPOR) - average
	Calorific value mixed waste	6.96	MJ/kg	Operational data (LIPOR) - average
	Electricity generation – biowaste	212.7	kWh/tonne	Based on 411.2 kWh/tonne for mixed waste (Operational data of LIPOR), adjusted according to heating value
	Revenue from electricity generation	21.7	€/tonne	Operational data (LIPOR) – considering the average value of 0.10 €/kWh
	Operational GHG emissions incineration process	0.0223+0.000196	Kg CO2 eq./kg OFMSW	EASETECH model, includes landfilling of bottom ash and all gaseous emissions to air (non-biogenic), variable share of electricity

AppxII–Figure 4: Parameter and values used in the Excel model – Central Incineration

3.2 Parameter used and masse balance for central anaerobic digestion

A mass balance was carried out to model realistic operations and obtain figures for the separated liquid and fibrous digestate streams (see AppxII-Figure 5). To ensure the inlet %DM content is below 15% for wet anaerobic digestion and to keep the recycle rate low,

750kg of process water were assumed to be added per 1000 kg of feed. A 2% methane loss was assumed in the AD process and 70% yield of digestible carbon. The recycle stream was disconnected and Excel Solver was used to solve the iteration until the values converged (according to the steps indicated on the figure, for the mass of solids as well as the mass of nutrients, carbon, water and volatile solids). The split of stream contents in the screw press separation was according to Drosg et al., (2015). Assumptions were used for the pre-treatment (to remove heavy and dry rejects such as soil from garden waste) and the post-treatment sequential batch reactor for nitrogen removal. All values used are shown below. The electricity consumption for the solid/liquid separation was based on the AD outlet throughput. The outlet stream values related to mass and composition were transferred to the EASETECH model, the solid digestate composted and the liquid digestate discharged to sewer except for the scenario "external land application" (in which no post-treatment nitrogen removal was applied). The liquid fraction of digestate was considered to be transported in case of productive (i.e. replacing fertiliser) application, using special trucks for liquid hazardous waste.



AppxII–Figure 5:Overall mass balance and specific component flows of the central anaerobic digestion plant

Category	Parameter	Value	Unit	Source
Collection	Pick-up efficiency biowaste - urban	463	Kg/h	Operational data (LIPOR) - extrapolated from dataset obtained from monitoring of waste truck fleet
	Pick-up efficiency biowaste – semi-urban	116	Kg/h	Operational data (LIPOR) - extrapolated from dataset obtained from monitoring of waste truck fleet
	Maximum truck capacity	12,000	kg	Operational data (LIPOR)
	Proportionality of pick-up rate to waste generation	46	%	Based on LIPOR collection monitoring data for the same route with different bin fill rates, means that if bins are twice as full, the pick-up efficiency increases by 46%
	Collection frequency – biowaste	3	1/week	Assumption based on the door-to-door collection models (LIPOR)
	Investment cost collection truck (12t)	85,000	€	Market data (LIPOR), estimation
	Lifetime collection truck	10	years	Operational data (LIPOR)
	Annual maintenance expenses	8,500	€/year	Assumption of 10% of investment cost
	Cost collection bin	12	€	Operational data (LIPOR) - 1 per household or 2.6 people
	Cost kitchen bin	3	€	Operational data (LIPOR) - 1 per household or 2.6 people
	Lifetime collection / kitchen bins	7.5	Years	Assumption
Treatment	Operational AD plant	52.6	€/tonne	Values in literature vary strongly by country and technology provider. Range reported between 50 and 109 €/tonne in Europe (Hogg, 2002). Selected value according to Hogg et al. (2007) with 70€/tonne (exchange rate GBP to EUR 1.16) minus aerobic treatment of solid fraction (~17.4 €/tonne, accounted in different step). Excluding digestate separation and liquid treatment (around 12€/tonne)
	Investment cost biogas & upgrading plant	268.90, 18.62 M	€/tonne, €	4000 GBP/kWe generation (Ng et al., 2019) adjusted for inflation and exchange rate (1.16) with 954 kWh/tonne feed biogas generation (143 Nm3/tonne) and 40% conversion efficiency in CHP, assumed same cost for CHP and upgrading plant (Carlini et al., 2017), includes pre-treatment, excl. Digestate treatment.
	Lifetime biogas plant	25	years	Assumption of project duration
	Investment cost soli-liquid separation plant	511,784	€	(Drosg et al., 2015) adjusted to throughput
	Lifetime separation plant	25	years	Assumption of project duration
	Share of labor cost biogas plant	24.3	%	Calculations according to (Hauser, 2017) adjusted for this study
	Electricity requirements solid/liquid separation	0.5	kWh/tonne	(Drosg et al., 2015)
	Revenue from biomethane	36.24	€/tonne biowaste	Based on 40 €/MWh sale price in Porto (estimation of a no feed-in tariff scenario) and 143.4 Nm3/tonne gas production, 5% upgrading and distribution losses and 6.6 kWh/Nm3 LHV. No subsidies included
	Cost for composting of solid fraction	51 + share capital investment	€/tonne	Operational data (LIPOR) - see composting costs
	Methane yield	85%	% of digestible C fraction	User defined in EASETECH, equates to 80 Nm3 biogas/tonne ww or 369 Nm3 biogas/tonne VS for food waste in line with average from empirical studies (Levis and Barlaz, 2013)
	Parasitic heat requirements	0.3	MJ/kg ww	To be supplied by natural gas, value from (Banks et al., 2011)
	Parasitic electricity requirements	0.049	kWh/kg ww	EASETECH, similar to (Banks et al., 2011)
	Operational GHG anaerobic digestion	0.03914+0.02484	Kg CO2 eq./kg OFMSW	EASETECH model, the share of electricity depends on the carbon intensity of the grid, includes fugitive emissions
	GHG emissions for biogas upgrading	0.000474+0.01038	Kg CO2 eq./kg OFMSW	EASETECH model, includes upgrading and compression, distribution loss, variable carbon intensity of electricity
	GHG emissions composting of solid fraction	0.00678+0.005202	Kg CO2 eq./kg OFMSW	EASETECH model, tunnel composting facility, variable carbon intensity of electricity
	Substitutional emission credits for biomethane	0.1597	Kg CO2 eq./kg OFMSW	EASETECH model, substitution of conventional natural gas, including combustion (equivalent to 2.19 kg CO2/m3 CH4)
	Electricity requirements pre-treatment	0.007	kWh /kg OFMSW	SUEZ, personal communication with Sales team for Re:Sep process (27.11.2019)
	Investment cost nitrogen removal (SBR)	1.93, 2.88	€ /kg N	(Jardin et al., 2006), inflation adjusted with 2.9% (equals 1.2 M€ investment cost)
	Electricity requirement nitrogen removal (SBR)	2.9	kWh /kg N	(Gustavsson, 2010)
	Operational cost nitrogen removal (SBR)	1,39, 2.07	€ /kg N	(Jardin et al., 2006), inflation adjusted with 2.9% (equals 12.6€/tonne)
	Sewage disposal cost	2.52	€ /m3	(WRAP Cymru, 2014)
	Sewage treatment emissions	0.0005	Kg CO2 eq. / l	(Parravicini et al., 2016)
	Landfill reject emissions	0.000712	Kg CO2 eq./kg OFMSW	EASETECH
Storage and transport	Capital cost liquid digestate storage	100	€/tonne	(Redman, 2008) – only for scenario regulatory changes
	Lifetime liquid digestate storage	25	years	Assumption, project duration – only for scenario regulatory changes
	Average storage of liquid digestate	2	months	Assumption, winter and summer 3 months, spring and fall 1 month – only for scenario regulatory changes
	Average diesel req. for liquid digestate transport	0.00006*120	l/kg	EASETECH model, for 120 km – only for scenario external land application
	Financial value liquid digestate	0.0038	€/kg	http://www.wrapcymru.org.uk/content/compost-calculator – only for scenario regulatory changes
	GHG emissions liquid digestate transport	0.02731	Kg CO2 eq./kg OFMSW	EASETECH model, for 120 km – only for scenario external land application
	Average diesel req. for composted digestate transport	0.0000152*120	l/kg	EASETECH model, for 120 km
	GHG emissions composted digestate transport	0.0006468	Kg CO2 eq./kg OFMSW	EASETECH model, for 120 km
	Sale value composted digestate	0.006	€/kg	https://fenix.ciencias.ulisboa.pt/downloadFile/1126037345798109/caso-pratico-8-Presenta-ETVO.pdf
Application	Land application of composted solids	0.001909	Kg CO2 eq./kg OFMSW	EASETECH, tractor application, off-gases, run-off
	Avoided emissions from composted solids (fertilizer)	0.008673	Kg CO2 eq./kg OFMSW	EASETECH, replacement including application
	Avoided emissions from digestate fibre use (reduced water)	0.000245	Kg CO2 eq./kg compost	Chron (2011) with 700 l/tonne compost retained, 0.00035 kg CO2/l water provision http://oco-carbon.com/metrics/embodied-carbon-of-water-update/
	Avoided emissions from digestate fibre (reduced soil erosion)	0.00343	Kg CO2 eq./kg compost	Chron (2011) with 41.31 kg of soil loss prevented per tonne of compost. EASETECH model with 82.95 kgCO2eq/tonne compost from green waste, assumption 1:1 soil-build up with compost
	Land application of liquid digestate	0.0581	Kg CO2 eq./kg OFMSW	EASETECH, tractor application, off-gases, run-off
	Avoided emissions liquid digestate (fertilizer)	0.09852	Kg CO2 eq./kg OFMSW	EASETECH, replacement including application
	Replaced mineral Phosphorus in liquid digestate	4.63e-4/0.841	Kg P / kg OFMSW	EASETECH, according to specific plant uptake
	Replaced mineral Phosphorus in composted solids	3.35e-4	Kg P / kg OFMSW	EASETECH, according to specific plant uptake

AppxII–Figure 6: Parameter and values used in the Excel model – Central anaerobic digestion

3.3 Parameter used for the different composting systems

Composting processes – general notes

To account for the different composting performance between home composting, compost islands (well maintained and mixed) and industrial tunnel composting, absolute values (kg/tonne) from experimental literature studies were chosen to derive the resulting emissions as a percentage of the inlet N content. Numerous empirical studies measuring N_2O emissions reflect a strong variation in both quantity and influencing factors. Given the high GHG emission factor of N_2O, the overall message of studies comparing composting with different

biowaste composting options depend strongly on the chosen values and can significantly vary (Saer et al., 2013).

The following information is reflected from these studies:

- The C:N ratio usually drops during composting (Kumar et al., 2009), indicating a higher decomposition of C than N, which was not necessarily reflected in the data.
- The aerobic decomposition of N usually leads to N_2, NH_3 and NO_x as gaseous emissions, with N_2O emissions showing higher values for less mixed and monitored composting processes with anaerobic pockets (Martínez-Blanco et al., 2010).
- Industrially produced compost usually has lower moisture content and higher mass compaction, indicating increased degradation compared with home composting for the same time period (Martínez-Blanco et al., 2010).
- Better aeration (e.g. in industrial facilities) also leads to higher degradations rates (Sonesson, 1996).

Aspect	Percentage	Application	Source
C degradation (food waste, bulking material)	63%	For home composting	(Andersen et al., 2011)
	77%	For industrial tunnel composting	(Andersen et al., 2011)
	70%	For compost islands (average value of two other technologies)	(Andersen et al., 2011)
N degradation	51%	For home composting	(Andersen et al., 2011)
	68%	For industrial tunnel composting	(Andersen et al., 2011)
	59.5%	For compost islands (average value of two other technologies)	(Andersen et al., 2011)
Moisture in compost	43%	For home composting (Jora reactor)	EASETECH
	35%	For industrial tunnel composting	EASETECH
	39%	For compost islands (average value of two other technologies)	EASETECH
NH_3 emissions (as % of N)	15.6%	For home composting	(Amlinger et al., 2008) backyard
	1.8%	For industrial tunnel composting	(Amlinger et al., 2008) tunnel
	7.5%	For compost islands	(Saer et al., 2013) Average of aerated non-industrial
N_2O emissions (as % of N)	4.7%	For home composting	(Andersen et al., 2011) Average from 6 trials of backyard composting
	0.3%	For industrial tunnel composting	(Amlinger et al., 2008) Tunnel
	1.1%	For compost islands	(Saer et al., 2013) Average of aerated non-industrial

AppxII–Figure 7: Degradation and gaseous emissions values used in this work for the different composting systems

Category	Parameter	Value	Unit	Source
Collection	All parameter same as for central anaerobic digestion	See above	See above	Operational data (LIPOR)
Treatment	Operational cost composting plant	51	€/tonne	Operational data (LIPOR)
	Investment cost compost plant	500€ / tonne	€/tonne	Investment cost for the composting plant of LIPOR adjusted for inflation - 30m EUR for design throughput of 60 kt
	Lifetime compost plant	25	years	Assumption of project duration
	Share of labor cost biogas plant	24.3	%	Assumed same as anaerobic digestion
	Operational GHG composting process	0.00646+0.01626	Kg CO2 eq./kg OFMSW	EASETECH model, the share of electricity depends on the carbon intensity of the grid
	Compaction or remaining mass	33.46	%	EASETECH
Transport	Average diesel req. for compost transport	0.0000152 *120	l/kg	EASETECH model, for 120 km
	Financial value Compost	0.011	€/kg OFMSW	Operational data (LIPOR)
	GHG emissions from compost transport	0.002228	Kg CO2 eq./kg OFMSW	EASETECH model, for 120 km
Application	Land application of compost	0.02236	Kg CO2 eq./kg OFMSW	EASETECH, tractor application, off-gases, run-off
	Avoided emissions from compost	0.04465	Kg CO2 eq./kg OFMSW	EASETECH, replacement including application
	Replaced mineral Phosphorus in compost	8.77e-4/0.841	Kg P / kg OFMSW	EASETECH, according to specific plant uptake
	Avoided emissions from water provision (productive, fields)	0.000245	Kg CO2eq/kg compost	Chron (2011), also see table 3.3
	Emissions associated to soil erosion prevention	0.00034	Kg CO2eq/kg compost	Chron (2011), also see table 3.3

AppxII–Figure 8: Parameter and values used in the Excel model – Central tunnel composting

Note: Farm tractor emissions were excluded in the home composting process. No rejects were assumed. No rejects were assumed for compost islands. Electricity was not considered for the compost island process. For urban farm application, no tractor emissions were considered.

Category	Parameter	Value	Unit	Source
Bulking material (BM)	Share of household garden waste (GW) considered as BM	25	%	Assumption based on EASETECH garden waste (20% branches, 5% trees)
	Share of electively collected green waste convertible to BM	50	%	Assumption based on EASETECH green waste (40% branches, 10% trees)
	Seasonal share of green waste	2.9/13.2/5.9/12.0	%	Waste composition analysis (LIPOR) - winter to autumn
	Separately collected GW - Espinho	30.86	tonne/year	Operational data (LIPOR)
	Separately collected GW - Gondomar	3,048.02	tonne/year	Operational data (LIPOR)
	Separately collected GW - Maia	2,131.48	tonne/year	Operational data (LIPOR)
	Separately collected GW - Matosinhos	3,944.98	tonne/year	Operational data (LIPOR)
	Separately collected GW - Porto	3,447.43	tonne/year	Operational data (LIPOR)
	Separately collected GW – Povoa de Varzim	936.58	tonne/year	Operational data (LIPOR)
	Separately collected GW – Valongo	2,571.09	tonne/year	Operational data (LIPOR)
	Bulk material required	1:1	Volume-based ratio	Good practices recommended from the Pontevedra scheme
	Density bulk material	300	Kg/m3	Operational data (LIPOR)
	Diesel required to convert GW into BM	0.002	l/kg GW	Operational data (LIPOR)
	Labour required to convert GW into BM	3.3e-4	h/kg	Operational data (LIPOR)
	Prevented cost of treatment for GW at central facility	40	€/tonne	Operational data (LIPOR), 51€ cost – 11€ revenue per tonne
	Investment cost BM shredder	40,000	€	Market data (LIPOR)
	Lifetime BM shredder	25	years	Assumption of project duration
	Delivery of BM	1	/week	Assumption based on operational data (LIPOR)
	Capacity electric van	1000	Kg	Market data - also for compost island surplus collection
	Investment cost electric van	15,000	€	Market data - also for compost island surplus collection
	Lifetime electric van	10	Years	Market data - also for compost island surplus collection
	Electricity use electric van	0.2	kWh/km	Market data - also for compost island surplus collection
	Stop duration of delivery and pick-up	0.2	hours	Assumption based on operational data (LIPOR)
	Shifts per week bulking material preparations	5	/week	Assumption based on operational data (LIPOR) – assumption no weekend work
Compost islands	Compaction in compost island	37.49	%	EASETECH
	Cost of kitchen bin	3	€/bin	Operational data (LIPOR)
	Lifetime kitchen bin	7.5	years	Operational data (LIPOR), also for home compost
	Minimum number of 1000l cubes	3	/island	Assumption based on community composting trial data
	Cost of 1000l cube with RFID	500+500	€/bin	Market data (LIPOR) - Material and construction cost
	Lifetime compost cube	25	years	Assumption of project duration
	Technicians per compost cubes	30	Cubes/technician	Assumption based on community composting trial data
	Compost collection	1	/month	Assumption based on community composting trial data
	GHG emissions compost island process	0.02378	Kg CO2eq/kg feed	EASETECH, includes BM
	Avoided emissions from fertilizer – compost islands	0.0481 / 0.0478	Kg CO2eq/kg feed	EASETECH, if applied productively. To peri-urban agriculture (with motorized application) / to urban farms
	GHG emissions from compost use and application - islands	0.0212 / 0.02075	Kg CO2eq/kg feed	EASETECH, applied too peri-urban agriculture (with motorized application) / to urban farms
	Emission balance from processing BM in central facility - process	0.007 + 0.0163	Kg CO2eq/kg BM	EASETECH model, the share of electricity depends on the carbon intensity of the grid
	Emission balance from processing BM in central facility – logistics and use	-0.007	Kg CO2eq/kg BM	EASETECH model, assumed 120 km transport and mechanized application
	Emission balance from processing BM in central facility - fertilizer	-0.023	Kg CO2eq/kg BM	EASETECH model, assumed productive application outside of region
	Diesel use for compost field application	0.00025	l/kg	EASETECH, compared with concentrated fertilizer granules
	Replaced mineral Phosphorus compost island	8.76e-4/0.841	Kg P / kg OFMSW	EASETECH (the phosphorus added due to bulking material was not considered as it is excluded in the other systems as well)
	Shifts per week compost island technicians	5	/week	Assumption considering no weekend work
Home composting	Compaction in home compost	38.26	%	EASETECH
	Cost of home composting unit	50	€/unit	Operational data (LIPOR)
	Lifetime home composting unit	15	years	Operational data (LIPOR)
	GHG emissions home compost process	0.129	Kg CO2eq/kg OFMSW	EASETECH
	Avoided emissions from fertilizer – home composting	0.0659	Kg CO2eq/kg OFMSW	EASETECH, if applied
	GHG emissions from compost use and application - home	0.03364	Kg CO2eq/kg OFMSW	EASETECH
	Replaced mineral Phosphorus home compost	8.76e-4/0.841	Kg P / kg OFMSW	EASETECH
Sink consideration	Seasonal application peri-urban field	5/45/5/45	%	Assumption, winter to autumn, compost
	Seasonal application urban farming	10/35/20/35	%	Assumption, winter to autumn, compost
	Seasonal application indoor households	20/30/25/35	%	Assumption, winter to autumn, compost
	Compost application rate (fields, urban)	4	Kg/m2/year	Assumption according to the recommendations of Agència Residus de Catalunya, 2 times 2 kg/m2 per year http://residus.gencat.cat/ca/inici
	Productive use for gardens (semi-urban)	1 (for 3,500 people/km2)	Kg/person/year	2.6 m2 for 2.6 people household with 2 kg/m2 application rate and 50% participation rate, with linear interpolation for each district (minimum garden use of 1 kg/person/year even if denser)
	Productive use for gardens (rural)	10 (for 500 people/km2)	Kg/person/year	26 m2 for 2.6 people household with 2 kg/m2 application rate and 50% participation rate, with linear interpolation for each district
	Productive use indoor	1.5	Kg/person/year	10 vases with 20x20 cm and 2 cm compost application = 4.8 kg / 2.6 people per household and 80% participation
	Avoided emissions from peat production	0.0775	Kg CO2eq/kg compost	EASETECH, 28% replacement rate, 0.2766 kg CO2eq/kg peat
	Avoided emissions from water provision (productive, fields)	0.000245	Kg CO2eq/kg compost	Chron (2011) with 700 l/tonne compost retained, 0.00035 kg CO2/l water provision http://oco-carbon.com/metrics/embodied-carbon-of-water-update/
	Emissions associated to soil erosion prevention	0.00034	Kg CO2eq/kg compost	Chron (2011) with 41.31 kg of soil loss prevented per tonne of compost. EASETECH model with 82.95 kgCO2eq/tonne compost from green waste, assumption 1:1 soil-build up with compost
	Financial value Compost	0.011	€/kg OFMSW	Operational data (LIPOR)
Transport to and from central facility	Investment cost collection truck (10t)	35,000	€	Market data (LIPOR)
	Lifetime collection truck	10	years	Operational data (LIPOR)
	Annual maintenance expenses	3,500	€/year	Assumption of 10% of investment cost
	Maximum truck capacity	10,000	kg	Operational data (LIPOR)
	Personnel required for truck	1	Person/truck	Operational data (LIPOR)
	Fuel use travelling	0.093	l/km	Market data (LIPOR)

AppxII-Figure 9: Parameter and values used in the Excel model for the local composting systems

4. Life cycle assessment in EASETECH

EASETECH V3.17 was used to model the emissions related to the systems. All impacts related to electricity were separately transferred to the Excel model and their associated emissions made dependent of the carbon intensity of the electricity grid. Biowaste from

households was considered to have 34.4% of garden waste and 65.6% of food waste (according to the biowaste composition in Porto, average between seasons). The garden waste and the bulking material compositions are indicated in AppxII-Figure 10. The new composition was 25.1% Garden waste, 47.8% food waste and 27.1% bulking material. Since some of the separately collected green waste from parks for bulking material is treated in the compost islands, their substituted treatment in the central facility was credited to this system (effectively negative emissions, reducing the benefits of the local composting systems). In all other systems it is therefore not additionally considered. Any logistics attributed to green waste from parks (e.g. transport from municipalities to the central facility) was neglected as a) it was assumed that these operations need to happen anyway in both cases, b) the actual routes and frequencies are unknown, c) its impact is likely very low and d) was not relevant for or within the scope of this study. Heavy clay soil was considered for the calculation of application and fertiliser replacement impacts (https://forest.jrc.ec.europa.eu/media/filer_public/a5/b2/a5b2ff38-2c48-4cb6-861a-fb93b30adea4/prt_soil.pdf). The emissions for compost or digestate land application have always been considered, irrespective of whether it was productively used or not.

Material fraction	%
Garden waste, Tree	10
Garden waste, Plants	49.8
Garden waste, Branches	40

Material fraction	%
Grass, Garden waste, Aarhus 2007	75.81
Branches, Garden waste, Aarhus 2007	19.34
Tree, Garden waste, Aarhus 2007	4.4
Stone, Garden waste, Aarhus 2007	0.25

AppxII-Figure 10: Composition of garden waste and bulking material

5. Location-allocation methodology for compost islands and home composting

1. Create Network database from OSM data http://gascuk.github.io/OpenStreetMap-ArcGIS/workflows/simplified/

2. Create roads layer from OSM data, select relevant area data

3. Determination of population considered for compost islands: Add New Fields in Urban Atlas 2012 polygons for classification ‘Urban Fabric’. Calculate New Field as population density by dividing POP2012 with Shape_Area. Copy CODE2012 into new field as Double entry, Reclassify another new field so that Codes of *Continuous urban fabric (S.L. : > 80%)* is 1 (considered for compost islands) and *Discontinuous medium density urban fabric (S.L. : 30% - 50%)* and lower density is 0 (considered to be home composting). Then Reclassify remaining *Discontinuous dense urban fabric (S.L. : 50% - 80%)* entries depending on the population density with <90 people/ha as 0 and =>90 people/ha as 1. Multiply the

POP2012 figure with the new 0/1 field to obtain the relevant population for the compost islands in a new field, e.g. “biowaste”. Finally carry out Feature to Point to create potential Demand Points.

4. Determination of road points as potential location for compost islands: Select fclass *secondary, tertiary, residential roads* in OSM road dataset and carry out Feature to Point. Load *Ecopontos* and create a 200m buffer zone around them, erase all road points within buffer and outside of relevant municipalities.

5. Create Location-Allocation layer: load road points layer and *Ecopontos* as Facilities, load population points as Demand Points (select Weight as the “biowaste” field. Settings of layer are Mode: Driving, Metric: Driving Distance, remove all restrictions (e.g. One-way). Choose 250 m as cut-off.

6. Results were visually sense-checked by LIPOR employees living in Porto and confirming the algorithm’s suitability (see AppxII-Figure 11).

7. Determine compost island number for each district: Select Maximize Coverage and Minimise Facilities. Create New Layer from Chosen Facilities, Spatial Join with Administrative Zones + Extract as Table (relevant entries are DemandWeight and Name_3

8. Each row in the table presents one compost island, the number of cubes was calculated by ROUNDUP (DemandWeight/60). 60 was the maximum number of people connected per bin to ensure sufficient maturation.



AppxII-Figure 11: Snapshot of locations of compost islands and populated areas associated with them

9. Every compost island location with less than 120 people connected to it (i.e. only 2 cubes per island) were considered to walk slightly further and adjoin another island where they are accounted for. If a district had no islands so far (e.g. because it is very rural), the people were assumed to do home composting – this is mainly due to the algorithm not always categorizing the type of the block according to reality.

6. Calculations implemented in the Excel model for collection, treatment and land application

Note: [] for explanations or values

General calculations

Applicable food waste = food waste generation [kg/person/day] * food waste sortation rate * degradable fraction

Applicable garden waste = green waste share [kg/person/day] / total generation * green waste sortation rate

Applicable biowaste = Applicable food waste + Applicable garden waste

GHG emissions from electricity = carbon intensity Portugal - % renewable penetration * (carbon intensity Portugal – carbon intensity France)

Biowaste delivered to island per district [weekly, depending on season] = sum population connected to CI * 7 * applicable food waste + applicable garden waste [depending on season]

CI technician working time per district = ROUNDUP (Sum of cubes in municipality / cubes per technician) *5 [days/week] * hours per day [7] * cubes per district / cubes per municipality

Jobs created = work hours / 35 [h/week] / *(52-6) [annual leave]

Calculation routine for mixed waste pick-up (with and without biowaste)

Mixed waste collected [per round, with biowaste] = Population [district] * mixed waste generation [kg/cap/day] * 7 / collection frequency

Mixed waste collected [per round, without biowaste] = Population [district] * mixed waste generation [kg/cap/day] * 7 / collection frequency

Pick-up rate [kg/h, with biowaste] = IF 1000 < pop. Density < 4000; 0.401 [m] * population density [x] + 410.67 [b]

Pick-up rate [without biowaste] = Pick-up rate [with biowaste] * (1+ Mixed waste collected [per round, without biowaste] / Mixed waste collected [per round, with biowaste]/ Mixed waste collected [per round, with biowaste] * Proportionality of pick-up rate to waste generation

Driving speed pick-up [km/h] = -0.00046 [m] * population density [x] + 7.16 [b]

Total distance driven during pick-up = Driving speed pick-up * mixed waste collected [per round] * pick-up rate

Total distance driven during non-pick-up = AVERAGE (Distance to central facility *2) * Number of shifts required per round

Number of shifts required per round = ROUNDUP (SUM (mixed waste collection [district] / pick-up rate [district]) [h total, municipality] / (shift duration – unloading time – AVERAGE (Distance to central facility *2 + unloading time))

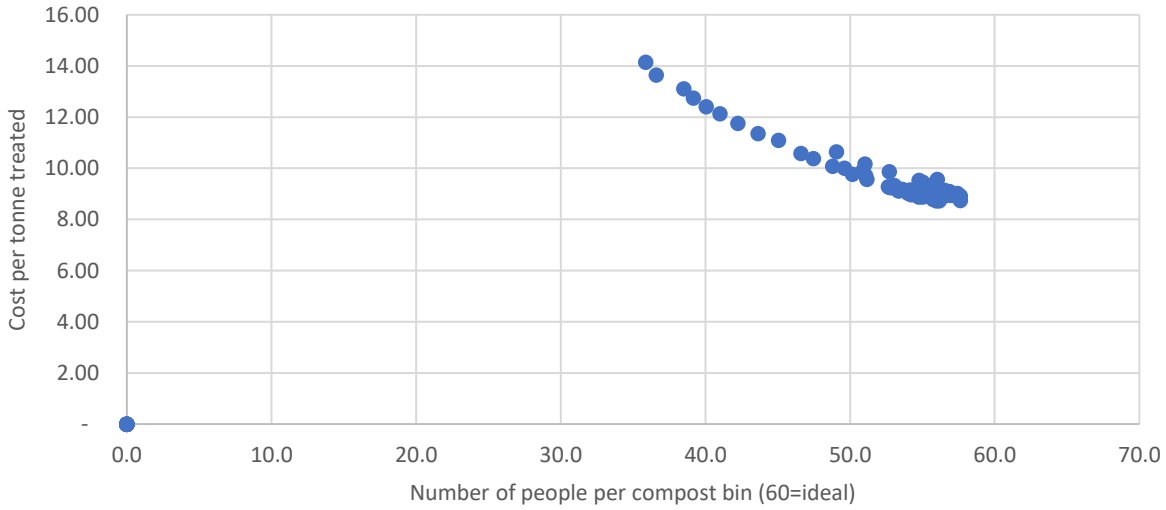
Share of vehicles required = ROUNDUP (Number of shifts required per round * shift duration / 7 * collection frequency [per week] / shift duration / shifts per day) + 1 [to account for vehicles in maintenance] * district share of required collection time

Share of employee hours required [per week] = Number of shifts required per round * shift duration * personnel per truck * collection frequency * district share of required collection time

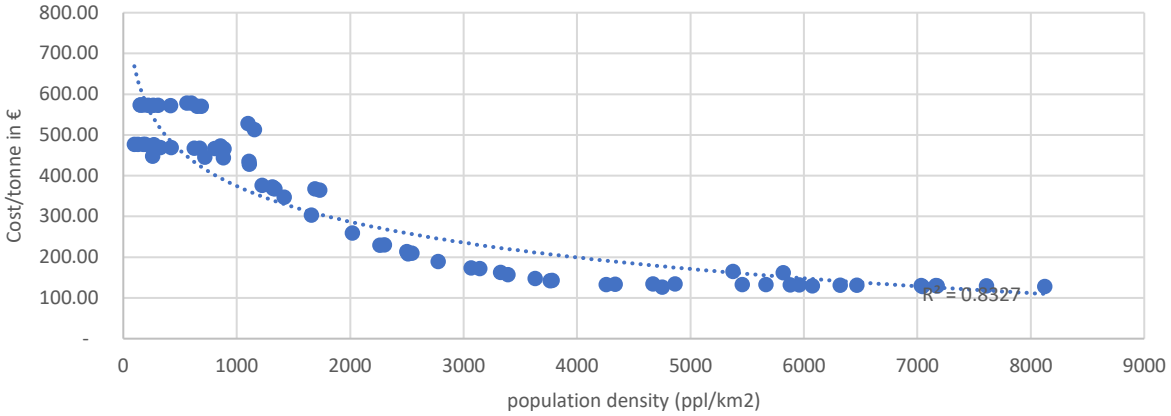
Fuel use [weekly] = Total distance driven during pick-up * fuel use pick-up + Total distance driven during non-pick-up * fuel use non-pick-up * collection frequency

Equations for the remaining aspects can be found in the Supplementary Information of Weidner et al. (2020) and include the calculation routine for biowaste pick-up, for waste collection cost and GHG emissions, incineration, anaerobic digestion and composting, for bulking material preparations, for bulking material logistics to CI, for the compost balance, for surplus compost collection, for GHG emissions from compost process application, and for the total annualised cost of local composting.

7. Further visualisation of results



AppxII-Figure 12: Relationship between the annualised cost per tonne treated of the local composting system per district with the number of people associated to each composting bin in the same district



AppxII-Figure 13: Relationship between the annualised cost per tonne for biowaste collection and the population density in each district. For districts with the same population density the different cost can be explained by the different distance to the treatment facilities

8. GHG emission reduction through electrified waste collection trucks

In this study, waste collection and transport were carried out by larger diesel trucks (10-22 tonne capacity). In the future, advances in truck electrification technology might lead to municipalities adopting electric waste truck fleets. A preliminary calculation using figures from table S1 can be used to assess the impact on GHG emissions per km driven.

Fuel use (average between collection and transport): 0.282 l diesel / km; GHG emissions of diesel: 3.83 kg CO2 / l = GHG emissions per kg driven for diesel trucks: 1.08 kg CO2 / km

Fuel use electric truck 12 tonne capacity: 1.06 kWh/km (Martins-Turner et al., 2020); Carbon intensity of electricity grid (2030 estimate for Portugal): 0.07 kg CO2/kWh = GHG emissions per kg driven for electric trucks: 0.074 kg CO2 / km (-93.1% difference in GHG emissions)

9. Comparison with other literature

The waste management cost figures from this study for centralised systems are similar to or slightly higher than what was reported in a cost-benefit analysis study performed in Denmark (Hogg et al., 2007): 177 €/tonne for incineration (vs 175 €/tonne); 240 €/tonne for composting (vs 303 €/tonne) and 230 €/tonne for AD (vs 298 €/tonne). The reason for this difference is mainly related to the higher collection costs observed in the collection area of LIPOR (227 €/tonne vs 188 €/tonne), which can be partly explained by the inclusion of more remote districts in the regional collection area of LIPOR. In most of the studies considering environmental impacts, GHG emissions are usually most favourable for AD, followed by incineration or composting and finally landfill as the worst option (Bernstad and La Cour

Jansen, 2012; Morris et al., 2013, 2017). Depending on the country and the methodology, detailed study results vary significantly, reflecting the dependencies of GHG emissions on local conditions such as the city layout, carbon intensity of the electricity grid (Vieira & Matheus, 2019) and potential carbon credits from (productive) land application. Salemdeeb et al. (2018) found that, for current electricity grids, incineration can achieve even more negative emissions across the life cycle than AD with composting generating net positive emissions. Confirming this, another study that included detailed calculations for collection, bin and handling requirements found that separated organic collection and AD with productive field application has higher climate impacts than mixed collection with incineration (Chiew et al., 2015). The high contributions to emissions from home composting schemes were also found by other studies (Lundie & Peters, 2005; Martínez-Blanco et al., 2010).

10. Applicability of results to other cases or regions

Due to the diversity of urban areas present in the associate municipalities of LIPOR, the regional results of the present study are transferable to a wide number of regions. Considering smaller administrative areas, it is possible to find in this study districts with similar population density, peri-urban farmland, distance to central facilities and potential for land conversion to UA. The sensitivities observed for the different scenarios on the regional level also apply to the district level. Moreover, the smaller the scale, the higher the probability of finding a specific scenario from the scenario analysis for which a given change can provide a more significant impact (e.g. districts with 100% potential for home composting will benefit more from promoting an improvement in composting practices).

In other regions and cases, individual cost items might change. Due to an indication of the labour cost share and the cost categories, the annualised cost approach allows for a straightforward modulation of relevant costs, such as capital costs or salaries.

11. Limitations and assumptions

This study analysed data concerning spatially sensitive logistics, sink capacities and household waste generation, as well as waste treatment and final disposal impacts. Conversely, it did not consider the carbon footprint of capital goods, some consumables (e.g. plastic waste bags) and the impacts of increased road traffic. There may be a lack of representativity in the models of biowaste collection since the truck monitoring information used to produce the models for collection consisted of a small number of pilot areas and only a limited number of circuits were analysed. This study considered only the waste produced in

households and excluded waste from restaurants and distribution chain and therefore the potential synergies which can be derived from integrated solutions. For the local composting model, it was also assumed that there is sufficient space for compost islands in the streets. This is generally the case for less dense urban and semi-urban districts but possibly not the case for very dense districts. Previous studies have shown that cities with higher population densities and certain city layouts may struggle to find locations covering every neighbourhood (Pai et al., 2019). Another assumption was that upgraded biogas would always replace natural gas from fossil sources. This may not always be valid in some locations, e.g. in summer when less space heating is required, if there are no industrial users or if the share of biomethane in the gas grid increases. This work assumed best available technologies for the incineration and composting plant, which may not be the case in all locations. Another limitation is the use of fixed values for many parameters instead of a distribution profile, e.g. capital cost, labour cost, energy recovery efficiency in incineration plants. Incorporating a probability distribution into the model was not feasible with Excel and other, more critical parameters, were chosen for the scenario analysis assessing the sensitivity of results to specific assumptions on how the future waste management system would operate.

A major limitation of this study is the lack of available consistent methods to estimate the impact of compost and digestate in global warming. Composting has a multitude of benefits that have been extensively studied qualitatively but there is limited quantitative evidence about long-term effects with high-quality data (e.g. carbon sequestration and soil built-up). These effects are further discussed in SI 6. Recent studies shed light on the likely underestimated effects regarding the carbon stored in soil (Tautges et al., 2019). The environmental impact assessment performed in this study only considered consistent and reliable data available, and therefore, it is important to stress out that it might understate the climate benefits of compost. Further research is recommended in this field. Moreover, this study also did not quantify the changes in soil carbon content when converting grassland (e.g. some of the greenspaces) into urban farms. Studies have shown that grassland, which benefits from year-round cover and potential input of carbon (e.g. animal excrements) has a higher total organic carbon content than typical farmland (e.g. monocultures, bare fields over winter, synthetic fertilization) (Jacobs et al., 2018). However, in this work we assume that good practice would minimise the impact of conversion through regular application of compost, diverse crop species and the use of cover crops (Tautges et al., 2019).

Appendix III: Supplementary Information of Chapter 5

1. LED lighting schedule, efficiency and direct cooling

Plant growth strongly depends on adequate light supply; increasing the average amount of light received leads to greater photosynthesis (up to a certain point) and thus the synthesis of sugars and other non-structural components, which in the end increase the structural biomass generated (Van Henten, 1994). Reference yield values, together with the daily light integral (in mol of photons per day) at which they were obtained, are used to determine the overall lighting requirement (DLI_{plant}). A comparison with the naturally available sunlight on a specific day ($DLI_{natural}$) determines the amount of additional light or moles of light required. It seems that the total amount supplied per day matters more than at which hour they are supplied (Proksch, 2017). At the same time, low solar radiation in the morning and early evening might hamper growth and shorten the effective photoperiod for a specific crop (Tewolde et al., 2018). Thus, the LEDs in greenhouses are considered to supply light in precisely those times at varying intensities to smooth the incoming light profile of the sun, which itself follows a positive sin curve. The following method was devised to obtain the I_{LED} or LED light output in W/m2 from the required DLI_{LED} or daily total light (i.e. photosynthetically active radiation, PAR) output. This will approximate the inverse of the solar radiation, dimming the intensity towards solar noon and increasing it again in the afternoon.

Step 1: From the daily solar radiation curves (see SI in Weidner and Yang (2019)), calculate the total (in Wh/(m^2*day)) and maximum (in Wh/h) solar radiation (only PAR component).

Step 2: Calculate the total Wh to be supplied by the LED (from mol/(m^2*day) to Wh/(m^2*day).

$$\sum_{0}^{23} I_{LED} = DLI_{LED} * \frac{222000 \frac{J}{mol}}{3600 \frac{s}{h}} \qquad \text{Eq. III-1}$$

Step 3: Add the PAR component of the solar radiation and the total LED output (PAR) and divide it by the photoperiod to obtain an assumed target intensity $I_{target,1st}$ (in W).

Step 4: The resulting target intensity value $I_{target,1st}$ is then used to plot the first approximation of the intensity with equation III-2. If the maximum of the solar radiation is lower than this target value, the first approximation will be the actual intensity.

$$I_{LED,1st} = I_{target,1st} - I_{solar,eff} * 0.45 \frac{mol\ PAR}{mol\ solar}$$ Eq.III-2

Step 5: If this is not the case, then all negative $I_{LED,1st}$ values are added, their hour count defined as *N* and subtracted from $I_{target,1st}$ as shown in equation III-3.

$$I_{target,2nd} = I_{target,1st} - \frac{I_{excess}}{t_{photo} - N}$$ Eq. III-3

Step 6: The second target intensity then determines the LED output by equation III-4.

$$I_{LED,2nd} = I_{target,2nd} - I_{solar,eff} * 0.45 \frac{mol\ PAR}{mol\ solar}$$ Eq. III-4

An illustration of the concept can be found in the Supplementary Information of Weidner et al. (2021). The standard efficiency, i.e. their ability to convert electrons into photons rather than heat, used in this study is 59% or 2.7 µmol/J, which is the average of current models from the largest producers. The efficiency is derived from the conversion factor 4.57 for light with a wavelength of 400 to 700 nm.

2. Mass and energy balances and general equations

2.1 Primary mass and energy balances

The energy balance considers the enthalpy of the CEA facility at the inlet and outlet of the HVAC system and vent openings and can be written as a first-order differential equation III-5.

$$\frac{dH_{air}}{dt} = F_{vent} * \left(h_{air,outside} - h_{air,out}\right) + F_{hvac} * (h_{air,hvac,out} - h_{air,out}) + Q_{total}$$ Eq. III-5

where $\frac{dH_{air}}{dt}$ is the change of enthalpy of the air (including both the dry air and the water vapour) in the space for growing, $h_{air,outside}$ is the outside air enthalpy, $h_{air,hvac,out}$ is the enthalpy of the HVAC outlet air. $h_{air,out}$ is the enthalpy of air at both the inlet of the HVAC system and the outlet of the vents. In practice, those would not necessarily be at exactly the same locations but for simplicity an average outlet condition is adopted for this zone. Q_{total} is the net enthalpy change introduced to the space for growing due to energy or mass flows other than the HVAC and venting air flow. For the PF, CGH and the OGH if venting was off, this would simplify to equation III-6.

$$\frac{dH_{air}}{dt} = F_{hvac} * (h_{air,hvac,out} - h_{air,out}) + Q_{total}$$ Eq. III-6

In our model implementation, the differential term was approximated by the finite difference method (equation III-7)

$$\frac{dH_{air}}{dt} \approx (h_{air,center,t} * Vol * \rho_{dry,center,t} - h_{air,center,t-1} * Vol * \rho_{dry,center,t-1})/\Delta t \quad \text{Eq. III-7}$$

where Δt is the interval from time t-1 to time t, which was set to 1 hour or 3600 s. The density used here is the dry air density. The calculation of centre and inlet conditions are based on achieving the above stated aims of the model. The enthalpy at the centre zone of the growing space is defined as shown in equation III-8.

$$h_{air,centre} \approx \left(h_{air,outside} * \frac{1}{2} + h_{air,out} * \frac{1}{2}\right) * \frac{F_{vent}}{F_{hvac} + F_{vent} + \frac{Vol * \rho_{dry,centre}}{3600}} + \left(h_{air,hvac,out} * \frac{1}{4} + h_{air,out} * \frac{3}{4}\right) * \frac{F_{hvac}}{F_{hvac} + F_{vent} + \frac{Vol * \rho_{dry,centre}}{3600}} + h_{air,out} * \frac{\frac{Vol * \rho_{dry,centre}}{3600}}{F_{hvac} + F_{vent} + \frac{Vol * \rho}{3600}} \quad \text{Eq. III-8}$$

The same relationship is used for the other air properties (density, specific humidity and temperature) by replacing the enthalpy term with the respective property. Akin to the centre zone, the inlet zone is defined as shown in equation III-9.

$$h_{air,inlet} \approx h_{air,outside} * \frac{F_{vent}}{F_{hvac} + F_{vent} + \frac{Vol * \rho_{dry,centre}}{3600}} + \left(h_{air,hvac,out} * \frac{1}{2} + h_{air,out} * \frac{1}{2}\right) * \frac{F_{hvac}}{F_{hvac} + F_{vent} + \frac{Vol * \rho_{dry,centre}}{3600}} + h_{air,out} * \frac{\frac{Vol * \rho_{dry,centre}}{3600}}{F_{hvac} + F_{vent} + \frac{Vol * \rho_{dry,centre}}{3600}} \quad \text{Eq. III-9}$$

The first terms in equation III-8 and III-9 describe the influence of venting on the zone (with a more pronounced plug flow reactor behaviour), the second term describe the influence of the HVAC outlet into the growing space (with a combined plug flow reactor and well-mixed space behaviour) and the third term accounts for the well-mixed space behaviour at low venting and HVAC flowrates. The inlet zone relation was used in the optimisation to derive the temperature dependent yield factor (see SI 4.2) and the adherence to climate setpoints (e.g. keeping the vapour pressure deficit between 0.4 and 1.2 kPa) in this zone.

Equation III-8 was then combined with equation III-6 and equation III-7 to derive the energy balance valid for all systems (derivations in the Supplementary Information of Weidner et al. (2021). Similar to the energy balance, the mass balance for water incorporates the specific

humidity ω in g water vapour per kg air at the centre zone, as well as the infiltration balance and the added water vapour from evapotranspiration and fogging.

The total amount of energy into the room is described by equation III-10, Q_{solar} and $Q_{inflitration}$ are specific to GHs.

$$Q_{total} = \left(Q_{structure} + Q_{LED,PAR} + Q_{LED,heat} + Q_{SH} + Q_{fans,hvac} + \left[Q_{solar} + Q_{inflitration}\right]\right) + h_{w,T_{center}} * m_{w,fog} + h_{sat,T_{leaf}} * m_{w,evap} \quad \text{Eq. III-10}$$

The total energy to be added or removed in the HVAC is calculated by equations III-11 and III-12.

$$Q_{cool,req} = \begin{cases} F_{hvac} * \left(h_{air,GH,out} - h_{air,equiv}\right) - m_{w,out} * h_{w,T_{equiv}} & if\ m_{w,out} > 0\ and\ h_{air.GH,out} > h_{air,hvac,out} \\ F_{hvac} * \left(h_{air,GH,out} - h_{air,hvac,out}\right) & if\ m_{w,out} = 0\ and\ h_{air.GH,out} > h_{air,hvac,out} \\ 0 & else \end{cases} \quad \text{Eq. III-11}$$

$$Q_{heat,req} = \begin{cases} F_{hvac} * \left(h_{air,hvac,out} - h_{air,equiv}\right) & if\ m_{w,out} > 0 \\ F_{hvac} * \left(h_{air,hvac,out} - h_{air,GH,out}\right) & if\ m_{w,out} = 0\ and\ \ h_{air,hvac,out} > h_{air,GH,out} \\ 0 & else \end{cases} \quad \text{Eq. III-12}$$

In the PF with continuous dehumidification, these simplify to equations III-14 and III-14.

$$Q_{cool,req} = F_{hvac} * \left(h_{air,hvac,in} - h_{air,equiv}\right) - m_{w,out} * h_{w,T_{equiv}} \quad \text{Eq. III-13}$$

$$Q_{heat,req} = F_{hvac} * \left(h_{air,hvac,out} - h_{air,equiv}\right) \quad \text{Eq. III-14}$$

2.2 Exchanges with the environment

To calculate Q_{total}, the following equations are employed (Eq. III-15 to III-20).

$$U_{GH} = \frac{U_{cover} * \left(A_{Roof} * f_{screen} + A_{wall,S} * f_{screen} + A_{walls,E,W} * \left(1 + f_{screen,EW}\right) * 0.5\right) + U_{wall} * A_{wall,N}}{A_{Roof} + A_{facade}} \quad \text{Eq. III-15}$$

$$Q_{GH} = Q_{structure} = U_{GH} * \left(T_{outside} - T_{center}\right) * \left(A_{roof} + A_{facade}\right) * \left(1 + f_{radiation}\right) \quad \text{Eq. III-16}$$

$$Q_{PF} = Q_{structure} = U_{wall} * \left(T_{air,outside} - T_{air,center}\right) * \left(A_{roof} + A_{facade}\right) \quad \text{Eq. III-17}$$

$$Q_{solar} = I_{solar,eff} * \left(1 - f_{production}\right) * A_{roof} + \left(I_{solar,eff} + I_{LED} - I_{net}\right) * A_{growing} \quad \text{Eq. III-18}$$

Source: (Graamans et al., 2018; N. Katsoulas et al., 2015)

$$A_{growing} = A_{roof} * f_{production} * N_{racks} \quad \text{Eq. III-19}$$

$$Q_{LED,PAR} = I_{LED} * \left((1 - CAC) + e^{-k_s * LAI} + \left(1 - \frac{PAR_{Plant}}{PAR_{LED}} \right) \right) * A_{growing} \quad \text{Eq. III-20}$$

Source: (Graamans et al., 2017; Nikolaos Katsoulas & Stanghellini, 2019; Toyoki Kozai, 2013)

Note: The above equations ensure that solar radiation and PAR not absorbed by plants are not double-counted in the energy balance.

$$Q_{LED,heat} = (Power_{LED} - I_{LED}) * A_{growing} * (1 - f_{LED\ cooling}) \quad \text{Eq. III-21}$$

$$Q_{cool,LED} = (Power_{LED} - I_{LED}) * A_{growing} * (f_{LED\ cooling}) \quad \text{Eq. III-22}$$

The energy and mass balance of infiltration and fogging are shown in equation III-23 to III-25.

$$Q_{infiltration} = AER_{infiltration} * Vol * \rho_{outside} * \left(1 - \frac{\omega_{outside}}{1000 + \omega_{outside}} \right) * \frac{h_{air,outside} - h_{air,center}}{3600} \quad \text{Eq. III-23}$$

Note: Q_infiltration already includes the balance enthalpy of in- and outgoing water vapour, hence it is excluded in Q_total. The specific enthalpy of air adopted here is per unit mass of dry air, hence $\rho_{outside}$ of wet air needs to be converted to the density of dry air (kg dry air per unit volume of air flow) using the specific humidity.

$$m_{w,balance,infiltration} = AER_{infiltration} * Volume * \rho_{centre} * (\omega_{centre} - \omega_{outside}) \quad \text{Eq. III-24}$$

$$E_{fog} = m_{w,fog} * 3600 * \frac{E_{fog,ref}}{\eta_{fog}} \quad \text{Eq.III-25}$$

The resource loss is shown by equations III-26 to III-28.

$$m_{CO2,loss,infiltration} = \frac{P_{atm} * Vol * AER_{infiltration}}{R * (T_{centre} + 273)} * \frac{C_{CO2,centre} - C_{CO2,ambient}}{1000000 \frac{1}{mol}} * \frac{MW_{CO2}}{1000 \frac{g}{kg}} \quad \text{Eq. III-26}$$

Note: There is no CO_2 loss at night as the interior air is only conditioned during the photo period. In the OGH, $CO_{2,centre}$ becomes $CO_{2,centre-1}$ to avoid a circular reference without significant impact on the results.

$$m_{w,balance,OGH} = m_{w,balance,infiltration} + F_{vent,dry} * (\omega_{GH,out} - \omega_{outside}) \quad \text{Eq. III-27}$$

Due to the dehumidification device, more water vapour from the outside might be condensed than what is being lost (e.g. if the outside air is very humid). To account for potentially negative and positive $m_{w,balance,infiltration}$ values, the balance values over the 24 hours are added up to obtain the loss.

$$m_{w,loss} = \sum_{1}^{24} m_{w,balance} * 3600 \frac{s}{h} \quad \text{Eq. III-28}$$

The irrigation water that is used by the plant for biomass growth is not considered in this study as it will be the same for the three systems. For the CGH, the ventilation represents additional exchange with the environment; the air velocity was calculated by equation III-29 (Graamans et al., 2020) and pressure drop and fan electricity by equations III-30 and III-31.

$$u_{vent,out} = \frac{F_{vent} * \left(1 + \frac{\omega_{GH,out}}{1000 \frac{g}{kg}}\right)}{\rho_{GH,out} * A_{sect} * f_{vent\ size}} \quad \text{Eq. III-29}$$

$$\Delta P_{vent} = u_{vent,out}^2 * \frac{\rho_{GH,out}}{2} + 3.4 * u_{vent,out}^2 + 4.9 * u_{vent,out} \quad \text{Eq. III-30}$$

$$E_{fans,vent} = \begin{cases} \frac{F_{vent}}{\rho_{outside}} * \frac{AER_{vent} - 4}{AER_{vent}} * \frac{\Delta P_{vent}}{\eta_{fans}} & if\ AER_{vent} > 4 \\ 0 & else \end{cases} \quad \text{Eq. III-31}$$

Note: For AER_vent <= 4/h natural ventilation was assumed (according to calculations with wind speeds of 2 m/s.

2.3 Carbon dioxide level in the open greenhouse

The CO_2 level at the centre was calculated using equations III-32 to III-35 for the OGH.

$$\frac{dn_{CO2}}{dt} = C_{CO2,outside} * n_{air,vent} + \frac{\left(m_{CO2,supply} - m_{CO2,loss,infiltration}\right) * \frac{1000g}{kg}}{MW_{CO2}} - C_{CO2,centre} * n_{air,vent} \quad \text{Eq. III-32}$$

$$n_{air,vent} = \frac{F_{vent} * 1000 \frac{g}{kg}}{MW_{air}} \quad \text{Eq. III-33}$$

$$\frac{dn_{CO2}}{dt} \approx \frac{\left(C_{CO2,centre} - C_{CO2,centre-1}\right) * \frac{Vol * P_{atm}}{R * (T_{centre} + 273)}}{\Delta t} \quad \text{Eq. III-34}$$

$$C_{CO2,centre} =$$

$$\frac{C_{CO2,outside} * n_{air,vent} + \frac{\left(m_{CO2,supply} - m_{CO2,loss,infiltration}\right) * \frac{1000g}{kg}}{MW_{CO2}} + C_{CO2,centre-1} * \frac{Vol * P_{atm}}{R * (T_{centre} + 273}}{\frac{Vol * P_{atm}}{R * (T_{centre} + 273)} * \frac{1}{3600} + n_{air,vent}} \quad \text{Eq. III-35}$$

The CO_2 supply during the photoperiod with venting in the OGH was regulated in order to balance CO_2 purchase cost and environmental impact with the increase in yield, while ensuring that it would not be lower than in the closed greenhouse if there was no venting (equation III-36).

$$m_{CO2,supply} = Y_{hourly}@1600ppm@T_{opt} * 0.3 + m_{CO2,loss,infiltration} \quad \text{Eq. III-36}$$

$$m_{CO2,supply} \leq \left(C_{CO2,target} - C_{CO2,outside}\right) * n_{air,vent} * MW_{CO2} * \frac{3600\frac{s}{h}}{1000\frac{g}{kg}} + \left(C_{CO2,target} - C_{CO2,center-1}\right) * \frac{Vol * P_{atm}}{R * (T_{centre} + 273)} * \frac{MW_{CO2}}{1000\frac{g}{kg}} * + m_{CO2,loss,infiltration} \quad \text{Eq. III-37}$$

Equation III-37 ensures that at no time more CO_2 is supplied than needed to maintain the target CO_2 concentration. The 0.3 kg CO_2/kg edible crop produced is derived from Hemming et al. [32] to reflect current best practice.

For the CGH, we found that the loss of CO_2 through the low infiltration rate could be compensated by typical CO_2 dosing rates even at 1600 ppm while staying in the range of kg CO_2/kg crop values reported by Hemming et al. [32]. The CO_2 level during the photo period was thus fixed in the CGH and supply would cease in the dark period to prevent wasting CO_2 when it does not increase plant growth. Equation III-38 thus simplifies in the dark period to

$$C_{CO2,centre} = \frac{\left(m_{CO2,loss,infiltration}\right) * \frac{1000g}{kg}}{MW_{CO2}} + C_{CO2,centre-1} * \frac{Vol * P_{atm}}{R * (T_{centre} + 273)} * \frac{1}{3600} \quad \text{Eq. III-38}$$
$$\frac{Vol * P_{atm}}{R * (T_{centre} + 273)} * \frac{1}{3600} +$$

The required supply to boost the CO_2 concentration at the beginning of the photoperiod is described by equation III-39 for both GHs.

$$m_{CO2,supply}@t(photo) = \frac{C_{CO2,target} - C_{CO2,centre-1}@t(photo) - 1}{1000000\frac{ppm}{mol}} * \frac{Vol * P_{atm}}{R * (T_{centre} + 273)} * \frac{MW_{CO2}}{1000\frac{g}{kg}}$$ Eq.III-39

In the case of the OGH, any ventilation flow rate determined by the optimisation higher than zero at 7 AM will lead to an initial CO_2 level below the target CO_2 level.

For the CGH, the total CO_2 supplied (and lost to the air) can be calculated for the day (except the first hour) with equation III-40:

$$m_{CO2,supply} = m_{CO2,loss,infiltration}$$ Eq. III-40

The mass of CO2 that needs to be supplied for plant growth was not considered in this study as it will be the same for all three systems (in terms of kg CO_2/kg produce) and typically discounted as biogenic in life cycle assessments of food system impacts.

2.4 Thermodynamic relations

The equations describing the behaviour of water in were used from https://www.hatchability.com/Vaisala.pdf and https://www.engineeringtoolbox.com/density-air-d_680.html. The pressure drop in the HVAC system is described below.

$$\Delta P_{hvac} = \frac{(V_{hvac} * 2118.9)^{1.9} * 0.109136}{(D_{duct} * 39.37)^{5.02}} * 8.162 * L_{duct} + \xi * \rho_{hvac,out} * \frac{u_{air,hvac}^2}{2}$$ Eq. III-41

Equation from https://www.engineeringtoolbox.com/sizing-ducts-d_207.html, ducts sized for air flows of AER = 10 and 10,000 m3 volume, with a maximum air speed of 12 m/s.

$$E_{fans,hvac} = Q_{fans.hvac} = V_{hvac} * \Delta P_{hvac} * \frac{1}{\eta_{fans}}$$ Eq. II-42

Source: (Graamans et al., 2020)

2.5 Physical relations

The physical relations describing the radiation into the greenhouse were taken from Vanthoor et al. (2011) and the radiation received by the plant bed from the sun and LEDs were taken from Graamans et al. (2018) and Kozai (2013). They are listed in 2.5 in the Supplementary Information of (Till Weidner et al., 2021).

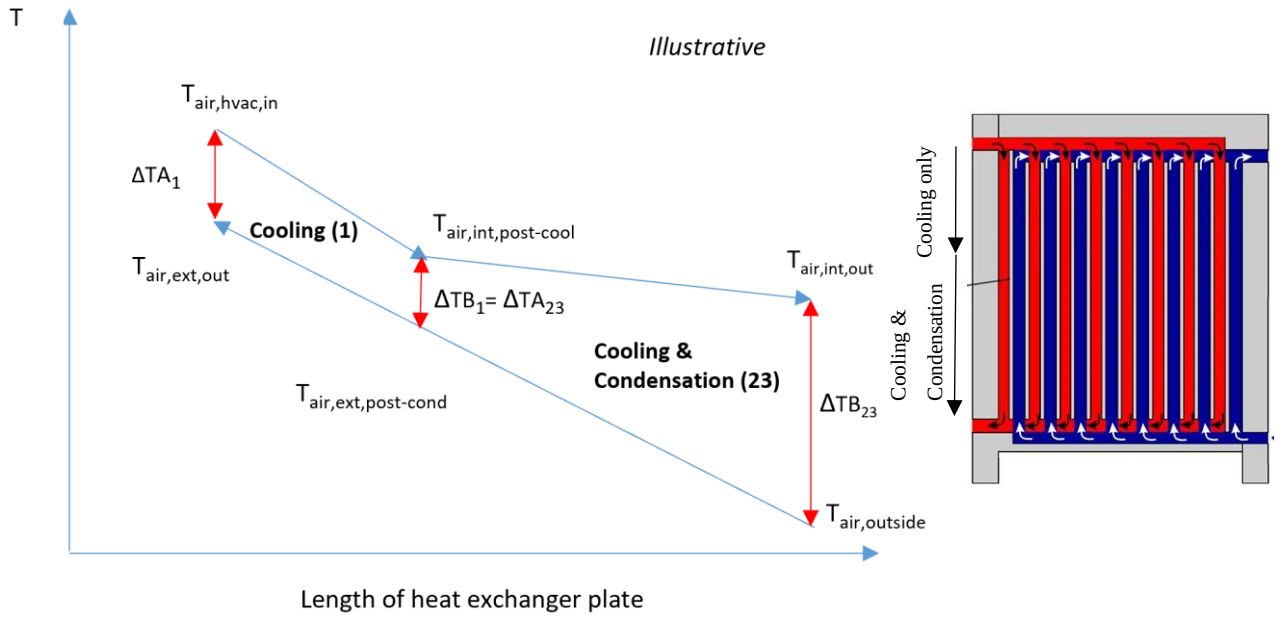
3. Design and concepts of the air handling unit

Ventilation is sometimes either not an option (PF and CGH) or has limited potential to keep climate parameters such as humidity in check, e.g. when the outside air is hotter or more humid than the inside air (Graamans et al., 2018). This study, therefore, considers a comprehensive air handling unit (AHU) to condition the circulating GH or PF air. It is equipped with an air-to-air heat exchanger ("free" cooling), a refrigeration cycle (RC) for condensing (dehumidification) and cooling of the internal air and an air-source heat pump (ASHP) to either increase air temperature after the condensation step or to simply heat the circulating air. Although ground-source heat pumps can be more efficient, ASHPs were chosen due to their lower upfront investment costs and their global applicability since they are not dependent on shallow, accessible and abundant groundwater. Such integrated AHUs are readily available on the market and can be customised for specific purposes (https://www.aaon.com/Documents/Sales/M2_ONLINE_160419.pdf).

In the PF, the sealed building combined with the evapotranspiration from plants results in permanent dehumidification requirements. Hence, the air in the AHU is cooled below the dew point and subsequently heated up again to the target temperature. In the CGH, the infiltrating air causes the AHU to vary in its operation depending on the circulating flowrate; the air is either dehumidified and heated up again, is simply cooled or heated without any change in the absolute humidity of the air stream (if the moisture removal through infiltration is equal or greater than the evapotranspiration). In the OGH, the AHU works together with the ventilation and fogging system to control the climate. The operation is similar to the CGH, but the AHU is combined with venting operations to reduce the overall energy consumption. Thus, the AHU either dehumidifies (cooling below the dew point with subsequent heating) or simply cools or heats the air, depending on the desired inlet zone conditions.

The electricity consumers of the AHU consist of two compressors (in the RC and ASHP) and several fans to overcome the pressure drop created by the smaller channels in the heat exchangers (see image on the left). There are in total 5 HEXs, i.e. air-to-air, refrigerant evaporator (between internal air and refrigerant) and condenser (between the refrigerant and outside air), ASHP evaporator (between the refrigerant and outside air) and condenser (between internal air and refrigerant). The air-to-air HEX requires two fans (outside and internal air), all other HEXs one internal air and one external air fan (the liquid within the tubes is propelled through the pressure difference created by the compressor). The air-to-air HEX is considered to be a counter-flow plate HEX while all other HEXs are cross-flow finned tube HEX in which the refrigerant circulates within the tubes.

To fully capture the influence of the outside climate and the requirements on the internal air conditioning in the optimisation, the electricity consumption of the six fans and two compressors were made wholly dependent on the cooling and heating load as well as the temperatures and absolute humidity of the AHU inlet, outlet and outside air. Previous studies either optimised the cooling and heating duty without further investigation how this would be realised in an HVAC system (Golzar et al., 2018; L. Li et al., 2020) or indicated the electricity consumption through constant heating and cooling COPs for a specific location (Graamans et al., 2018). To satisfy the requirements for detail and flexibility, this work builds on the methodology developed by Graamans et al. [9] and incorporates concepts such as a) the NTU method (Incropera et al., 2006) combined with b) a distinction between cooling and cooling with condensation of the internal air in the air-to-air HEX, c) state variable plotting to obtain empirical polynomial equations (e.g. temperature, enthalpy and entropy of the refrigerant in the RC) and d) heat integration between the ASHP and RC condensers.



AppxIII-Figure 1: Illustrative T-L diagram of the air-to-air heat exchanger, containing a cooling only zone and a zone in which water vapour is continuously condensed as air is fully saturated. The image on the right illustrates how this would look like in a schematic of a plate heat exchanger (from https://whatispiping.com/plate-heat-exchanger-with-steam-1/)

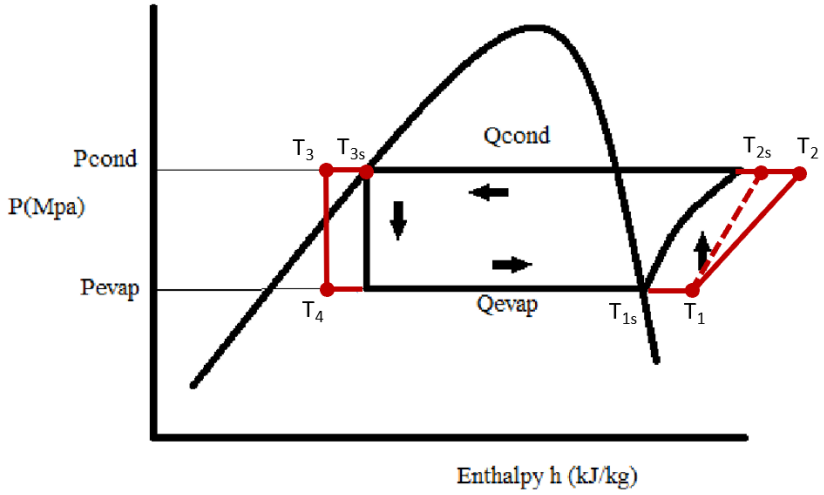
The air-to-air HEX is added to the system to make use of cold outside air in winter or cold regions. The HEX will need to be able to both cool the internal air to the target temperature and dehumidify it (see AppxIII-Figure 1). The latter occurs when the temperature reaches its saturation point for a given absolute humidity and continues until the target absolute humidity

is reached (defined as step 23). This process is different from a cooling-only process (defined as step 1) since the heat capacity ratio between the streams differs for the two steps. An iterative process using the NTU-method was developed to account for this.

1. Based on the value of the decision variables $u_{air,ext}$ (external air velocity) and $f_{a2a,share}$(amount of internal air sent through air-to-air HEX), the model assessed whether the potential duty is higher than the duty required for step 1. If so, the area of the HEX was divided by the share of step 1 duty to the potential duty to obtain a cooling ratio splitting the available HEX area.
2. The remaining area was used to determine the potential duty for step 23 and the resulting external air temperature after the condensation step.
3. The external air temperature and available HEX area for step 1 were then used to recalculate the step 1 duty.
4. The error between the required duty and the recalculated duty was used to refine the cooling ratio.
5. Steps 2 to 4 were repeated 4 times which appeared sufficient to reach a convergence
6. The final cooling ratio was used to determine the actual step 23 duty and thus the remaining cooling duty to be realised by the RC.
7. The value of the decision variables determined the fan power consumption requirements and the optimisation routine compared those with the energy savings in the RC achieved by the air-to-air HEX, finding the optimum balance between the two options.

The RC was modelled in three steps. First, the outside air and target temperature after the RC, either T_{equiv} (if condensation is required) or $T_{hvac,out}$, were used to determine the operating conditions of the refrigeration cycle, i.e. the evaporator and condenser temperature. Saturated refrigerant properties and a P-t diagram (see AppxIII-Figure 2) were used to derive polynomial equations for enthalpy and entropy (depending on temperature values).

These would then indicate the refrigerant enthalpy at the relevant locations within the RC, allowing to calculate the COP and electricity consumption of the compressor.



AppxIII-Figure 2: Illustrative P-h diagram of the refrigeration cycle. The red lines describe the subcooling and superheating.

Second, the required refrigerant flow determines the cooling requirements in the condenser section, which was realised by a) reheating the internal air stream if it was required and desired and b) by an air-cooled HEX for the remaining part. Reheating the internal stream means a reduced or nullified requirement for the ASHP to reheat the internal air stream (see AppxIII-Figure 1). The optimisation ensured that the most energy-efficient pathway is chosen, balancing "free" air2air cooling (which, if used for the complete cooling requirements, would necessitate the ASHP to deliver all reheating requirements) with refrigerant cycle cooling.

Third, the required outside air flows and thus fan power consumptions were assessed and combined with the power consumption of the internal air fans and the compressor. The remaining heating duty was to be covered by the ASHP, for which an empirical relation related outside air temperature to the power consumption. This relation was also used when the HVAC was only used for heating. The COP for LED cooling was assessed with fixed inlet and outlet water temperatures. The developed methodology results in similar COP values as indicated by other studies for cooling (Kozai et al., 2019; Tong et al., 2013) and heating (Ahmadi et al., 2018; Sarbu & Sebarchievici, 2014).

All equations used for the calculations of the air-to-air heat exchanger and the refrigeration cycle can be found in section 3 of the Supplementary Information in Weidner et al., (2021). The heat exchanger calculations were carried out according to http://www.heattransferconsult.nl/Tradi_Plate_Calc.html,

https://cheguide.com/air_cooled_exch.html, Graamans et al. (2020) and the NTU method (Incropera et al., 2006).

All HEXs were designed to cope with the maximum expected heating and cooling duties (around 750 kW) while occupying only a stretch of 2 m along the North wall. This led to relatively large HEX areas which might result in high investment costs. A full economic analysis would be needed to strike a balance between capital investment and energy savings, which is out of the scope of this work. The dimensions of the three types of HEX (counter-flow plate, air to air; cross-flow finned tube, internal air to refrigerant; cross-flow finned tube, refrigerant to external air) are listed below in AppxIII-Table 1.

AppxIII-Table 1: Dimension of the heat exchangers in the air conditioning system

Design air-to-air HEX	**Dimen-sions**	**Design finned tubes of air-to-refrigerant HEX**	**Dimen-sions**	**Design air-to-refrigerant HEX (other parameter)**	**Dimensions internal air HEX**	**Dimen-sions external air HEX**
Number of plates	200	Tube outer diameter	1 inch	Number of tube rows	15	12
Plate length	12 m	External area of bundle face area	26.8 m^2/m^2	Total external area (APSF)	402 m^2/m^2	321.6 m^2/m^2
Plate width	4 m	APF	m^2/m tube	Height (y-axis to flow)	4.5 m	2 m
Plate distance	8 cm	Fin height	1.59 cm	Width (x-axis to flow)	2 m	10 m
Plate thickness	2 cm	Fins per meter	394	Face area	9 m^2	20 m^2
Total flow area	3.2 m^2	Wall thickness	1.5 mm	Finned tube area	3,618 m^2	6,432
Total HEX area	9,600 m^2	Flow area per tube	3.94 cm^2	Number of tubes	1,064	378
Width of HEX	2 m	Tube inner radius	1.12 cm	Length (z-axis to flow)	1.28 m	1.03 m

4. Model parameter

4.1 Evapotranspiration

Several physical and empirical models have been proposed which aim to correlate the transpiration rate of plants to measurable parameters in the greenhouse (Nikolaos Katsoulas & Stanghellini, 2019). It seems that all of those models result in some over- or underestimation compared with experimental data, in particular when considering early plant stages, different crops or parameters close to zero (Kirnak et al., 2002; F. Villarreal-Guerrero et al., 2012). In this study, the model by Graamans et al. [17] was selected due to its ease of application with climate and crop variables obtainable or determinable from commonly available data. A topic of debate is the calculation of the r_s value, the stomatal resistance (F. Villarreal-Guerrero et al., 2012). We found that all of the proposed relations showed significant over- or underestimation for conditions at which the model was not validated, such as high VPD, very low radiation or low air velocities typically found in PF. We thus defined the terms in the r_s equation empirically by minimising the error for two sets of experimentally obtained ET values with known conditions (Graamans et al., 2017; Pamungkas et al., 2014). The CO_2 term was taken from Stanghellini (1987), the temperature term was dropped as it is both very plant-specific and excluded in most models due to its interrelation with other parameters, e.g. VPD (Nikolaos Katsoulas & Stanghellini, 2019). The VPD term was the most sensitive one, and a linear relation resulted in the smallest deviation from measurements and reflected the ET vs VPD curves from experimental studies (Kirnak et al., 2002; Pamungkas et al., 2014). The hyperbolic VPD term leads to very large r_s values at higher VPD values (above 1 kPa, outside the applicability range reported in (Stanghellini, 1987)), which would lead to a drop in evapotranspiration rates at higher VPD values, something not observed in the previously mentioned studies for plant factories or for plants in general (Massmann et al., 2019). The small values of the radiation terms C1 and C2 suggested by other works result in a sharp drop of the overall radiation term of 1 at very low light levels (Stanghellini, 1987) and could thus not represent measurements taken at those conditions. The terms used in Graamans et al. [17] make it less sensitive but were also empirically determined for a specific set of measurements not covering all ranges. Since we used watts instead of photosynthetic photon flux density in this work, we adjusted $r_{s,min}$, C1 and C2 values from curve fitting and least deviation from measurements. Finally, ET was equated to ET0, as suggested by crop coefficients close to 1 (Pamungkas et al., 2014).

4.2 Crop growth and yield

The yield-light dependency was chosen from Graamans et al. [7] and Van Henten [18]; doubling the DLI output increases the crop growth by a factor of 1.74 for all crops, similar to findings from other experiments (Proietti et al., 2004; Qaddoum et al., 2013). The target DLI determined the whitewash (light, 25% reduction or strong, 50% reduction) for the GHs as described in S1.3. This more rigid control of solar radiation in GHs (as opposed to flexible shading screens for example) meant that for months which did not require additional lighting in GHs, slightly more PAR than the target DLI was received by the plants. This was accounted for by adjusting the yield according to equation III-42.

$$YF_{correction} = \left(\frac{DLI_{actual}}{DLI_{target}} - 1\right) * 0.74 + 1 \quad \text{Eq. III-42}$$

The yield-CO_2 dependency (Equation III-43) was chosen from (L. Li et al., 2020) as it is in line with results from other works (Erwin & Gesick, 2017; Proksch, 2017). The yield-temperature dependency equation (Equation III-44) was chosen from Li et al. [34] and maximum temperatures were adjusted (between indicated value and 40 C) to reflect the possibility to obtain adequate yields for certain crops above the indicated temperatures (Graamans et al., 2018).

$$YF_{CO2} = \frac{1 - e^{-0.003} * (CO2_{centre} - 56)}{1 - e^{-0.003} * (CO2_{ref} - 56)} \quad \text{Eq. III-43}$$

$$YF_T = \frac{T_{max} - T_{air}}{T_{max} - T_{opt}} * \left(\frac{T_{air}}{T_{opt}}\right)^{\frac{T_{opt}}{T_{max} - T_{opt}}} \quad \text{Eq. III-44}$$

$$YF_{total} = YF_{CO2} * \left(\frac{YF_{T,center} * 4 + YF_{T,GH_{in}} + YF_{T,GH_{out}}}{6}\right) * YF_{rad} * YF_{correction} \quad \text{Eq. III-45}$$

Since a temperature gradient exists within the structure with the more optimum temperature in the centre, an approximation of the integral was carried out to account for this (Equation III-45).

Note: in the PF and CGH, the suffix *GH,in* becomes *hvac,out* and *GH,out* becomes *hvac,in*. The temperature yield factor differs between the locations in the greenhouse and is represented by a sin-curve, hence an approximation of the integral is used in this equation.

4.3 Duration and timing of photoperiod

The length of the photoperiod in GH was assumed to be at least 12 hours, from 7 AM to 7 PM, and longer for summer days when the solar radiation in a given hour before 7 AM or after 7 PM was above 50 W/m^2. This ensured minimum energy requirements for cooling when the sun hours are longer. The length of the PF was adjusted to the recommended photoperiod for each crop (Shao et al., 2016) and thus the vegetable basket proxy. The daily yield was divided by the length of the photoperiod in hours to obtain the hourly yield. Moreover, the photoperiod in PF is considered to be at night to reduce cooling costs associated with waste heat from artificial lighting (Graamans et al., 2018). The slightly higher duration of the photoperiod in the PF is assumed to not negatively affect the yield but helps to distribute the cooling load for the PF.

4.4 Crop properties and parameter table

The theoretical optimum and maximum temperature range values in AppxIII-Table 2 for tomatoes, bell peppers, broccoli and zucchini were obtained from (L. Li et al., 2020) and growers' recommendations. The minimum and maximum temperatures to be realised during the different periods by growers are also shown in AppxIII-Table 2 below.

The photoperiod, reference yield at 800 ppm CO_2 (using the harvest index) and default DLI values were selected for bell pepper (Schnitzler et al., 2004; Shao et al., 2016), lettuce, spinach, broccoli (L. Li et al., 2020; Shao et al., 2016), zucchini (www.greenhousegrower.com/production/zucchini-in-the-greenhouse/) and tomato (Benis et al., 2017c; B. H.E. Vanthoor, de Visser, et al., 2011) with slight adjustments based on LED suppliers' recommendations (www.horti-growlight.com/typical-ppfd-dli-values-per-crop).

To the authors' knowledge, there has so far been no attempt to produce statistically significant information on achievable yields at certain DLI levels and fixed conditions (e.g. temperature, VPD). Hence, these values reflect the authors best attempt to consolidate multiple sources and sometimes incongruent information (e.g. the tomato yield at a given DLI ranged from 30 kg/m2 at 25.9 mol/day (T. Kozai et al., 2019) to 74 kg/m2 at 20 mol/day (Benis et al., 2017c)). They serve here as a basis for the modelling effort and might differ in practice and between cultivars. The LAI was assumed to be constant for each crop given the different growth stages present in typical GH and PF; 2.1 for lettuce (Graamans et al., 2018), 2.8 for tomato (Benis et al., 2017c) and 2.5 for the basket.

AppxIII-Table 2: Composition of the vegetable basket and properties of the crops considered in it

Crop	Share in basket	Photoperiod PF (h)	Reference yield (kg m^{-2} $year^{-1}$)	Default DLI (mol day^{-1})	T_{opt}, T_{max} (C)	T_{min}, T_{max} (photo, C)	T_{min}, T_{max} (night, C)
Lettuce	12%	16	52.6	11.5	18, 33.5	11.6, 24.1	6, 14
Tomato	40%	12	56.0	16	27, 40	20.6, 32.5	15, 23
Broccoli	12%	16	18.1	12.4	16, 29	10.5, 21.2	4, 12
Bell pepper	12%	12	16.6	15	24, 38.5	17.3, 30	12, 20
Spinach	12%	16	27.8	10.7	18, 36	11, 25	6, 14
Zucchini	12%	16	8.5	10.8	18, 35	11.3, 24.6	6, 14
Vegetable basket	-	14	38.0	13.7	22.1, 36.6	15.6, 28.0	10.1, 18.1

5. Exterior climate

5.1 Latitude and sun-hours

The latitude is an indicator of the daily hours of sunshine, depending on the day of the year. Third-order polynomial equations were developed, which relate the latitude to the average daily sun hours for a given month. Data was obtained from https://www.engr.scu.edu/~emaurer/tools/calc_solar_cgi.pl. The equations were of the form $sun\ hours = a * x^3 + b * x^2 + c * x * d$, with x being the latitude.

5.2 Extraction of climate data for the metropolitan regions

The local values were aggregated to an average for each region, and an attempt was made to ensure the regions are roughly similar in size. The administrative boundaries were either country (level 1), state (level 2) or county (level 3). Each country defines their administrative boundaries differently (e.g. in some cases, the county level is the municipal level while in other cases states are called regions or prefectures), so for easier comparison, the definition by GADM was used here (https://gadm.org/download_world.html). The monthly temperature (min, max), water vapour pressure and solar radiation (daily average total) values were extracted from https://www.worldclim.org/.

5.3 Selection of regions

AppxIII-Table 3: List of regions and their climatic properties used in this study

Name of the region	Administrative type (level)	Average DLI natural (PAR, mol/(m2* day))	Mean annual temperature (C)	Climate zone (Köppen climate zone classification)	Latitude
Reykjavik region (Iceland)	Counties (3)	15.40	4.7	Cfc / ET	64.15 N
Stockholm region (Sweden)	States (2)	19.69	7.0	Cfb	59.46 N
Tokyo region (Japan)	States (2)	26.17	15.6	Cfa	35.51 N
Massachusetts (US)	State (2)	26.46	9.8	Cfa / Dfb	42.26 N
Tasmania (Australia)	State (2)	27.96	12.4	Cfb	41.97 S
Singapore	Country (1)	32.49	26.8	Af	1.35 N
Santiago region (Chile)	States (2)	33.71	14.6	Csb	33.59 S
Maricopa county (Arizona, US)	County (3)	39.73	21.94	Bwh	33 N
Gauteng (South Africa)	State (2)	40.35	16.0	Cwb	26.11 S
United Arab Emirates	Country (1)	42.83	26.7	Bwh	23.91 N

6. Optimisation routine

The optimisation was carried out with a Solver macro in Excel to facilitate the selection of different locations, crops and settings. This made it necessary to split the optimisation into two steps (specific energy and evapotranspiration balance), using multiple loops with convergence to update the conditions at the centre of the facility. The optimisation was finished when venting and HVAC flowrate, temperature and VPD would not change more than 2.5%, usually achieved within four iterations (10-30 seconds per hourly optimisation). The GRG non-linear engine was used with a convergence of 0.001.

7. Scenario analysis

Besides the choice of crop, a range of other parameters also has a considerable influence on the results. AppxIII-Table 4 shows these scenarios, listed by assumptions, design variables and control variables. Some of those parameters and the decisions taken are explained below.

AppxIII-Table 4: Overview of the 18 scenarios used in the parametric sensitivity analysis

Category	#	Aspect	Standard value	Scenario analysis
Physical behaviour assumptions	1	Minimum stomatal resistance	60	82
	2	Permissible VPD range	4 to 12 kPa	6 to 10 kPa
	3	LED efficiency	59%	75%
	4	U-value of the cover	GH: 2 (ETFE) and 2.27 (PC), PF: 0.3	Twice as much
	5	Permissible temperature differences in the refrigeration cycle	ΔTcond = 15 ΔTevap = 8	ΔTcond = 8 ΔTevap = 5
Design variables	6	Building size	Volume fixed	Half the floor area
	7	Geometry	Rectangular (W/L=0.5)	Square (W/L=1)
	8	Size of heat exchangers	See AppxIII-Table 1	Half as much area
	9	Target DLI	13.7 mol/(m^2*day)	Twice as much
	10	CO2 supply intensity	0.3 kg CO_2/kg yield	No limit (PF only)
	11	Crop	Basket	Lettuce
	12, 13	Climate preference	Mild	Warm, Cold
	14	LED water cooling	Variable (GHs only)	Off
	15	LED dimming (GHs only)	To compensate low sunshine in the morning and afternoon (GHs only)	Fixed power (250 µmol/m^2/s)
Control variables	16	Optimised parameter	Specific energy	Energy consumption only
	17	Air-to-air cooling	Variable bypass	Off
	18	Variable LED cooling	Variable (GHs only)	Fixed on
	19	Yield optimisation	Minimisation of hourly specific energy	Maximisation of hourly yield

Geometry

Since the greenhouse is East-West oriented, the geometry determines the length of the sturdy wall not facing the sun (North for above the equator and South for below) and thus indirectly the overall U-value and the design of the AHU. The standard value is width /length = 0.5.

Results are also obtained for width /length = 1, essentially a square. Further, the size of the building is doubled in one of the scenarios.

LED efficiency

The efficiency of LEDs has increased over the last year, and further technological advancement causes this trend likely to continue (Gómez & Izzo, 2018). The sensitivity of the results due to LED efficiency and the comparative benefit to GH and PF is assessed with an efficiency value of 75% or 3.5 µmol/J (https://www.horti-growlight.com/coolpack-horti-led-top-light).

U-value of walls

The overall heat transfer coefficient describes the possible heat exchange driven by a difference in temperature between inside and outside air. In continental and colder climate zones, winter heating is a significant contributor to the annual heating requirements (Benis et al., 2017a). The choice of ethylene tetrafluoroethylene film is thus justified from an energy perspective. However, it might not be realisable in every circumstance, e.g. due to the availability of equipment required to install it. Moreover, some plant factories might be situated in very well-insulated buildings. To assess the effect of the U-value and thus the wall material on the total energy consumption, results are also obtained for a U-value of 0.05 W/(m^2*C) for PF and twice the U-value for PC (2*2.27 W(m^2*C)) and ETFE (2*2 W(m^2*C)).

Light intensity

Increasing the moles of PAR received per day comes with diminishing returns for higher light levels (Proksch, 2017). Considering that artificial lighting is the primary electricity consumer in PF (Graamans et al., 2018) and GH in less sunny climates (Till Weidner & Yang, 2019), balancing the light supplied with the power consumption is a way to increase profits by reducing the cost per kg of crop produced (Golzar et al., 2018). The reference yield values were obtained at the indicated Default DLI which for lettuce can be equated with 16 hours of 250 µmol/(m^2*s). This was assumed to be common practice and thus chosen for the default case while a doubling of the light intensity (for lettuce 500 µmol/(m^2*s) and thus the DLI required was also assessed. Increasing the DLI much further than that was found to increase yield only marginally while almost linearly increasing the electricity consumption and was thus not selected.

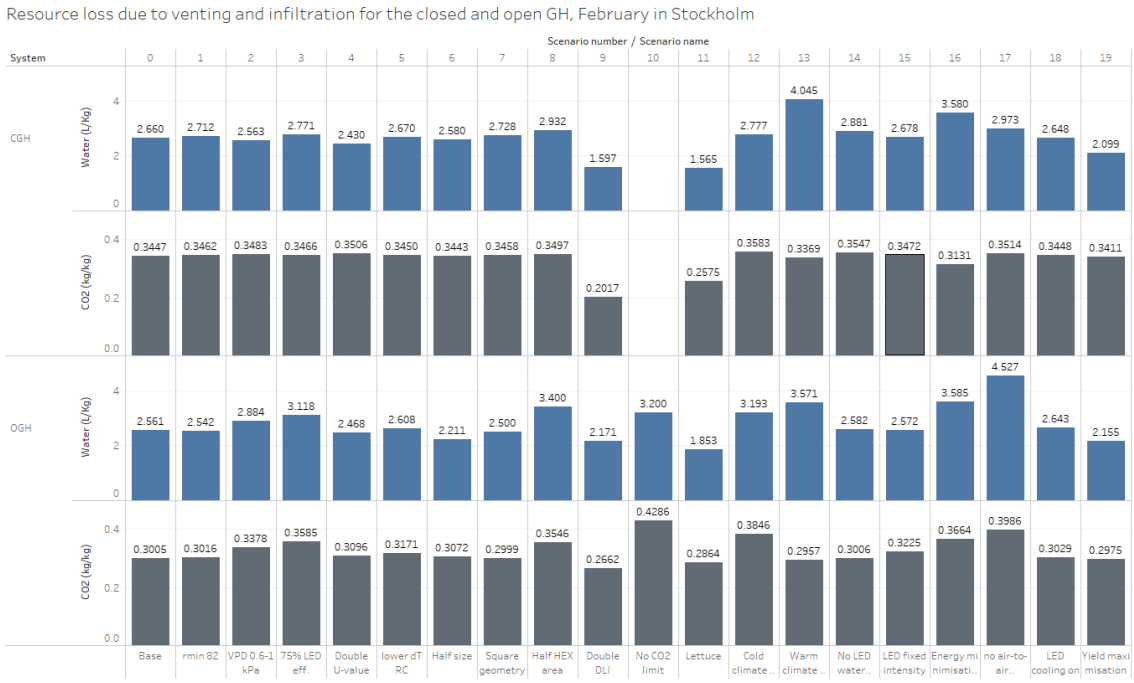
CO_2 concentration in the air

The positive influence of CO_2 on crop growth is well known. However, some discrepancies exist for the effect on the photosynthesis rate of a higher CO_2 concentration between 1200 and 1600 ppm. Some models suggest that increasing the CO_2 concentration at higher light intensities has a more substantial effect on the yield compared with the same increase at lower light intensities (Graamans et al., 2018; Van Henten, 1994), or similarly, that the photosynthesis rate reaches its maximum at lower CO_2 concentrations when the light intensity is lower (Pan et al., 2020). Others suggest that the effect of increased CO_2 levels in the air is less dependent on the light intensity (L. Li et al., 2020; Proksch, 2017). The photosynthesis rate increase calculated in one study (Graamans et al., 2018) for switching the CO_2 concentration from 400 to 1600 ppm at 250 µmol m^{-2} s^{-1} (a more than three times higher photosynthesis rate) could not be confirmed by reports from growers considering the actual yield of crops (Iddio et al., 2020). Hence, the simplified model from Li et al. [34] is employed for this work. Since CO_2 is contained with PF and CGH, a target CO_2 concentration of 1600 ppm is considered as the default and 400 ppm as an assessment of the influence on the comparative results between the growing practices.

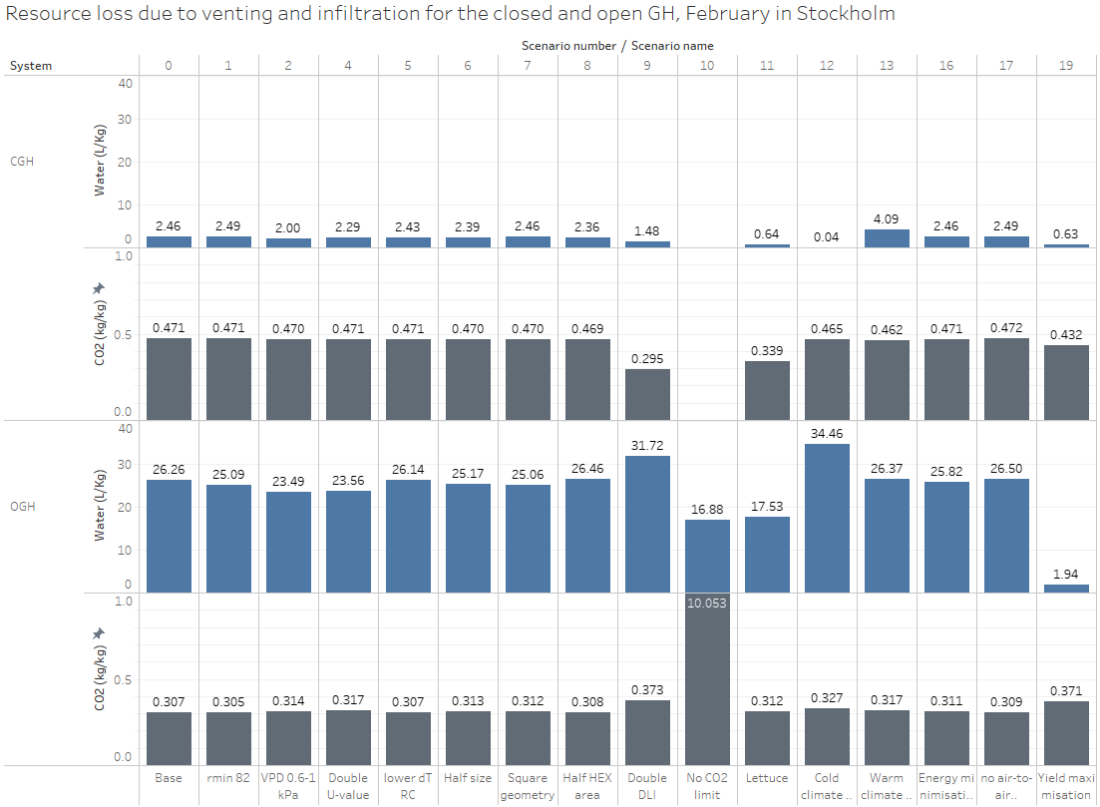
Optimisation of specific energy and variable cooling

The operations of a climate-optimised greenhouse require a high level of sensors and automation in practice which not every grower desires or can afford. To test the influence on the specific energy obtained without such measures, the optimisation is carried out for a hypothetical “non-optimised” case in which a) LEDs are constantly fully water-cooled or have a constant light intensity during their active hours (GH-only), b) an air-to-air heat exchanger which can’t be flexibly bypassed (either on or off) and c) the objective function during the day or photoperiod is the total electricity consumption (which would reduce controlling complexity). The latter means that the temperature limits are set to 85% of the maximum yield during the day and that the potential productivity loss due to venting (lower CO_2 levels) is ignored in the optimisation. Regarding the constant or non-dimmable light intensity of the LEDs, an output of 250 µmol/m^2/s was assumed, and the required hours of operation calculated as described in SI 2.5. To compare this with the optimised versions, the effects on yield of the resulting climate are still considered and the specific energy is nevertheless chosen as the target indicator.

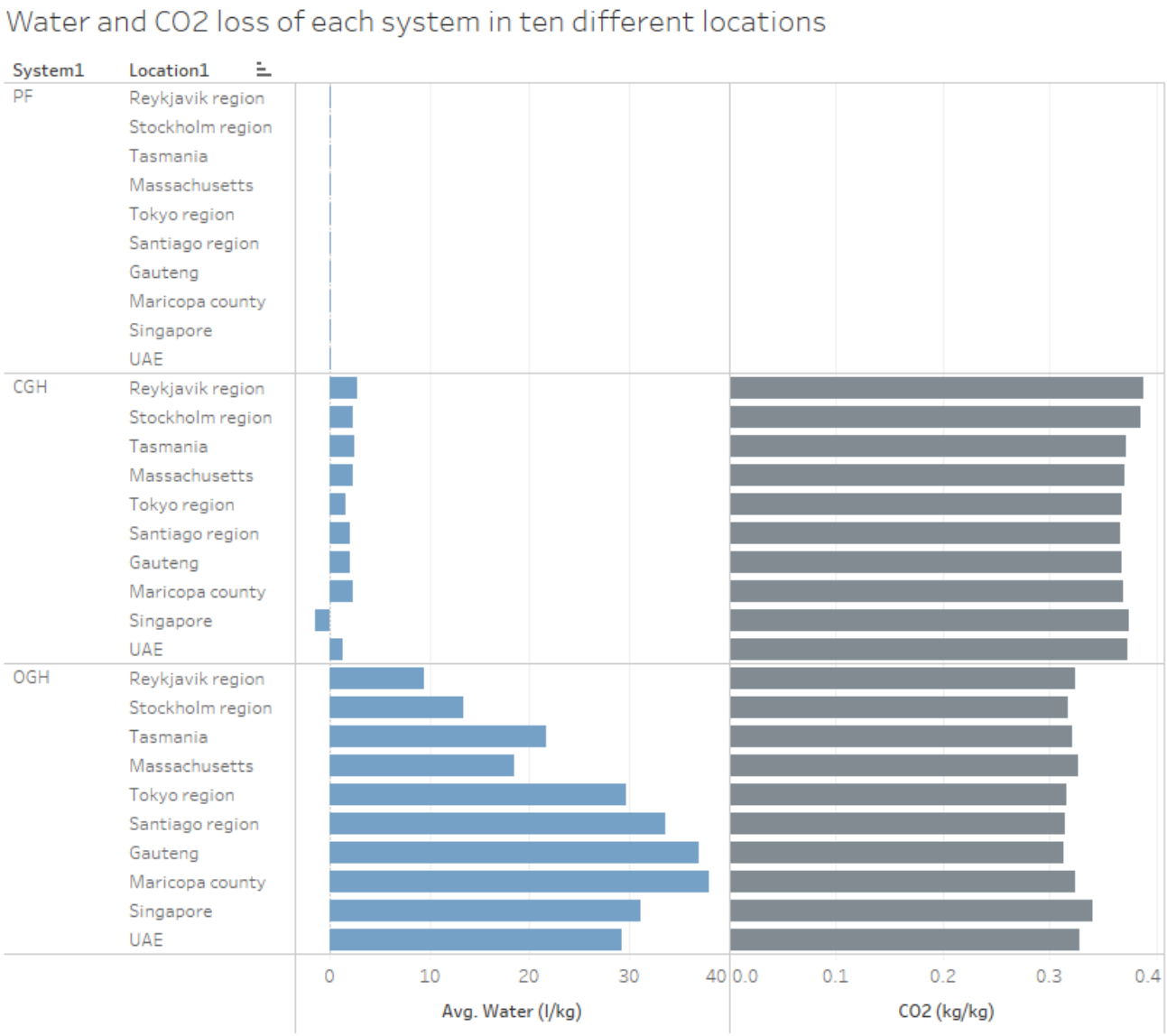
8. Additional results



AppxIII-Figure 3: Water and CO_2 loss for the three CEA systems and 18 scenarios for February in Stockholm



AppxIII-Figure 4: Water and CO_2 loss for the three CEA systems and 18 scenarios for July in Stockholm



AppxIII-Figure 5:Water and resource loss for the three systems (PF, CGH, OGH) at different locations. Plant uptake of water and CO_2 was not considered in this comparison.

9. Further comparison with other studies

The simulation and optimisation of indoor climate control have been carried out by other studies as well. Similar results were obtained in this for ventilation rates (Federico Villarreal-Guerrero et al., 2012), the difference between inside and outside winter temperatures (Shen et al., 2018), between day and night setpoints (Golzar et al., 2018), and the curves or development of temperature, VPD and evapotranspiration flux during the day (F. Villarreal-Guerrero et al., 2012). Different results for inside vs outside summer temperatures were obtained by Van Beveren et al. [12], which stems from the influence of temperature on yield considered in this study, as the objective of other control studies was to minimising energy consumption by keeping the temperature within a wide temperature range, rather than

optimising for specific energy. Further, relative humidity and temperature during a summer day were different in Katsoulas et al. [17], with lower relative humidity at high temperatures. Although this makes climate control easier, these settings would have violated the maximum VPD of 1.2 in this work. A growers guideline by a leading software provider for vertical farms assumes around 90 W for LEDs and 51.2 W combined for climate control, resulting in 22.1 kWh/kg for the yield and photoperiod assumed in this study (iFarm, n.d.). The small discrepancy can partly be explained by the gains through yield-energy optimisation in the present work. A description of how the values of the individual studies considered in Chapter 5 section 5.3.4. were conducted can be found in section 10 of the Supplementary Information of Weidner et al. (2021).

10. Nomenclature

Variables

Symbol	Description	Value (unit)
$\frac{\Delta h}{\Delta T}$	Change of saturated air enthalpy between for a given temperature range	kJ/(kg*C)
$h_{air,suffix}$	Enthalpy of moist air, dry mass basis	kJ/kg
$h_{sat,cond}$	Enthalpy of the saturated refrigerant vapour in the condenser	kJ/kg
$h_{w,T_{equiv}}$	Enthalpy of condensed water	kJ/kg
A_{suffix}	Respective area of the roof (roof), cardinal direction facing walls (E/S/W/N), all walls (façade), sum of all plant beds (growing), intersectional area or width * times (sect)	m^2
$C_{CO2,centre}$	CO_2 concentration in the air in the centre of the facility	Mol CO_2/mol of air
$C_{CO2,target}$	Target CO_2 concentration in the air	Mol CO_2/mol of air
$C_{air,ext}$	Heat capacity rate external air	J/K
$C_{air,int,1}$	Heat capacity rate internal air for cooling only (decrease in temperature, no condensation)	J/K
$C_{air,int,23}$	Heat capacity rate internal air cooling and condensation (decrease in temperature and ω)	J/K
C_{min}	Smaller heat capacity rate of respective air flows (1 for cooling only, 23 for cooling and condensation)	J/K
C_r	Heat capacity rate ratio of respective air flows	-
C_w	Heat capacity of water	4.19 kJ/(kg*C)
E_{heat}	Electricity consumption of the air-source heat pump	W
E_{ASHP}	Electricity consumption of HVAC heating coil (heat pump)	W
E_{RC}	Electricity consumption of HVAC refrigeration system	W

$E_{comp,ref}$	Electricity consumption of the compressor in the refrigeration cycle	W
$E_{cool,LED}$	Electricity consumption of LED cooling system	W
$E_{fan,ref,ext}$	Electricity consumption of the fan in the air-cooled condenser of the refrigeration cycle	W
$E_{fan,ref,int}$	Electricity consumption of the internal air fan to overcome the pressure drop in the finned tube heat exchanger of the refrigeration cycle	W
$E_{fans,hvac}$	Electricity consumption fans in HVAC system	W
$E_{fans,a2a,ext}$	Electricity consumption of the external air fans for the air to air HEX	W
$E_{fans,a2a,int}$	Electricity consumption of the internal air fans for the air to air HEX	W
$E_{fans,vent}$	Electricity consumption venting fans	W
E_{fog}	Electricity consumption of fogging system (OGH only)	W
E_{total}	Total electricity consumption	W
E_{vent}	Electricity consumption of venting fans	W
E_{vent}	Electricity consumption of ventilation system (OGH only)	W
F_{hvac}	Dry mass flow of hvac system	Kg/s
$F_{GH,in}$	Dry air mass flow rate entering the GH	Kg/s
$F_{air,a2a,ext}$	Outside air flow in the plate HEX	Kg/s
$F_{air,a2a,int}$	Internal air flow in the plate HEX	Kg/s
$F_{air,cond,req}$	Required outside air flow in the air-cooled condenser of the refrigeration cycle	Kg/s
F_{vent}	Dry mass flow of ventilation system (OGH only)	Kg/s
F_{vent}	Dry air mass flow rate of venting air	Kg/s
$I_{LED,canopy}$	Radiation of the LEDs received by the plant bed	W_{PAR}/m^2
I_{LED}	Radiation of the LEDs at the light fixture	W_{PAR}/m^2
$I_{net,PAR}$	Net radiation, solar and LED combined (PAR)	W_{PAR}/m^2
I_{net}	Net radiation, solar and LED combined (full spectrum)	W/m^2
$I_{solar,sky}$	Irradiation	$Wh/(m^2*h)$
$I_{solar,eff}$	Irradiation reaching into the greenhouse	$Wh/(m^2*h)$
I_{target}	The intensity of combined solar and LED radiation which approximates a uniform light supply	W_{PAR}/m^2
$PPFD_{LED}$	Photosynthetic photon flux density	$\mu mol/(m^2*s)$
$Power_{LED}$	Power consumption per unit area of LED	W_e/m^2
$P_{sat,suffix}$	Water vapour pressure of saturated air	hPa

$P_{w,suffix}$	Water vapour pressure	hPa
$Q_{heat,ASHP}$	Remaining heating duty to be realised by the air-source heat pump	W
$Q_{LED,heat}$	Heat gain from the waste heat of the LEDs	W
$Q_{LED,PAR}$	Heat gain from the light of the LEDs not absorbed by plants	W
Q_{PF}	Heat transfer between the plant factory and the environment	W
$Q_{cool,LED}$	Water cooling of LED cooling load	W
$Q_{fans,hvac}$	Heat gain from fans in hvac system	W
Q_{fog}	Sensible heat removed through fogging	W
$Q_{infiltration}$	Energy gain or loss due to infiltrating air	W
Q_{solar}	Heat gain from solar radiation not absorbed by plants	W
$Q_{structure}$	Heat transfer between the building structure and the environment	W
Q_{total}	Total heat balance	kW
$T_{air,equiv}$	Target temperature for required condensation (Ps@T_equiv = Pw,hvac,out)	C
$T_{air,suffix}$	Air temperature at given location	C
$T_{condens}$	Saturation temperature of the internal air at its water vapour pressure at the inlet of the hvac	C
T_{leaf}	Temperature of leaf surface	C
T_{max}	Maximum growing temperature of specific crop	C
T_{opt}	Optimum growing temperature of specific crop	C
U_{hex}	Heat transfer coefficient for heat exchanger, either air to air (a2a) or refrigeration cycle finned tube (ref)	W/(m2*C)
U_{GH}	Overall heat transfer coefficient for the greenhouse structure	W/(m2*C)
U_{GH}	Overall heat transfer coefficient for the greenhouse structure	W/(m2*C)
$V_{hvac,out}$	Volumetric flowrate at exit of HVAC system	m^3/s
Vol	Volume of CEA facility	m^3
X_{suffix}	Absolute humidity	g/m^3
Y_{hourly}	Attributed hourly yield	$Kg/(m^2*h)$
$Y_{ref,annual}$	Annual reported yield for year-round growing for specific crop at reference conditions	$Kg/(m^2*year)$
f_D	Darcy friction factor	-
$f_{LED\ cooling}$	Share of LED waste heat water cooled, 1 in PF	%
$f_{a2a,share}$	Share of total hvac flow sent through plate HEX (optimisation variable)	%

$f_{cooling\ ratio}$	Ratio of the area considered to be used for the cooling-only (1) step versus the total HEX area	%
$m_{CO2,loss}$	Mass of CO_2 lost	Kg/s
$m_{R134A,ref}$	Refrigerant flowrate	Kg/s
$m_{w,balance}$	Water lost or collected to environmental exchange	g/s
$m_{w,evap}$	Mass of water evaporated from plants	Kg H_2O/s
$m_{w,fog}$	Mass of water flow through fogging device	kg/s
$m_{w,infiltration}$	Mass of water introduced through venting	Kg/s
$m_{w,loss}$	Water lost to the environment due to infiltration and venting during a 24 hour period	g/day
$m_{w,out}$	Flowrate of condensed water	kg/s
n_{CO2}	Moles of CO2 in the growing facility	mol
$n_{air,vent}$	Molar flowrate air venting	Mol/s
r_a	Aerodynamic resistance to transpiration	s/m
r_c	Canopy resistance to transpiration, r_s /2	s/m
t_{photo}	Daily photoduration	h/day
$u_{air,a2a,ext}$	Outside air velocity in the plate HEX (optimisation variable)	m/s
$u_{air,a2a,int}$	Internal air velocity in the plate HEX	m/s
$u_{air,cond}$	Velocity of outside air in the air-cooled condenser of the refrigeration cycle	m/s
$u_{air,int,ref}$	Internal air velocity in the finned tube HEX (evaporator) of the refrigeration cycle	m/s
$u_{vent,out}$	Velocity of air through vent openings	m/s
ΔP_{hvac}	Pressure drop in the HVAC duct	Pa
ΔP_{vent}	Static and dynamic pressure drop delivered by the venting fans	Pa
AER_{hvac}	Air exchange rate of HVAC system	AE/h
AER_{vent}	Air exchange rate of ventilation system (only OGH, 0 for PF and CGH)	AE/h
$CO2_{loss}$	Carbon dioxide lost to the environment due to infiltration and venting	Kg/s
COP_{heat}	Coefficient of Performance for heating of HVAC cooling system	-
COP_{ASHP}	Coefficient of performance of the air-source heat pump	-
COP_{comp}	Coefficient of performance of the compressor in the refrigeration cycle	-
$COP_{cool,LED}$	Coefficient of Performance of LED cooling system	

COP_{cool}	Coefficient of Performance for cooling of HVAC cooling system	-
$DLI_{LED,canopy}$	Total moles of light received by the plant canopy	Mol PAR/(m2*day)
DLI_{LED}	Total moles of light produced by the LEDs	Mol PAR/(m2*day)
$DLI_{natural}$	Daily light integral solar radiation	Mol PAR/(m2*day)
DLI_{plant}	Daily light integral required	Mol PAR/(m2*day)
ET	Evapotranspiration	Kg/(h*m^2) or mm/h
LH	Latent heat transfer from plants to environment due to transpiration	W/m^2
SE_{hourly}	Specific energy consumption (for given hour of photoperiod)	Wh/kg
$SE_{product}$	Specific energy consumption as average during one month (or year)	Wh/kg
SH	Sensible heat transfer from plants to environment due to evapotranspiration balance	W/m^2
VCD	Vapour concentration difference at the leaf surface	g/m^3
VPD_{leaf}	Vapour pressure difference between air and saturated air at the leaf surface temperature	hPa
VPD_{suffix}	Vapour pressure difference of air	hPa
Vol	Volume of greenhouse or plant factory	m^3
YF_{CO2}	Yield factor due to varying CO_2 concentration in the air	-
YF_T	Yield factor due to varying air temperature	-
YF_{total}	Product of all yield factors for a given hour	-
λ_{suffix}	Latent heat of vaporisation at the temperature of the location indicated by the suffix	kJ/kg
$\rho_{air,suffix}$	Density of dry air	Kg/m^3
ρ_{suffix}	Density of wet air	Kg/m^3
ω_{suffix}	specific humidity of water in air	g/kg

Suffixes

Location	Description
centre	Air condition at the centre zone (half-way between East and West wall) of the GH or PF
equiv	Air condition after the condensation step in the HVAC system
hvac,in	Air condition at the inlet of the HVAC system
hvac,out	Air condition at the outlet of the HVAC system

In	Air condition at the inlet zone of the facility, influenced by the hvac_out flow and venting (OGH)
leaf	Air and water conditions at the leaf surface of the plants
out	Air condition at the exit zone of the facility, which is also hvac_in and the venting outlet
outside	Air condition at the outside of the facility

Fixed variables

Name	**Description**	**Value (unit)**	**Source**
$\dot{m}_{CO2,supply,ma}$	Maximum CO_2 dosing capacity per unit area	0.015 kg/(m^2*hr)	Based on 150 kg/ha/h (Kempkes & Janse, 2016)
$\dot{m}_{w,fog,max}$	Maximum fogging capacity per unit area	0.5 kg/(m^2*hr)	(Bram H.E. Vanthoor, Gázquez, et al., 2012)
$A_{hex,a2a}$	Heat transfer area of plate HEX	9,600 m^2	Based on design for feasible dimensions and potential to cover cooling load with reasonable COP when outside temperatures are below 0 C
$A_{hex,ref,ext}$	Finned Hex area (condenser) of the refrigeration cycle	6,432 m^2	Based on design for feasible dimensions and ability to cool down the refrigerant with outside air for the maximum hvac cooling load (~750 kW)
$A_{hex,ref,int}$	Finned Hex area (evaporator) of the refrigeration cycle	3,618 m^2	Based on design for feasible dimensions and ability to cool down the refrigerant with outside air for the maximum hvac cooling load (~750 kW)
A_{duct}	Duct intersectional area of HVAC system	2.32 m^2	Designed for 12 m/s, 10 AE/h and 10,000 m3
$A_{face,ref,int}$	Face area of the finned tube HEX (evaporator) of the	9 m^2	Based on design for feasible dimensions and ability to cool down the refrigerant with outside air for the maximum hvac cooling load (~750 kW)

	refrigeration cycle		
A_{fch}	Area of each channel between two plates in the plate HEX	0.032 m^2	http://www.heattransferconsult.nl/Tradi_Plate_Calc.html
C_1	First radiation term for rs	90.1	Based on empirical model constructed from experimental measurements from Graamans et al. [7] and Pamungkas et al. [46]
C_2	2nd radiation term for rs	11.3	Based on empirical model constructed from experimental measurements from Graamans et al. [7] and Pamungkas et al. [46]
C_3	VPD term for rs	4.3	Based on empirical model constructed from experimental measurements from Graamans et al. [7] and Pamungkas et al. [46]
C_4	CO_2 term for rs	6.1E-07	(Stanghellini, 1987)
$C_{CO2,amb}$	Ambient CO_2 concentration in the air	415 ppm	
$C_{CO2,ref}$	Reference CO_2 concentration in the air for yield figures	800 ppm	(Shao et al., 2016)
$C_{p,air}$	Heat capacity of air	1.005 kJ/(kg*K)	
$C_{p,liquid}$	Refrigerant liquid heat capacity	1.44 kJ/(kg*K)	https://www.gas-servei.com/images/Technical-data-sheet-R134a-ENGLISH.pdf
$C_{p,vapour}$	Refrigerant vapour heat capacity	0.85 kJ/(kg*K)	https://www.gas-servei.com/images/Technical-data-sheet-R134a-ENGLISH.pdf
C_w	Heat capacity of liquid water	4.19 kJ/(kg*K)	
D_{duct}	Duct diameter of HVAC system	1.72 m	Designed for 12 m/s, 10 AE/h and 10,000 m^3

D_{leaves}	Average leaf diameter	0.08 m	(Graamans et al., 2017; Nikolaos Katsoulas & Stanghellini, 2019)
D_{plate}	Distance between plates in plate HEX	0.008 m	Based on design for feasible dimensions and potential to cover cooling load with reasonable COP when outside temperatures are below 0 C
$E_{fog,ref}$	Reference electricity consumption of fogging system	2.41 Wh/l	Calculated assuming 70 bar pressure (http://www.fogsis.com/haber-fogging-system-and-efficient-greenhouse-79.html) using pump head (https://www.engineeringtoolbox.com/pump-head-pressure-d_663.html) and power consumption relations (https://www.engineeringtoolbox.com/water-pumping-costs-d_1527.html)
L_{plate}	Length of the plate in the plate HEX	12 m	Based on design for feasible dimensions and potential to cover cooling load with reasonable COP when outside temperatures are below 0 C
N_{plate}	Number of plates in plate HEX	200	Based on design for feasible dimensions and potential to cover cooling load with reasonable COP when outside temperatures are below 0 C
N_{racks}	Number of growing racks	4 (PF), 1 (GH)	Assumption for PF based on building height 8m and stack height 1.5m
$\frac{PAR_{canopy}}{PAR_{LED}}$	Share of LED light reaching the plant bed	89% for plant factories (due to reflective surfaces within the racks), 79% for greenhouses	(Kozai, 2013)
$P_{air,atm}$	Ambient pressure	101325 Pa	
$T_{evap,LED}$	Temperature in the evaporator (refrigerant) for LED cooling	10 C	15 C as difference assumed, LEDs kept at 25 C
U_{cover}	Overall heat transfer coefficient for the cover	2 ETFE, 2.27 PC, 0.5 RLC W/(m^2*C)	(Pakari & Ghani, 2019; Proksch, 2017)
U_{wall}	Overall heat transfer coefficient	0.3 W/(m^2*C)	(Castleton et al., 2010)

	for the wall or building		
W_{plate}	Width of plate in plate HEX	4 m	Based on design for feasible dimensions and potential to cover cooling load with reasonable COP when outside temperatures are below 0 C
$f_{LED,cooling}$	Share of waste heat absorbed by water cooling	0 – 0.85	Decision variable in optimisation, maximum of 85% from Mechatronix (Personal communication)
$f_{production}$	Share of the ground area used for plant beds	82% (GH), 60% (PF)	GH: (Villarreal-Guerrero et al., [13], PF: assumption based on higher requirements for machinery, automation and higher growing racks
$f_{radiation}$	Factor accounting for radiative heat loss	20%	(Castleton et al., 2010)
$f_{shading}$	Effect on solar transmissivity through structural shading	95 %	Assumption based on typical greenhouse design
$f_{screen,EW}$	Thermal day screen covering East (afternoon) and West (morning) facing walls	100% (off), 57% (on)	https://fyi.extension.wisc.edu/energy/files/2016/09/ThermalCurtains.pdf
f_{screen}	Thermal night screen covering	100% (off), 57% (on)	https://fyi.extension.wisc.edu/energy/files/2016/09/ThermalCurtains.pdf
$f_{vent\ size}$	Typical share of vent opening compared with GH height	19%	(B. H.E. Vanthoor, Stanghellini, et al., 2011)
$f_{whitewash}$	Whitewash for reduced solar light transmission	75% for light and 50% for strong	(Bram H.E. Vanthoor, Stigter, et al., 2012)
k_s	Reflection coefficient	0.7	(Nikolaos Katsoulas & Stanghellini, 2019)

$r_{s,min}$	Minimum stomatal resistance to transpiration	29 s/m	Based on empirical model constructed from experimental measurements from Graamans et al. [7] and Pamungkas et al. [46]
$AER_{hvac,max}$	Maximum air exchange rate in the HVAC system	100 AE/h	Assumption
$AER_{infiltration}$	Equivalent air exchange rate from air infiltration	0.25 AE/h	(Shin & Nam, 2015)
$AER_{vent,max}$	Maximum ventilation rate	40 AE/h	Assumption
AER_{min}	Minimum air exchange rate in the facility	0.75 AE/h	Assumption to ensure sufficient air flow to distribute CO_2, moisture and heat
CAC	Cumulative area cover, share of plant leaf cover in plant bed	90%	(Graamans et al., 2018)
LAI	Leaf area index	2.1 (lettuce), 2.8 (tomato)	(Benis et al., 2017c; Graamans et al., 2017)
MW_{h2o}	Molecular weight water	18 g/mol	
MW_{CO2}	Molecular weight CO_2	44.01 g/mol	
MW_{air}	Molecular weight air	28.96 g/mol	
R	Specific gas constant	8.314 J/(mol*K)	
Ra	Individual gas constant air	286.9 J/(kg*K)	

Rw	Individual gas constant water vapour	461.5 J/(kg*K)	
VPD_{max}	Maximum permissible vapour pressure deficit	12 hPa	(Shamshiri, Jones, et al., 2018)
VPD_{min}	Minimum permissible vapour pressure deficit	4 hPa	(Shamshiri, Jones, et al., 2018)
YF_{rad}	Yield factor influenced by the radiation	1 for default (reference), 1.74 for "high lighting"	(Graamans et al., 2018; Shao et al., 2016)
ξ	Minor Dynamic Loss Coefficient	4.15	4*0.7 (90° bend with vanes) + 1 (flow from duct) + 0.35 (flow away from duct) https://www.engineeringtoolbox.com/minor-loss-air-ducts-fittings-d_208.html
η_{LED}	Conversion efficiency LED	0.52 W_{PAR} / W_e	(Graamans et al., 2018)
η_{fans}	Fan efficiency	65%	(Graamans et al., 2020)
η_{fog}	Fogging system efficiency (share of water droplets evaporated before falling to the ground)	68%	(Federico Villarreal-Guerrero et al., 2012)
λ_{tube}	Thermal conductivity of tube or plate (copper core with aluminium fins)	380 W/(m*C)	(Graamans et al., 2020)
τ_{cover}	Solar transmissivity	83% (ETFE), 70% (PC), 28% (RLC)	(Proksch, 2017)

$\epsilon_{surface}$	Surface roughness	0.0000015 m	https://www.pumpfundamentals.com/PIPE%20ROUGHNESS%20VALUES.pdf

Appendix IV – Supplementary information to Chapter 6

1. Further information about methods, parameters and assumptions used in this study

1.1 Composition and micronutrient characteristics of the vegetable basket

Table S1: Vegetable basket composition and properties. The average nutrient score determines how much fresh produce would be required per person (50% of RNI equals 376.8 g). The loss combined with the length of the growing period determines any required overproduction to satisfy nutrient needs. The basket properties are derived from the weighted contributions (share in basket) of each crop. The composition is equal to that in Chapter 4 to allow for a comparison of CEA with open-field farming.

Crop	**Share in basket**	**Max. reported yield ($kg/m^2/year$)**	**Nutrient score (%RNI / 100 g)**	**Preservation method**	**Initial loss**
Bell pepper	12%	7.3	17.18	Freeze	15.3%
Broccoli	12%	2.8	17.10	Freeze	10.6%
Lettuce	12%	4.1	11.22	Not applicable	Not applicable
Tomato	40%	12.5	8.64	Canning	19.9%
Spinach	12%	3.6	28.09	Freeze	22.1%
Summer squash	12%	4.9	8.19	Canning	38.1%
Basket	100%	7.6	13.27	Mixed	21.5%

1.2 Land availability for energy generation

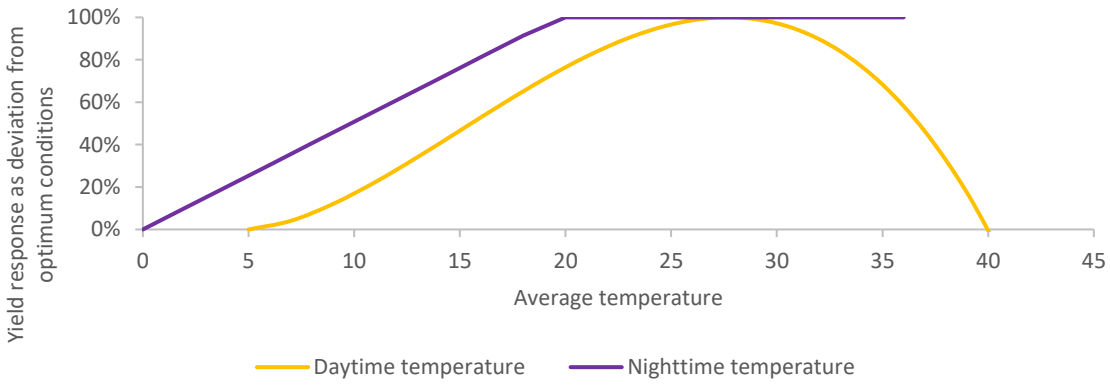
The potential land availability for renewable energy generation has been the subject of many studies with vastly different assumptions. Although they agreed on excluding conservation use and wetland, estimates for relevant land cover categories such as grassland, shrubland and sparsely vegetated land ranged from very low (Deng et al., 2015; Zappa & van den Broek, 2018) to almost 100% (Domínguez Bravo et al., 2007; Hoogwijk et al., 2004). A primary reason for this is the differing level of ambition, ranging from current political feasibility (Deng et al., 2015) to hypothetical or technically realisable (Hoogwijk et al., 2004). In general, the land availability differed between onshore wind and solar PV, with onshore wind

being more favourable in forests (Lopez et al., 2012) and possible in steeper areas (Hoefnagels et al., 2011; Q. Wang et al., 2014) or higher altitudes (Deng et al., 2015; Hoogwijk et al., 2004) compared with solar PV. On the other hand, urban areas (mainly rooftops) were considered partly available for solar PV, with reported potentials of around 1-15% of the total urban land (Domínguez Bravo et al., 2007; Miskin et al., 2019; C. D. Yue & Wang, 2006).

1.3 Productivity of open-field farming

A host of conditions influence local crop growth, such as summer temperature and precipitation, soil conditions, and plant care factors such as irrigation, drainage and fertilisation (Archontoulis et al., 2020). Compared to specific vegetables, wheat and other staple crops have been thoroughly studied. Although the behaviour of specific vegetable cultivars likely differs, this work considers the empirically derived tendencies to be applicable to the vegetable basket as well. The hypothetical yield model thus also draws from studies investigating different staple crops, mainly concerning the effects of precipitation and soil characteristics.

For temperature, a relationship between annual growing degree days (GDD, the annual sum of all average daily temperatures above a specific cardinal temperature) and annual yield (Qadir & Malik, 2007), as well as the favourability of crop production (Ramankutty et al. 2002) exists while at the same time, large diurnal temperature extremes negatively affect yield



AppxIV-Figure 1: Effect of temperature on vegetable growth. The average day and night time temperature are characteristic for each month. The y-axis describes the yield deviation from that of optimum conditions and thus productivity decrease for the specific month. The equations to derive the daytime temperature curve are shown in Aslam et al.(Aslam et al., 2017)

(Vogel et al., 2019). An adapted model calculates Wang-Engel Degree Days (WEDD) using upper and lower bounds, and an optimum temperature was proposed (E. Wang & Engel, 1998) and tested (Aslam et al., 2017; L. Li et al., 2020). Still, optimum temperatures differ for the photoperiod and night-time (Parthasarathi et al., 2013; S. Singh, 2018) and are observed in practice for vegetable production (Benis et al., 2017c). This study, therefore, uses two different temperature correlations depending on the time of day (see AppxIV-Figure 1).

The average day and night time temperatures of each month were approximated from WorldClim (Fick & Hijmans, 2017) data (minimum and maximum temperatures) via the equations below.

$$T_{day,avg} = (T_{max} - T_{min}) * 0.75 + T_{min}$$

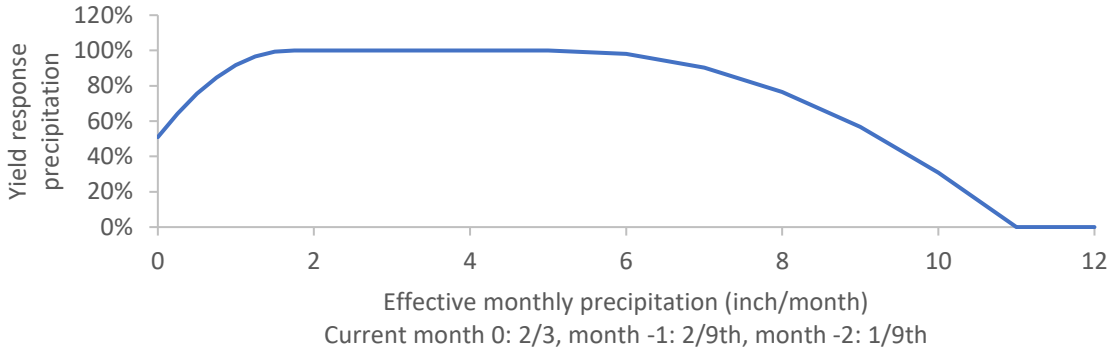
$$T_{night,avg} = (T_{max} - T_{min}) * 0.25 + T_{min}$$

The moisture index, as an indication of the interplay between evapotranspiration and precipitation, has been used to predict the favourability of crop production (Ramankutty et al., 2002). Although it is calculated by daily precipitation rates, its value does not describe the seasonal characteristics of rainfall and thus the conditions when most crop production might occur. Optimum amounts of rainfall (around 3.2 inch/month for wheat) and a strong negative effect on annual yields of staple crops for very high and close-to-zero seasonal precipitation have been observed (Archontoulis et al., 2020; Rosenzweig et al., 2002). The shape of this crop response curve seems to depend on crop type, soil type and groundwater conditions (Martinez-Feria & Basso, 2020). Excessive rainfall, e.g. during monsoon season (Biswas, 2016; Hazra, 2008) or unusual events (Li et al., 2019), have detrimental effects on yields due to soil erosion and plant diseases. Damages during floods make up the majority of harvest loss(FAO, n.d.). Dry spells and droughts also have a negative effect (Feng & Hao, 2020). The impact of excessive rainfall was considered to be more challenging to mitigate than too little rainfall. The yield response to precipitation is shown in AppxIV-Figure 2 and derived from the equation below.

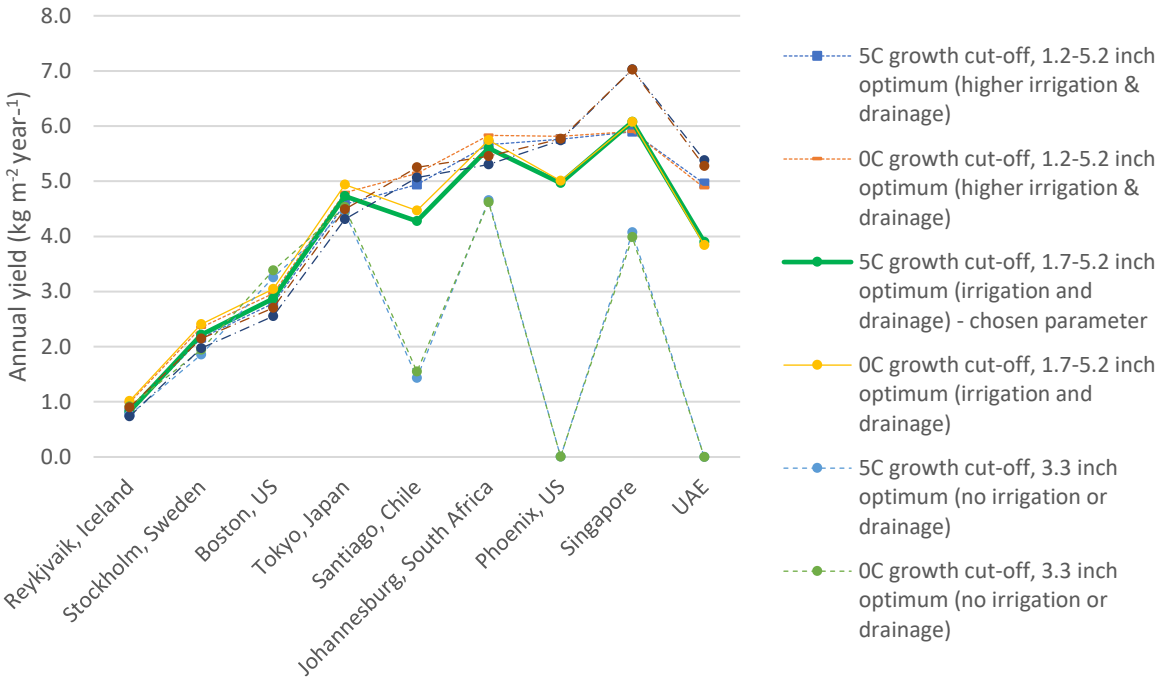
$$Yield\ response\ precipitation\ (\%) = \begin{cases} -17 * (EP - 1.7)^2 + 100 & if\ EP < 1.7 \\ -3 * (EP - 5.2)^2 + 100 & if\ EP > 5.2 \\ 100 & else \end{cases}$$

An approximation of soil water storage effects defines effective precipitation (EP, in inch) considering precipitation (P) during the previous months as described in the equation below.

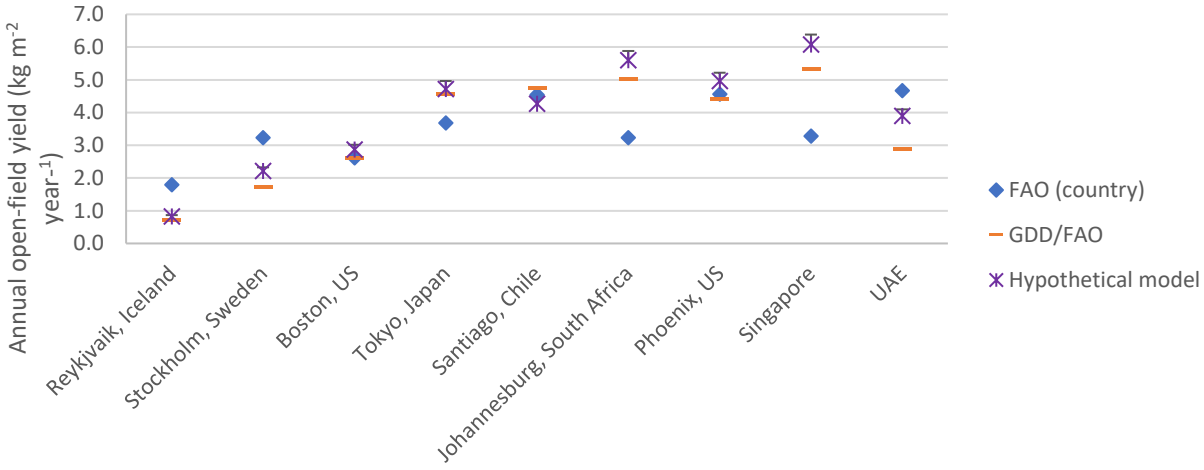
$$EP = P_0 * \frac{2}{3} + P_{-1} * \frac{2}{9} + P_{-2} * \frac{1}{9}$$



AppxIV-Figure 2: Effect of monthly precipitation on vegetable growth. Between 1.7 and 5.2 inch effective monthly precipitation, no negative effect on yields was assumed for the specific month.



AppxIV-Figure 3: Sensitivity analysis for the effect of the effective precipitation influence on annual yields. Excluding the influence of rainfall favours arid (Maricopa County, UAE) and very wet climates (Singapore), while irrigation and drainage ameliorate the impacts of a strong influence of precipitation



AppxIV-Figure 4: Comparison of hypothetical model results for open-field production with reported FAO figures (sometimes influenced by greenhouse production) and growing degree days (GDD) adjusted to FAO figures. The negative error bars for the hypothetical yield model visualise the average yield reductions due to extreme climatic anomalies

1.4 Length of the growing period and overproduction factor

The local annual yield was adjusted by the overproduction factor (OP). It incorporates the initial processing loss (24.6%), the daily loss (0.1%) and the length of the growing period (LGP) adjusted by the first productive month without harvest, resulting in the length of the harvest period (LHP). The steady consumption of stored food means the average length of the stored food is the total duration divided by 2. If the LGP is below 365, the OP is thus derived via the following steps:

$$percentage\ harvest\ period\ within\ year = LHP\% = \frac{LGP - 30.5}{365}$$

$$percentage\ loss\ of\ stored\ food = Loss\% = \frac{\left(365 - (LGP - 30.5)\right)}{2} * \frac{0.1}{100} + \frac{24.6}{100}$$

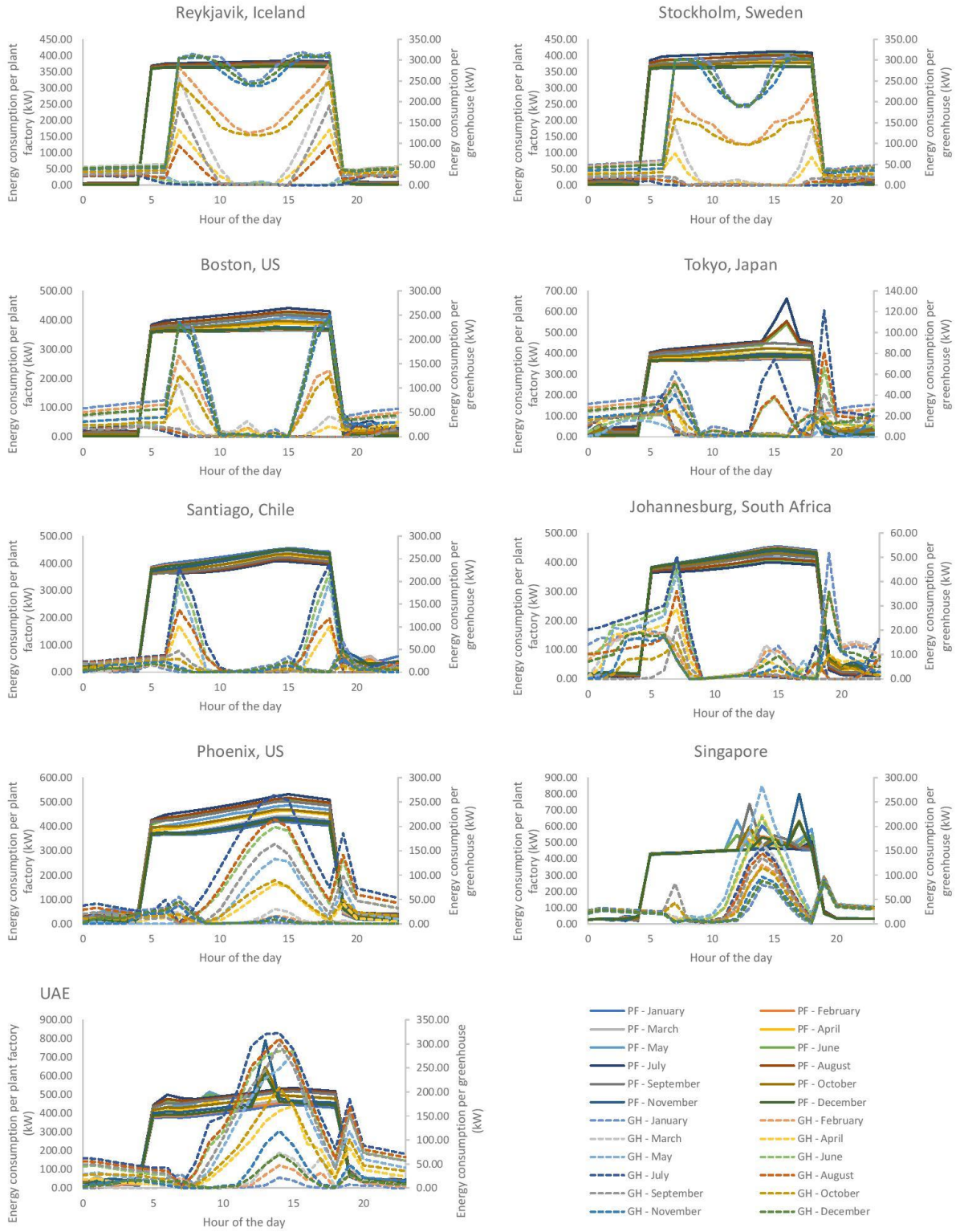
$$pood\ to\ be\ produced = annual\ demand * LHP\% + \frac{annual\ demand * (1 - LHP\%)}{1 - Loss\%}$$

$$overproduction\ factor\ (OS) = \frac{food\ to\ be\ produced}{annual\ demand}$$

$$OP = \frac{annual\ demand * LHP\% + \frac{annual\ demand * (1 - LHP\%)}{1 - Loss\%}}{annual\ demand}$$

$$OP = LHP\% + \frac{1 - LHP\%}{1 - Loss\%} = \frac{LGP - 30.5}{365} + \frac{(1 - \frac{LGP - 30.5}{365})}{1 - \left(\frac{\left(365 - (LGP - 30.5)\right)}{2} * \frac{0.1}{100} + \frac{24.6}{100}\right)}$$

1.5 Energy consumption modelling and hourly profiles of CEA facilities



AppxIV-Figure 5: Monthly facility load curves for all regions. Note: The units on the two y-axis are different, the primary (left) y-axis describes the energy consumption of plant factories, the secondary y-axis (right) describes the energy consumption of greenhouses.

Less sunny regions (Reykjavik, Stockholm, Boston, Santiago) rely on supplemental lighting in winter and have thus a high load in the morning and evening hours. Very hot regions required substantial mechanical cooling in the summer months when ventilation was insufficient for climate control. The spikes for plant factories in the afternoon hours are due to less efficient cooling (air-to-air cooling was not feasible anymore) when the daytime temperature was at its highest. The early morning and early evening spikes for greenhouses (especially pronounced in Tokyo and Johannesburg) are due to a change in permissible temperature and humidity ranges between day- and night-time settings. It is important to note that those spikes are only moderate, as indicated by the different scaling of the y-axis on each graph (lowest for Tokyo and Johannesburg).

1.6 Renewable electricity: grid optimisation and land-use efficiency

To address the concerns of land impacts of CEA facilities, realistic and fair assumptions need to be made. First, constructing vast quantities of CEA facilities requires additional renewable energy generation potential. Second, the burden on the existing grid should be minimised. Both statements are relevant in a low-carbon world, in which increased electrification and renewable penetration make it substantially more challenging to balance the grid and provide energy security (Oyekale et al., 2020). The implication is that the CEA facilities should be considered prosumers (Laugs et al., 2020) and be powered quasi-independently by renewable energy infrastructure that behaves similar to a microgrid (Kapica, 2020). Simultaneously, this infrastructure would be connected to a regional grid with high renewable penetration and adequate balancing sources, such as biomass, hydropower or nuclear plants. The question is how economics would dictate such a microgrid design with low levels of grid interaction. Several studies have investigated the economic trade-off between the amount of storage (storage days), the share of dispatchable or balancing energy and the overproduction factor (i.e. more energy is produced than required, also called oversizing factor (Dujardin et al., 2017), generation factor (Johlas et al., 2020) or overcapacity (Moore, 2020)) for fully or mostly renewable electricity grids. Short-term energy storage is expensive, and installing more renewable generation capacity than required reduces storage requirements exponentially and thus total system costs (Moore, 2020). At some level of overproduction, these savings become less pronounced (Johlas et al., 2020), with an optimum between 0.3 (Johlas et al., 2020) and 1.0 (Moore, 2020) storage days and 40 (Johlas et al., 2020; Putnam & Perez, 2018) to 50 (Moore, 2020)‘(Dujardin et al., 2017) per cent overcapacity. Equally, introducing some level of dispatchable energy, e.g. 5 (Johlas et al., 2020; Perez et al., 2019b) to 20 (Dujardin et

al., 2017) per cent, can lead to import-free (Dujardin et al., 2017) or significantly cheaper (Putnam & Perez, 2018) regional grid operations. The amount of dispatchable energy is constrained by the local availability of more steady renewable energy sources, such as hydropower or biomass. Considering local grid imbalances, relying only on local storage alone comes at a high cost but half a day of storage can eliminate most imbalances, even without a regional grid (Laugs et al., 2020).

The land-use efficiencies of renewables follow different principles for onshore wind and solar PV and are expected to improve with time. For wind turbines, the turbine, hub height and blade length are the most decisive parameters (Saunders, 2020). Studies investigating the actual footprint of wind farms range between around 3 (Denholm et al., 2009; McDonald et al., 2009; Miskin et al., 2019) to 6 (Zappa & van den Broek, 2018) MW/km^2 with a projection for 2030 (Zappa & van den Broek, 2018) for 8 MW/km^2. The direct land footprint of the turbines, including access roads, was considered relatively low, from 1% (Denholm et al., 2009; McGowan & Connors, 2000) to 5% (McGowan & Connors, 2000; Saunders, 2020), with a lower footprint in areas where wind turbines were co-located with agriculture and existing roads (McGowan & Connors, 2000). This study uses a conservative measure of 5% since no double-use of agricultural land was permitted. For solar PV panels, the panel efficiency and the filling ratio (how much of the land is covered by effective panel area) are most relevant. Panel efficiencies have increased rapidly over the last decades; hence assessments of land-use efficiencies of existing plants with older panels might be on a lower end (MacKay, 2013; Zappa & van den Broek, 2018), while projections for the future have a wide range, depending on the technology (IRENA, 2019), with an estimate of 24.4% after 2040 (Bloomberg, 2019). The filling ratio depends on the technology (e.g. axial adjustment and sunlight tracking) and the economic constraints on the land, ranging from 14% for old plants to a feasible maximum of 80% (MacKay, 2013). An average of modern utility-scale plants had a filling ratio of 36.6% (Zappa & van den Broek, 2018). Combined land-use efficiencies (LUE) based on nominal power for existing plants ranged from 17.6 MW/km^2 for older plants to 25.4 and 36.8 MW/km^2 for more recent plants on public and private land, respectively (Saunders, 2020). Since this work considers a more efficient panel (21%) with a nominal capacity per unit area of 209.375 W/m^2, the average filling ratio of 36.6% would lead to a land-use efficiency based on nominal power of 76.6 MW/km^2.

1.7 Project settings and equipment data for Homer Pro

PV solar: Panel – SunPower X21-335-BLK with 21% efficiency, 335 kWp per 1.6 m^2 panel area, Capital cost 1,000 $ per kW capacity (Fu et al., 2009), O&M cost 0.3% of capital cost (default value), Lifetime: 25 years, derating factor: 88%, inverter efficiency: 95%, No solar tracking

Wind: Generic 1.5 MW (infinite search space) and Enercon E-115 EP3 E3 4,2 MW (1-10 search space), Capital cost 1,350 $ per kW capacity (Milborrow, 2020; Orrell et al., n.d.), O&M cost 1% of capital cost (default value), Lifetime 20 years, hub height: 80m (1.5 MW), 122 m (4.2 MW), Turbine losses (3%), Default power curve

Storage: Generic 100 kWh Li-ion, Capital cost 220 $ per kWh capacity (IRENA, 2018) , O&M cost 0.1% of capital cost (default value), Roundtrip efficiency 90%, Lifetime: 15 years, throughput: 300,000 kWh, minimum state of charge 20%

Converter: Capital cost 300 $ per kWh capacity (default value), No O&M cost , Inverter efficiency 95%, rectifier efficiency 95%, Lifetime: 15 years

Advanced Grid: Emissions: 30 g CO_2/kWh, 50 $/tonne carbon price (assuming low carbon dispatchable energy), Power price 10 ct/kWh, Prohibit any grid sales, Maximum net grid purchases: 10% of annual load (scenarios with 0% of the annual load or no restrictions)

Resources: Scale wind speed at 50m to average value extracted from ArcGIS Pro

Project: Economics: 6% nominal discount rate (scenario with 9%), 2% inflation, 25 years project lifetime

1.8 Calculation of per person and relative land-use

Two types of land use considerations were relevant to this study. First, the land use per person for each growing method, considering the direct land use through farming, the required capacity of renewable energy generation capacity (which depends on the energy-efficiency of CEA farming in a particular location and the favourability for renewable energy production as simulated by Homer Pro) and the renewable energy technology-specific land use efficiency (LUE, see AppxIV 1.6). The per-person land use was also influenced by the potential for co-generation of wind and solar PV, determined by the ratio between land suitable for hybrid use and land suitable only for one of the two types. Second, the relative land use characteristics consider the land area available for crop production and energy generation and describe the agricultural land-sparing potential relative to the land requirements for renewable energy generation.

$$solar\ PV\ land\ use\ per\ person = \frac{capacity\ solar\ PV}{LUE_{PV} * regional\ population}$$

$$wind\ land\ use\ per\ person = \frac{capacity\ onshore\ wind}{LUE_{wind} * regional\ population}$$

$$land\ to\ be\ colocated\ per\ person = MIN(\frac{solar\ PV\ land\ use\ per\ person}{0.95}, wind\ land\ use\ per\ person * \frac{land\ suitable\ for\ colocation}{land\ available\ for\ wind\ turbines})$$

The co-location potential was limited either by the amount of land used for solar panels, which can be placed between the wind turbines (accounting for the 5% footprint of turbines) or the share of wind turbines that would be placed on co-location land, assuming equal distribution (determined by the share of land suitable for co-location compared with the land available for wind generation), whichever is smaller.

This effectively considers the setting as if all available land for renewable energy is used for energy generation according to the most economical split recommended by the grid optimisation. For a single renewable energy project with a different demand profile and cost structure, the co-location area could naturally be 100% of the land used, depending on the location. The amount of land suitable for co-location constitutes an overlap of the respective land available for either solar PV or wind and is thus already part of the estimated land for each (e.g. 10 km^2 available for solar PV and wind energy, each with a co-location suitability of 5 km^2 means 15 km^2 is in total available for renewable energy generation).

$$solar\ PV\ (only)\ land\ use\ per\ person = solar\ PV\ land\ use\ per\ person - land\ to\ be\ colocated\ per\ person * (1 - 0.05)$$

$$wind\ (only)\ land\ use\ per\ person = wind\ land\ use\ per\ person - land\ to\ be\ colocated\ per\ person$$

$$additional\ land\ required\ without\ colocation = land\ to\ be\ colocated * 0.95$$

These equations lead to the results illustrated in Figure 6-4 in the main text.

The relative land use can be assessed in multiple ways. In this study, the relative land use of solar PV and wind energy generation was combined in one number, considering land saving potentials due to co-location. An alternative illustration would be to split the relative land use for both types of renewable energy generation, which was considered less useful here in conveying high-level outcomes comparing the nine regions.

$$Share\ of\ land\ required\ for\ renewable\ energy\ generation$$

$$= \frac{(solar\ PV\ land\ use\ per\ person + wind\ land\ use\ per\ person) * regional\ population}{land\ available\ for\ wind\ turbines + land\ available\ for\ solar\ PV - land\ suitable\ for\ co\ location * 0.05}$$

The "Renewable energy land abundance relative to the demand for powering CEA" term shown in figure X in the main text is the inverse of the equation above.

The agricultural land sparing potential was calculated by considering the land not needed anymore for open-field vegetable production and the footprint of the greenhouses.

$$land\ sparing\ potential = \frac{Land\ use\ per\ person\ open\ field * regional\ population - [footprint\ growing\ facilities]}{existing\ agricultural\ land}$$

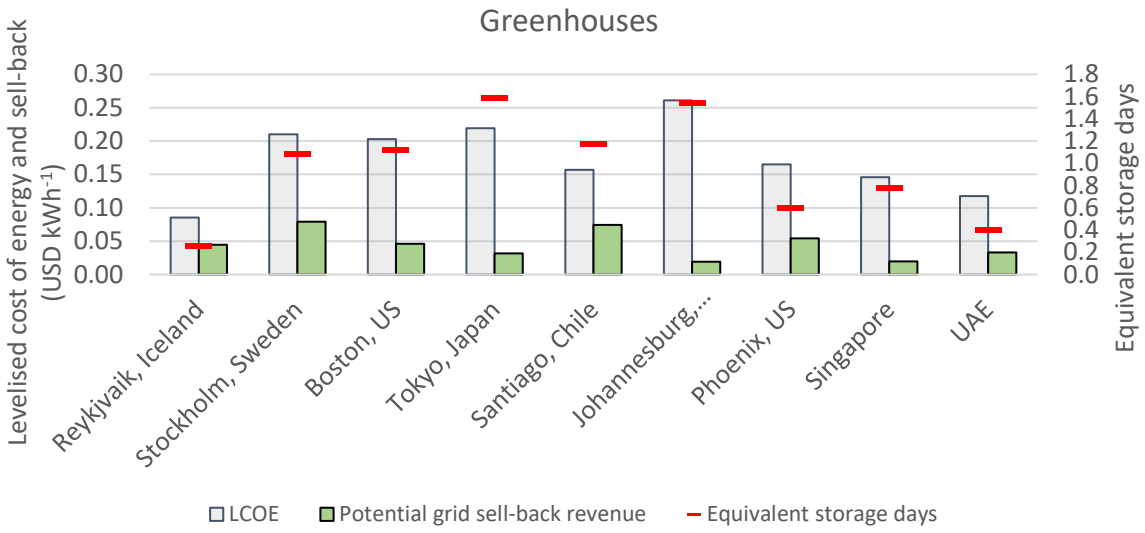
For an alternative scenario, it was assumed that the current agricultural land was also partly available for energy generation through agriphotovoltaic and wind turbines placed between fields. For agriphotovoltaic, it was assumed that the negative effect on the crops is kept to a minimum by sparsely allocating the solar panels with 1/4th of the land use efficiency previously assumed, hence 25% of agricultural land was considered available for solar PV. For wind turbines, a clearing of 5% of the project area was required, effectively reducing the agricultural output and thus the land-sparing potential of CEA farming. It was assumed that the wind turbines would be distributed among farm and non-farm land according to the ratio between them.

$$Share\ of\ land\ required\ for\ renewable\ energy\ generation\ (alternative\ scenario)$$

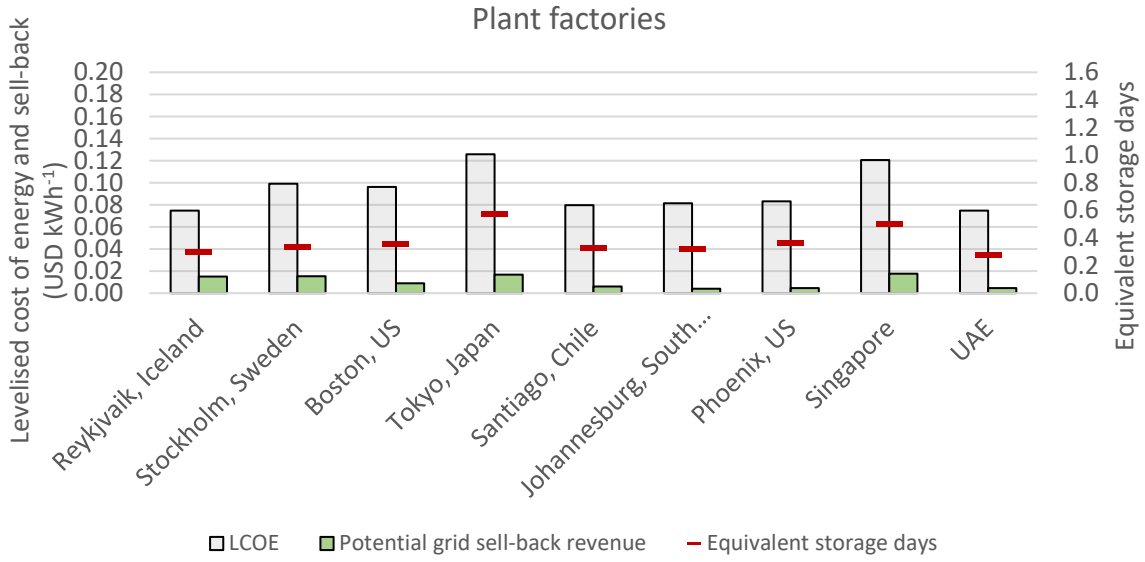
$$= \frac{(solar\ PV\ land\ use\ per\ person + wind\ land\ use\ per\ person) * regional\ population}{land\ available\ for\ solar\ PV + land\ available\ for\ wind\ turbines - land\ suitable\ for\ co\ location * 0.05 + agricultural\ land * (1 + 0.25)}$$

$$land\ sparing\ potential\ (alternative\ scenario) = \Big(Land\ use\ per\ person\ open\ field * regional\ population - [footprint\ growing\ facilities] - wind\ land\ use * 0.05 * \frac{agricultural\ land}{land\ available\ for\ wind\ turbines + agricultural\ land}\Big) * \frac{1}{existing\ agricultural\ land}$$

2.2. Cost of energy and storage requirements



AppxIV-Figure 6: Results from the grid cost optimisation with Homer Pro for greenhouses; the levelised cost of energy (LCOE) indicates the cost per unit energy considering infrastructure, project duration and output. The potential grid sell-back revenue assumes that all overgeneration can be utilised regionally and is discounted with the same rate as the LCOE. The equivalent storage days relate the storage capacity with the daily electricity generation. A value of 1 indicates that the average generation of 1 full day can be stored in a battery. Due to the high cost of energy storage, this parameter had a strong influence on the LCOE.



AppxIV-Figure 7: Results from the grid cost optimisation with Homer Pro for plant factoriess; the levelised cost of energy (LCOE) indicates the cost per unit energy considering infrastructure, project duration and output. The potential grid sell-back revenue assumes that all overgeneration can be utilised regionally and is discounted with the same rate as the LCOE. The equivalent storage days relate the storage capacity with the daily electricity generation. A value of 1 indicates that the average generation of 1 full day can be stored in a battery.

The LCOE for PFs is significantly correlated with the need for storage (AppxIV-Figure 7), which was higher when relying on solar PV only. Less optimal wind conditions (e.g. Stockholm and Boston) also increased the LCOE. Night-time operations in PFs and offshore wind scenarios always led to higher costs and installed capacities due to the lack of otherwise load-matching solar PV, even in windy locations such as Reykjavik. For GHs, the LCOE (AppxIV-Figure 6) was highest for locations with strong fluctuations in the daily load curves (e.g. Johannesburg and Tokyo) and lowest for locations with favourable renewable energy sources (e.g. wind in Reykjavik and solar PV in UAE).

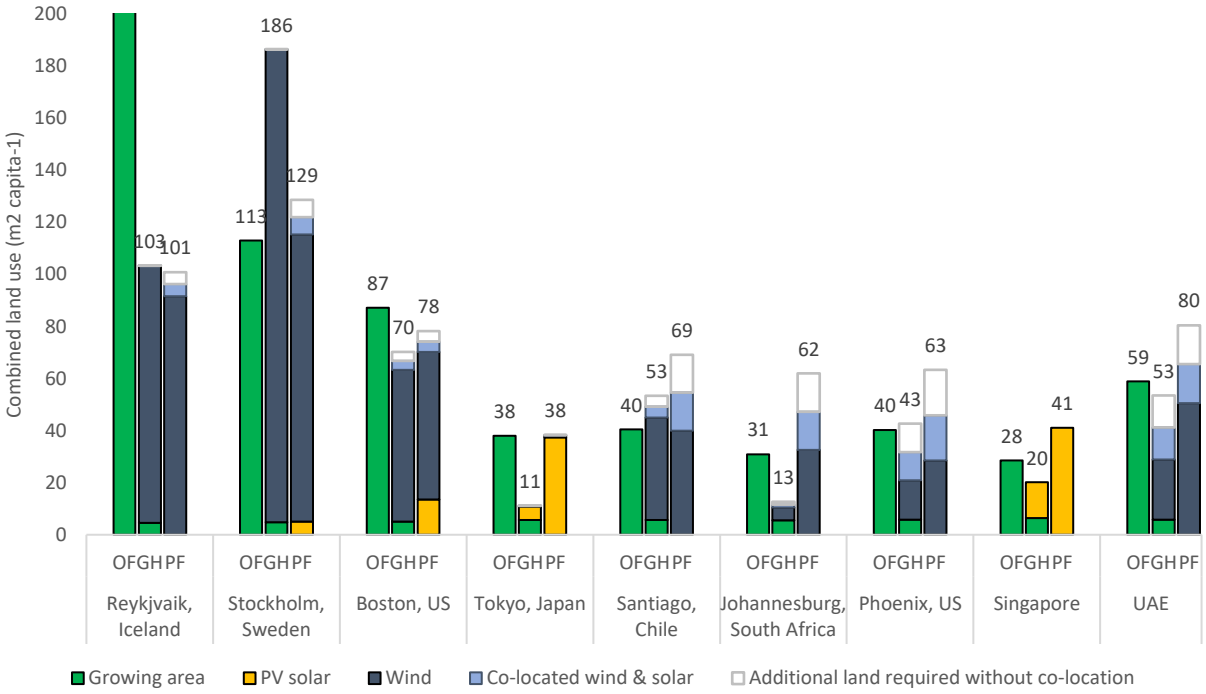
The sensitivity of results to a higher discount rate was little. A stronger sensitivity was observed for grid interaction limits: if they were removed, the LCOE dropped by up to 25%, and the overgeneration ratio was negative (implying a high grid contribution), while having no access to dispatchable grid energy increased the LCOE by up to 37% and the overgeneration ratio by up to 172% (with corresponding implications on land use). The majority of overgeneration in GHs occurred during winter midday in cold and temperate regions, in summer of cold locations (no lighting required), or in winter of hot locations (no cooling required). These spikes deserve special attention when considering the regional demand balance between CAE and other sectors.

2.3. Alternative scenarios for combined land use and influencing factors

If Boston, Tokyo and Singapore were also able to employ wind to achieve a lower energy cost, PFs would require significantly more land than open-field farming (AppxIV-Figure 8). The combined land use for plant factories differs quite significantly between the regions. The main driver for this is the share between solar PV and wind but also the overgeneration as a result of the daily and seasonal mismatch between demand and supply, which was mitigated by an economic trade-off between energy storage and installing more capacity. The total required capacity was influenced, in turn, by a) fluctuations of load or energy demand, (e.g. when air-to-air cooling was not feasible in the afternoon hours in Tokyo, Singapore and UAE), b) an unfavourable complementarity between seasonal characteristics of solar radiation and wind power (e.g. very low wind speed in some seasons in Singapore) and c) the energy demand per facility (cooling was more energy-intensive in hot climates). The seasonal non-complementarity for a region between solar PV and wind was calculated as shown below, using monthly and annual average values of global horizontal irradiation (GHI) and wind power, calculated using the power curve of the turbines and the wind speed.

$$\left[\sum_{i=1}^{12} ABS\left(\frac{x_{GHI,i} - AVG_{GHI}}{AVG_{GHI}} + \frac{x_{wind\ power,i} - AVG_{wind\ power}}{AVG_{wind\ power}}\right)\right] * \frac{1}{12}$$

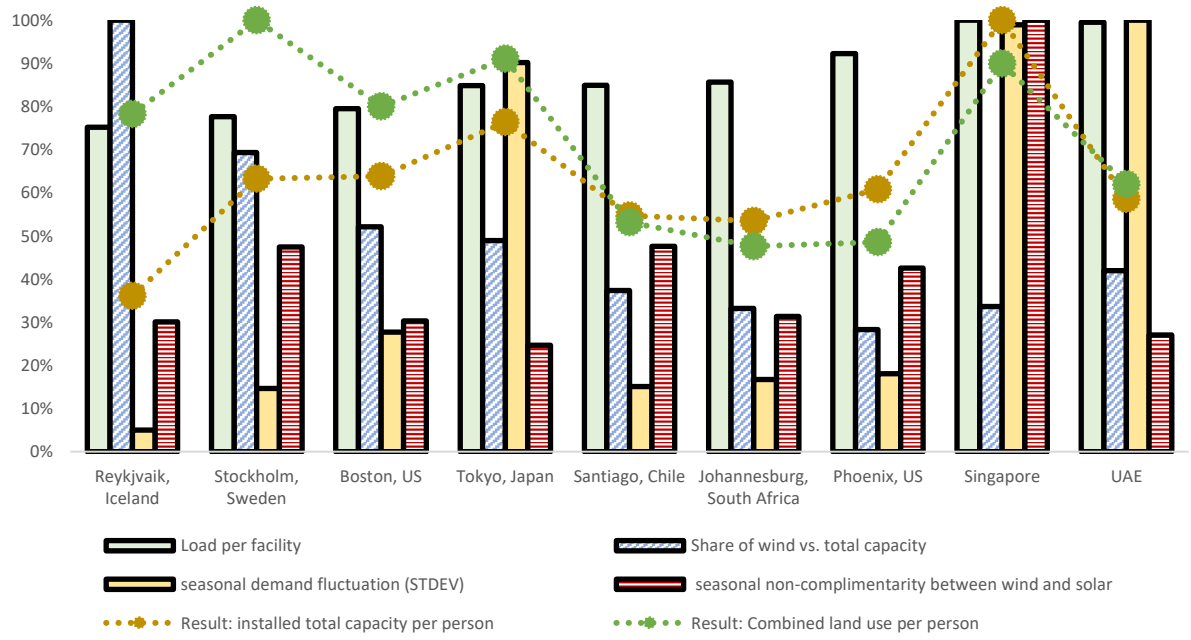
AppxIV-Figure 9 shows the relative values for each of these parameters compared with the maximum value of all regions. AppxIV-Figure 10 visualises the combined land required for increased yields in CEA facilities (50% more in GHs, up from around 30 to 35 kg/m^2 for the basket, and 75% more in PFs, up from around 40 kg m^2 based on the previous work in



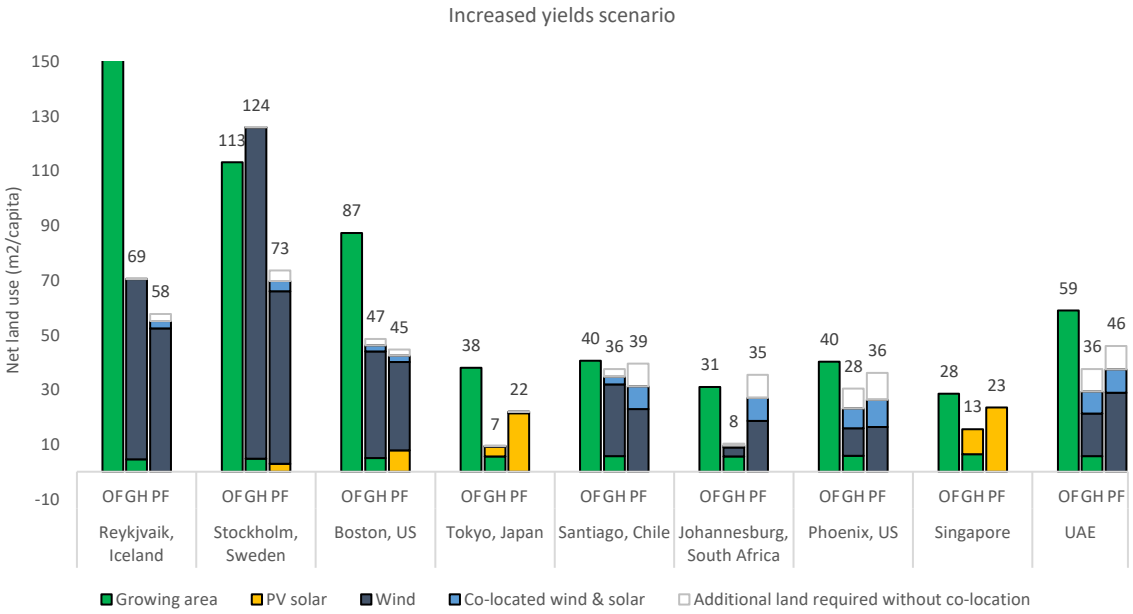
AppxIV-Figure 8: Combined land use efficiency of the three growing techniques without land restrictions on wind energy in Singapore and Tokyo. The land required to generate the required electricity is included and hybrid land use is preferred.

Chapter 5, which suggests that advances in science and growing practices have a significant impact on the comparative results. A re-calculation of the combined land use as if all excess energy could be utilised within the region for other purposes is presented in AppxIV-Figure 11, implying a reduced hypothetical land allocation of the solar and wind farms to CEA production. In that case, the land use of GHs (which remains to be the lowest) is reduced more than that of the PF since the fluctuating load profile is more relevant for the former. This means that finding a regional use for excess energy is more relevant and impactful for GHs, while PFs would now require less land overall than open-field farming in all locations except Johannesburg. The sensitivity of results to the land-use efficiency of solar panels is shown in AppxIV-Figure 12, indicating that a threshold panel density exists to equalise the combined

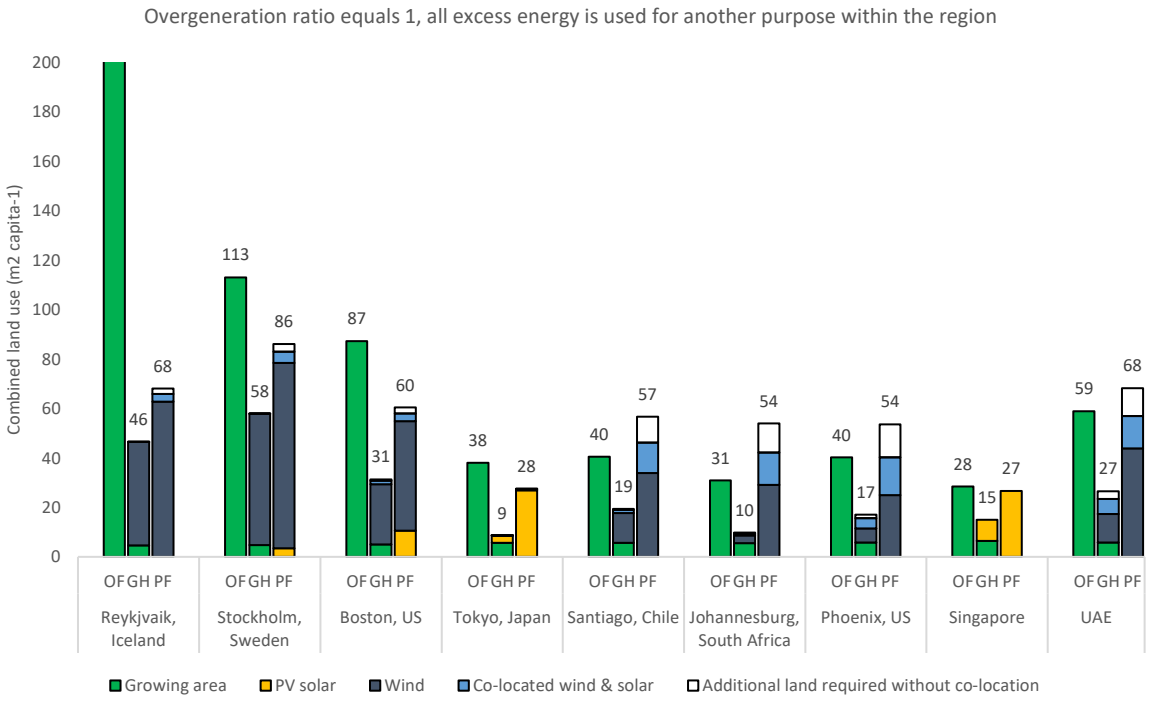
land use for open-field farming and PFs, except in Johannesburg and UAE (where PF always requires more or less land than open-field farming, respectively).



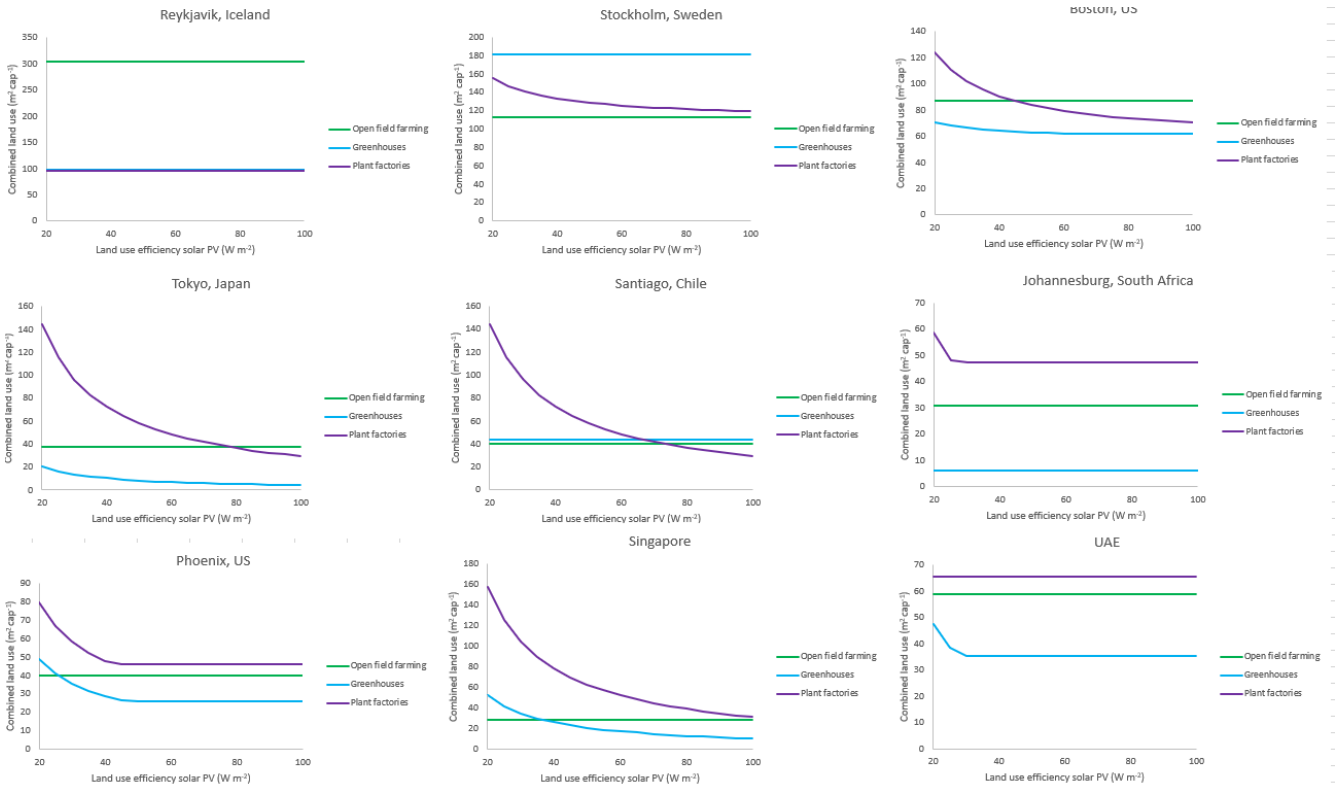
Appx IV-Figure 9: Overview of aspects influencing the combined land use per person of PFs. All values are displayed relative to the maximum value in a region for the specific category. The dotted lines between the regions are only for trend visualisation. A low value for seasonal wind and solar mismatch describes a favourable seasonal match.



AppxIV-Figure 10: Combined land use efficiency of the three growing techniques, considering a yield increase of 50% in greenhouses and 75% in plant factories. The land required to generate the required electricity is included and hybrid land use is preferred. The value for open field farming in Iceland is 305.1 m^2/capita.

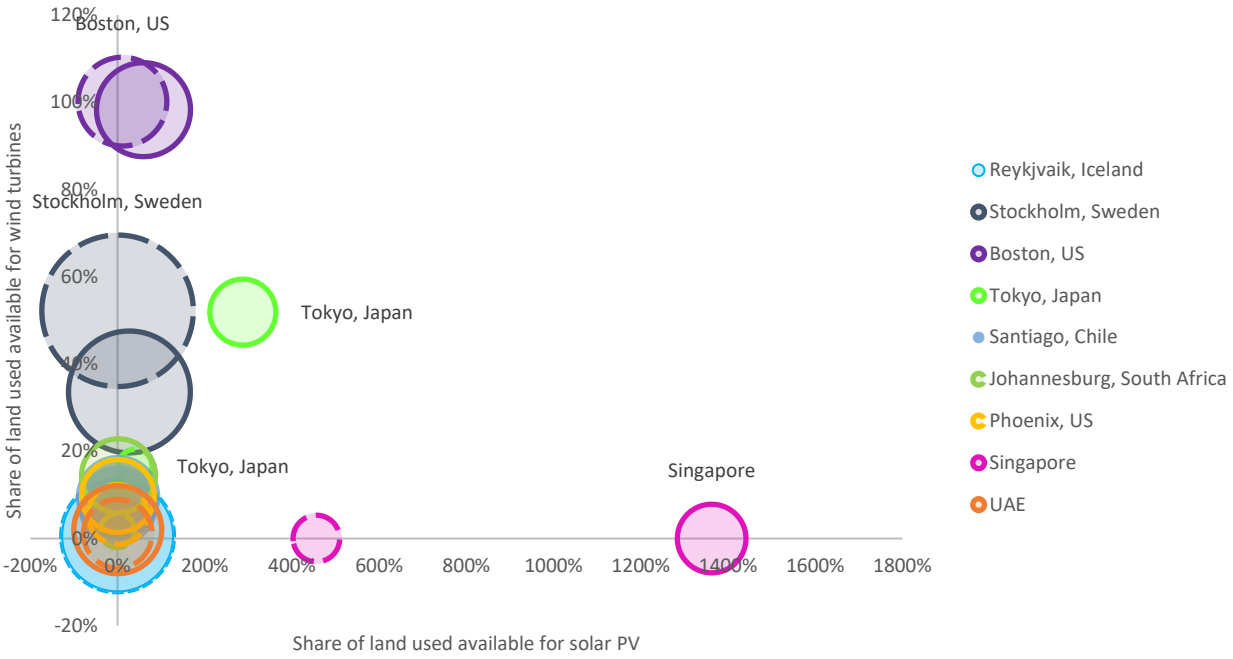


AppxIV-Figure 11: Combined land use efficiency of the three growing techniques, considering an overproduction factor of 1 (i.e. electricity generation equals consumption). The land required to generate the required electricity is included and hybrid land use is preferred. The value for open field farming in Iceland is 305.1 m^2 $capita^{-1}$.

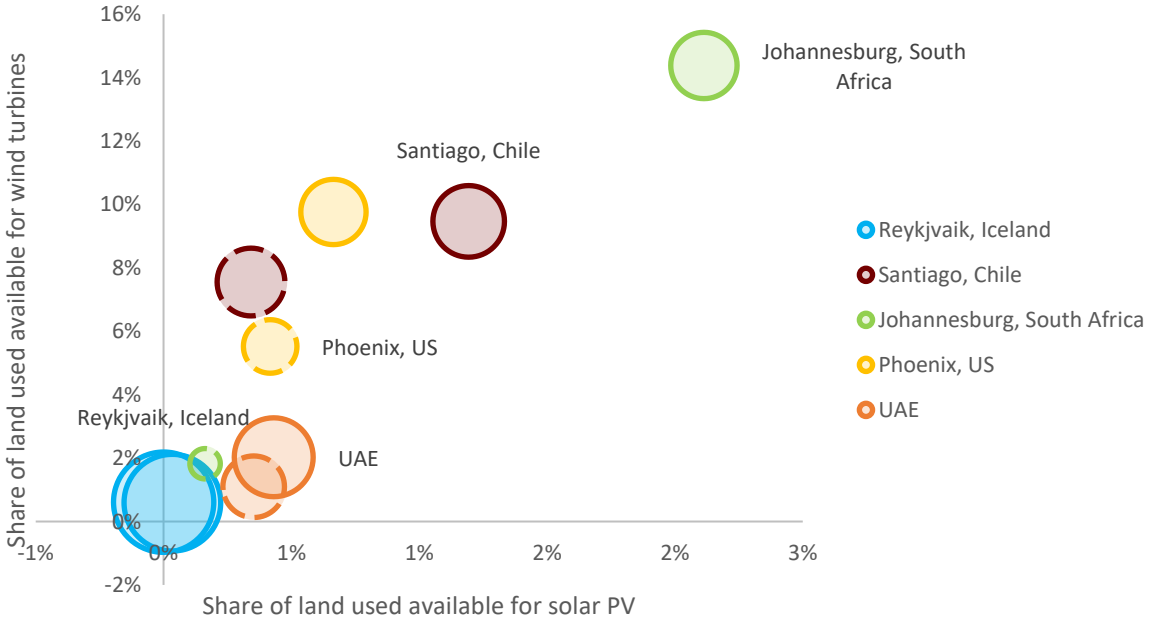


AppxIV-Figure 12: Sensitivity of combined land use to the land use efficiency of solar PV.

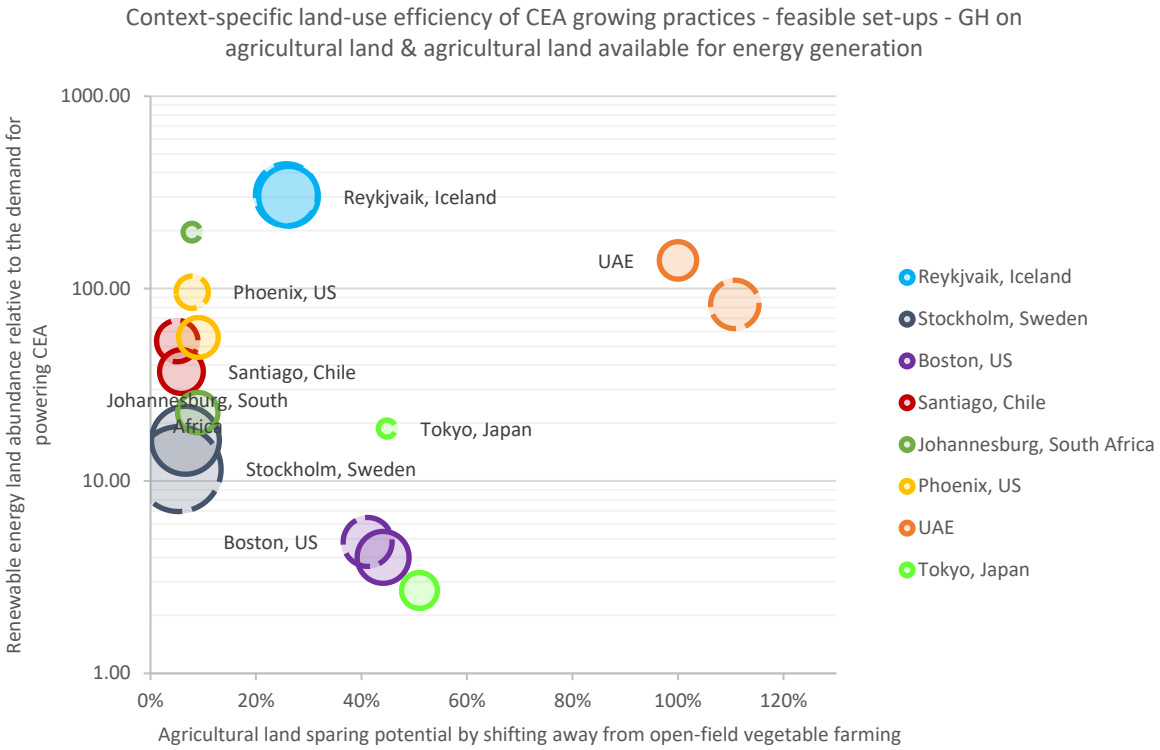
2.4. Alternative scenarios for the relative land use



AppxIV-Figure 13: Relative land use requirements of the CEA practices by the type of land available for either solar PV or wind turbines. The bubble size depicts the net land use per person subtracted with savings of co-locating solar PV and wind. The dashed-line circle is for greenhouses and the solid-line circle is for plant factories.



AppxIV-Figure 14: Relative land use requirements of the CEA practices by the type of land available for either solar PV or wind turbines akin to AppxIV-Figure 13, only showing the regions with a small required share of the available land for energy generation. The bubble size depicts the net land use per person subtracted with savings of co-locating solar PV and wind. The dashed-line circle is for greenhouses and the solid-line circle is for plant factories.



AppxIV-Figure 15: Relative land use requirements of the CEA practices akin to figure 5 in the main text. Agricultural land was considered partly suitable for renewable energy generation. The bubble size depicts the net land use per person subtracted with savings of co-locating solar PV and wind. The dashed-line circle is for greenhouses and the solid-line circle is for plant factories.

References

Adhikari, B. K., Trémier, A., Martinez, J., & Barrington, S. (2010). Home and community composting for on-site treatment of urban organic waste: Perspective for Europe and Canada. *Waste Management and Research*, *28*(11), 1039–1053. https://doi.org/10.1177/0734242X10373801

Agritecture. (2020). *2020 Global CEA Census Report*.

Ahemd, H. A., Al-Faraj, A. A., & Abdel-Ghany, A. M. (2016). Shading greenhouses to improve the microclimate, energy and water saving in hot regions: A review. In *Scientia Horticulturae* (Vol. 201, pp. 36–45). Elsevier B.V. https://doi.org/10.1016/j.scienta.2016.01.030

Ahmadi, M. H., Ahmadi, M. A., Sadaghiani, M. S., Ghazvini, M., Shahriar, S., & Alhuyi Nazari, M. (2018). Ground source heat pump carbon emissions and ground-source heat pump systems for heating and cooling of buildings: A review. *Environmental Progress and Sustainable Energy*, *37*(4), 1241–1265. https://doi.org/10.1002/ep.12802

Alexander, P., Brown, C., Arneth, A., Finnigan, J., Moran, D., & Rounsevell, M. D. A. (2017). Losses, inefficiencies and waste in the global food system. *Agricultural Systems*, *153*, 190–200. https://doi.org/10.1016/j.agsy.2017.01.014

Alshrouf, A. (2017). Hydroponics , Aeroponic and Aquaponic as Compared with Conventional Farming. *American Scientific Research Journal for Engineering, Technology, and Sciences*, *27*(1), 247–255.

Alvarenga, P., Mourinha, C., Farto, M., Santos, T., Palma, P., Sengo, J., Morais, M. C., & Cunha-Queda, C. (2015). Sewage sludge, compost and other representative organic wastes as agricultural soil amendments: Benefits versus limiting factors. *Waste Management*, *40*, 44–52. https://doi.org/http://dx.doi.org/10.1016/j.wasman.2015.01.027

Arbel, A., Yekutieli, O., & Barak, M. (1999). Performance of a fog system for cooling greenhouses. *Journal of Agricultural and Engineering Research*, *72*(2), 129–136. https://doi.org/10.1006/jaer.1998.0351

Archontoulis, S. V., Castellano, M. J., Licht, M. A., Nichols, V., Baum, M., Huber, I., Martinez-Feria, R., Puntel, L., Ordóñez, R. A., Iqbal, J., Wright, E. E., Dietzel, R. N., Helmers, M., Vanloocke, A., Liebman, M., Hatfield, J. L., Herzmann, D., Córdova, S. C., Edmonds, P., … Lamkey, K. R. (2020). Predicting crop yields and soil-plant nitrogen dynamics in the US Corn Belt. *Crop Science*, *60*(2), 721–738. https://doi.org/10.1002/csc2.20039

Aslam, M. A., Ahmed, M., Stöckle, C. O., Higgins, S. S., ul Hassan, F., & Hayat, R. (2017). Can growing degree days and photoperiod predict spring wheat phenology? *Frontiers in Environmental Science*, *5*(SEP), 1–10. https://doi.org/10.3389/fenvs.2017.00057

Astrup, T., Møller, J., & Fruergaard, T. (2009). Incineration and co-combustion of waste: Accounting of greenhouse gases and global warming contributions. *Waste Management and Research*, *27*(8), 789–799. https://doi.org/10.1177/0734242X09343774

Aubry, C., Jean-Paul, G. B., & Koegler, M. (2017). *Climate Innovation Potentials of Urban Agriculture (CIPUrA) Geographic Pathfinder*.

Audsley, E., Brander, M., Chatterton, J., Murphy-Bokern, Webster, & Williams. (2009). *How*

Low can we go? An assessment of greenhouse gas emissions from the UK food system and the scope reduction by 2050 (Issue November).

Avgoustaki, D. D., & Xydis, G. (2020). Indoor vertical farming in the Urban nexus context: Business growth and resource savings. *Sustainability (Switzerland)*, *12*(5), 1–18. https://doi.org/10.3390/su12051965

Bahers, J. B., & Giacchè, G. (2019). Towards a metabolic rift analysis: The case of urban agriculture and organic waste management in Rennes (France). *Geoforum*, *98*(February 2018), 97–107. https://doi.org/10.1016/j.geoforum.2018.10.017

Bakos, G. C., Fidanidis, D., & Tsagas, N. F. (1999). Greenhouse heating using geothermal energy. *Geothermics*, *28*(6), 759–765. https://doi.org/10.1016/S0375-6505(99)00041-3

Baltzell, A. H. (2011). *The Suitability of Worm Castings & Compost Tea in Organic Hydroponic Lettuce Propagation*. University of Arizona.

Banks, C. J., Chesshire, M., Heaven, S., & Arnold, R. (2011). Anaerobic digestion of source-segregated domestic food waste: Performance assessment by mass and energy balance. *Bioresource Technology*, *102*(2), 612–620. https://doi.org/10.1016/j.biortech.2010.08.005

Barbosa, G. L., Almeida Gadelha, F. D., Kublik, N., Proctor, A., Reichelm, L., Weissinger, E., Wohlleb, G. M., & Halden, R. U. (2015). Comparison of land, water, and energy requirements of lettuce grown using hydroponic vs. Conventional agricultural methods. *International Journal of Environmental Research and Public Health*, *12*(6), 6879–6891. https://doi.org/10.3390/ijerph120606879

Béné, C. (2020). Resilience of local food systems and links to food security – A review of some important concepts in the context of COVID-19 and other shocks. In *Food Security* (Vol. 12, Issue 4, pp. 805–822). Springer. https://doi.org/10.1007/s12571-020-01076-1

Benis, K., & Ferrão, P. (2017). Potential mitigation of the environmental impacts of food systems through urban and peri-urban agriculture (UPA) – a life cycle assessment approach. *Journal of Cleaner Production*, *140*, 784–795. https://doi.org/10.1016/j.jclepro.2016.05.176

Benis, K., Reinhart, C., & Ferrão, P. (2017a). Building-Integrated Agriculture (BIA) In Urban Contexts : Testing A Simulation-Based Decision Support Workflow. *15th IBPSA Conference San*. https://doi.org/10.26868/25222708.2017.479

Benis, K., Reinhart, C., & Ferrão, P. (2017b). Building-Integrated Agriculture (BIA) In Urban Contexts: Testing A Simulation-Based Decision Support Workflow. *Journal of Cleaner Production*, *147*(August), 589–602. https://doi.org/10.1016/j.jclepro.2017.01.130

Benis, K., Reinhart, C., & Ferrão, P. (2017c). Development of a simulation-based decision support workflow for the implementation of Building-Integrated Agriculture (BIA) in urban contexts. *Journal of Cleaner Production*, *147*, 589–602. https://doi.org/10.1016/j.jclepro.2017.01.130

Benke, K., & Tomkins, B. (2017). Future food-production systems: Vertical farming and controlled-environment agriculture. *Sustainability: Science, Practice, and Policy*, *13*(1), 13–26. https://doi.org/10.1080/15487733.2017.1394054

Bernstad, A., & La Cour Jansen, J. (2012). Review of comparative LCAs of food waste management systems - Current status and potential improvements. *Waste Management*,

32(12), 2439–2455. https://doi.org/10.1016/j.wasman.2012.07.023

Bianchi-Aguiar, T., Carravilla, M. A., & Oliveira, J. F. (2011). Vehicle routing for mixed solid waste collection. *VII ALIO–EURO – Workshop on Applied Combinatorial Optimization*, 137–140. http://core.ac.uk/download/pdf/20444408.pdf#page=150

Biswas, S. C. (2016). *Vegetable cultivation in the monsoon season in Bangladesh Vegetable cultivation in the monsoon season in Bangladesh*. *August*. https://doi.org/10.13140/RG.2.1.1226.5209

Bloomberg. (2019). *New Energy Outlook 2019*.

Boldrin, A., Andersen, J. K., Møller, J., Christensen, T. H., & Favoino, E. (2009). Composting and compost utilization: Accounting of greenhouse gases and global warming contributions. *Waste Management and Research*, *27*(8), 800–812. https://doi.org/10.1177/0734242X09345275

Boskovic, G., Jovicic, N., Jovanovic, S., & Simovic, V. (2016). Calculating the costs of waste collection: A methodological proposal. *Waste Management and Research*, *34*(8), 775–783. https://doi.org/10.1177/0734242X16654980

Bosompem, C., Stemn, E., & Fei-Baffoe, B. (2016). Multi-criteria GIS-based siting of transfer station for municipal solid waste: The case of Kumasi Metropolitan Area, Ghana. *Waste Management and Research*, *34*(10), 1054–1063. https://doi.org/10.1177/0734242X16658363

Boulard, T., Raeppel, C., Brun, R., Lecompte, F., Hayer, F., Carmassi, G., & Gaillard, G. (2011). Environmental impact of greenhouse tomato production in France. *Agronomy for Sustainable Development*, *31*(4), 757–777. https://doi.org/10.1007/s13593-011-0031-3

Bowman, J. (2017). *Tradeoffs in aquaponics vs hydroponics, by the numbers*. https://medium.com/edenworks/tradeoffs-in-aquaponics-vs-hydroponics-by-the-numbers-6d12b0ecd0af

Brogaard, L. K., & Christensen, T. H. (2016). Life cycle assessment of capital goods in waste management systems. *Waste Management*, *56*, 561–574. https://doi.org/10.1016/j.wasman.2016.07.037

Bruni, C., Akyol, C., Cipolletta, G., Eusebi, A. L., Caniani, D., Masi, S., Colon, J., & Fatone, F. (2020). Decentralized community composting: Past, present and future aspects of Italy. *Sustainability (Switzerland)*, *12*(8). https://doi.org/10.3390/SU12083319

Buchhorn, M., Smets, B., Bertels, L., Lesiv, M., Tsendbazar, N.-E., Masiliunas, D., Linlin, L., Herold, M., & Fritz, S. (2020). *Copernicus Global Land Service: Land Cover 100m: Collection 3: epoch 2019: Globe (Version V3.0.1) [Data set]*. https://doi.org/10.5281/zenodo.3939050

Bugbee, B. (2004). Nutrient Management in Recirculating Hydroponic Culture. *Acta Horticulturae*, *648*, 99–112. https://doi.org/10.17660/ActaHortic.2004.648.12

Calvert, K., & Mabee, W. (2015). More solar farms or more bioenergy crops? Mapping and assessing potential land-use conflicts among renewable energy technologies in eastern Ontario, Canada. *Applied Geography*, *56*, 209–221. https://doi.org/10.1016/j.apgeog.2014.11.028

Cameira, M. R., Tedesco, S., & Leitão, T. E. (2014). Water and nitrogen budgets under different production systems in Lisbon urban farming. *Biosystems Engineering*, *125*, 65–

79. https://doi.org/10.1016/j.biosystemseng.2014.06.020

Castleton, H. F., Stovin, V., Beck, S. B. M., & Davison, J. B. (2010). Green roofs; Building energy savings and the potential for retrofit. *Energy and Buildings*, *42*(10), 1582–1591. https://doi.org/10.1016/j.enbuild.2010.05.004

Chiew, Y. L., Spångberg, J., Baky, A., Hansson, P. A., & Jönsson, H. (2015). Environmental impact of recycling digested food waste as a fertilizer in agriculture - A case study. *Resources, Conservation and Recycling*, *95*(2015), 1–14. https://doi.org/10.1016/j.resconrec.2014.11.015

Chinta, Y. D., Kano, K., Widiastuti, A., Fukahori, M., Kawasaki, S., Eguchi, Y., Misu, H., Odani, H., Zhou, S., Narisawa, K., Fujiwara, K., Shinohara, M., & Sato, T. (2014). Effect of corn steep liquor on lettuce root rot (Fusarium oxysporum f.sp. lactucae) in hydroponic cultures. *Journal of the Science of Food and Agriculture*, *94*(11), 2317–2323. https://doi.org/10.1002/jsfa.6561

Cho, J., Park, S. M., Reum Park, A., Lee, O. C., Nam, G., & Ra, I. H. (2020). Application of photovoltaic systems for agriculture: A study on the relationship between power generation and farming for the improvement of photovoltaic applications in agriculture. *Energies*, *13*(18), 1–18. https://doi.org/10.3390/en13184815

Choab, N., Allouhi, A., El Maakoul, A., Kousksou, T., Saadeddine, S., & Jamil, A. (2019). Review on greenhouse microclimate and application: Design parameters, thermal modeling and simulation, climate controlling technologies. *Solar Energy*, *191*(May), 109–137. https://doi.org/10.1016/j.solener.2019.08.042

CIESIN. (2018). *Gridded Population of the World, Version 4 (GPWv4): Population Count Adjusted to Match 2015 Revision of UN WPP Country Totals, Revision 11*. NASA Socioeconomic Data and Applications Center (SEDAC). https://doi.org/10.7927/H4PN93PB

Cleveland, D. (1997). *Are urban gardens an efficient use of resources?* Arid Langs Newsletter No. 42. https://cals.arizona.edu/OALS/ALN/aln42/cleveland.html

Clinton, N., Stuhlmacher, M., Miles, A., Uludere Aragon, N., Wagner, M., Georgescu, M., Herwig, C., & Gong, P. (2018). A Global Geospatial Ecosystem Services Estimate of Urban Agriculture. *Earth's Future*. https://doi.org/10.1002/2017EF000536

Colasanti, K., & Hamm, M. W. (2010). Assessing the local food supply capacity of Detroit, Michigan. *Journal of Agriculture, Food Systems, and Community Development*, *1*(2), 41–58. https://doi.org/10.5304/jafscd.2010.012.002

Comesaña, I. V., Alves, D., Mato, S., Romero, X. M., & Varela, and B. (2017). Decentralized Composting of Organic Waste in a European Rural Region: A Case Study in Allariz (Galicia, Spain). In F.-C. Mihai (Ed.), *Solid Waste Management in Rural Areas*. Intech Open.

Proposal for a Directive of the European Parliament and of the Council amending Directive 2008/98/EC on waste, (2018) (testimony of Council of the European Union).

Cuce, E., Harjunowibowo, D., & Cuce, P. M. (2016). Renewable and sustainable energy saving strategies for greenhouse systems: A comprehensive review. *Renewable and Sustainable Energy Reviews*, *64*, 34–59. https://doi.org/10.1016/j.rser.2016.05.077

David, A. (2013). *Technical document on municipal solid waste organics processing*.

http://publications.gc.ca/collections/collection_2013/ec/En14-83-2013-eng.pdf

Davis, K. F., Downs, S., & Gephart, J. A. (2021). Towards food supply chain resilience to environmental shocks. *Nature Food*, *2*(1), 54–65. https://doi.org/10.1038/s43016-020-00196-3

Dehaene, M., Tornaghi, C., & Sage, C. (2014). Urban Metabolism and Urban Agriculture : How might growing food in cities ‘ mend ’ the metabolic rift ? *Urban Agriculture Europe*, 1–15.

Deng, Y. Y., Haigh, M., Pouwels, W., Ramaekers, L., Brandsma, R., Schimschar, S., Grözinger, J., & de Jager, D. (2015). Quantifying a realistic, worldwide wind and solar electricity supply. *Global Environmental Change*, *31*, 239–252. https://doi.org/10.1016/j.gloenvcha.2015.01.005

Denholm, P., Hand, M., Jackson, M., & Ong, S. (2009). Land Use Requirements of Modern Wind Power Plants in the United States. *National Renewable Energy Laboratory*, *Technical*(August), 46. http://www.osti.gov/bridge%0Ahttp://www.osti.gov/servlets/purl/964608-LaTU8c/

Deswal, M., & Laura, J. S. (2018). *Selection Of Collection Sites And Optimization Of Waste Bins of Rohtak City , Selection Of Collection Sites And Optimization Of Waste Bins Of Rohtak City , Haryana (India). April*.

Dhunny, A. Z., Doorga, J. R. S., Allam, Z., Lollchund, M. R., & Boojhawon, R. (2019). Identification of optimal wind, solar and hybrid wind-solar farming sites using fuzzy logic modelling. *Energy*, *188*, 116056. https://doi.org/10.1016/j.energy.2019.116056

Dimambro, M., Steiner, J., & Rayns, F. (2015). *Literature review : Digestate use in protected horticulture* (Issue March).

Doherty, K. (2015). *Urban agriculture and ecosystem services:a typology and toolkit for planners* [University of Massachusetts Amherst]. http://scholarworks.umass.edu/masters_theses_2

Domínguez Bravo, J., García Casals, X., & Pinedo Pascua, I. (2007). GIS approach to the definition of capacity and generation ceilings of renewable energy technologies. *Energy Policy*, *35*(10), 4879–4892. https://doi.org/10.1016/j.enpol.2007.04.025

Dorr, E., Sanyé-Mengual, E., Gabrielle, B., Grard, B. J. P., & Aubry, C. (2017). Proper selection of substrates and crops enhances the sustainability of Paris rooftop garden. *Agronomy for Sustainable Development*, *37*(5). https://doi.org/10.1007/s13593-017-0459-1

Drew, F., & Rhee, K. S. (1980). Energy Use, Cost, and Product Quality in Preserving Vegetables At Home By Canning, Freezing, and Dehydration. *Journal of Food Science*, *45*(6), 1561–1565. https://doi.org/10.1111/j.1365-2621.1980.tb07563.x

Drosg, B., Fuchs, W., Al Seadi, T., Madsen, M., & Linke, B. (2015). Nutrient Recovery by Biogas Digestate Processing. In *IEA Bioenergy*. https://doi.org/10.13140/rg.2.1.3182.6403

Dujardin, J., Kahl, A., Kruyt, B., Bartlett, S., & Lehning, M. (2017). Interplay between photovoltaic, wind energy and storage hydropower in a fully renewable Switzerland. *Energy*, *135*, 513–525. https://doi.org/10.1016/j.energy.2017.06.092

Edwards, J., Othman, M., Crossin, E., & Burn, S. (2018). Life cycle assessment to compare

the environmental impact of seven contemporary food waste management systems. *Bioresource Technology*, *248*, 156–173. https://doi.org/10.1016/j.biortech.2017.06.070

EEA. (n.d.). *Corine Land Cover*. https://land.copernicus.eu/pan-european/corine-land-cover/clc2018

Ellis, F., & Sumberg, J. (1998). Food production, urban areas and policy responses. *World Development*, *26*(2), 213–225. https://doi.org/10.1016/S0305-750X(97)10042-0

Erwin, J., & Gesick, E. (2017). Photosynthetic responses of swiss chard, kale, and spinach cultivars to irradiance and carbon dioxide concentration. *HortScience*, *52*(5), 706–712. https://doi.org/10.21273/HORTSCI11799-17

EU fruit and vegetables market observatory. (2020). *The tomato market in the EU: Vol 1.: Production, areas and yields*. https://ec.europa.eu/info/sites/info/files/food-farming-fisheries/farming/documents/tomatoes-production_en.pdf

FAO. (n.d.). *Damage and losses from climate-related disasters in agricultural sectors*. Retrieved February 28, 2021, from www.fao.org/3/a-i5128e.pdf

FAO. (2021). *FAOSTAT*. FAOSTAT Statistics Database. http://www.fao.org/faostat/en/#home

Feng, S., & Hao, Z. (2020). Quantifying likelihoods of extreme occurrences causing maize yield reduction at the global scale. *Science of the Total Environment*, *704*, 135250. https://doi.org/10.1016/j.scitotenv.2019.135250

Fick, S. E., & Hijmans, R. J. (2017). WorldClim 2: new 1-km spatial resolution climate surfaces for global land areas. *International Journal of Climatology*, *37*(12), 4302–4315. https://doi.org/10.1002/joc.5086

Fink, M., Feller, C., Scharpf, H. C., Weier, U., Maync, A., Ziegler, J., Paschold, P. J., & Strohmeyer, K. (1999). Nitrogen, phosphorus, potassium and magnesium contents of field vegetables - Recent data for fertiliser recommendations and nutrient balances. *Journal of Plant Nutrition and Soil Science*, *162*(1), 71–73. https://doi.org/10.1002/(SICI)1522-2624(199901)162:1<71::AID-JPLN71>3.0.CO;2-0

Fisch-Informationszentrum. (2016). *Fischwirtschaft - Daten und Fakten*. https://doi.org/10.1007/s11298-013-0792-x

Foley, J. A., DeFries, R., Asner, G. P., Barford, C., Bonan, G., Carpenter, S. R., Chapin, F. S., Coe, M. T., Daily, G. C., Gibbs, H. K., Helkowski, J. H., Holloway, T., Howard, E. A., Kucharik, C. J., Monfreda, C., Patz, J. A., Prentice, I. C., Ramankutty, N., & Snyder, P. K. (2005). Global consequences of land use. In *Science* (Vol. 309, Issue 5734, pp. 570–574). American Association for the Advancement of Science. https://doi.org/10.1126/science.1111772

Forchino, A. A., Lourguioui, H., Brigolin, D., & Pastres, R. (2017). Aquaponics and sustainability: The comparison of two different aquaponic techniques using the Life Cycle Assessment (LCA). *Aquacultural Engineering*, *77*, 80–88. https://doi.org/10.1016/j.aquaeng.2017.03.002

Forkes, J. (2007). Nitrogen balance for the urban food metabolism of Toronto, Canada. *Resources, Conservation and Recycling*, *52*(1), 74–94. https://doi.org/10.1016/j.resconrec.2007.02.003

Fthenakis, V., & Kim, H. C. (2009). Land use and electricity generation: A life-cycle analysis.

Renewable and Sustainable Energy Reviews, *13*(6–7), 1465–1474. https://doi.org/10.1016/j.rser.2008.09.017

Fu, R., Feldman, D., & Margolis, R. (2009). *U.S. Solar Photovoltaic System Cost Benchmark: Q1 2018*. www.nrel.gov/publications.

Fujiwara, K., Aoyama, C., Takano, M., & Shinohara, M. (2012). Suppression of Ralstonia solanacearum bacterial wilt disease by an organic hydroponic system. *Journal of General Plant Pathology*, *78*(3), 217–220. https://doi.org/10.1007/s10327-012-0371-0

GADM. (n.d.). Retrieved February 25, 2021, from https://gadm.org/download_world.html

Gallardo, A., Bovea, M. D., Colomer, F. J., Prades, M., & Carlos, M. (2010). Comparison of different collection systems for sorted household waste in Spain. *Waste Management*, *30*(12), 2430–2439. https://doi.org/10.1016/j.wasman.2010.05.026

Gao, L., & Bryan, B. A. (2017). Finding pathways to national-scale land-sector sustainability. *Nature*, *544*(7649), 217–222. https://doi.org/10.1038/nature21694

Ghoulem, M., El Moueddeb, K., Nehdi, E., Boukhanouf, R., & Kaiser Calautit, J. (2019). Greenhouse design and cooling technologies for sustainable food cultivation in hot climates: Review of current practice and future status. *Biosystems Engineering*, *183*, 121–150. https://doi.org/10.1016/j.biosystemseng.2019.04.016

Global Footprint Network. (2021). *Free Public Data Set - Global Footprint Network*. https://www.footprintnetwork.org/licenses/public-data-package-free/

Godfray, H. C. J., Beddington, J. R., Crute, I. R., Haddad, L., Lawrence, D., Muir, J. F., Pretty, J., Robinson, S., Thomas, S. M., & Toulmin, C. (2010). Food security: The challenge of feeding 9 billion people. In *Science* (Vol. 327, Issue 5967, pp. 812–818). https://doi.org/10.1126/science.1185383

Goldstein, B., Hauschild, M., Fernandez, J., & Birkved, M. (2016). Testing the environmental performance of urban agriculture as a food supply in northern climates. *Journal of Cleaner Production*, *135*, 984–994. https://doi.org/10.1016/j.jclepro.2016.07.004

Goldstein, B., Hauschild, M., Fernández, J., & Birkved, M. (2016). Urban versus conventional agriculture, taxonomy of resource profiles: a review. *Agronomy for Sustainable Development*, *36*(1), 1–19. https://doi.org/10.1007/s13593-015-0348-4

Goldstein, B. P., Hauschild, M. Z., Fernández, J. E., & Birkved, M. (2017). Contributions of Local Farming to Urban Sustainability in the Northeast United States. *Environmental Science and Technology*, *51*(13), 7340–7349. https://doi.org/10.1021/acs.est.7b01011

Golzar, F., Heeren, N., Hellweg, S., & Roshandel, R. (2018). A novel integrated framework to evaluate greenhouse energy demand and crop yield production. *Renewable and Sustainable Energy Reviews*, *96*(April), 487–501. https://doi.org/10.1016/j.rser.2018.06.046

Golzar, F., Heeren, N., Hellweg, S., & Roshandel, R. (2019). A comparative study on the environmental impact of greenhouses: A probabilistic approach. *Science of the Total Environment*, *675*, 560–569. https://doi.org/10.1016/j.scitotenv.2019.04.092

Gómez, C., & Izzo, L. G. (2018). Increasing efficiency of crop production with LEDs. *AIMS Agriculture and Food*, *3*(2), 135–153. https://doi.org/10.3934/agrfood.2018.2.135

Gondhalekar, D., & Ramsauer, T. (2017). Urban Climate Nexus City : Operationalizing the

urban Water- Energy-Food Nexus for climate change adaptation in Munich , Germany. *Urban Climate*, *19*, 28–40. https://doi.org/10.1016/j.uclim.2016.11.004

González-Sierra, R. P., Arizmendiarrieta, J. S., Sánchez, B. P., Iriarte, I. I., & Duarte, G. N. (2019). *Community Composting: A Practical Guide for Local Management of Biowaste*. *April*. https://zerowasteeurope.eu/downloads/community-composting-a-practical-guide-for-local-management-of-biowaste/

Graamans, L., Baeza, E., van den Dobbelsteen, A., Tsafaras, I., & Stanghellini, C. (2018). Plant factories versus greenhouses: Comparison of resource use efficiency. *Agricultural Systems*, *160*(July 2017), 31–43. https://doi.org/10.1016/j.agsy.2017.11.003

Graamans, L., Tenpierik, M., van den Dobbelsteen, A., & Stanghellini, C. (2020). Plant factories: Reducing energy demand at high internal heat loads through façade design. *Applied Energy*, *262*(February), 114544. https://doi.org/10.1016/j.apenergy.2020.114544

Graamans, L., van den Dobbelsteen, A., Meinen, E., & Stanghellini, C. (2017). Plant factories; crop transpiration and energy balance. *Agricultural Systems*, *153*, 138–147. https://doi.org/10.1016/j.agsy.2017.01.003

Graham-Rowe, D. (2011). Agriculture: Beyond food versus fuel. *Nature*, *474*(7352 SUPPL.). https://doi.org/10.1038/474S06a

Grard, B. J.-P., Bel, N., Marchal, N., Madre, F., Castell, J.-F., Cambier, P., Houot, S., Manouchehri, N., Besancon, S., Michel, J.-C., Chenu, C., Frascaria-Lacoste, N., & Aubry, C. (2015). Recycling urban waste as possible use for rooftop vegetable garden. *Future of Food: Journal on Food, Agriculture and Society*, *3*(1), 21–34. http://futureoffoodjournal.org/index.php/journal/article/view/141

Grewal, S. S., & Grewal, P. S. (2012). Can cities become self-reliant in food? *Cities*, *29*(1), 1–11. https://doi.org/10.1016/j.cities.2011.06.003

Guo, W., Zhou, Y., Zhu, N., Hu, H., Shen, W., Huang, X., Zhang, T., Wu, P., & Li, Z. (2018). On site composting of food waste: A pilot scale case study in China. *Resources, Conservation and Recycling*, *132*(September 2017), 130–138. https://doi.org/10.1016/j.resconrec.2018.01.033

H Adwiraah, S Oldenburg, I Körner, R. S. (2012). Bioresources inventory. GIS-based identification, quantification and characterisation methods. *ORBIT*, 80–87.

Haberman, D., Gillies, L., Canter, A., Rinner, V., Pancrazi, L., & Martellozzo, F. (2014). The Potential of Urban Agriculture in Montréal: A Quantitative Assessment. *ISPRS International Journal of Geo-Information*, *3*(3), 1101–1117. https://doi.org/10.3390/ijgi3031101

Hall, E. (1989). The Garden History Society Hot Walls : An Investigation of Their Construction in Some Northern Kitchen Gardens. *Garden History*, *17*(1), 95–107.

Hamm, M., Frison, E., & Tirado von der Pahlen, M. (2018). Human health, diets and nutrition: missing links in eco-agri-food systems. *TEEB for Agriculture and Food: Scientifc and Economic Foundations*, *UN Environment Geneva*.

Harbick, K., & Albright, L. D. (2016). Comparison of energy consumption: Greenhouses and plant factories. *Acta Horticulturae*, *1134*, 285–292. https://doi.org/10.17660/ActaHortic.2016.1134.38

Harris, J., Depenbusch, L., Pal, A. A., Nair, R. M., & Ramasamy, S. (2020). Food system

disruption: initial livelihood and dietary effects of COVID-19 on vegetable producers in India. *Food Security*, *12*(4), 841–851. https://doi.org/10.1007/s12571-020-01064-5

Hart, M. R., Quin, B. F., & Nguyen, M. L. (2004). Phosphorus Runoff from Agricultural Land and Direct Fertilizer Effects. *Journal of Environment Quality*, *33*(6), 1954. https://doi.org/10.2134/jeq2004.1954

Hazra, P. (2008). Upgradation of the vegetable production scenario of Bangladesh: suggested strategy. *J. Agrofor. Environ*, *2*(2), 201–204.

Health Canada. (n.d.). *Canada's Food Guide*. Retrieved November 26, 2018, from https://www.canada.ca/content/dam/hc-sc/migration/hc-sc/fn-an/alt_formats/hpfb-dgpsa/pdf/food-guide-aliment/view_eatwell_vue_bienmang-eng.pdf

Health Canada. (2005). Nutrient Value of Some Common Foods. *Canadian Nutrient File*, 1–54. http://www.hc-sc.gc.ca/fn-an/nutrition/fiche-nutri-data/index_e.html

Hemming, S., De Zwart, F., Elings, A., Righini, I., & Petropoulou, A. (2019). Remote control of greenhouse vegetable production with artificial intelligence—greenhouse climate, irrigation, and crop production. *Sensors (Switzerland)*, *19*(8). https://doi.org/10.3390/s19081807

Hernandez, O. L., Calderín, A., Huelva, R., Martínez-Balmori, D., Guridi, F., Aguiar, N. O., Olivares, F. L., & Canellas, L. P. (2014). Humic substances from vermicompost enhance urban lettuce production. *Agronomy for Sustainable Development*, *35*(1), 225–232. https://doi.org/10.1007/s13593-014-0221-x

Herrero, M., Thornton, P. K., Mason-D'Croz, D., Palmer, J., Benton, T. G., Bodirsky, B. L., Bogard, J. R., Hall, A., Lee, B., Nyborg, K., Pradhan, P., Bonnett, G. D., Bryan, B. A., Campbell, B. M., Christensen, S., Clark, M., Cook, M. T., de Boer, I. J. M., Downs, C., … West, P. C. (2020). Innovation can accelerate the transition towards a sustainable food system. *Nature Food*, *1*(5), 266–272. https://doi.org/10.1038/s43016-020-0074-1

Hertel, S., Navarro, P., Deegener, S., & Körner, I. (2015). Biogas and nutrients from blackwater, lawn cuttings and grease trap residues???experiments for Hamburg???s Jenfelder Au district. *Energy, Sustainability and Society*, *5*(1). https://doi.org/10.1186/s13705-015-0057-5

Hoefnagels, R., Junginger, M., Panzer, C., Resch, G., Vienna, T. U., Held, A., & Isi, F. (2011). *Long Term Potentials and Costs of RES Part I: Potentials, Diffusion and Technological learning*. www.reshaping-res-policy.eu

Hogg, D., Gibbs, A., Favoino, E., & Ricci, M. (2007). *Managing biowastes from households in the uk : applying life-cycle thinking in the framework of cost-benefit analysis appendices to the main report* (Issue May).

HOMER. (n.d.). Retrieved March 1, 2021, from https://www.homerenergy.com

Hoogwijk, M., de Vries, B., & Turkenburg, W. (2004). Assessment of the global and regional geographical, technical and economic potential of onshore wind energy. *Energy Economics*, *26*(5), 889–919. https://doi.org/10.1016/j.eneco.2004.04.016

Huang, C., Duiker, S. W., Deng, L., Fang, C., & Zeng, W. (2015). Influence of precipitation on maize yield in the eastern United States. *Sustainability (Switzerland)*, *7*(5), 5996–6010. https://doi.org/10.3390/su7055996

Iddio, E., Wang, L., Thomas, Y., McMorrow, G., & Denzer, A. (2020). Energy efficient

operation and modeling for greenhouses: A literature review. *Renewable and Sustainable Energy Reviews*, *117*(October 2019), 109480. https://doi.org/10.1016/j.rser.2019.109480

IEA. (2019). *World Energy Outlook 2019*. https://www.iea.org/reports/world-energy-outlook-2019

IEA. (2020). *World Energy Outlook 2020*. https://www.iea.org/reports/world-energy-outlook-2020

iFarm. (n.d.). *How Much Electricity Does a Vertical Farm Consume Using iFarm technologies?* Retrieved March 26, 2021, from https://ifarm.fi/blog/2020/12/how-much-electricity-does-a-vertical-farm-consume

Incropera, F. P., DeWitt, D. P., Bergman, T. L., & Lavine, A. S. (2006). *Fundamentals of Heat and Mass Transfer* (6th ed.). John Wiley & Sons.

ipiff. (2021, May 4). *The International Platform of Insects for Food and Feed*. https://ipiff.org/wp-content/uploads/2021/05/May-04-2021-PR-novel-food-vote-2-1.pdf

IRENA. (2018). *Technology Beif: Biogas for Road Vehicles* (Issue March). https://www.irena.org/publications/2017/Mar/Biogas-for-road-vehicles-Technology-brief

IRENA. (2019). Future of solar Photovoltaic. In *International Renewable Energy Agency (IRENA)*. www.irena.org/publications

Jacobs, A., Flessa, H., Don, A, Heidkamp A, Prietz R, Dechow R, G., A, Poeplau C, Riggers C, Schneider F, Tiemeyer B, Vos C, W. M., Müller T, Säurich A, Fahrion-Nitschke A, Gebbert S, Jaconi A, K. H., & A, L. (2018). *Landwirtschaftlich genutzte Böden in Deutschland - Ergebnisse der Bodenzustandserhebung*. https://doi.org/10.3220/REP1542818391000

Jaunich, M. K., Levis, J. W., Barlaz, M. A., & DeCarolis, J. F. (2016). Lifecycle Process Model for Municipal Solid Waste Collection. *Journal of Environmental Engineering*, *142*(8), 04016037. https://doi.org/10.1061/(asce)ee.1943-7870.0001065

Johlas, H., Witherby, S., & Doyle, J. R. (2020). Storage requirements for high grid penetration of wind and solar power for the MISO region of North America: A case study. *Renewable Energy*, *146*, 1315–1324. https://doi.org/10.1016/j.renene.2019.07.043

Joly, G. (2018). *Valorising Organic Waste using the Black Soldier Fly (Hermetia illucens), in Ghana* [KTH Royal Institue of Technology]. http://www.diva-portal.org/smash/record.jsf?pid=diva2%3A1196375&dswid=878

Kapica, J. (2020). Wind and photovoltaic potential in Europe in the context of mid-term energy storage. *Journal of Renewable and Sustainable Energy*, *12*(3), 034101. https://doi.org/10.1063/1.5131560

Katsoulas, N., Sapounas, A., De Zwart, F., Dieleman, J. A., & Stanghellini, C. (2015). Reducing ventilation requirements in semi-closed greenhouses increases water use efficiency. *Agricultural Water Management*, *156*, 90–99. https://doi.org/10.1016/j.agwat.2015.04.003

Katsoulas, Nikolaos, & Stanghellini, C. (2019). Modelling crop transpiration in greenhouses: Different models for different applications. *Agronomy*, *9*(7), 1–17. https://doi.org/10.3390/agronomy9070392

Kawamura-Aoyama, C., Fujiwara, K., Shinohara, M., & Takano, M. (2014). Study on the

hydroponic culture of lettuce with microbially degraded solid food waste as a nitrate source. *Japan Agricultural Research Quarterly*, *48*(1), 71–76. https://doi.org/10.6090/jarq.48.71

Kazem, H. A., Al-Badi, H. A. S., Al Busaidi, A. S., & Chaichan, M. T. (2017). Optimum design and evaluation of hybrid solar/wind/diesel power system for Masirah Island. *Environment, Development and Sustainability*, *19*(5), 1761–1778. https://doi.org/10.1007/s10668-016-9828-1

Kempkes, F. L. K., & Janse, J. (2016). *Cultivation and energy 2SaveEnergy greenhouse*. http://edepot.wur.nl/385097

Keng, Z. X., Chong, S., Ng, C. G., Ridzuan, N. I., Hanson, S., Pan, G. T., Lau, P. L., Supramaniam, C. V., Singh, A., Chin, C. F., & Lam, H. L. (2020). Community-scale composting for food waste: A life-cycle assessment-supported case study. *Journal of Cleaner Production*, *261*, 121220. https://doi.org/10.1016/j.jclepro.2020.121220

Khattab, N. M., Badr, M. A., Maalawi, K. Y., El Shenawy, E. T., El Ghetany, H. H., & Ibrahim, M. M. (2016). Hybrid renewable energy system for water desalination: A case study for small green house hydroponic cultivation in Egypt. *ARPN Journal of Engineering and Applied Sciences*, *11*(21), 12380–12390.

Kibler, K. M., Reinhart, D., Hawkins, C., Motlagh, A. M., & Wright, J. (2018). Food waste and the food-energy-water nexus: A review of food waste management alternatives. *Waste Management*, *74*, 52–62. https://doi.org/10.1016/j.wasman.2018.01.014

Kim, J. Y., Koide, D., Ishihama, F., Kadoya, T., & Nishihiro, J. (2021). Current site planning of medium to large solar power systems accelerates the loss of the remaining semi-natural and agricultural habitats. *Science of The Total Environment*, *779*, 146475. https://doi.org/10.1016/j.scitotenv.2021.146475

Kinney, C. A., Furlong, E. T., Zaugg, S. D., Burkhardt, M. R., Werner, S. L., Cahill, J. D., & Jorgensen, G. R. (2006). Survey of organic wastewater contaminants in biosolids destined for land application. *Environmental Science and Technology*, *40*(23), 7207–7215. https://doi.org/10.1021/es0603406

Kinnunen, P., Guillaume, J. H. A., Taka, M., D'Odorico, P., Siebert, S., Puma, M. J., Jalava, M., & Kummu, M. (2020). Local food crop production can fulfil demand for less than one-third of the population. *Nature Food*, *1*(4), 229–237. https://doi.org/10.1038/s43016-020-0060-7

Kirnak, H., Hansen, R. C., Keener, H. M., & Short, T. H. (2002). An evaluation of physically based and empirically determined evapotranspiration models for nursery plants. *Turkish Journal of Agriculture and Forestry*, *26*(6), 355–362. https://doi.org/10.3906/tar-0112-4

Kittas, C., Boulard, T., & Papadakis, G. (1997). Natural ventilation of a greenhouse with ridge and side openings: Sensitivity to temperature and wind effects. *Transactions of the American Society of Agricultural Engineers*, *40*(2), 415–425. https://doi.org/10.13031/2013.21268

Koc, A., Turk, S., & Şahin, G. (2019). Multi-criteria of wind-solar site selection problem using a GIS-AHP-based approach with an application in Igdir Province/Turkey. *Environmental Science and Pollution Research*, *26*(31), 32298–32310. https://doi.org/10.1007/s11356-019-06260-1

Kopittke, P. M., Menzies, N. W., Wang, P., McKenna, B. A., & Lombi, E. (2019). Soil and

the intensification of agriculture for global food security. In *Environment International* (Vol. 132, p. 105078). Elsevier Ltd. https://doi.org/10.1016/j.envint.2019.105078

Kozai, T., Niu, G., & Takagaki, M. (2019). *Plant Factory - An Indoor Vertical Farming System for Efficient Quality Food Production*. Academic Press.

Kozai, Toyoki. (2013). Resource use efficiency of closed plant production system with artificial light: Concept, estimation and application to plant factory. *Proceedings of the Japan Academy Series B: Physical and Biological Sciences*, *89*(10), 447–461. https://doi.org/10.2183/pjab.89.447

Kuijpers, W. J. P., van de Molengraft, M. J. G., van Mourik, S., van 't Ooster, A., Hemming, S., & van Henten, E. J. (2019). Model selection with a common structure: Tomato crop growth models. *Biosystems Engineering*, *187*, 247–257. https://doi.org/10.1016/j.biosystemseng.2019.09.010

Kulak, M., Graves, A., & Chatterton, J. (2013). Reducing greenhouse gas emissions with urban agriculture: A Life Cycle Assessment perspective. *Landscape and Urban Planning*, *111*(1), 68–78. https://doi.org/10.1016/j.landurbplan.2012.11.007

Kumar, P. R., Jayaram, A., & Somashekar, R. K. (2009). Assessment of the performance of different compost models to manage urban household organic solid wastes. *Clean Technologies and Environmental Policy*, *11*(4), 473–484. https://doi.org/10.1007/s10098-009-0204-9

Kummu, M., Kinnunen, P., Lehikoinen, E., Porkka, M., Queiroz, C., Röös, E., Troell, M., & Weil, C. (2020). Interplay of trade and food system resilience: Gains on supply diversity over time at the cost of trade independency. *Global Food Security*, *24*(February), 100360. https://doi.org/10.1016/j.gfs.2020.100360

KZNDARD. (n.d.). *Length of growing period:* Retrieved November 26, 2018, from https://www.kzndard.gov.za/images/Documents/Horticulture/Veg_prod/length_of_growing_period.pdf

Lade, S. J., Steffen, W., de Vries, W., Carpenter, S. R., Donges, J. F., Gerten, D., Hoff, H., Newbold, T., Richardson, K., & Rockström, J. (2020). Human impacts on planetary boundaries amplified by Earth system interactions. *Nature Sustainability*, *3*(2), 119–128. https://doi.org/10.1038/s41893-019-0454-4

Laugs, G. A. H., Benders, R. M. J., & Moll, H. C. (2020). Balancing responsibilities: Effects of growth of variable renewable energy, storage, and undue grid interaction. *Energy Policy*, *139*, 111203. https://doi.org/10.1016/j.enpol.2019.111203

Leung Pah Hang, M. Y., Martinez-Hernandez, E., Leach, M., & Yang, A. (2016). Designing integrated local production systems: A study on the food-energy-water nexus. *Journal of Cleaner Production*, *135*, 1065–1084. https://doi.org/10.1016/j.jclepro.2016.06.194

Leung Pah Hang, M. Y., Martinez-Hernandez, E., Leach, M., & Yang, A. (2017). Insight-Based Approach for the Design of Integrated Local Food-Energy-Water Systems. *Environmental Science and Technology*, *51*(15), 8643–8653. https://doi.org/10.1021/acs.est.7b00867

Li, L., Li, X., Chong, C., Wang, C. H., & Wang, X. (2020). A decision support framework for the design and operation of sustainable urban farming systems. *Journal of Cleaner Production*, *268*, 121928. https://doi.org/10.1016/j.jclepro.2020.121928

Li, M., Ho, K. K. H. Y., Hayes, M., & Ferruzzi, M. G. (2019). *The Roles of Food Processing in Translation of Dietary Guidance for Whole Grains, Fruits, and Vegetables*. https://doi.org/10.1146/annurev-food-032818

Li, Y., Guan, K., Schnitkey, G. D., DeLucia, E., & Peng, B. (2019). Excessive rainfall leads to maize yield loss of a comparable magnitude to extreme drought in the United States. *Global Change Biology*, *25*(7), 2325–2337. https://doi.org/10.1111/gcb.14628

LIPOR. (n.d.). *Horta à Porta*. https://www.lipor.pt/pt/educacao-ambiental/horta-da-formiga/agricultura-biologica/horta-a-porta/

López-Mosquera, M. E., Fernández-Lema, E., Villares, R., Corral, R., Alonso, B., & Blanco, C. (2011). Composting fish waste and seaweed to produce a fertilizer for use in organic agriculture. *Procedia Environmental Sciences*, *9*, 113–117. https://doi.org/10.1016/j.proenv.2011.11.018

Lopez, A., Roberts, B., Heimiller, D., Blair, N., & Porro, G. (2012). U.S. Renewable Energy Technical Potentials: A GIS-Based Analysis. *National Renewable Energy Laboratory Document*, *1*(7), 1–40.

López, A., Valera, D. L., Molina-Aiz, F. D., & Peña, A. (2012). Sonic anemometry to evaluate airflow characteristics and temperature distribution in empty Mediterranean greenhouses equipped with pad-fan and fog systems. *Biosystems Engineering*, *113*(4), 334–350. https://doi.org/10.1016/j.biosystemseng.2012.09.006

Love, D. C., Fry, J. P., Li, X., Hill, E. S., Genello, L., Semmens, K., & Thompson, R. E. (2015). Commercial aquaponics production and profitability: Findings from an international survey. *Aquaculture*, *435*, 67–74. https://doi.org/10.1016/j.aquaculture.2014.09.023

Lunag, M. N., Elauria, J. C., & Burguillos, J. D. (2020). Community-based bin design approach: an initial stage toward urban composting at a hill station, Philippines. *Environment, Development and Sustainability*, *0123456789*. https://doi.org/10.1007/s10668-020-00746-6

Lundie, S., & Peters, G. M. (2005). Life cycle assessment of food waste management options. *Journal of Cleaner Production*, *13*(3), 275–286. https://doi.org/10.1016/j.jclepro.2004.02.020

MacKay, D. J. C. (2013). Solar energy in the context of energy use, energy transportation and energy storage. *Philosophical Transactions of the Royal Society A: Mathematical, Physical and Engineering Sciences*, *371*(1996), 20110431. https://doi.org/10.1098/rsta.2011.0431

Mago, P., Chamra, L., & Hueffed, A. (2009). A review on energy, economical, and environmental benefits of the use of CHP systems for small commercial buildings for the North American climate. *International Journal of Energy Research*, *33*, 1252–1265. https://doi.org/10.1002/er

Makkar, H. P. S., Tran, G., Heuzé, V., & Ankers, P. (2014). State-of-the-art on use of insects as animal feed. *Animal Feed Science and Technology*, *197*, 1–33. https://doi.org/10.1016/J.ANIFEEDSCI.2014.07.008

Manikandan, K., & Vethamoni, I. (2017). A review: Crop modeling in vegetable crops. *Journal of Pharmacognosy and Phytochemistry*, *6*(4), 1006–1009. http://www.phytojournal.com/archives/2017/vol6issue4/PartO/6-4-4-958.pdf

Martellozzo, F., Landry, J. S., Plouffe, D., Seufert, V., Rowhani, P., & Ramankutty, N. (2014). Urban agriculture: A global analysis of the space constraint to meet urban vegetable demand. *Environmental Research Letters*, *9*(6). https://doi.org/10.1088/1748-9326/9/6/064025

Martin, M., Poulikidou, S., & Molin, E. (2019). *Exploring the Environmental Performance of Urban Symbiosis for Vertical Hydroponic Farming*. 10–12.

Martínez-Blanco, J., Colón, J., Gabarrell, X., Font, X., Sánchez, A., Artola, A., & Rieradevall, J. (2010). The use of life cycle assessment for the comparison of biowaste composting at home and full scale. *Waste Management*, *30*(6), 983–994. https://doi.org/10.1016/j.wasman.2010.02.023

Martinez-Feria, R. A., & Basso, B. (2020). Unstable crop yields reveal opportunities for site-specific adaptations to climate variability. *Scientific Reports*, *10*(1), 1–10. https://doi.org/10.1038/s41598-020-59494-2

Martins-Turner, K., Grahle, A., Nagel, K., & Dietmar, G. (2020). Electrification of Urban Freight Transport – a Case Study of the Food Retailing Industry. *The 9th International Workshop on Agent-Based Mobility, Traffic and Transportation Models, (ABMTRANS) April 6 - 9, 2020, Warsaw, Poland*.

Marucci, A., & Cappuccini, A. (2016). Dynamic photovoltaic greenhouse: Energy balance in completely clear sky condition during the hot period. *Energy*, *102*, 302–312. https://doi.org/10.1016/j.energy.2016.02.053

Massmann, A., Gentine, P., & Lin, C. (2019). When Does Vapor Pressure Deficit Drive or Reduce Evapotranspiration? *Journal of Advances in Modeling Earth Systems*, *11*(10), 3305–3320. https://doi.org/10.1029/2019MS001790

Mayer, F., Bhandari, R., Gäth, S. A., Himanshu, H., & Stobernack, N. (2020). Economic and environmental life cycle assessment of organic waste treatment by means of incineration and biogasification. Is source segregation of biowaste justified in Germany? *Science of the Total Environment*, *721*, 137731. https://doi.org/10.1016/j.scitotenv.2020.137731

Mazzanti, M., & Zoboli, R. (2011). Waste Generation, Incineration and Landfill Diversion: De-Coupling Trends, Socio-Economic Drivers and Policy Effectiveness in the EU. *SSRN Electronic Journal*. https://doi.org/10.2139/ssrn.1314222

McClintock, N. (2010). Why farm the city? Theorizing urban agriculture through a lens of metabolic rift. *Cambridge Journal of Regions, Economy and Society*, *3*(2), 191–207. https://doi.org/10.1093/cjres/rsq005

McDonald, R. I., Fargione, J., Kiesecker, J., Miller, W. M., & Powell, J. (2009). Energy sprawl or energy efficiency: Climate policy impacts on natural habitat for the United States of America. *PLoS ONE*, *4*(8). https://doi.org/10.1371/journal.pone.0006802

McGowan, J. G., & Connors, S. R. (2000). Windpower: A turn of the century review. *Annual Review of Energy and the Environment*, *25*, 147–197. https://doi.org/10.1146/annurev.energy.25.1.147

Mead, B. R., Christiansen, P., Davies, J. A. C., Falagán, N., Kourmpetli, S., Liu, L., Walsh, L., & Hardman, C. A. (2021). Is urban growing of fruit and vegetables associated with better diet quality and what mediates this relationship? Evidence from a cross-sectional survey. *Appetite*, *163*(October 2020), 105218. https://doi.org/10.1016/j.appet.2021.105218

Milborrow, D. (2020, January 31). *Energy cost analysis 2020: Wind is ready for zero-subsidy future*. https://www.windpowermonthly.com/article/1671659/energy-cost-analysis-2020-wind-ready-zero-subsidy-future

Milbrandt, A. (2005). A geographic perspective on the current biomass resource availability in the United States. *NREL Technical Report*, *December*, 1–50. https://doi.org/NREL/TP-560-39181

Miskin, C. K., Li, Y., Perna, A., Ellis, R. G., Grubbs, E. K., Bermel, P., & Agrawal, R. (2019). Sustainable co-production of food and solar power to relax land-use constraints. *Nature Sustainability*, *2*(10), 972–980. https://doi.org/10.1038/s41893-019-0388-x

Mohareb, E., Heller, M., Novak, P., Goldstein, B., Fonoll, X., & Raskin, L. (2017). Considerations for reducing food system energy demand while scaling up urban agriculture. *Environmental Research Letters*, *12*(12). https://doi.org/10.1088/1748-9326/aa889b

Møller, J., Boldrin, A., & Christensen, T. H. (2009). Anaerobic digestion and digestate use: Accounting of greenhouse gases and global warming contribution. *Waste Management and Research*, *27*(8), 813–824. https://doi.org/10.1177/0734242X09344876

Moore, N. (2020). Large Scale Grid Integration of Wind and Solar Power with Storage. *Macalester Journal of Physics and Astronomy*, *8*(1), 13.

Morris, J., Brown, S., Cotton, M., & Matthews, H. S. (2017). Life-Cycle Assessment Harmonization and Soil Science Ranking Results on Food-Waste Management Methods. *Environmental Science and Technology*, *51*(10), 5360–5367. https://doi.org/10.1021/acs.est.6b06115

Morris, J., Scott Matthews, H., & Morawski, C. (2013). Review and meta-analysis of 82 studies on end-of-life management methods for source separated organics. *Waste Management*, *33*(3), 545–551. https://doi.org/10.1016/j.wasman.2012.08.004

Mugica, Y., & Spacht, A. (2017). *San Francisco Composting from fork to farm and back* (Issue November). https://www.nrdc.org/sites/default/files/food-matters-san-francisco-composting-cs.pdf

Nadal, A., Alamús, R., Pipia, L., Ruiz, A., Corbera, J., Cuerva, E., Rieradevall, J., & Josa, A. (2017). Urban planning and agriculture. Methodology for assessing rooftop greenhouse potential of non-residential areas using airborne sensors. *Science of the Total Environment*, *601–602*, 493–507. https://doi.org/10.1016/j.scitotenv.2017.03.214

Namany, S., Al-Ansari, T., & Govindan, R. (2019). Optimisation of the energy, water, and food nexus for food security scenarios. *Computers and Chemical Engineering*, *129*. https://doi.org/10.1016/j.compchemeng.2019.106513

Nemś, A., Nemś, M., & Świder, K. (2018). Analysis of the possibilities of using a heat pump for greenhouse heating in Polish climatic conditions-A case study. *Sustainability (Switzerland)*, *10*(10). https://doi.org/10.3390/su10103483

Nie, Y., Avraamidou, S., Xiao, X., Pistikopoulos, E. N., Li, J., Zeng, Y., Song, F., Yu, J., & Zhu, M. (2018). A Food-Energy-Water Nexus approach for land use optimization. *Science of the Total Environment*, *659*, 7–19. https://doi.org/10.1016/j.scitotenv.2018.12.242

Nigussie, A., Kuyper, T. W., & Neergaard, A. de. (2015). Agricultural waste utilisation

strategies and demand for urban waste compost: Evidence from smallholder farmers in Ethiopia. *Waste Management*, *44*, 82–93. https://doi.org/10.1016/j.wasman.2015.07.038

Noche, B., Chinakupt, T., Rhoma, F. A., & Jawale, M. (2010). Optimization model for solid waste management system network design case study. *2010 The 2nd International Conference on Computer and Automation Engineering, ICCAE 2010*, *5*, 230–236. https://doi.org/10.1109/ICCAE.2010.5451476

O'Sullivan, C. A., Bonnett, G. D., McIntyre, C. L., Hochman, Z., & Wasson, A. P. (2019). Strategies to improve the productivity, product diversity and profitability of urban agriculture. *Agricultural Systems*, *174*(December 2018), 133–144. https://doi.org/10.1016/j.agsy.2019.05.007

Opitz, I., Doernberg, A., Specht, K., & Piorr, A. (2017). *Future|Food|Commons: Alternative Food Networks at the urban-rural interface*. *July*. https://www.researchgate.net/publication/320346028%0AFuture%7CFood%7CCommons:

Orrell, A., Preziuso, D., Foster, N., Morris, S., & Homer, J. (n.d.). *2018 Distributed Wind Market Report*. Retrieved March 1, 2021, from http://www.ntis.gov/about/form.aspx

Orsini, F., Gasperi, D., Marchetti, L., Piovene, C., Draghetti, S., Ramazzotti, S., Bazzocchi, G., & Gianquinto, G. (2014). Exploring the production capacity of rooftop gardens (RTGs) in urban agriculture: the potential impact on food and nutrition security, biodiversity and other ecosystem services in the city of Bologna. *Food Security*, *6*(6), 781–792. https://doi.org/10.1007/s12571-014-0389-6

Orsini, F., Kahane, R., Nono-Womdim, R., & Gianquinto, G. (2013). Urban agriculture in the developing world: A review. *Agronomy for Sustainable Development*, *33*(4), 695–720. https://doi.org/10.1007/s13593-013-0143-z

Oyekale, J., Petrollese, M., Tola, V., & Cau, G. (2020). Impacts of renewable energy resources on effectiveness of grid-integrated systems: Succinct review of current challenges and potential solution strategies. *Energies*, *13*(18). https://doi.org/10.3390/en13184856

Pai, S., Ai, N., & Zheng, J. (2019). Decentralized community composting feasibility analysis for residential food waste: A Chicago case study. *Sustainable Cities and Society*, *50*(June), 101683. https://doi.org/10.1016/j.scs.2019.101683

Pakari, A., & Ghani, S. (2019). Evaluation of a novel greenhouse design for reduced cooling loads during the hot season in subtropical regions. *Solar Energy*, *181*(September 2018), 234–242. https://doi.org/10.1016/j.solener.2019.02.006

Pamungkas, A. P., Hatou, K., & Morimoto, T. (2014). Evapotranspiration Model Analysis of Crop Water Use in Plant Factory System. *Environmental Control in Biology*, *52*(3), 183–188. https://doi.org/10.2525/ecb.52.183

Pan, T., Wang, Y., Wang, L., Ding, J., Cao, Y., Qin, G., Yan, L., Xi, L., Zhang, J., & Zou, Z. (2020). Increased CO2 and light intensity regulate growth and leaf gas exchange in tomato. *Physiologia Plantarum*, *168*(3), 694–708. https://doi.org/10.1111/ppl.13015

Pantanella, E., Cardarelli, M., Colla, G., Rea, E., & Marcucci, A. (2012). Aquaponics vs. hydroponiics: production and quality of lettuce crop. *Acta Horticulturae*, *927*, 887–893. https://doi.org/10.17660/ActaHortic.2012.927.109

Parry, D. (2016). Municipal food waste management options: climate and economic impacts. In *Sowing Seeds in the City* (pp. 107–123). Springer.

Parthasarathi, T., Velu, G., & Jeyakumar, P. (2013). Impact of Crop Heat Units on Growth and Developmental Physiology of Future Crop Production: A Review. *Research & Reviews : Journal of Crop Science and Technology*, *2*(1), 11–18. http://www.stmjournals.com/sci/index.php?journal=RRJoCST&page=article&op=view&path%5B%5D=311%5Cn

Perez, M., Perez, R., Rábago, K. R., & Putnam, M. (2019a). Overbuilding & curtailment: The cost-effective enablers of firm PV generation. *Solar Energy*, *180*(September 2018), 412–422. https://doi.org/10.1016/j.solener.2018.12.074

Perez, M., Perez, R., Rábago, K. R., & Putnam, M. (2019b). Overbuilding & curtailment: The cost-effective enablers of firm PV generation. *Solar Energy*, *180*, 412–422. https://doi.org/10.1016/j.solener.2018.12.074

Peters, C. J., Bills, N. L., Lembo, A. J., Wilkins, J. L., & Fick, G. W. (2012). Mapping potential foodsheds in New York State by food group: An approach for prioritizing which foods to grow locally. *Renewable Agriculture and Food Systems*, *27*(2), 125–137. https://doi.org/10.1017/S1742170511000196

Poggi, F., Firmino, A., & Amado, M. (2018). Planning renewable energy in rural areas: Impacts on occupation and land use. *Energy*, *155*, 630–640. https://doi.org/10.1016/j.energy.2018.05.009

Powell, J. P., & Reinhard, S. (2015). Measuring the effects of extreme weather events on yields. *Weather and Climate Extremes*, *12*, 69–79. https://doi.org/10.1016/j.wace.2016.02.003

Proietti, S., Moscatello, S., Leccese, A., Colla, G., & Battistelli, A. (2004). The effect of growing spinach (Spinacia oleracea L.) at two light intensities on the amounts of oxalate, ascorbate and nitrate in their leaves. *Journal of Horticultural Science and Biotechnology*, *79*(4), 606–609. https://doi.org/10.1080/14620316.2004.11511814

Proksch, G. (2017). *Creating Urban Agricultural Systems - An Integrated Approach to Design*. Routledge.

Purkayastha, D., Majumder, M., & Chakrabarti, S. (2015). Collection and recycle bin location-allocation problem in solid waste management : A review. *Pollution*, *1*(2), 175–191. https://jpoll.ut.ac.ir/article_52927_7f3c6c2744324db252eaead57db03019.pdf

Putnam, M., & Perez, M. (2018). Solar Potential Analysis Report. In *MN Solar Pathways*. https://energy.gov/solar-office.

Qaddoum, K., Hines, E. L., & Iliescu, D. D. (2013). Yield Prediction for Tomato Greenhouse Using EFuNN. *ISRN Artificial Intelligence*, *2013*, 1–9. https://doi.org/10.1155/2013/430986

Qadir, G., & Malik, M. A. (2007). Growing degree days and yield relationship in sunflower (Helianthus annuus L.). *International Journal of Agriculture and Biology (Pakistan), January 2007*.

Rafie-Majd, Z., Pasandideh, S. H. R., & Naderi, B. (2018). Modelling and solving the integrated inventory-location-routing problem in a multi-period and multi-perishable product supply chain with uncertainty: Lagrangian relaxation algorithm. *Computers and*

Chemical Engineering, *109*, 9–22. https://doi.org/10.1016/j.compchemeng.2017.10.013

Ramankutty, N., Foley, J. A., Norman, J., & McSweeney, K. (2002). The Global Distribution of Cultivable Lands : Current Patterns and Sensitivity to Possible Climate Change. *Global Ecology & Biogeography*, *11*(5), 377–392.

Rasheed, A., Lee, J. W., & Lee, H. W. (2018). Development and optimization of a building energy simulation model to study the effect of greenhouse design parameters. *Energies*, *11*(8). https://doi.org/10.3390/en11082001

Richards, T. J., & Rickard, B. (2020). COVID-19 impact on fruit and vegetable markets. *Canadian Journal of Agricultural Economics*, *68*(2), 189–194. https://doi.org/10.1111/cjag.12231

Richardson, J. J., & Moskal, L. M. (2016). Urban food crop production capacity and competition with the urban forest. *Urban Forestry & Urban Greening*, *15*, 58–64. https://doi.org/10.1016/j.ufug.2015.10.006

Rickman, J. C., Bruhn, C. M., & Barrett, D. M. (2007). Nutritional comparison of fresh, frozen, and canned fruits and vegetables II. Vitamin A and carotenoids, vitamin E, minerals and fibe. *Journal of the Science of Food and Agriculture*, *1243*(December 2006), 1237–1243. https://doi.org/10.1002/jsfa

Righi, S., Oliviero, L., Pedrini, M., Buscaroli, A., & Della Casa, C. (2013). Life Cycle Assessment of management systems for sewage sludge and food waste: Centralized and decentralized approaches. *Journal of Cleaner Production*, *44*(2013), 8–17. https://doi.org/10.1016/j.jclepro.2012.12.004

Rijsdijk, A. A., & Vogelezang, J. V. M. (2000). Temperature integration on a 24-hour base: a more efficient climate control strategy. *Acta Horticulturae*, *519*, 163–170. https://doi.org/10.17660/ActaHortic.2000.519.16

Robb, D. H. F., MacLeod, M., Hasan, M. R., & Soto, D. (2017). Greenhouse gas emissions from aquaculture: A life cycle assessment of three Asian systems. *FAO Fisheries and Aquaculture Technical Paper*, *609*, I,III,IV,VIII,XI,XII,XIII,XIV,1-92. https://doi.org/10.1515/eko-2015-0009

Romeo, D., Vea, E. B., & Thomsen, M. (2018). Environmental Impacts of Urban Hydroponics in Europe: A Case Study in Lyon. *Procedia CIRP*, *69*(May), 540–545. https://doi.org/10.1016/j.procir.2017.11.048

Rosenzweig, C., Tubiello, F. N., Goldberg, R., Mills, E., & Bloomfield, J. (2002). Increased crop damage in the US from excess precipitation under climate change. *Global Environmental Change*, *12*(3), 197–202. https://doi.org/10.1016/S0959-3780(02)00008-0

Ruiter, H. De, Macdiarmid, J. I., Matthews, R. B., & Smith, P. (2016). Exploring a 'Healthy Foodshed': Land Use Associated with UK Fruit and Vegetables Supply. *Land Use Competition*, 247–261. https://doi.org/10.1007/978-3-319-33628-2

Russo, G., Anifantis, A. S., Verdiani, G., & Mugnozza, G. S. (2014). Environmental analysis of geothermal heat pump and LPG greenhouse heating systems. *Biosystems Engineering*, *127*, 11–23. https://doi.org/10.1016/j.biosystemseng.2014.08.002

S2G Ventures. (2020). *Growing Beyond the Hype : Controlled Environment Agriculture*.

Sabiiti, G., Ininda, J. M., Ogallo, L. A., Ouma, J., Artan, G., Basalirwa, C., Opijah, F.,

Nimusiima, A., Ddumba, S. D., Mwesigwa, J. B., Otieno, G., & Nanteza, J. (2018). Adapting agriculture to climate change: Suitability of banana crop production to future climate change over uganda. In *Climate Change Management* (pp. 175–190). Springer. https://doi.org/10.1007/978-3-319-64599-5_10

Saer, A., Lansing, S., Davitt, N. H., & Graves, R. E. (2013). Life cycle assessment of a food waste composting system: Environmental impact hotspots. *Journal of Cleaner Production*, *52*, 234–244. https://doi.org/10.1016/j.jclepro.2013.03.022

Saha, M., & Eckelman, M. J. (2017). Growing fresh fruits and vegetables in an urban landscape: A geospatial assessment of ground level and rooftop urban agriculture potential in Boston, USA. *Landscape and Urban Planning*, *165*(August 2016), 130–141. https://doi.org/10.1016/j.landurbplan.2017.04.015

Salemdeeb, R., Bin Daina, M., Reynolds, C., & Al-Tabbaa, A. (2018). An environmental evaluation of food waste downstream management options: a hybrid LCA approach. *International Journal of Recycling of Organic Waste in Agriculture*, *7*(3), 217–229. https://doi.org/10.1007/s40093-018-0208-8

Salomone, R., Saija, G., Mondello, G., Giannetto, A., Fasulo, S., & Savastano, D. (2017). Environmental impact of food waste bioconversion by insects: Application of Life Cycle Assessment to process using Hermetia illucens. *Journal of Cleaner Production*, *140*, 890–905. https://doi.org/10.1016/j.jclepro.2016.06.154

Sanjuan-Delmás, D., Llorach-Massana, P., Nadal, A., Ercilla-Montserrat, M., Muñoz, P., Montero, J. I., Josa, A., Gabarrell, X., & Rieradevall, J. (2018). Environmental assessment of an integrated rooftop greenhouse for food production in cities. *Journal of Cleaner Production*, *177*, 326–337. https://doi.org/10.1016/j.jclepro.2017.12.147

Sanyé-Mengual, E., Martinez-Blanco, J., Finkbeiner, M., Cerdà, M., Camargo, M., Ometto, A. R., Velásquez, L. S., Villada, G., Niza, S., Pina, A., Ferreira, G., Oliver-Solà, J., Montero, J. I., & Rieradevall, J. (2018). Urban horticulture in retail parks: Environmental assessment of the potential implementation of rooftop greenhouses in European and South American cities. *Journal of Cleaner Production*, *172*, 3081–3091. https://doi.org/10.1016/j.jclepro.2017.11.103

Sarbu, I., & Sebarchievici, C. (2014). General review of ground-source heat pump systems for heating and cooling of buildings. *Energy and Buildings*, *70*, 441–454. https://doi.org/10.1016/j.enbuild.2013.11.068

Sasse, J.-P., & Trutnevyte, E. (n.d.). *Regional impacts of electricity system transition in Central Europe until 2035 Achieving current electricity sector targets in Central Europe*. https://doi.org/10.1038/s41467-020-18812-y

Saunders, P. J. (2020). *Land Use Requirements of Solar and Wind Power Generation: Understanding a Decade of Academic Research ENERGY INNOVATION REFORM PROJECT*. www.innovationreform.org

Schmutz, U., Kneafsey, M., Sarrouy Kay, C., Doernberg, A., & Zasada, I. (2017). Sustainability impact assessments of different urban short food supply chains: examples from London, UK. *Renewable Agriculture and Food Systems*, 1–11. https://doi.org/10.1017/S1742170517000564

Schnitzler, W. H., Sharma, A. K., Gruda, N. S., & Heuberger, H. T. (2004). A low-tech hydroponic system for bell pepper (capsicum annuum L.) production. *Acta Horticulturae*, *644*, 47–53. https://doi.org/10.17660/ActaHortic.2004.644.3

Seifert, C., & Moss, L. (2020). *Understanding Soil Productivity Ratings*. Granular, Inc. https://granular.ag/blog/understanding-soil-productivity-ratings/

Shamshiri, R. R., Jones, J. W., Thorp, K. R., Ahmad, D., Man, H. C., & Taheri, S. (2018). Review of optimum temperature, humidity, and vapour pressure deficit for microclimate evaluation and control in greenhouse cultivation of tomato: A review. *International Agrophysics*, *32*(2), 287–302. https://doi.org/10.1515/intag-2017-0005

Shamshiri, R. R., Kalantari, F., Ting, K. C., Thorp, K. R., Hameed, I. A., Weltzien, C., Ahmad, D., & Shad, Z. M. (2018). Advances in greenhouse automation and controlled environment agriculture: A transition to plant factories and urban agriculture. *International Journal of Agricultural and Biological Engineering*, *11*(1), 1–22. https://doi.org/10.25165/j.ijabe.20181101.3210

Shao, Y., Heath, T., & Thu, Y. (2016). Developing an economic estimation system for vertical farms. *International Journal of Agricultural and Environmental Information Systems*, *7*(2).

Shen, Y., Wei, R., & Xu, L. (2018). Energy consumption prediction of a greenhouse and optimization of daily average temperature. *Energies*, *11*(1). https://doi.org/10.3390/en11010065

Shiina, T., Hosokawa, D., Roy, P., Nakamura, N., Thammawong, M., & Orikasa, T. (2011). Life cycle inventory analysis of leafy vegetables grown in two types of plant factories. *Acta Horticulturae*, *919*, 115–122. https://doi.org/10.17660/ActaHortic.2011.919.14

Shiina, T., Hosokawa, D., Roy, P., Orikasa, T., Nakamura, N., & Thammawong, M. (2011). Life cycle inventory analysis of leafy vegetables grown in two types of plant factories. *Acta Horticulturae*, *919*(December), 115–122. https://doi.org/10.17660/ActaHortic.2011.919.14

Shin, H. H., & Nam, S. W. (2015). Validation of load calculation method for greenhouse heating design and analysis of the influence of infiltration loss and ground heat exchange. *Korean Journal of Horticultural Science and Technology*, *33*(5), 647–657. https://doi.org/10.7235/hort.2015.15007

Shinkuma, T., & Nguyen Thi Minh Huong. (2009). The flow of E-waste material in the Asian region and a reconsideration of international trade policies on E-waste. *Environmental Impact Assessment Review*, *29*(1), 25–31. https://doi.org/10.1016/j.eiar.2008.04.004

Shinohara, M., Aoyama, C., Fujiwara, K., Watanabe, A., Ohmori, H., Uehara, Y., & Takano, M. (2011). Microbial mineralization of organic nitrogen into nitrate to allow the use of organic fertilizer in hydroponics. *Soil Science and Plant Nutrition*, *57*(2), 190–203. https://doi.org/10.1080/00380768.2011.554223

Shoup, M. E. (n.d.). *Pandemic accelerates demand for fresh food and gives rise to the "contemporary consumer."* Retrieved March 16, 2021, from https://www.foodnavigator-usa.com/Article/2020/10/28/Pandemic-accelerates-demand-for-fresh-food-and-gives-rise-to-the-contemporary-consumer

Silva, S., Alçada-Almeida, L., & Dias, L. C. (2014). Biogas plants site selection integrating Multicriteria Decision Aid methods and GIS techniques: A case study in a Portuguese region. *Biomass and Bioenergy*, *71*, 58–68. https://doi.org/10.1016/j.biombioe.2014.10.025

Singh, A., & Singh, G. S. (2017). Vermicomposting: A sustainable tool for environmental

equilibria. *Environmental Quality Management*, *27*(1), 23–40. https://doi.org/10.1002/tqem.21509

Singh, S. (2018). Agrometeorological Requirements for Sustainable Vegetable Crops Production. *Journal of Food Protection*, *2*(3), 1–22.

Sioen, G. B., Sekiyama, M., Terada, T., & Yokohari, M. (2017). Post-disaster food and nutrition from urban agriculture: A self-Sufficiency analysis of Nerima ward, Tokyo. *International Journal of Environmental Research and Public Health*, *14*(7), 1–20. https://doi.org/10.3390/ijerph14070748

Sioen, G. B., Terada, T., Sekiyama, M., & Yokohari, M. (2018). Resilience with mixed agricultural and urban land uses in Tokyo, Japan. *Sustainability (Switzerland)*, *10*(2), 1–27. https://doi.org/10.3390/su10020435

Slater, R., & Aiken, M. (2015). Can't You Count? Public Service Delivery and Standardized Measurement Challenges – The Case of Community Composting. *Public Management Review*, *17*(8), 1085–1102. https://doi.org/10.1080/14719037.2014.881532

Sliz-Szkliniarz, B. (2013). Assessment of the renewable energy-mix and land use trade-off at a regional level: A case study for the Kujawsko-Pomorskie Voivodship. *Land Use Policy*, *35*, 257–270. https://doi.org/10.1016/j.landusepol.2013.05.018

Slorach, P. C., Jeswani, H. K., Cuéllar-Franca, R., & Azapagic, A. (2020). Environmental sustainability in the food-energy-water-health nexus: A new methodology and an application to food waste in a circular economy. *Waste Management*, *113*, 359–368. https://doi.org/10.1016/j.wasman.2020.06.012

Smit, J., & Nasr, J. (1992). Urban agriculture for sustainable cities: using wastes and idle land and water bodies as resources. In *Environment and Urbanization* (Vol. 4, Issue 2, pp. 141–152). https://doi.org/10.1177/095624789200400214

Sokolow, J., Kennedy, G., & Attwood, S. (2019). Managing Crop tradeoffs: A methodology for comparing the water footprint and nutrient density of crops for food system sustainability. *Journal of Cleaner Production*, *225*, 913–927. https://doi.org/10.1016/j.jclepro.2019.03.056

Sonesson, U. (1996). *Modelling of the Compost and Transport Process in the ORWARE Simulation Model* (p. 35). http://pub.epsilon.slu.se/3833/1/sonesson_u_091216.pdf

Springmann, M., Clark, M., Mason-D'Croz, D., Wiebe, K., Bodirsky, B. L., Lassaletta, L., de Vries, W., Vermeulen, S. J., Herrero, M., Carlson, K. M., Jonell, M., Troell, M., DeClerck, F., Gordon, L. J., Zurayk, R., Scarborough, P., Rayner, M., Loken, B., Fanzo, J., … Willett, W. (2018). Options for keeping the food system within environmental limits. *Nature*, *562*(7728), 519–525. https://doi.org/10.1038/s41586-018-0594-0

Ssenyimba, S., Kiggundu, N., & Banadda, N. (2020). Designing a solar and wind hybrid system for small-scale irrigation: A case study for Kalangala district in Uganda. *Energy, Sustainability and Society*, *10*(1), 1–18. https://doi.org/10.1186/s13705-020-0240-1

Stacey, N. T., & Hildebrandt, D. (2018). Quantitative modeling of a greenhouse as a bioreactor to process power station emissions. *Environmental Progress and Sustainable Energy*, *37*(5), 1774–1780. https://doi.org/10.1002/ep.12824

Stanghellini, C. (1987). *Transpiration of Greenhouse Crops*. Wageningen University.

Stanhill, G. (1980). The energy cost of protected cropping: A comparison of six systems of

tomato production. *Journal of Agricultural Engineering Research*, *25*(2), 145–154. https://doi.org/10.1016/0021-8634(80)90055-4

Stoknes, K., Scholwin, F., Krzesiński, W., Wojciechowska, E., & Jasińska, A. (2016). Efficiency of a novel "Food to waste to food" system including anaerobic digestion of food waste and cultivation of vegetables on digestate in a bubble-insulated greenhouse. *Waste Management*, *56*, 466–476. https://doi.org/10.1016/j.wasman.2016.06.027

Sumathi, V. R., Natesan, U., & Sarkar, C. (2008). GIS-based approach for optimized siting of municipal solid waste landfill. *Waste Management*, *28*(11), 2146–2160. https://doi.org/10.1016/j.wasman.2007.09.032

Tautges, N. E., Chiartas, J. L., Gaudin, A. C. M., O'Geen, A. T., Herrera, I., & Scow, K. M. (2019). Deep soil inventories reveal that impacts of cover crops and compost on soil carbon sequestration differ in surface and subsurface soils. *Global Change Biology*, *February*, 1–14. https://doi.org/10.1111/gcb.14762

Teitel, M., Ziskind, G., Liran, O., Dubovsky, V., & Letan, R. (2008). Effect of wind direction on greenhouse ventilation rate, airflow patterns and temperature distributions. *Biosystems Engineering*, *101*(3), 351–369. https://doi.org/10.1016/j.biosystemseng.2008.09.004

Teixeira, C. A., Russo, M., Matos, C., & Bentes, I. (2014). Evaluation of operational, economic, and environmental performance of mixed and selective collection of municipal solid waste: Porto case study. *Waste Management and Research*, *32*(12), 1210–1218. https://doi.org/10.1177/0734242X14554642

Teo, Y. L., & Go, Y. I. (2021). Techno-Economic-Environmental Analysis of Solar/Hybrid/Storage for Vertical Farming System: A Case Study, Malaysia. *Renewable Energy Focus*. https://doi.org/10.1016/j.ref.2021.02.005

Tewolde, F. T., Shiina, K., Maruo, T., Takagaki, M., Kozai, T., & Yamori, W. (2018). Supplemental LED inter-lighting compensates for a shortage of light for plant growth and yield under the lack of sunshine. *PLoS ONE*, *13*(11), 1–14. https://doi.org/10.1371/journal.pone.0206592

Theurl, M. C., Haberl, H., Erb, K. H., & Lindenthal, T. (2014). Contrasted greenhouse gas emissions from local versus long-range tomato production. *Agronomy for Sustainable Development*, *34*(3), 593–602. https://doi.org/10.1007/s13593-013-0171-8

Tong, Y., Kozai, T., & Ohyama, K. (2013). Performance of household heat pumps for nighttime cooling of a tomato greenhouse during the summer. *Applied Engineering in Agriculture*, *29*(3), 414–421. https://doi.org/10.13031/aea.29.9984

Trlica, A. (2016). Soil Carbon Sequestration and Organic Wastes. In *Sowing Seeds in the City* (pp. 153–159). Springer.

UNEP. (n.d.). *Environmental Data Explorer - The Environmental Database*. Retrieved February 25, 2021, from http://geodata.grid.unep.ch/results.php

UNICEF. (2016). *Global Nutrition Report 2016 From Promise to Impact Ending Malnutrition by 2030*. https://doi.org/10.2499/9780896299948

USDA. (2020). *Vegetables 2019 Summary*.

USEPA. (2013). *Municipal Solid Waste in The United States*. https://archive.epa.gov/epawaste/nonhaz/municipal/web/pdf/mswcharacterization_fnl_060713_2_rpt.pdf

USGS. (2016). *GAP/LANDFIRE National Terrestrial Ecosystems 2011*. U.S. Geological Survey. https://doi.org/https://doi.org/10.5066/F7ZS2TM0

Vallati, A., Grignaffini, S., & Romagna, M. (2015). A New Method to Energy Saving in a Micro Grid. *Sustainability*, *7*(10), 13904–13919. https://doi.org/10.3390/su71013904

Van Beveren, P. J. M., Bontsema, J., Van Straten, G., & Van Henten, E. J. (2015). Minimal heating and cooling in a modern rose greenhouse. *Applied Energy*, *137*, 97–109. https://doi.org/10.1016/j.apenergy.2014.09.083

van der Velde, M., Tubiello, F. N., Vrieling, A., & Bouraoui, F. (2012). Impacts of extreme weather on wheat and maize in France: Evaluating regional crop simulations against observed data. *Climatic Change*, *113*(3–4), 751–765. https://doi.org/10.1007/s10584-011-0368-2

Van Henten, E. J. (1994). Validation of a dynamic lettuce growth model for greenhouse climate control. *Agricultural Systems*, *45*(1), 55–72. https://doi.org/10.1016/S0308-521X(94)90280-1

van Huis, A. (2013). Potential of Insects as Food and Feed in Assuring Food Security. *Annual Review of Entomology*, *58*(1), 563–583. https://doi.org/10.1146/annurev-ento-120811-153704

Vanthoor, B. H.E., de Visser, P. H. B., Stanghellini, C., & van Henten, E. J. (2011). A methodology for model-based greenhouse design: Part 2, description and validation of a tomato yield model. *Biosystems Engineering*, *110*(4), 378–395. https://doi.org/10.1016/j.biosystemseng.2011.08.005

Vanthoor, B. H.E., Stanghellini, C., Van Henten, E. J., & De Visser, P. H. B. (2011). A methodology for model-based greenhouse design: Part 1, a greenhouse climate model for a broad range of designs and climates. *Biosystems Engineering*, *110*(4), 363–377. https://doi.org/10.1016/j.biosystemseng.2011.06.001

Vanthoor, Bram H.E., Gázquez, J. C., Magán, J. J., Ruijs, M. N. A., Baeza, E., Stanghellini, C., van Henten, E. J., & de Visser, P. H. B. (2012). A methodology for model-based greenhouse design: Part 4, economic evaluation of different greenhouse designs: A Spanish case. *Biosystems Engineering*, *111*(4), 336–349. https://doi.org/10.1016/j.biosystemseng.2011.12.008

Vanthoor, Bram H.E., Stigter, J. D., van Henten, E. J., Stanghellini, C., de Visser, P. H. B., & Hemming, S. (2012). A methodology for model-based greenhouse design: Part 5, greenhouse design optimisation for southern-Spanish and Dutch conditions. *Biosystems Engineering*, *111*(4), 350–368. https://doi.org/10.1016/j.biosystemseng.2012.01.005

Vanthoor, Bram H E. (2011). *A model based greenhouse design method*. Wageningen University.

Vázquez, M. A., & Soto, M. (2017). The efficiency of home composting programmes and compost quality. *Waste Management*, *64*, 39–50. https://doi.org/10.1016/j.wasman.2017.03.022

Vieira, V. H. A. de M., & Matheus, D. R. (2019). Environmental assessments of biological treatments of biowaste in life cycle perspective: A critical review. *Waste Management and Research*, *37*(12), 1183–1198. https://doi.org/10.1177/0734242X19879222

Villarreal-Guerrero, F., Kacira, M., Fitz-Rodríguez, E., Kubota, C., Giacomelli, G. A., Linker,

R., & Arbel, A. (2012). Comparison of three evapotranspiration models for a greenhouse cooling strategy with natural ventilation and variable high pressure fogging. *Scientia Horticulturae*, *134*, 210–221. https://doi.org/10.1016/j.scienta.2011.10.016

Villarreal-Guerrero, Federico, Kacira, M., Fitz-Rodríguez, E., Linker, R., Kubota, C., Giacomelli, G. A., & Arbel, A. (2012). Simulated performance of a greenhouse cooling control strategy with natural ventilation and fog cooling. *Biosystems Engineering*, *111*(2), 217–228. https://doi.org/10.1016/j.biosystemseng.2011.11.015

Vogel, E., Donat, M. G., Alexander, L. V., Meinshausen, M., Ray, D. K., Karoly, D., Meinshausen, N., & Frieler, K. (2019). The effects of climate extremes on global agricultural yields. *Environmental Research Letters*, *14*(5). https://doi.org/10.1088/1748-9326/ab154b

Walker, M., Theaker, H., Yaman, R., Poggio, D., Nimmo, W., Bywater, A., Blanch, G., & Pourkashanian, M. (2017). Assessment of micro-scale anaerobic digestion for management of urban organic waste: A case study in London, UK. *Waste Management (New York, N.Y.)*, *61*, 258–268. https://doi.org/10.1016/j.wasman.2017.01.036

Wang, E., & Engel, T. (1998). Simulation of phenological development of wheat crops. *Agricultural Systems*, *58*(1), 1–24. https://doi.org/10.1016/S0308-521X(98)00028-6

Wang, Q., M'Ikiugu, M. M., & Kinoshita, I. (2014). A GIS-based approach in support of spatial planning for renewable energy: A case study of Fukushima, Japan. *Sustainability (Switzerland)*, *6*(4), 2087–2117. https://doi.org/10.3390/su6042087

Ward, J., & Symons, J. (2017). Optimising Crop Selection for Small Urban Food Gardens in Dry Climates. *Horticulturae*, *3*(2), 33. https://doi.org/10.3390/horticulturae3020033

Watkiss, P. (2009). *Comparative Life Cycle Assessment of Food Commodities Procured for UK Consumption through a Diversity of Supply Chains: Appendix 2* (Vol. 5, Issue 020, pp. 1–27). https://doi.org/10.1109/TELSKS.2003.1246180

Webb, J., Williams, A. G., Hope, E., Evans, D., & Moorhouse, E. (2013). Do foods imported into the UK have a greater environmental impact than the same foods produced within the UK? *International Journal of Life Cycle Assessment*, *18*(7), 1325–1343. https://doi.org/10.1007/s11367-013-0576-2

Weidner, T., & Yang, A. (2020). The potential of urban agriculture in combination with organic waste valorization: Assessment of resource flows and emissions for two european cities. *Journal of Cleaner Production*, *244*. https://doi.org/10.1016/j.jclepro.2019.118490

Weidner, Till, Graça, J., Machado, T., & Yang, A. (2020). Comparison of local and centralized biowaste management strategies – A spatially-sensitive approach for the region of Porto. *Waste Management*, *118*, 552–562. https://doi.org/10.1016/j.wasman.2020.09.013

Weidner, Till, & Yang, A. (2019). The potential of urban agriculture in combination with organic waste valorization: Assessment of resource flows and emissions for two european cities. *Journal of Cleaner Production*, *244*, 118490. https://doi.org/10.1016/j.jclepro.2019.118490

Weidner, Till, Yang, A., & Hamm, M. W. (2019). Consolidating the current knowledge on urban agriculture in productive urban food systems: Learnings, gaps and outlook. *Journal of Cleaner Production*, *209*, 1637–1655.

https://doi.org/10.1016/J.JCLEPRO.2018.11.004

Weidner, Till, Yang, A., & Hamm, M. W. (2021). Energy optimisation of plant factories and greenhouses for different climatic conditions. *Energy Conversion and Management*.

Weithmann, N., Möller, J. N., Löder, M. G. J., Piehl, S., Laforsch, C., & Freitag, R. (2018). Organic fertilizer as a vehicle for the entry of microplastic into the environment. *Science Advances*, *4*, 1–8. https://doi.org/10.1126/sciadv.aap8060

White, J. T., & Bunn, C. (2017). Growing in Glasgow: Innovative practices and emerging policy pathways for urban agriculture. *Land Use Policy*, *68*(July), 334–344. https://doi.org/10.1016/j.landusepol.2017.07.056

Widener, M. J., Metcalf, S. S., & Bar-Yam, Y. (2012). Developing a mobile produce distribution system for low-income urban residents in food deserts. *Journal of Urban Health*, *89*(5), 733–745. https://doi.org/10.1007/s11524-012-9677-7

Wielemaker, R. C., Weijma, J., & Zeeman, G. (2018). Harvest to harvest: Recovering nutrients with New Sanitation systems for reuse in Urban Agriculture. *Resources, Conservation and Recycling*, *128*, 426–437. https://doi.org/10.1016/j.resconrec.2016.09.015

Wikipedia. (n.d.-a). *Greater Tokyo Area*. Retrieved February 25, 2021, from https://en.wikipedia.org/wiki/Greater_Tokyo_Area

Wikipedia. (n.d.-b). *Mälaren Valley*. Retrieved February 25, 2021, from https://en.wikipedia.org/wiki/Mälaren_Valley

Wikipedia. (n.d.-c). *Metropolregion Greater Boston*. Retrieved February 25, 2021, from https://de.wikipedia.org/wiki/Metropolregion_Greater_Boston

Wilhelm, J. A., & Smith, R. G. (2017). Ecosystem services and land sparing potential of urban and peri-urban agriculture: A review. *Renewable Agriculture and Food Systems*, 1–14. https://doi.org/10.1017/S1742170517000205

Willett, W., Rockström, J., Loken, B., Springmann, M., Lang, T., Vermeulen, S., Garnett, T., Tilman, D., DeClerck, F., Wood, A., Jonell, M., Clark, M., Gordon, L. J., Fanzo, J., Hawkes, C., Zurayk, R., Rivera, J. A., De Vries, W., Majele Sibanda, L., … Murray, C. J. L. (2019). Food in the Anthropocene: the EAT–Lancet Commission on healthy diets from sustainable food systems. In *The Lancet* (Vol. 393, Issue 10170, pp. 447–492). Lancet Publishing Group. https://doi.org/10.1016/S0140-6736(18)31788-4

Willmott, C., & Feddema, J. (1992). A more rational climatic moisture index. *Professional Geographer*, *44*(1), 84–88. https://doi.org/10.1111/j.0033-0124.1992.00084.x

Wind Farms Adapt to Forest Conditions - Renewable Energy World. (n.d.). Retrieved February 25, 2021, from https://www.renewableenergyworld.com/wind-power/wind-farms-adapt-to-forest-conditions/#gref

WRAP. (2016). *Field experiments for quality digestate and compost in agriculture DC- Agri Recycling to agricultural land*. *February*. www.wrap.org.uk/dc-agri-reports.%0Ahttp://www.wrap.org.uk/sites/files/wrap/WRAP_DC-Agri_research_summary.pdf

Wrighton, S., & Reiter, K. (2016). CycleLogistics – Moving Europe Forward! *Transportation Research Procedia*, *12*, 950–958. https://doi.org/10.1016/J.TRPRO.2016.02.046

Xiao, X., Mazza, L., Yu, Y., Cai, M., Zheng, L., Tomberlin, J. K., Yu, J., van Huis, A., Yu, Z., Fasulo, S., & Zhang, J. (2018). Efficient co-conversion process of chicken manure into protein feed and organic fertilizer by Hermetia illucens L. (Diptera: Stratiomyidae) larvae and functional bacteria. *Journal of Environmental Management*, *217*, 668–676. https://doi.org/10.1016/j.jenvman.2018.03.122

Xie, Z., Game, E. T., Hobbs, R. J., Pannell, D. J., Phinn, S. R., & McDonald-Madden, E. (2020). Conservation opportunities on uncontested lands. *Nature Sustainability*, *3*(1), 9–15. https://doi.org/10.1038/s41893-019-0433-9

Y. Tong, T. Kozai, N. Nishioka, & K. Ohyama. (2012). Reductions in Energy Consumption and CO2 Emissions for Greenhouses Heated with Heat Pumps. *Applied Engineering in Agriculture*, *28*(3), 401–406. https://doi.org/10.13031/2013.41488

Yin, P. Y., Cheng, C. Y., Chen, H. M., & Wu, T. H. (2020). Risk-aware optimal planning for a hybrid wind-solar farm. *Renewable Energy*, *157*, 290–302. https://doi.org/10.1016/j.renene.2020.05.003

Yoder, R. E., Odhiambo, L. O., & Wright, W. C. (2005). Effects of Vapor-Pressure Deficit and Net-Irradiance Calculation Methods on Accuracy of Standardized Penman-Monteith Equation in a Humid Climate. *Journal of Irrigation and Drainage Engineering*, *131*(3), 228–237. https://doi.org/10.1061/(ASCE)0733-9437(2005)131:3(228)

Yue, C. D., & Wang, S. S. (2006). GIS-based evaluation of multifarious local renewable energy sources: A case study of the Chigu area of southwestern Taiwan. *Energy Policy*, *34*(6), 730–742. https://doi.org/10.1016/j.enpol.2004.07.003

Yue, D., Pandya, S., & You, F. (2016). Integrating Hybrid Life Cycle Assessment with Multiobjective Optimization: A Modeling Framework. *Environmental Science & Technology*, *50*(3), 1501–1509. https://doi.org/10.1021/acs.est.5b04279

Zappa, W., & van den Broek, M. (2018). Analysing the potential of integrating wind and solar power in Europe using spatial optimisation under various scenarios. *Renewable and Sustainable Energy Reviews*, *94*(August), 1192–1216. https://doi.org/10.1016/j.rser.2018.05.071

Zasada, I., Schmutz, U., Wascher, D., Kneafsey, M., Corsi, S., Mazzocchi, C., Monaco, F., Boyce, P., Doernberg, A., Sali, G., & Piorr, A. (2017). Food beyond the city - Analysing foodsheds and self-sufficiency for different food system scenarios in European metropolitan regions. *City, Culture and Society*, *January*, 0–1. https://doi.org/10.1016/j.ccs.2017.06.002

Zhang, Shanhong, Guo, Y., Zhao, H., Wang, Y., Chow, D., & Fang, Y. (2020). Methodologies of control strategies for improving energy efficiency in agricultural greenhouses. In *Journal of Cleaner Production* (Vol. 274, p. 122695). Elsevier Ltd. https://doi.org/10.1016/j.jclepro.2020.122695

Zhang, Shengbo, & Schulman, B. (2017). A Numerical Model for Simulating the Indoor Climate inside the Growing Chambers of Vertical Farms with Case Studies. *International Journal of Environmental Science and Development*, *8*(10), 728–735. https://doi.org/10.18178/ijesd.2017.8.10.1047

Zhang, Siduo, Bi, X. T., & Clift, R. (2013). A Life Cycle Assessment of integrated dairy farm-greenhouse systems in British Columbia. *Bioresource Technology*, *150*, 496–505. https://doi.org/10.1016/j.biortech.2013.09.076

Ziegler, F., Nilsson, P., Mattsson, B., & Walther, Y. (2003). Life Cycle assessment of frozen cod fillets including fishery-specific environmental impacts. *The International Journal of Life Cycle Assessment*, *8*(1), 39–47. https://doi.org/10.1007/BF02978747